5-30-2014

Electrochemical Control of Bacterial Persister Cells

Tagbo Herman Roland Niepa
Syracuse University

Abstract:

The emergence of antibiotic-resistant bacteria has presented an increasing challenge to infection control. Conventional methods of antibacterial treatment involving high dose of antibiotics or surgical intervention have proven insufficient for eradicating persistent infections, such as those associated with medical implants. It is well recognized that bacterial populations commonly contain a small percentage of phenotypic variants, known as persister cells, which are metabolically inactive and extremely tolerant to antibiotics. When the antibiotic treatment is stopped, surviving persister cells can regenerate the bacterial population with a similar percentage of persister cells. Thus, persistence presents a great challenge to curing chronic infections.

In this study, we introduced a novel method for controlling bacterial persistence based on a phenomenon we named electrochemical control of persister cells (ECCP). We demonstrate that bacterial persister cells can be effectively eliminated by low-level direct currents (DCs); e.g. treatment with 70 μA/cm^2 DC for 1 h using stainless steel (SS) 304 reduced the number of viable planktonic persister cells of *Pseudomonas aeruginosa* PAO1 by 98% compared to the untreated control. In addition to persister killing by applying DC alone, synergistic effects were observed when treating persister cells with 70 μA/cm^2 DC and 1.5 μg/mL tobramycin together using SS 304 electrodes. The same level of DC was also found to be cidal to biofilm associated persister cells of *P. aeruginosa* PAO1. Based on this discovery, the electrophysiological properties of *P. aeruginosa* PAO1 cells treated with 70 μA/cm^2 DC using carbon and SS 304 electrodes were characterized both at the cellular and genetic levels to understand the mechanism of

ECCP. We found that DC treatments affected surface charge and membrane integrity of *P. aeruginosa*, leading to increase intracellular concentration of metal cations as observed via scanning electron microscopy-energy dispersive spectroscopy (SEM-EDS) analysis. Moreover, electrochemical treatments mediated via carbon electrodes provoked the permeabilization of the cells to extracellular materials, and increased their susceptibility to antibiotics, which led to complete eradication of the persisters. These findings are corroborated by DNA microarray analysis, which revealed that DC treatments have profound effects on the physiology of persister cells, altering the regulation of genes involved in antibiotic resistance, pyocin-related functions, and SOS response. Comparative transmission electron microscopy (TEM) studies of the stationary phase *P. aeruginosa* PAO1 cells confirmed that DC treatments resulted in the compartmentalization of intracellular contents, release of outer membrane vesicles, or cell lysis.

To design novel systems to effectively control infections associated with biofilms and persister cells, the safety and the efficacy of ECCP were evaluated in co-culture models with human epithelial cells and *P. aeruginosa* PAO1. In addition, a pilot animal study was conducted to investigate the effects of electrochemical currents using a rabbit model of sinus infections. *P. aeruginosa* PAO1 was used to induce rhinosinusitis in rabbits, which were then treated with antibiotics, or antibiotics with electrical current, and compared with the untreated controls. The results of this study validated the effectiveness of electrochemical treatment in reducing both biofilms and planktonic cells *in vivo*. Overall, these findings improved the understanding of the electrophysiology of bacterial persister cells, and provided new insight for designing novel systems to effectively

control infections associated with biofilms and persister cells.

Keywords: Persisters, biofilms, direct current (DC), electrochemical treatments, electrodes, metal cations, 2-chamber system, co-culture, epithelial cells, rabbit model, sinusitis.

ELECTROCHEMICAL CONTROL OF BACTERIAL PERSISTER CELLS

By

Tagbo Herman Roland Niepa

B.S. Syracuse University, USA, 2009

DISSERTATION

Submitted in partial fulfillment of the requirements for the

degree of Doctor of Philosophy in Chemical Engineering

Syracuse University

May 2014

I dedicate this work to
my daugthers, Herlynn Edugie Niepa and Lisette Eliyah Niepa,
my wife Edugie Ruby Niepa
my mother Elisabeth Nehi Ble Niepa

ACKNOWLEDGEMENTS

First, I would like to thank Dr. Dacheng Ren for having me in his Lab since 2008. It has been a long a great journey working closely with him. He has been a role model, a leader, an advisor, and a mentor. I am extremely grateful for this opportunity he offered me in 2010, when he asked me to join his Lab as a graduate. Today, I am about to leave his Lab, and looking back I do have any regret because I have made the best choice.

Second, I would like to thank the committee members of my PhD. Dissertation who took time out of their busy schedule to listen to my stories. Over the path of this adventure, they have guided me, and will continue to be part of my academic life because of the good relationship we built. I would like to thank Dr. Jeremy Gilbert, Dr. James Dabrowiak, Dr. Jing An, Dr. Rebecca Bader and Dr. Hasenwinkel for the inspiration they all gave me. Next to them, I would like to mention Dr. Gina Lee-Glauser and Dr. Trish Lowney, who have been great mentors from the day I met them. Through them, I would love to thank Syracuse University, the office of Research, the College of Engineering, the Department of Biomedical and Chemical Engineering, the Syracuse Biomaterial Institute.

Third, I would like to thank close collaborators such Dr. Parul Goyal, Dr. Greg Haveman, Dr. Marcus Jones, Dr. Robert P. Smith, Dr. Deborah Kerwwod, Dr. Sheng Zhang, Wenjing Bao, Shiril Sivan, and Luana Blaszczyk, who contributed to make this work successful.

My fourth thought goes toward my Dear lab mates from the Ren lab and some colleagues who contributed to my scientific growth. I am thinking of Jiachuan Pan, Huan Gu, Huiqing Adonis Zheng, Xiangyu Yao, Geetika Choudhary, Ali Adem Bahar, Fangchao Song, Li Zhang, Grace Altimus, Nick Kelley, Meagan Garafalo, Robert Neiberger, Jing Wang “77”, Shuyuan Ma.

I have decided to have a special paragraph to acknowledge four precious people, who taught me how to be a good mentor, a good teacher: Jennifer Mary Puthota, Henry Lars Peterson, Shanelle Simone Gayle and Laura Mary Shepenger. These students of “mine” have been a precious asset, as we built precious mentor-mentor relationship while collaborating on this project. Laura and Henry deserve to be mentioned twice for their devotion and determination to make “it” happen.

I would love to acknowledge The National Science Foundation and Blue Highway Inc. for supporting this work through my doctoral fellowships and research grants.

My upmost gratitude goes to my Family who has been very supportive. They never judged me for my shortcomings; instead, they continued to provide love and encouragement, which was needed to become successful. Special Thanks to Lisette, Herlynn and Edugie Niepa, to my Mother, Sibblings, in-laws, and to everyone who supported me or inspired me. Thank you all…

TABLE OF CONTENTS

LIST OF TABLES

LIST OF FIGURES

CHAPTER 1

MOTIVATION, HYPOTHESIS, AND OBJECTIVES

1.1 MOTIVATIONS

1.1.1 Antibiotic-resistant infections

The discovery of penicillin in 1929 opened an exciting era of antibiotic therapy, in which millions of lives were saved from microbial infections. Over the years, however, microorganisms have developed an extraordinary level of resistance against commonly used antibiotics. For the past two decades, the so-called ESKAPE pathogens[1] (*Enterococcus faecium, Staphylococus aureus, Klebsiella pneunomoniae, Acinetobacter baumanii, Pseudomonas aeruginosa,* and *Enterobacteriaceae*) have caused an increasing problem of drug-resistant infections. In addition, species including *Clostridium difficile* and *Streptococcus pneunomoniae* have been reported in major cases of hospital-acquired infections in the U.S. last year, affecting 250,000 and 1,200,000 people, respectively (*Antibiotic resistance Threats in the United States, 2013 CDC report*). Such drug-resistant infections are associated with high mortality and morbidity, as well as massive financial loss. For example, in 2008 alone, the cost of inpatient services associated with antibiotic-resistant infections was estimated to $20 billion[2], with a $35 billion loss of work productivity.

Antibiotic resistance is inherent to the bacterial cell and its occurrence in nosocomial infections seriously compromises the safety of many surgical procedures. In addition to the development of drug resistance through mutation and gene transfer, bacteria also tolerate antibiotics through intrinsic mechanisms, especially those associated with implanted medical devices. Metals, ceramics and polymers are among the materials commonly used for making medical devices. However, once a medical device is

implanted in the host, it is immediately surrounded with blood plasma and become rapidly coated with proteins such as fibrin and fibronectin[3]. These substrates carry receptors for bacterial pathogens, which, if present, can form multicellular structures, known as biofilms [4]. Biofilm cells are embedded in a slimy polysaccharide matrix secreted by the attached cells. The biofilm matrix can retard the penetration of certain antibiotics. In addition, the presence of the persisters, a dormant sub-population that is highly tolerant to antibiotics, renders biofilms more difficult to eradicate. After antibiotic treatments, the surviving persister cells could wake up and regenerate new cell populations within the biofilm. Collectively, biofilm cells are 500-5000 times more tolerant to antibiotics than their planktonic counterparts. Due to close contact, biofilm cells can exchange genetic material and spread drug resistant genes[5]. As a consequence, a chronic infection can develop and lead to prolonged hospitalization, device failure, or related complications such as implant replacements, amputations and even the death of the patient [6].

1.1.2 New antimicrobial strategies

Bacterial resistance to antibiotics presents an increasing threat to public health and economy. To address this problem, new methods need to be developed to effectively prevent biofilm formation and eradicate biofilm and persister cells. Over the past two decades, a number of molecules have been shown to be promising candidates, since they target biofilm formation and virulence, instead of general growth of microbes. Biofilm inhibition can also be pursued by engineering antifouling surfaces with specific surface chemistry and topography. Topographic and (bio) chemical modifications can inhibit

initial attachment of bacterial cells to device surfaces by repelling or directly killing bacterial cells. A variety of techniques have been developed to functionalize surfaces with covalent bonds or electrochemical interactions. Functional groups can be linked to metal surfaces by coating with self-assembly monolayer (SAM), polyelectrolytes, nanogel, and layer-by-layer coatings [7,8].

Since most of the medical devices are made with metal materials, it is important to understand the interaction between bacterial cells and metals or their corrosion products. Fe, Cr, Ni, Co and Mn are listed among the cations comprised in stainless steel (SS) and these metal cations were reported with various effects on bacteria. Cations generated from SS at μM [9] to mM range [10] exhibited low cidal effects on *P. aeruginosa*, suggesting that this bacterium can tolerate a slow release of metal ions as it occurs during electrochemical corrosion. However, the use of electrical factors could improve the killing effects of these cations on bacterial cells. Several studies have shown that electrical currents (DCs in the range of μA to mA/cm² and 100 kHz to 10 MHz of alternating currents or ACs) delivered for several hours (in most cases) with diverse electrode materials have bacteriostatic or biocidal effects on bacteria [11-15]. Similar currents were also found to enhance the effects of antibiotics on biofilms, an interesting phenomenon known as bioelectric effects[16-19]. For instance, Busscher *et al*. demonstrated that the detachment of bacteria from medical relevant SS could be achieved using electrical currents in the mA range[20-22]. The treatment of bacteria with relatively low electrical current and antibiotics has shown that individual cells, biofilm-embedded cells

and persisters of *P. aeruginosa* can be successfully controlled[23]. These preliminary studies set a new perspective for the treatment of implant-associated infections.

1.2 RESEARCH HYPOTHESIS AND OBJECTIVES

Biofilm formation and bacterial persistence play a very important role in chronic infections. Antibiotics consistently fail to control such infections due to slow growth and dormancy of the biofilms and persister cells. Thus, antimicrobial approaches that work independently of the bacterial growth phase have a good potential to control bacterial persistence and medical implant-associated infections.

The discovery of bioelectric effects brought an exciting opportunity for engineering new therapeutic methods. However, the underlying mechanism of this phenomenon is not well understood, which limits the applications of this technology. Inspired by previous works on bioelectric effects, we hypothesize that appropriate levels of electric current can kill bacterial persister cells and such effects can be enhanced though synergistic effects with antibiotics. To test this central hypothesis and reveal the underlying mechanism, this study was conducted with the central goal of understanding the effects of DC on persister cells at both cellular and genetic levels, as well as *in vivo* using a rabbit model of sinusitis.

The major goals and specific aims are summarized in Fig. 1.1. The proposed study was carried out in three specific aims:

Aim 1 (Chapter 3 & 4): ***To study the effects of low-level DC on the viability of PAO1 persister cells is characterized.*** *P. aeruginosa* PAO1 is selected as the model of this study to test the effects of DC on its persistence. Our results showed that the persister

cells can be eradicated after treatment with 70 μA/cm^2 DC for 1 h, a phenomenon named as electrochemical control of persister cells (ECCP). This phenomenon was further investigated to understand how the physiochemical factors (current/voltage, ions, and antibiotics) affect the viability of the persister cells.

Aim 2 (Chapter 5, 6, 7 & 8): ***To understand the mechanisms of ECCP by characterizing the effects of DC on the morphology, the electrophysiology and the gene expression of the PAO1 cells***. The effects of ECs on the electrophysiology of persister cells were characterized using electrochemical measurements including zeta-potential, SEM-EDS. Also, the morphological changes of *P. aeruginosa* cells due to DC treatment were investigated using SEM, TEM, and AFM. The effects of electrochemical stresses were also studied using DNA microarrays to identify genes affected by DC. The interaction between the antibiotic and the metal cations were also investigation to comprehend synergy in electrochemical treatments.

Aim 3 (Chapter 8 & 9): ***To evaluate the safety and efficacy of ECCP in a co-culture model and a rabbit model.*** In these tests, the efficacy of ECCP was evaluated *in vitro* using a co-culture model of human cells and *P. aeruginosa* PAO1. Also the effectiveness of electrochemical treatments in killing biofilm cells was investigated in a rabbit model.

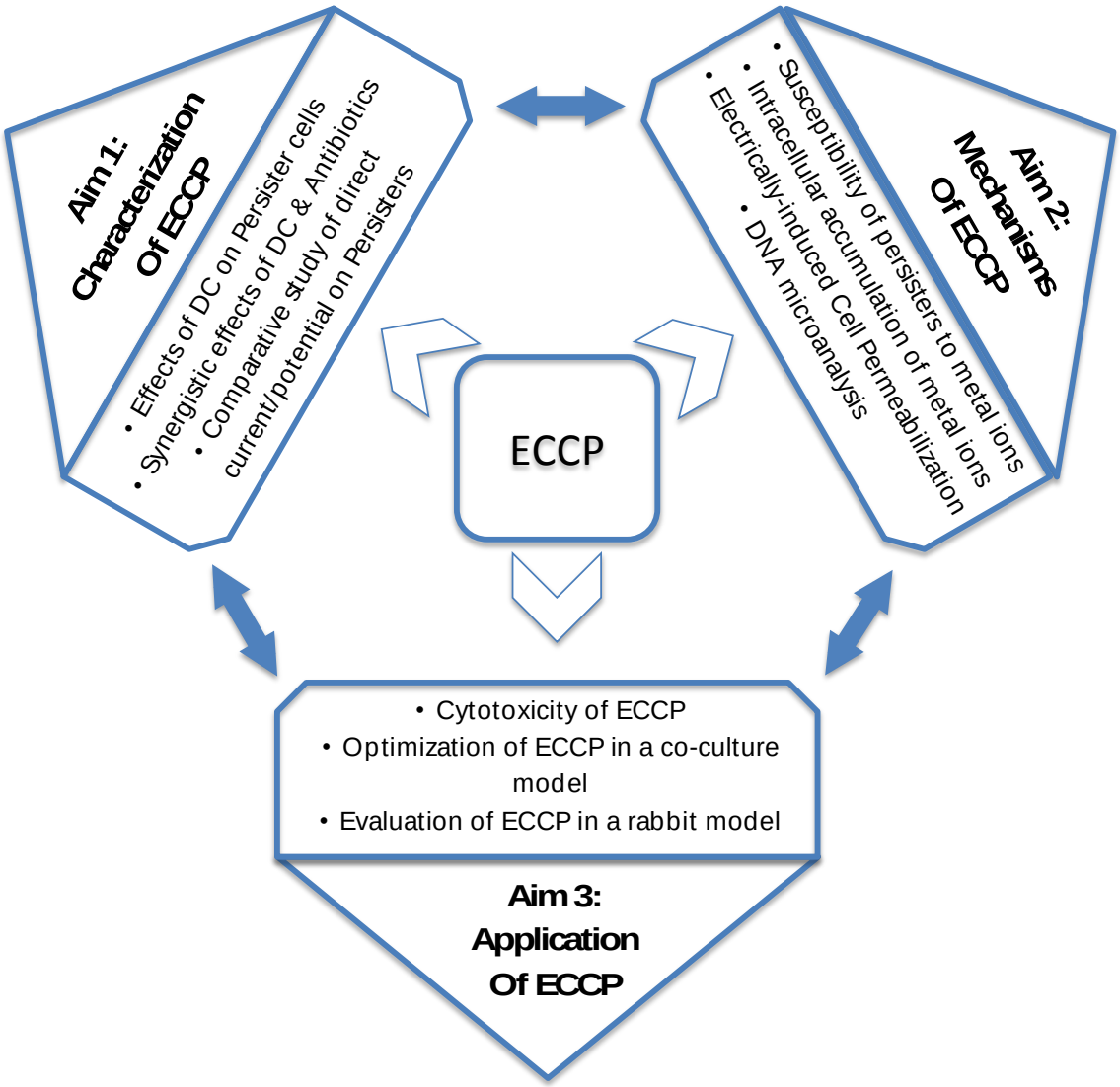

Figure 1.1: Overall plan for the study of the Electrochemical Control of Bacterial Persister Cells (ECCP). The specific aims and major subtasks of each aim are shown.

1.3 REFERENCES

1 **Boucher, H. W., Talbot, G. H., Bradley, J. S., Edwards, J. E., Gilbert, D., Rice, L. B., Scheld, M., Spellberg, B. & Bartlett, J.** Bad bugs, no drugs: no ESKAPE! An update from the Infectious Diseases Society of America. *Clinical infectious diseases : an official publication of the Infectious Diseases Society of America* **48**, 1-12, doi:10.1086/595011 (2009).

2 **Scott, R**. The Direct Medical Costs of Healthcare-Associated Infections in US Hospitals and the Benefits of Prevention. Division of Healthcare Quality Promotion National Center for Preparedness, Detection, and Control of Infectious Diseases Coordinating Center for Infectious Diseases Centers for Disease Control and Prevention March 2009 (2009).

3 **Savage, D. C. & Fletcher, M**. *Bacterial adhesion: mechanisms and physiological significance*. (Plenum Press, 1985).

4 **von Eiff, C., Kohnen, W., Becker, K. & Jansen, B**. Modern strategies in the prevention of implant-associated infections. *Int J Artif Organs* **28**, 1146-1156 (2005).

5 **Dzidic, S. & Bedekovic, V**. Horizontal gene transfer-emerging multidrug resistance in hospital bacteria. *Acta pharmacologica Sinica* **24**, 519-526 (2003).

6 **Adya, N., Alam, M., Ravindranath, T., Mubeen, A. & Saluja, B**. Corrosion in titanium dental implants: literature review. *The Journal* **5**, 127 (2005).

7 **Schuler, M., Trentin, D., Textor, M. & Tosatti, S. G. P**. Biomedical interfaces: titanium surface technology for implants and cell carriers. *Nanomedicine* **1**, 449-463 (2006).

8 **Kharlampieva, E., Kozlovskaya, V. & Sukhishvili, S. A**. Layer by Layer Hydrogen Bonded Polymer Films: From Fundamentals to Applications. *Advanced Materials* **21**, 3053-3065 (2009).

9 **Niepa, T. H., Gilbert, J. L. & Ren, D**. Controlling *Pseudomonas aeruginosa* persister cells by weak electrochemical currents and synergistic effects with tobramycin. *Biomaterials* **33**, 7356-7365, doi:10.1016/j.biomaterials.2012.06.092 (2012).

10 **Harrison, J. J., Turner, R. J. & Ceri, H**. Persister cells, the biofilm matrix and tolerance to metal cations in biofilm and planktonic *Pseudomonas aeruginosa*. *Environmental Microbiology* **7**, 981-994 (2005).

11 **Rosenberg, B**. Some biological effects of platinum compounds. *Platinum Metals Review* **15**, 42-51 (1971).

12 **Bolton, L., Foleno, B., Means, B. & Petrucelli, S**. Direct-current bactericidal effect on intact skin. *Antimicrobial agents and chemotherapy* **18**, 137-141 (1980).

13 **Del Pozo, J. L., Rouse, M. S., Mandrekar, J. N., Steckelberg, J. M. & Patel, R**. The electricidal effect: reduction of *Staphylococcus* and *Pseudomonas* biofilms by prolonged exposure to low-intensity electrical current. *Antimicrobial agents and chemotherapy* **53**, 41-45 (2009).

14 **Giladi, M. *et al***. Microbial growth inhibition by alternating electric fields in mice with *Pseudomonas aeruginosa* lung infection. *Antimicrobial agents and chemotherapy* **54**, 3212-3218 (2010).

15 **Spadaro, J., Berger, T., Barranco, S., Chapin, S. & Becker, R**. Antibacterial effects of silver electrodes with weak direct current. *Antimicrobial agents and chemotherapy* **6**, 637-642 (1974).

16 **Costerton, J. W., Ellis, B., Lam, K., Johnson, F. & Khoury, A. E**. Mechanism of electrical enhancement of efficacy of antibiotics in killing biofilm bacteria. *Antimicrobial agents and chemotherapy* **38**, 2803-2809 (1994).

17 **Lewinson, O., Lee, A. T. & Rees, D. C**. A P-type ATPase importer that discriminates between essential and toxic transition metals. *Proceedings of the National Academy of Sciences* **106**, 4677-4682 (2009).

18 **Del Pozo, J. L., Rouse, M. S., Mandrekar, J. N., Sampedro, M. F., Steckelberg, J. M. & Patel, R.** Effect of electrical current on the activities of antimicrobial agents against *Pseudomonas aeruginosa, Staphylococcus aureus, and Staphylococcus epidermidis* biofilms. *Antimicrobial agents and chemotherapy* **53**, 35-40 (2009).

19 **Jass, J., Costerton, J. & Lappin-Scott, H.** The effect of electrical currents and tobramycin on *Pseudomonas aeruginosa* biofilms. *Journal of Industrial Microbiology & Biotechnology* **15**, 234-242 (1995).

20 **Van Der Borden, A. J., Van Der Werf, H., Van Der Mei, H. C. & Busscher, H. J**. Electric current-induced detachment of *Staphylococcus epidermidis* biofilms from surgical stainless steel. *Applied and Environmental Microbiology* **70**, 6871 (2004).

21 **Van der Borden, A., Van der Mei, H. & Busscher, H.** Electric block current induced detachment from surgical stainless steel and decreased viability of *Staphylococcus epidermidis*. *Biomaterials* **26**, 6731-6735 (2005).

22 **Van der Borden, A., Van der Mei, H. & Busscher, H.** Electric current induced detachment of *Staphylococcus epidermidis* strains from surgical stainless steel. *Journal of Biomedical Materials Research Part B: Applied Biomaterials* **68**, 160-164 (2004).

23 **Ren, D., Zhang, M., Niepa, T. & Gilbert, J**. (Google Patents, 2010).

CHAPTER 2

LITTERATURE REVIEW ON

ELECTROCHEMICAL TREATMENT OF BACTERIA

2.1. UNMET CHALLENGES IN CONTROLLING BACTERIAL INFECTIONS

2.1.1. Implant-associated infections

The preponderance of antibiotic-resistant microorganisms in public and medical environments constitutes a serious concern to health-care. The ability of certain microorganisms to persist on dry surfaces from days to weeks, and in some extreme cases, even months, increases the risk of cross-contaminations and disease outbreaks [1]. For instance, it is reported that *Enterococcus faecium* could reside on inanimate surfaces for up to 4 months [2], *Staphylococcus aureus* for up to 7 months [2], *Klebsiella pneumoniae* up to 30 months [3,4], *Acinetobacter baumanii* up to 5 months [5-7], *Pseudomonas aeruginosa* up to 60 months [3,6,8], and *Enterobacter* species for 5 to 49 days [6]. These six pathogens constitute the so-called ESKAPE pathogens, and are known for escaping from the treatment of commonly used antibiotics. By persisting on surfaces for such long period of time, these microorganisms could compromise the safety of many medical procedures, especially the implantation of medical devices.

Each year, millions of individuals receive medical implants to substitute failing body components. Such procedures, however, can lead to major complications due to the adherence of antibiotic-resistant microorganisms. Indeed, infection associated with indwelling medical devices accounts for half of the cases of hospital-acquired infections[9]. The mechanism of cell adhesion to indwelling medical devices relies on multiple physicochemical factors, by which bacteria overcome a series of repulsive forces (e.g. Van der Waals forces), and hydrophobic interactions to initiate attachment and stable adherence to the substrate[10,11]. Some electrochemical interactions between metal-based

surfaces and the host cells are viewed as one of the most common source of bacterial infection. Once a medical device is implanted in a host, the surface is immediately surrounded by blood plasma. Because of physical properties of the implanted devices such as wettability (or hydrophilicity), surface roughness, and the surface charge, the implants are rapidly coated with body fluid involving platelets and glycoproteins such as fibrin and fibronectin[12]. Fibronectins commonly possess specific sets of receptors that mammalian cells bind during normal wound healing [13]. However, these receptors are also used by bacteria to attach to tissues and indwelling devices covered with the host proteins. The role of fibronectin in promoting *S. aureus* contamination has been confirmed in vivo [14]. *S. aureus* expresses fibronectin-binding proteins FnBPA and FnBPB, which promote such adherence of this bacterium to the terminal domain of the 5 type I module of the fibronectin [15].

The attachment of bacteria to indwelling medical devices lead to the formation of a slimy bacterial macrostructure, known as biofilm, with the bacterial cells embedded in a self-produced polysaccharide matrix. The diffusion barrier presented by this matrix and the slow growth of the biofilm cells collectively render the biofilm cells up to 1000 times more tolerant to antibiotics than their planktonic counterparts. The challenges represented by biofilm infections associated with implanted medical devices can be even bigger due to the physicochemical properties of the devices. In the case of metal-based devices, wear and reduction of the oxide layer covering metals generates free metabolites and ions, which contribute to the proliferation of the cells and the biofilms[11,16]. As a consequence, a

chronic infection can develop, which could lead to other complications such as device failure, prolonged hospitalization, sepsis, and even patient death[17].

2.1.2. Bacterial antibiotic-resistance

Antibiotic-resistant infections can cause prolonged hospitalization and require higher doses of antimicrobials to treat, if work at all. Recently, the combination of multiple antibiotics has become the most preferred approach to control these infections. However, finding the right combination can be challenging since many species are resistant to more than one antibiotic. *P. aeruginosa,* for instance, was found to resist to many antibiotic including fluoroquinolones, β-lactams and aminoglycosides[18].

Bacteria can resist drugs through acquired mechanisms such as reduced permeability of outer membrane due to mutation, degrading the drug molecules through enzymatic processes and modifying the intracellular targets of the antibiotic. For example, the process of inactivation of aminoglycosides can occur by acetylation, phosphorylation or adenylation at critical sites of this molecule [19].

In addition to resistance based on mutations and activities against specific antibiotics, bacteria can also obtain resistance through intrinsic mechanisms such as the, extrusion of antibiotics by drug efflux pumps and by forming biofilms[20]. The transmembrane efflux pumps play an important role in drug resistance. Nikaido and colleagues showed that CmLA is a transporter that can pump chloramphenicol out of *P.*

aeruginosa. According to this model, an amphililic antimicrobial may cross the bilayer membrane but will be driven out of the cell by the efflux transporter.

2.1.3. Bacterial Biofilms

Biofilms are sessile communities of microorganisms organized in a self-created extracellular matrix, which separates the cells from their immediate environment and provides the cells with protection against external physicochemical stresses. Due to the ubiquitous presence of biofilms in nature, the first time a biofilm was observed can be dated back to the invention of the microscope. However, the concept of biofilm was not introduced until William Costerton published his seminar paper describing bacterial biofilm as a well-organized community of microorganisms. Since then, many studies have been published attempting to elucidate the mechanisms of biofilm formation and their significance[21]. Previous studies have well-characterized the structural organization[22,23] of biofilms and their implications to the medical field[24].

In 2008, Monds *et al*.[25] proposed a model of microbial biofilm formation comprising five steps including reversible and irreversible attachments of the cells, microcolonies formation, maturation (formation of the 3D structure) and finally dispersion which allows the biofilm cells to return planktonic state. The initial attachment of bacterial cells to a surface is reversible and involves motility [26]. Gram-negative bacteria, such as *Pseudomonas aeruginosa*, motility functions via flagella and pili allow the cells to sense the local environment[27] and initiate irreversible adhesion leading to

secretion of polymeric substance. Caiazza *et al*.[28] reported that the cytoplasmic protein SadB contributes to the irreversible attachment and the development of microcolonies.

The production of the EPS matrix is a dynamic process involving communication with the host environment and among bacterial cells through quorum-sensing[29-31]. The molecular mechanism behind the EPS product is not fully understood; however, it is well known that the structure of the EPS is dependent on carbon source availability[32]. In fact, polysaccharides, glycolipids, amino acids, proteins and even extracellular DNAs (e-DNAs) have all be found as key components of the EPS matrix of certain species[33]. It is important to know that EPS is not s solid material but have pores and channels for nutrients and waste removal[34]. Collectively, the EPS matrix constitutes a diffusion barrier for both antimicrobials and nutrients. Therefore, a concentration gradient exists for added compounds, resulting in the starvation of the cells located in the most inner part of the biofilm, and associated drug tolerance.

Although the functions of EPS components are not fully understood, it is clear that the EPS matrix provides important protection to bacterial cells from hydrostatic and chemical challenges. Dispersion of bacterial cells occurs when the EPS matrix is disrupted using surfactants such as Triton-X 100[35]. In dental and hydraulic environments, high shear stress is required to remove biofilm plaques. Dispersion caused by these types of applications is known as passive dispersion[36]. In contrast, an active dispersion is a coordinated event where biofilm-embedded bacterial cells initiate detachment to become free-swimming cells. It is believed that active detachment is a survival strategy for

biofilm cells to live in low-nutrient conditions and plays an important role in spreading infections[37]. The return to a planktonic state is highly dependent on the intra and extra-biofilm signaling and requires the activities of EPS degrading enzymes. The generation of reactive oxygen intermediates (e.g. hydrogen peroxide) or reactive nitrogen intermediate (e.g. nitric oxide) from the host environment can result in cell lysis and therefore induce the expression of matrix degrading enzymes as stress response [38].

As discussed above, bacterial drug resistance is based on multiple mechanisms. For planktonic cells, the mutation of drug targets, the activities of the efflux pumps, the modification or degradation of drug molecules by secreted enzymes all contribute to multidrug resistance. In contrast, the biofilm cells exhibit common resistance to essentially all antibiotics up to one thousand times higher than the cells in their planktonic state. An important factor of biofilm associated drug resistance resides in the structure of exopolysaccharide matrix protecting the cells. As discussed previously, the EPS matrix regulates the nutrient transport and assists the biofilm development. One of the main features of the biofilm is the oxygen and nutrient concentration gradients between the outside and inside of the biofilm. During antibiotic treatment the concentration gradient allows the inner cells to survive better due to the low drug concentration and low metabolic activities (antibiotics are more effective against metabolically active cells)[39]. Meanwhile, the death and lysis of the other larger cells add e-DNA to the biofilm. Lawenza has demonstrated that e-DNA provokes a cation limitation within the biofilm which modified the LPS structure. As a consequence, the LPS modification lowers the permeability of the bacterial outer membrane and induces

drug resistance. For example, addition of e-DNA at a sub-inhibitory concentration results in a 2560-fold increase in cationic peptide resistance and 640-fold increase in aminoglycoside resistance[40]. Hence, the production of the EPS matrix does not only provide the biofilm cells a physical barrier, but also influence the physiology of the biofilm cells and the interaction between drug molecules and bacteria.

2.1.4. Bacterial persistence

In addition to the above mechanism, recent research has shown that a subpopulation of metabolically inactive cells, known as persister cells are also highly tolerant to antibiotics. The first indication of persister cells was reported in 1944 by Joseph Bigger, who noticed a failure of penicillin to sterilize *S. aureus* infections[41]. However, with the emergence of the antibiotic-resistant strain, its persister cells were largely overlooked for decades. About 40 years after Bigger's intriguing finding, Harris Moyed conducted a study to understand (at the genetic level) the phenotypic variance between successive generations of *E. coli* persisters isolated with ampicillin (Amp). It was discovered that the high persistence gene (*hipA)* increased the frequency of persister cells; however, its deletion did not prevent Hip mutants from forming persisters[42]. Kim Lewis and colleagues conducted similar experiments and discovered that a small subpopulation of *E. coli*, *P. aeruginosa*, and *S. aureus* could survive high drug concentrations and maintain a constant cell density after treatment with increasing concentrations of ampicillin (Amp), ofloxacin (Ofx), and ciprofloxacin (Cip) & penicillin. When this surviving population was cultured again without antibiotics, it harbored a similar subpopulation, which could tolerate the antibiotics to the same extent[43]. This

finding proves that the persister cells are phenotypic variants with increased tolerance to antibiotics.

Since then, studies have been conducted to better understand bacterial persistence, and understand its relevance to multidrug-resistance[44,45]. Later, it was found that the persister cells also exist in biofilms[46] and play a role in chronic biofilms infections[47]. Now, it is well established that the presence of the persister cells renders biofilms more difficult to eradicate. In the absence of antibiotics, the persister cells have the ability to wake up and regenerate new cell populations within the biofilms[48]. The clinical relevance of persister cells becomes more clear with the isolation of *P. aeruginosa* strain having high persistence frequency from cystic fibrosis patients[49].

Many studies have been conducted to understand the mechanism of persister formation and develop strategies to control bacterial persistence. Genetic studies have revealed that persister genes are redundant. In addition to *hipA*, genes such as *GlpD* (encoding *sn*-glycerol-3-phosphate dehydrogenase), *plsB* (encoding *sn*-glycerol-3-phosphate acyltransferase), respectively, *phoU*, and *hfg* (encoding for regulators), and *hha* and *cspD* (encoding for toxins) have all been reported to control persister formation in *E. coli* [50-52]. Other studies on the effects of physicochemical factors have shown that antibiotics[53], signaling molecules[54-56], and oxidative stress[57] could induce persister formation. The strategies to control persister cells reported to date include those using peptides[58], quorum sensing inhibitor molecules[59-61], metal elements[62,63], and direct

current[64] (part of this research). The physicochemical factors can either kill the persisters alone, or sensitize them to antimicrobials.

2.2. ELECTROCHEMICAL TREATMENTS OF BACTERIAL CELLS

2.2.1. Effects of electric currents on bacterial cells

2.2.1.1. Alternating currents

The study of the effects of electric currents on bacteria is not new. Treatment of bacterial cells with alternating currents (AC) was reported in 1915 by Beattie *et al.*[65], and in 1919 Anderson *et al.*[66]. In 1925, Beattie and Lewis reported the bactericidal effects of 2 A (ampere) AC corresponding to a field comprised between 3000-4000 V, which was then used for sterilization of milk[67]. Over the years, more studies were performed to explain the mechanism of the bactericidal effects of electric current. Hence, in 1962, Brandt *et al*. proposed that the bactericidal effects of the electric discharges were due to the generation of oxidizing species and free radical[68].

Three years later, Barnett Rosenberg discovered that treatment with alternating current at 2 A (corresponding to $50x10^5$ c/s) generated using platinum electrodes resulted in 300 times elongation *of E. coli* K12 cells[69]. However, the bacteriostatic effects observed were not linked to reactive oxygen radicals, as they were not found into the solution. Instead, the oxidation of the platinum electrodes lead to the formation of Pt-based species which interfere with the genetic material of the cells, preventing them to complete cells division[70]. This finding led to the development of the exciting field of metallodrug complexes, which has found applications in cancer chemotherapy[71].

The lethal effects of low-level AC on bacteria were also investigated. For instance, Pareilleux *et al*.[72] demonstrated that low-level AC ranging from 10 to 200 mA using platinum or stainless steel (SS) electrodes affected the viability of *E. coli*. While 20 mA AC did not have any effects of the cell viability, the cells were killed by 4 logs and 7 logs, with the treatments using 60 mA and 120 mA AC, respectively. However, Rower *et al*.[73] reported different results during the testing of *E. coli* cells with Platinum wire. It appeared that the 15-30 mA AC level generated using platinum did not have any effect on cell viability.

2.2.1.2. Direct currents (DC)

The effects of DC on the viability of bacterial cells were first tested in the early 70's. Treatment of *E. coli* with total DC comprised between 1 and 140 using platinum electrodes were described for their bactericidal effects by Rowley *et al*.[73]. However, different effects were reported when the study was performed in vivo. The treatment of wounds infected with *P. aeruginosa* using copper-mediated DC ranging from 200-1000 μA for 72 h exhibited bacteriostatic effects[74].

The effects of the electrodes material have been investigated by Baranco *et al*.[75], who determined that antimicrobial activity of the lower level DCs in the range of 40 to 400 μA (mediated using SS, platinum, gold or silver electrodes) on the viability of *S. aureus*, and observed variable levels of killing.

Later, the activity of silver ions in the presence of low-level DC ranging between 5-40 μA were tested on oral bacteria by Thibodeau *et al.*[76] and demonstrated that supplementation of silver ions to DC treatment had dose-dependent killing effects on oral bacteria, resulting in 2 to 6 logs of killing in the range of DC tested compared to the untreated control. This study demonstrated that silver ions could maintain its antimicrobial activities even in the presence of reduced current. This study brought more attention to the antimicrobial activities of silver ions, which were then used to test on Gram-positive and Gram-negative microorganisms such as *S. aureus*, *P. aeruginosa*[77-79]. The studies of bacterial control with electrical currents are summarized in Table 2.1.

2.2.2. Effects of electrochemical factors on bacterial cells

In most of the previous studies, high field strength discharges were performed in short time pulses to determine the effect on cells viability. Gilliand *et al*. [91] investigated the effects of multiple cycles of 10 kV electrical discharges generated using copper electrodes on bacterial cells including *E. coli*, *Streptococcus faecalis*, vegetative cells and spores of *Bacillus subtilis*. The result of that study demonstrated cells lysis occurred and the effects were attributed to the generation of cupric ions, which increase the toxicity level of the treating solution, and result in cell killing. However, the cells responded differently to the treatments based on their size. For instance, bacteriophages were more readily killed by the treatment than bacterial cells. Similar studies were performed by Hulsheger *et al*.[92,93] and demonstrated that Gram-negative bacteria were more resistance to the electric shock generated by strong electric fields.

Table 2.1: Effects of electric currents (AC and DCs) on bacterial cells

Current/Voltage Level	DC	electrodes material	*Bacterial Species*	Findings	Ref
2 A	AC	Platinum wire	*E coli*	Bacteriostatic effects	Rosenberg *et al*.[69]
1 mA, 14 mA, and 140 mA	DC	Platinum wire	*E coli*	bactericidal effects	Rowley *et al*.[73]
1 mA	DC	Copper mesh in gauze	*P aeruginosa*	bactericidal effects	Rowley *et al*.[74]
DC; 40 and 400 μA	DC	Silver, platinum, gold, stainless steel	*S aureus*	bactericidal effects	Baranco *et al* [75]
5 μA	DC	Silver	*Oral bacteria*	bactericidal effects	Thibodeau *et al*[76]
100 μA	DC	Silver wire	*S. aureus, P. aeruginosa*	bactericidal effects	Ong *et al* [77]
26 μA - 800 μA	DC	Silver wire and silver nylon	*Gram-positive, Gram-negative*	bactericidal effects	Laatsch *et al*.[79]
0.7-1.8 mA/cm^2	DC	CDC biofilm reactors	*S. epidermidis, Gram negative*	bactericidal effects	Sandvik *et al*.[80]
3.1 mA/cm^2	DC	Platinum wire	*Klebsiella pneumoniae, P fluorescens, P aeruginosa*	reduction of cathodic biofilms	Stoodley *et al*.[81]
−800 to +800 μA	DC		*Streptococcus oralis J22*	Reversible attachment	Poortinga *et al*.[82,83]
65uA	DC	Indium tin oxide	*Streptococcus oralis J22, Staphylococcus epidermidis 3399, and A. naeslundii 147, A. naeslundii T14V-J1*	Detachment	Van Der Borden *et al*.[84,85]
60 μA and 100 μA	DC	Stainless-steel	*S epidermidis*	Detachment	Van Der Borden *et al*.[86]
3.7 μA/mm^2	DC	Stainless-steel	Mixed-Species	loss of bioelectric effects	Shirtliff *et al*.[87]
20-2000 μA	DC	Stainless steel or graphite cylinders	*Pseudomonas aeruginosa, Staphylococcus aureus, and Staphylococcus epidermidis*	bactericidal effect	Del pozo *et al*.[88]
200 μA	DC	stainless steel	*Staphylococcus epidermidis*	Electricidal effect in rabbit model of osteomyelitis	Del Pozo *et al*.[89]
180A/m^2	DC	Agarose	*E coli*	augmentation of biomass	Chang *et al*.[90]

Further analyses were conducted by Gilliand *et al*. [94] to evaluate the effects of 10 kV electrical discharges generated using aluminum electrodes. Under these conditions, it was discovered that some metabolic activities of the cells, as well as their membrane properties were altered by the treatment. However, it was believed that cell death was induced by the heat, mechanical shock engendered by the flows of ions and reactive oxygen species surrounding the cells. According to Zimmermann *et al*.[95,96], the ions flow of ions generated by the high electric field could disrupt of the cell membrane. These results corroborate with other findings, confirming that the lethal activities of electric fields are through the direct effects on cell properties and indirect effects associated with heat, ion flow or generated reactive species[97-99].

Recently, the effects of low electric field on bacterial growth have caused attention in the field of orthopedic and dental implants. The interaction between body fluid and alloys used for these implants generate an electrical potential, a phenomenon known as galvanism. On dental implants this potential could be as high as 900 mV. Some studies have been conducted to explore the effects such electric potential on oral bacterial cells. In a recent study, Zituni *et al*.[100] demonstrated that *S. aureus* was found more sensitive to the low level fields compared to *E. coli*, suggesting that oral galvanism could potentially affect oral ecosystem. The studies of bacterial control with electric fields are summarized in Table 2.2.

Table 2.2: Electric field effects on bacterial cells

Current/Voltage Level	DC	electrodes material	*Bacterial Species*	Findings	Ref
			effects of electric field (ACs)		
20 kV 0.1-50Hz	PEF	pulse generator equipped cell	*E coli K12*	Antimicrobial effects	Hulsheger *et al.*[93]
20 kV 0.1-50Hz	PEF	pulse generator equipped cell	*P. aeruginosa, S. aureus, E. coli, E. coli K12, Klebsiella pneumoniae, Listeria monocytogens I, Listeris monocytogens II, Candida albicans*	Antimicrobial effects	Hulsheger *et al.*[92]
1-4V	HVPC	Silver nylon cloth	*P aeruginosa, S. aureus, and Candida albicans*	Antimicrobial effects	Marino *et al.*[101]
150-300V	HVPC	Stainless-steel	*P aeruginosa, S. aureus, and E. coli*	Antimicrobial effects (Cathode)	Kincaid *et al.*[102]
500V	HVPC	Stainless-steel	*P aeruginosa, S. aureus, and E. coli, Klebsiella*	Antimicrobial effects	Szuminsky *et al.*[103]
10V/m	HVPC	Gold electrode	*P aeruginosa, S. aureus, and E. coli*	Anodic field inhibition	Zituni *et al.*[100]
0.1-50Hz	PEF		*P aeruginosa*	antibiotic susceptibility increases	Ali *et al.*[104]
10 MHz	LIEF	insulated electrode	*P aeruginosa*	inhibition in a lung model of infections	Giliadi *et al.*[105]
15-30V	HSEF	titanium	*Staphylococcus aureus*	decrease of biofilms on anodized nanotubular	Ercan *et al.*[106]
0.5 to 5 V	HSEF	Interdigitated electrodes	*P aeruginosa*	biofilm inhibition	Perez-Roa *et al.*[107]
1.5V	HSEF	stainless steel	*Pseudomonas aeruginosa*	Biofilm removal	Dargahi *et al.*[108]

LIEF: Low intensity electric field
PEF: Pulse Electric Field
HVPC: High Voltage Pulse Current
HSEF: High strength electric field

2.2.3. Medical implication of the electrochemical currents

Although AC has been found to sterilize milk using ampere-level AC generated with the high electric field, and cause the filamentous structure of *E. coli* due to bacteriostatic effects of, the attempt to apply electric currents to cure infection was not taken until 1974. Rowley *et al.*[74] performed the first in vivo study of DC treatment and

demonstrated that the co-treatment of *P. aeruginosa* infected wounds with 200-1000 μA total DC using copper mesh electrode and aerosporim-polymyxin B sulfate resulted in synergistic killing effects, a phenomenon. In 1992, Khoury and Costerton [109] discovered a phenomenon, names as bioelectric effects, in which synergistic killing of biofilm cells was obtained using 15 $\mu A/cm^2$ DC or 1.5 V/cm^2 and antibiotics including Tob. Costerton *et al*.[110] further investigated the mechanism of the bioelectric effects, which led to a renewed interest in the field of DC treatment of bacterial infection.

Since the published report of Costerton[109,110], a number of studies have been published to describe the effect of DC or AC in killing medical relevant planktonic and biofilm cells. In 1995, Jass and Costerton[111] demonstrated the effect of 1mA DC and Tob on killing *P. aeruginosa* biofilm cells in an electrical colonization cell[111]. In a similar setting, it was found that the activity of ciprofloxacin (Cip) polymyxin B was enhanced by 2 logs in a 12 h treatment and 3 logs in a 24 h treatment with 20 mA/cm^2 DC[112]. More bacterial species including *Klebsiella pneumonia, Pseudomonas fluorescens, P. aeruginosa* were tested with DC. For instance, Wellman *et al*. [113] used a mixed biofilm culture system composed of *K. pneumonia* and *P. aeruginosa* to demonstrate dose dependent bioelectric effects with increasing level of DC. To understand the effects of DC on the morphology of the biofilms, Stoodley *et al*. tested the bioelectric effects on the biofilms of multiple species including *Klebsiella pneumoniae*, *P. fluorescens*, *P. aeruginosa*, *Streptococcus oralis J22*, on platinum wire electrode and found that the viability of cathodic biofilm cells was reduced by 74%, while the biofilm on the anode increased in size after 3 days of treatment[81].

Table 2.3: Synergistic killing effects between electric currents and antibiotics

Current/Voltage Level		electrode materials	Antibiotics	Bacterial Species	Findings	Ref
			effect of direct current			
1 mA	DC	Copper mesh in gauze	Polymyxin B	*P aeruginosa*	synergy	Rowley *et al.*[74]
9-20 mA/cm^2	DC	Electrical colonization cell (ECC)	Tobramycin	*P aeruginosa*	synergy	Jass *et al.* [111]
9 mA/cm^2	DC	Electrical colonization cell (ECC)	Ciprofloxacin polymyxin B	*P aeruginosa*	synergy	Jass *et al.*[112]
1 mA	DC	Platinum wire	Tobramycin	Mixed- Species	synergy	Wellman *et al.*[113]
2 mA	DC	Stainless steel wire	Tobramycin	*Pseudomonas aeruginosa*	synergy	Stewart *et al.*[114]
20-2000 μA	DC	Stainless steel or graphite cylinders	Cefepime, Ciprofloxacin, Tobramycin, Daptomycin, Erythromycin, Linezolid, Minocycline, Moxifloxacin, Rifampin, Trimethoprim-sulfamethoxazole, Vancomycin	*Pseudomonas aeruginosa, Klebsiella pneumoniae, Staphylococcus epidermidis, Escherichia coli, and Streptococcus gordonii.*	synergy	Del Pozo *et al.*[115]
4V/cm, 100 kHz and 50 MHz	AC	Conductive electrodes	Chloramphenicol	*S aureus, P. aeruginosa*	synergy	Giliadi *et al.*[116]
<100 μA/cm^2	DC	stainless steel	Tobramycin	*P aeruginosa*	Synergy	Costerton *et al.*[110]
- 2.1 mA/cm^2 with +/- 12 V/cm	DC	Stainless steel	kathon, glutaraldehyde, and quaternary ammonium compound	*Pseudomonas aeruginosa*	Synergy	Blenkinsopp *et al.*[117]
6 mA/cm^2 current density, 5-20 MHz	RFC	stainless steel	gentamicin and with oxytetracycline	*P aeruginosa*	Synergy	Caubet *et al.*[118]

RFC: Radio frequency current

Overtime, more complex electrochemical system was constructed to study to understand of role of ROS in DC treatment. Stewart *et al.*[114] tested DC using carbon or SS electrodes were generated across an electrochemical chamber containing *P. aeruginosa* in the presence or absence antibiotic. The synergy between Tob and DC was studied under various pHs to control the concentration of dissolved oxygen. It was

concluded that the ROS contributes to the enhanced killing of the *P. aeruginosa* cells. The species electrolytes and their roles in the efficacy of the DC treatment were studied by Shirtliff *et al.*[87]. It was found that the chloride ions in the electrolyte are important to achieve synergistic killing effects in killing bacteria with DC and antibiotics.

The effects of electrochemical factors on bacteria have also been evaluated in vivo. Busscher *et al.*[82,84-86] first reported that bacterial adhesion on metal surfaces could be controlled by weak electric field or currents (either positively or negatively depending on the direction of current between -800 to 800 μA)[82,83]. This technology was translated in two in vivo studies, in which adhesion of *Staphylococcus epidermidis* to stainless steel-based implant was prevented[86] and biofilms were removed by applying the current before the treatment[85]. The studies of bacterial control with electrochemical factors are summarized in Table 2.3.

Overall, these study shows that the electrochemical factors including DC, AC, electric field and generated species could be used to effectively control bacterial cells. However, there is still a little known of the mechanism of these effects. Instead, the phenomena described the bactericidal activity of electrochemical treatments of various species. However, the genetic or cellular understanding of electrochemical control of bacterial cells could lead to the development of more effective design, which could improve antibiotic activity, and reveal new target for bacterial control through antimicrobial. Moreover, it is unknown if these technologies could remediate the challenge associated with the presence of the persister cells. Thus, this study aims to

contribute to the field of electrochemical treatment of bacteria by revealing the mechanisms of killing of drug resistant persister cells using DC.

2.3 TECHNIQUES APPLIED IN THE STUDY

2.3.1 Electrochemical measurements

Electrochemical treatment of bacterial cells: This study aims to understand the response of PAO1, a model bacterial strain to low-level direct currents (DCs). Thus, the electrochemical treatments are performed in the chronopotentiometric or galvanostatic mode. An electrochemical cell can be constructed in a 3-electrodes configuration. Stainless steel (SS) 304, carbon, or TGON (a graphite-based material) were used as working and counter electrodes, together with an Ag/AgCl saturated reference electrode in this study. Three electrochemical systems were designed for this study: (1) a 1-chamber system that hosts all the electrodes in a single cuvette (See Chapter 3 and 4); (2) a 2-chamber system consisted of 2 chambers (hosting the counter and the working electrode separately) connected with a salt bridge (See Chapter 4). (3) A flow cell system, which contains all the three electrodes and allows imaging of the experiment (Chapter 8). Using a potentiostat, a constant low-level DC is applied and the number of viable cells is quantified. In addition, anodic or cathodic electrode potential (E_{pa} or E_{pc}) as well as the electric field (E) are recorded to differentiate the effects of the electrochemical factors (DC, electric field, potential, redox reactions) on the viability of the persisters.

Electrode polarization: To study the electrochemical properties of an electrode, a polarization curve need to be recorded. A polarization curve provides critical information

about the rate of charge exchanges between the electrodes and electrolytes, which could be obtained by performing a scan on a range of potential while recording the current density. The corrosion potential (E_{corr}) or open-circuit potential (OCP) is the equilibrium potential, at which the cathodic and the anodic currents are equal. The current at OCP is usually referred to as i_{corr}. The OCP potential is important for determining if the electrode behaves as an anode or a cathode. During an active corrosion, the overpotential (the difference between the electrode potential and the OCP) increases as a function of current density; whereas the current density does not change during passivation of the electrode in spite of overpotential. Polarization curves have been a very useful tool for determining the electrochemical species released at different time points of an electrochemical treatment [24]. This method is used in this study to compare the electrochemistry of different electrode materials.

Cyclic Voltammetry (CV). CV was performed to investigate the electrochemical properties of the Tobramycin (Tob), the primary antibiotic supplemented to the DC treatment in this study, to understand synergistic interaction between metal ions and antibiotics in persister control. In principle, a CV plot displays electric potential associated with the redox reactions of a compound. In this method, a series of voltages is applied in a forward or reverse order to an inert electrode (e.g. gold, platinum

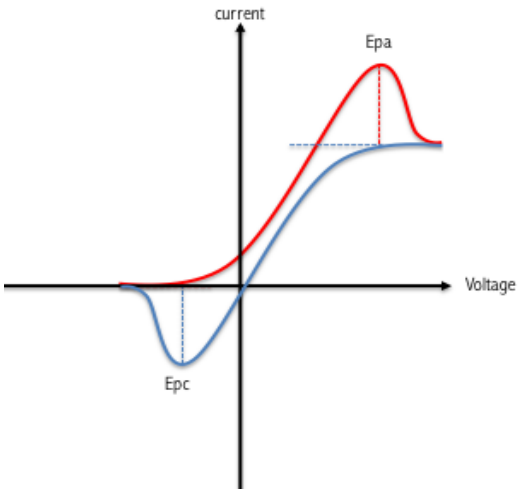

Figure 2.1: Cyclic voltammogram.

or glassy carbon) at a specific scan rate to evaluate the rate of electron exchange between the material and the solution of interest. The forward scan of the working electrode leads to the oxidation of the reactants until complete depletion, which is represented by the red peak in Fig. 2.1. Then, the oxidation current drops due to diffusion limitation of the reactants. When a reducing potential is applied (reverse scan), electrons are supplemented to the reactants until the amount of reactants available at the electrode deplete. The rate of charge exchange is proportional to the recorded current, and is used to generate a cyclic voltammogram (Fig. 2.1). Thus, the reversibility of a reaction could be determined based on the value of peaks at cathodic or anodic electrode potentials (Epc or Epa). If the redox reaction is reversible, the peak of E_{pc} is equal to that of E_{pa}. In this study, this method was are used to determine the stability of metal drug complexes formed during the electrochemical treatment of PAO1 cells in the presence of Cr ions and Tob.

Zeta potential: Measurement of the surface charge of colloidal systems is a very useful tool for predicting the effect of ionic strength on particle (e.g. coagulation of flocculation)[25]. Zeta potential or ζ-potential characterizes the electrokenetic potential of a charged particle in a colloidal suspension or the electrostatic potential between the particle and the charge molecules in the vicinity of particle. Once a charged particle is suspended in an aqueous solution, ionic bonds are formed between the particle and molecules with countercharges, referred to as the stern layer (Fig. 2.2). Additional molecules from charges opposite to that of the particle could interact with the stern layer to counterbalance the overall charge of the particle and form a so-called diffused layer. The diffuse layer is separated from the rest of the solution by a slipping plane. The

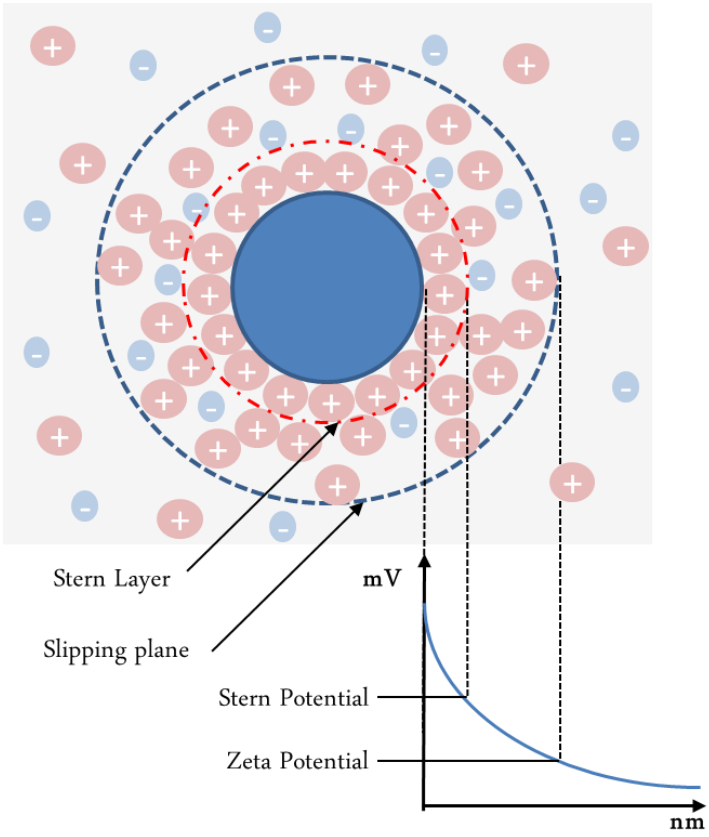

Figure 2.2: Illustration of the zeta potenital of a negatively charged particle in an aqueous solution (Updated from Larryisgood)

potential of the double-layer contributes to the ζ-potential and is proportional to both the surface potential of the particle and the ionic strength of the solution. The electrophoretic mobility (μ) of the particle across a well-defined electric field (E) is used to determine the ζ-potential according to the following relationship[26]:

$$\zeta = \frac{\mu\,\eta}{\varepsilon_o\,\varepsilon_r}\ ,\quad \mu = \frac{\nu}{E}$$

in which ζ: Zeta-potential

μ: electrophoretic mobility

η: viscosity of the suspension

ε_o: permittivity of the free space

ε_r: permittivity of the suspension

ν: velocity of the particles

Bacteria commonly possess a charge surface due to their transmembrane lipoproteins. The surface charge of the cell contributes greatly to the cell homeostasis and to the ability of the cell to control influx and efflux of small molecules. Thus, cell depolarization could lead to disruption of the membrane functions and cell death[27,28]. In this study the ζ-potential was used to evaluate the surface charge of DC-treated PAO1 cells and control cells to investigate the effects of the DC treatments[29].

2.3.2 Spectroscopy Techniques

Inductively Coupled Plasma-Mass Spectroscopy (ICPMS): ICP-MS is a powerful technique that can quantitatively characterize the elements in a sample, including both metal and some non-metal species. In contrast to many other mass spectroscopy systems, ICP-MS relies on the ionic state of the analytes in a chamber filled with an electrically conductive gas (e.g. argon), referred to as plasma. The plasma is energized at a radiofrequency by means of an electric coil, which results in the desolvation, atomization, and ionization of the sample. Using a quadrupole mass spectrometer, the ions are then separated based on a mass-to-charge ratio[30]. This method was used in this study to determine the composition of the electrolyte generated during DC treatments. ICP-MS was also used to quantify the amount of metal ions interacting with the cells in the absence and presence of an antibiotic.

Nuclear Magnetic Resonance (NMR): NMR relies on the ability of atomic nuclei to absorb and emit electromagnetic radiation in the presence of a static magnetic field. The

quantum magnetic properties of the atomic nuclei are determined by the specific structure of a compound and could be attributed to particular chemical elements at a known resonance frequency. The state of the atomic nuclear energy generated at these resonance frequencies is collected to elaborate the NMR spectroscopy on the basis of population distribution. For the purpose of this study, NMR-HSQC (heteronuclear single-quantum coherence) was performed on solutions containing metal ions and antibiotics including tobramycin (Tob) and kanamycin (Kan). HSQC is a two dimensional heteronuclear experiment which characterizes the correlation between proton and carbon of the molecule of interest. It is a powerful tool to determine structural changes in chemical compounds under different conditions. In this study, HSQC-NMR was used to investigate the structural dynamics of Tob and Kan and evaluate the possibility of formation of antibiotic-metal ion complexes.

Ultraviolet (UV) - visible Spectroscopy: The UV-visible spectroscopy measures the light absorbance of compounds exposed to light wavelengths ranging from 200 to 800 nm. During a UV-visible scan, light is projected through a sample, which absorbs some of the UV or visible photons. An absorption spectrum for the scan is created by computing the ratio of the transmitted (detected) light over the total light projected. Because of the electromagnetic radiation generated by the photon is rich in energy, the absorbance results in additional energy being transmitted to the molecules (sample). These molecules originally possess an electronic potential energy, a vibrational potential energy, and a rotational potential energy [31]. Therefore, the radiation could generate enough energy to increase the electronic potential energy of the molecules and change the electronic the

configuration by moving the electrons from a lower energy level to a higher one, e.g. a non-bonding-antibonding (n-π*) or a bonding –anti-bonding (π-π*) transition. Hence, structural change in molecule could be identified by the change in band and intensity of the absorbance spectrum. For instance the transition metals absorb light at wavelength between 300 and 700 nm. Therefore, the change of the electronic configuration of a molecule after mixing with another compound could be determined by the broadening of the absorbance band and the change in the intensity of the band. In this study, UV-visible spectroscopy was used to evaluate the interactions between Cr^{3+} and Tob.

2.3.3 Imaging

Atomic Force Microscopy: Atomic force microscopy (AFM) is a type of surface imaging technique, which evaluates the topographic profile of a sample based on intermolecular interactions between the tip of a cantilever and the sample. During surface scan, a light is emitted on the cantilever and the deflection of the light is detected to generate the image of the scanned surface. AFM has been a very useful tool to study the viscoelastic properties of samples including bacterial cells. In our study, AFM was performed to determine the change in the stiffness of PAO1 cells before and after electrochemical treatments.

Electron Microscopy (EM): Electron microscopy is an imaging technique that uses electrons instead of light. Because electrons emit very lower wavelength in comparison to photon, EM has the advantage of showing very small features. To capture an EM image, a high voltage is generated between a negatively charged filament and a positively

charged anode to drive an electron beam from the filament. The beam is oriented toward the sample by a series of electrostatic and electromagnetic lenses. When an electron hits the sample, it is deflected as back-scattered electron (BSE), secondary electron or X-ray, which is captured by a detector to generate an image. In this study, two types of EM are used: The scanning electron microscopy (SEM) and transmission electron microscopy (TEM). To perform SEM, the sample is coated with a conductive material, such as gold or platinum. The interaction between the electron beam and the sample is recorded to generate the SEM images. In contrast to SEM, TEM samples are stained with contrast agents, which are made of heavy metals. The contrast agents that penetrate the cells are detected to generate the TEM images. TEM and SEM in this study were used to investigate the changes that occur to the PAO1 cells treated with DC.

Fluorescence Microscopy: Fluorescence microscopy is a widely used optical microscopy technique, in which a sample is stained with fluorescent dyes that can absorb and emit light at different wavelengths. In this study, fluorescence microscopy was used to evaluate change in the cell viability or to track the movement of bacteria under the DC treatments.

2.3.4 Genomics and Proteomics

Information about the expression profile of genes and proteins is invaluable for understanding the physiology of the cells. In this study, DNA microarray analysis was performed to obtain the transcriptional profiles of PAO1 cells with or without DC treatment. Gene profiling with DNA microarrays is a mature technology, which can

quantify the expression level of every genes in an organism. This method relies on hybridization of complementary DNAs (cDNAs) with the DNA probes on the microarray, allowing the identification and the quantification of the expressed genes [32].

Similar to DNA microarrays, techniques have been developed to obtain protein expression profile of an organism. One of such methods, 2D gel electrophoresis was used in this study to determine the difference in protein expression between cells treated with DC vs. untreated cells.

2.4. REFERENCES

1 **Kramer, A., Schwebke, I. & Kampf, G.** How long do nosocomial pathogens persist on inanimate surfaces? A systematic review. *BMC infectious diseases* **6**, 130 (2006).

2 **Neely, A. N. & Maley, M. P.** Survival of enterococci and staphylococci on hospital fabrics and plastic. *Journal of clinical microbiology* **38**, 724-726 (2000).

3 **Scott, E. & Bloomfield, S. F.** The survival and transfer of microbial contamination via cloths, hands and utensils. *Journal of Applied Bacteriology* **68**, 271-278 (1990).

4 **Mitscherlich, E. & Marth, E. H.** *Microbial survival in the environment. Bacteria and rickettsiae important in human and animal health*. (Springer-Verlag, 1984).

5 **Webster, C., Towner, K. J. & Humphreys, H.** Survival of Acinetobacter on three clinically related inanimate surfaces. *Infection Control and Hospital Epidemiology* **21**, 246-246 (2000).

6 **Neely, A. N. A** survey of gram-negative bacteria survival on hospital fabrics and plastics. *Journal of Burn Care & Research* **21**, 523&hyhen (2000).

7 **Wendt, C., Dietze, B., Dietz, E. & Rüden, H.** Survival of *Acinetobacter baumannii* on dry surfaces. *Journal of clinical microbiology* **35**, 1394-1397 (1997).

8 **Dickgiesser, N.** Untersuchungen über das Verhalten grampositiver und gramnegativer Bakterien in trockenem und feuchtem Milieu. *Zentbl. Bakteriol. Mikrobiol. Hyg. I Abt. Orig. B* **167**, 48-62 (1978).

9 **Darouiche, R. O.** Treatment of infections associated with surgical implants. *The New England journal of medicine* **350**, 1422-1429, doi:10.1056/NEJMra035415 (2004).

10 **Gristina, A. G., Hobgood, C. D., Webb, L. X. & Myrvik, Q. N.** Adhesive colonization of biomaterials and antibiotic resistance. *Biomaterials* **8**, 423-426 (1987).
11 **Gristina, A. G.** Biomaterial-centered infection: microbial adhesion versus tissue integration. *Science* **237**, 1588-1595 (1987).
12 **Savage, D. C. & Fletcher, M.** *Bacterial adhesion: mechanisms and physiological significance*. (Plenum Press, 1985).
13 **Ruoslahti, E.** Fibronectin and its receptors. *Annual review of biochemistry* **57**, 375-413 (1988).
14 **Fischer, B., Vaudaux, P., Magnin, M., El Mestikawy, Y., Vasey, H., Lew, D. P., Proctor, R. A.** Novel animal model for studying the molecular mechanisms of bacterial adhesion to bone‐implanted metallic devices: role of fibronectin in *Staphylococcus aureus* adhesion. *Journal of orthopaedic research* **14**, 914-920 (1996).
15 **Sottile, J., Schwarzbauer, J., Selegue, J. & Mosher, D.** Five type I modules of fibronectin form a functional unit that binds to fibroblasts and *Staphylococcus aureus*. *Journal of Biological Chemistry* **266**, 12840-12843 (1991).
16 **Comizzoli, R., Frankenthal, R., Milner, P. & Sinclair, J.** Corrosion of electronic materials and devices. *Science* **234**, 340-345 (1986).
17 **Adva, N., Alam, M., Ravindranath, T., Mubeen, A. & Saluja, B.** Corrosion in titanium dental implants: literature review. *Journal of Indian Prosthodontic Society* **5** (2005).
18 **Nordmann, P., Naas, T., Fortineau, N. & Poirel, L.** Superbugs in the coming new decade; multidrug resistance and prospects for treatment of *Staphylococcus aureus, Enterococcus spp.* and *Pseudomonas aeruginosa* in 2010. *Current opinion in microbiology* **10**, 436-440 (2007).
19 **Poole, K.** Aminoglycoside resistance in *Pseudomonas aeruginosa*. *Antimicrobial agents and chemotherapy* **49**, 479-487 (2005).
20 **Nikaido, H.** Prevention of drug access to bacterial targets: permeability barriers and active efflux. *Science* **264**, 382-388 (1994).
21 **Costerton, J. W., Cheng, K. J., Geesey, G. G., Ladd, T. I., Nickel, J. C., Dasgupta, M. & Marrie, T. J.** Bacterial biofilms in nature and disease. *Annual Reviews in Microbiology* **41**, 435-464 (1987).
22 **Stoodley, P., Sauer, K., Davies, D. & Costerton, J. W.** Biofilms as complex differentiated communities. *Annual Reviews in Microbiology* **56**, 187-209 (2002).
23 **Costerton, J. W., Lewandowski, Z., Caldwell, D. E., Korber, D. R. & Lappin-Scott, H. M.** Microbial biofilms. *Annual Reviews in Microbiology* **49**, 711-745 (1995).
24 **Hoyle, B. D. & Costerton, J. W.** in *Progress in Drug Research/Fortschritte der Arzneimittelforschung/Progrès des recherches pharmaceutiques* 91-105 (Springer, 1991).
25 **Monds, R. D. & O'Toole, G. A.** The developmental model of microbial biofilms: ten years of a paradigm up for review. *Trends in microbiology* **17**, 73-87 (2009).
26 **O'Toole, G., Kaplan, H. B. & Kolter, R.** Biofilm formation as microbial development. *Annual Reviews in Microbiology* **54**, 49-79 (2000).

27 **O'Toole, G. A. & Kolter, R.** Flagellar and twitching motility are necessary for *Pseudomonas aeruginosa* biofilm development. *Molecular microbiology* **30**, 295-304 (1998).
28 **Caiazza, N. C. & O'Toole, G. A.** SadB is required for the transition from reversible to irreversible attachment during biofilm formation by *Pseudomonas aeruginosa* PA14. *Journal of bacteriology* **186**, 4476-4485 (2004).
29 **Miller, M. B. & Bassler, B. L.** Quorum sensing in bacteria. *Annual Reviews in Microbiology* **55**, 165-199 (2001).
30 **Singh, P. K., Schaefer, A. L., Parsek, M. R., Moninger, T. O., Welsh, M. J. & Greenberg, E. P.** Quorum-sensing signals indicate that cystic fibrosis lungs are infected with bacterial biofilms. *Nature* **407**, 762-764 (2000).
31 **Waters, C. M. & Bassler, B. L.** Quorum sensing: cell-to-cell communication in bacteria. *Annu. Rev. Cell Dev. Biol.* **21**, 319-346 (2005).
32 **Sutherland, I. W.** Biofilm exopolysaccharides: a strong and sticky framework. *Microbiology* **147**, 3-9 (2001).
33 **Flemming, H.-C. & Wingender, J.** The biofilm matrix. *Nature Reviews Microbiology* **8**, 623-633 (2010).
34 **Flemming, H.-C., Neu, T. R. & Wozniak, D. J.** The EPS matrix: the "house of biofilm cells". *Journal of bacteriology* **189**, 7945-7947 (2007).
35 **Chen, X. & Stewart, P. S.** Biofilm removal caused by chemical treatments. *Water research* **34**, 4229-4233 (2000).
36 **Kaplan, J. á.** Biofilm dispersal: mechanisms, clinical implications, and potential therapeutic uses. *Journal of dental research* **89**, 205-218 (2010).
37 **Hall-Stoodley, L., Costerton, J. W. & Stoodley, P.** Bacterial biofilms: from the natural environment to infectious diseases. *Nature Reviews Microbiology* **2**, 95-108 (2004).
38 **Barraud, N., Hassett, D. J., Hwang, S. H., Rice, S. A., Kjelleberg, S., Webb, J. S.** Involvement of nitric oxide in biofilm dispersal of *Pseudomonas aeruginosa*. *Journal of bacteriology* **188**, 7344-7353 (2006).
39 **Ashby, M., Neale, J., Knott, S. & Critchley, I.** Effect of antibiotics on non-growing planktonic cells and biofilms of *Escherichia coli*. *Journal of Antimicrobial Chemotherapy* **33**, 443-452 (1994).
40 **Mulcahy, H., Charron-Mazenod, L. & Lewenza, S.** Extracellular DNA chelates cations and induces antibiotic resistance in *Pseudomonas aeruginosa* biofilms. *PLoS pathogens* **4**, e1000213 (2008).
41 **Bigger, J.** Treatment of staphylococcal infections with penicillin by intermittent sterilisation. *The Lancet* **244**, 497-500 (1944).
42 **Moyed, H. S. & Bertrand, K. P.** hipA, a newly recognized gene of *Escherichia coli* K-12 that affects frequency of persistence after inhibition of murein synthesis. *Journal of bacteriology* **155**, 768-775 (1983).
43 **Keren, I., Kaldalu, N., Spoering, A., Wang, Y. & Lewis, K.** Persister cells and tolerance to antimicrobials. *FEMS microbiology letters* **230**, 13-18 (2004).
44 **Kohanski, M. A., Dwyer, D. J. & Collins, J. J.** How antibiotics kill bacteria: from targets to networks. *Nature Reviews Microbiology* **8**, 423-435 (2010).
45 **Cohen, N. R., Lobritz, M. A. & Collins, J. J.** Microbial Persistence and the Road to Drug Resistance. *Cell host & microbe* **13**, 632-642 (2013).

46 **Lewis, K.** in *Bacterial biofilms* 107-131 (Springer, 2008).
47 **Lewis, K.** Multidrug tolerance of biofilms and persister cells. *Current topics in microbiology and immunology* **322**, 107-131 (2008).
48 **Fux, C., Costerton, J., Stewart, P. & Stoodley, P.** Survival strategies of infectious biofilms. *Trends in microbiology* **13**, 34-40 (2005).
49 **Mulcahy, L. R., Burns, J. L., Lory, S. & Lewis, K.** Emergence of *Pseudomonas aeruginosa* strains producing high levels of persister cells in patients with cystic fibrosis. *Journal of bacteriology* **192**, 6191-6199 (2010).
50 **Spoering, A. L., Vulić, M. & Lewis, K.** GlpD and PlsB participate in persister cell formation in *Escherichia coli*. *Journal of bacteriology* **188**, 5136-5144 (2006).
51 **Li, Y. & Zhang, Y.** PhoU is a persistence switch involved in persister formation and tolerance to multiple antibiotics and stresses in *Escherichia coli*. *Antimicrobial agents and chemotherapy* **51**, 2092-2099 (2007).
52 **Kim, Y. & Wood, T. K.** Toxins Hha and CspD and small RNA regulator Hfq are involved in persister cell formation through MqsR in *Escherichia coli*. *Biochemical and biophysical research communications* **391**, 209-213 (2010).
53 **Dörr, T., Vulić, M. & Lewis, K.** Ciprofloxacin causes persister formation by inducing the TisB toxin in *Escherichia coli*. *PLoS biology* **8**, e1000317 (2010).
54 **Vega, N. M., Allison, K. R., Khalil, A. S. & Collins, J. J.** Signaling-mediated bacterial persister formation. *Nature chemical biology* **8**, 431-433 (2012).
55 **Dörr, T., Lewis, K. & Vulić, M.** SOS response induces persistence to fluoroquinolones in *Escherichia coli*. *PLoS genetics* **5**, e1000760 (2009).
56 **Möker, N., Dean, C. R. & Tao, J.** *Pseudomonas aeruginosa* increases formation of multidrug-tolerant persister cells in response to quorum-sensing signaling molecules. *Journal of bacteriology* **192**, 1946-1955 (2010).
57 **Wu, Y., Vulić, M., Keren, I. & Lewis, K.** Role of oxidative stress in persister tolerance. *Antimicrobial agents and chemotherapy* **56**, 4922-4926 (2012).
58 **Bahar, A. A. & Ren, D.** Antimicrobial Peptides. *Pharmaceuticals* **6**, 1543-1575 (2013).
59 **Pan, J., Bahar, A. A., Syed, H. & Ren, D.** Reverting antibiotic tolerance of Pseudomonas aeruginosa PAO1 persister cells by (Z)-4-bromo-5-(bromomethylene)-3-methylfuran-2 (5H)-one. *PloS one* **7**, e45778 (2012).
60 **Pan, J., Song, F. & Ren, D.** Controlling persister cells of *Pseudomonas aeruginosa* PDO300 by (*Z*)-4-bromo-5-(bromomethylene)-3-methylfuran-2 (5 *H*)-one. *Bioorganic & medicinal chemistry letters* **23**, 4648-4651 (2013).
61 **Pan, J. *et al.*** (Z)-4-Bromo-5-(bromomethylene)-3-methylfuran-2 (5H)-one sensitizes *Escherichia coli* persister cells to antibiotics. *Applied microbiology and biotechnology* **97**, 9145-9154 (2013).
62 **Harrison, J. J. *et al.*** Persister cells mediate tolerance to metal oxyanions in *Escherichia coli*. *Microbiology* **151**, 3181-3195 (2005).
63 **Harrison, J. J., Turner, R. J. & Ceri, H.** Persister cells, the biofilm matrix and tolerance to metal cations in biofilm and planktonic *Pseudomonas aeruginosa*. *Environmental microbiology* **7**, 981-994 (2005).
64 **Niepa, T. H., Gilbert, J. L. & Ren, D.** Controlling *Pseudomonas aeruginosa* persister cells by weak electrochemical currents and synergistic effects with

tobramycin. *Biomaterials* **33**, 7356-7365, doi:10.1016/j.biomaterials.2012.06.092 (2012).

65 **Beattie, J.** Report on the electrical treatment of milk to the city of Liverpool. *Liverpool: C. Tinling and Co* (1915).

66 **Anderson, A. K. & Finkelstein, R.** A study of the electro-pure process of treating milk. *Journal of dairy science* **2**, 374-406 (1919).

67 **Beattie, J. M. & Lewis, F.** The Electric Current (Apart from the Heat Generated). A Bacteriologibal Agent in the Sterilization of Milk and Other Fluids. *Journal of Hygiene* **24**, 123-137 (1925).

68 **Brandt, B. , Edebo, L., Heden, C. G., Hjortzberg-Nordlund, B., Selin, I. & Tigerschiold, M.** The effect of submerged electrical discharges on bacteria. *Tek. Vetenskaplig Forskning* **33**, 222-229 (1962).

69 **Rosenberg, B., Van Camp, L. & Krigas, T.** Inhibition of cell division in *Escherichia coli* by electrolysis products from a platinum electrode. *Nature* **205**, 698-699 (1965).

70 **Rosenberg, B., Renshaw, E., Vancamp, L., Hartwick, J. & Drobnik, J.** Platinum-induced filamentous growth in *Escherichia coli*. *Journal of bacteriology* **93**, 716-721 (1967).

71 **Johnstone, T. C., Alexander, S. M., Lin, W. & Lippard, S. J.** Effects of Monofunctional Platinum Agents on Bacterial Growth: A Retrospective Study. *Journal of the American Chemical Society* (2013).

72 **Pareilleux, A. & Sicard, N.** Lethal effects of electric current on *Escherichia coli*. *Applied microbiology* **19**, 421-424 (1970).

73 **Rowley, B. A.** Electrical Current Effects on E. coil Growth Rates. *Experimental Biology and Medicine* **139**, 929-934 (1972).

74 **Rowley, B. A., McKenna, J. M., Chase, G. R. & Wolcott, L. E.** The influence of electrical current on an infecting microorganism in wounds. *Annals of the New York Academy of Sciences* **238**, 543-551 (1974).

75 **Barranco, S., Spadaro, J., Berger, T. & Becker, R.** In vitro effect of weak direct current on *Staphylococcus aureus*. *Clinical orthopaedics and related research* **100**, 250-255 (1974).

76 **Thibodeau, E., Handelman, S. & Marquis, R.** Inhibition and killing of oral bacteria by silver ions generated with low intensity direct current. *Journal of dental research* **57**, 922-926 (1978).

77 **Ong, P. C.** *Antibacterial effects of a silver electrode carrying micro-amperage direct current in-vitro*, Marquette University, (1994).

78 **Kloth, L. C.** Electrical stimulation for wound healing: a review of evidence from in vitro studies, animal experiments, and clinical trials. *The international journal of lower extremity wounds* **4**, 23-44 (2005).

79 **Laatsch, L., Ong, P. & Kloth, L.** In vitro effects of two silver electrodes on select wound pathogens. *J Clin Electrophysiol* **7**, 10-15 (1995).

80 **Sandvik, E. L., McLeod, B. R., Parker, A. E. & Stewart, P. S.** Direct Electric Current Treatment under Physiologic Saline Conditions Kills *Staphylococcus epidermidis* Biofilms via Electrolytic Generation of Hypochlorous Acid. *PloS one* **8**, e55118 (2013).

81 **Stoodley, P. & Lappin-Scott, H.** Influence of electric fields and pH on biofilm structure as related to the bioelectric effect. *Antimicrobial agents and chemotherapy* **41**, 1876-1879 (1997).

82 **Poortinga, A. T., Smit, J., van der Mei, H. C. & Busscher, H. J.** Electric field induced desorption of bacteria from a conditioning film covered substratum. *Biotechnology and bioengineering* **76**, 395-399 (2001).

83 **Poortinga, A. T., Bos, R. & Busscher, H. J.** Reversibility of bacterial adhesion at an electrode surface. *Langmuir : the ACS journal of surfaces and colloids* **17**, 2851-2856 (2001).

84 **Van Der Borden, A. J., Van Der Mei, H. C. & Busscher, H. J.** Electric block current induced detachment from surgical stainless steel and decreased viability of *Staphylococcus epidermidis*. *Biomaterials* **26**, 6731-6735 (2005).

85 **Van Der Borden, A. J., Van Der Werf, H., Van Der Mei, H. C. & Busscher, H. J.** Electric current-induced detachment of *Staphylococcus epidermidis* biofilms from surgical stainless steel. *Applied and environmental microbiology* **70**, 6871-6874 (2004).

86 **Van der Borden, A. J., Maathuis, P. GM., Engels, E., Rakhorst, G., van der Mei, H. C., Busscher, H. J., Sharma, P. K.** Prevention of pin tract infection in external stainless steel fixator frames using electric current in a goat model. *Biomaterials* **28**, 2122-2126 (2007).

87 **Shirtliff, M. E., Bargmeyer, A. & Camper, A. K.** Assessment of the ability of the bioelectric effect to eliminate mixed-species biofilms. *Applied and environmental microbiology* **71**, 6379-6382 (2005).

88 **Del Pozo, J. L., Rouse, M. S., Mandrekar, J. N., Steckelberg, J. M. & Patel, R.** The electricidal effect: reduction of Staphylococcus and Pseudomonas biofilms by prolonged exposure to low-intensity electrical current. *Antimicrobial agents and chemotherapy* **53**, 41-45, doi:10.1128/AAC.00680-08 (2009).

89 **Del Pozo, J. L., Rouse, M. S., Euba, G., Kang, C., Mandrekar, J. N., Steckelberg, J. M., Patel, R.** The electricidal effect is active in an experimental model of *Staphylococcus epidermidis* chronic foreign body osteomyelitis. *Antimicrobial agents and chemotherapy* **53**, 4064-4068 (2009).

90 **Chang, Y. H. D., Grodzinsky, A. J. & Wang, D. I.** Augmentation of mass transfer through electrical means for hydrogel - entrapped *Escherichia coli* cultivation. *Biotechnology and bioengineering* **48**, 149-157 (1995).

91 **Gilliland, S. & Speck, M.** Inactivation of microorganisms by electrohydraulic shock. *Applied microbiology* **15**, 1031-1037 (1967).

92 **Hülsheger, H., Potel, J. & Niemann, E.-G.** Electric field effects on bacteria and yeast cells. *Radiation and environmental biophysics* **22**, 149-162 (1983).

93 **Hülsheger, H. & Niemann, E.-G.** Lethal effects of high-voltage pulses on *E. coli* K12. *Radiation and Environmental Biophysics* **18**, 281-288 (1980).

94 **Gilliland, S. & Speck, M.** Mechanism of the bactericidal action produced by electrohydraulic shock. *Applied microbiology* **15**, 1038-1044 (1967).

95 **Zimmermann, U., Schulz, J. & Pilwat, G.** Transcellular Ion Flow in *Escherichia coli* B and Electrical Sizing of Bacterias. *Biophysical journal* **13**, 1005-1013 (1973).

96 **Zimmermann, U., Pilwat, G., Beckers, F. & Riemann, F.** Effects of external electrical fields on cell membranes. *Bioelectrochemistry and bioenergetics* **3**, 58-83 (1976).

97 **Sale, A. & Hamilton, W.** Effects of high electric fields on microorganisms: I. Killing of bacteria and yeasts. *Biochimica et Biophysica Acta (BBA)-General Subjects* **148**, 781-788 (1967).

98 **Grahl, T. & Märkl, H.** Killing of microorganisms by pulsed electric fields. *Applied microbiology and biotechnology* **45**, 148-157 (1996).

99 **Sato, M., Ohgiyama, T. & Clements, J. S.** Formation of chemical species and their effects on microorganisms using a pulsed high-voltage discharge in water. *Industry Applications, IEEE Transactions on* **32**, 106-112 (1996).

100 **Zituni, D., Schütt-Gerowitt, H., Kopp, M., Krönke, M., Addicks, K., Hoffmann, C., Hellmich, M., Faber, F., Niedermeier, W.** The growth of *Staphylococcus aureus* and *Escherichia coli* in low-direct current electric fields. *International journal of oral science* (2013).

101 **Marino, A. A., Deitch, E. A., Albright, J. A. & Specian, R. D.** Electrical augmentation of the antimicrobial activity of silver-nylon fabrics. *Journal of Biological Physics* **12**, 93-98 (1984).

102 **Kincaid, C. B. & Lavoie, K. H.** Inhibition of bacterial growth in vitro following stimulation with high voltage, monophasic, pulsed current. *Physical Therapy* **69**, 651-655 (1989).

103 **Szuminsky, N. J., Albers, A. C., Unger, P. & Eddy, J. G.** Effect of narrow, pulsed high voltages on bacterial viability. *Physical therapy* **74**, 660-667 (1994).

104 **Ali, F. M., Elkhatib, A. M., Aboutalib, W. M., Abdelbacki, A. M., Khalil, A. M. & Serag, N.** Control of the Activity of *Pseudomonas aeruginosa* by Positive Electric Impulses at Resonance Frequency. *Journal of American Science* **10**, 9 (2013).

105 **Giladi, M., Porat, Y., Blatt, A., Shmueli, E., Wasserman, Y., Kirson, E. D., Palti, Y.** Microbial growth inhibition by alternating electric fields in mice with *Pseudomonas aeruginosa* lung infection. *Antimicrobial agents and chemotherapy* **54**, 3212-3218 (2010).

106 **Ercan, B., Kummer, K. M., Tarquinio, K. M. & Webster, T. J.** Decreased *Staphylococcus aureus* biofilm growth on anodized nanotubular titanium and the effect of electrical stimulation. *Acta biomaterialia* **7**, 3003-3012 (2011).

107 **Perez-Roa, R. E., Rodolfo E., Tompkins, D. T., Paulose, M., Grimes, C. A., Anderson, M. A. & Noguera, D. R.** Effects of localised, low-voltage pulsed electric fields on the development and inhibition of *Pseudomonas aeruginosa* biofilms. *Biofouling* **22**, 383-390 (2006).

108 **Dargahi, M., Hosseinidoust, Z., Tufenkji, N. & Omanovic, S.** Investigating Electrochemical Removal of Bacterial Biofilms from Stainless Steel Substrates. *Colloids and Surfaces B: Biointerfaces* (2014).

109 **Khoury, A. E., Lam, K., Ellis, B. & Costerton, J. W.** Prevention and control of bacterial infections associated with medical devices. *ASAIO journal* **38**, M174-M178 (1992).

110 **Costerton, J. W., Ellis, B., Lam, K., Johnson, F. & Khoury, A. E.** Mechanism of electrical enhancement of efficacy of antibiotics in killing biofilm bacteria. *Antimicrobial agents and chemotherapy* **38**, 2803-2809 (1994).

111 **Jass, J., Costerton, J. & Lappin-Scott, H.** The effect of electrical currents and tobramycin on P*seudomonas aeruginosa* biofilms. *Journal of industrial microbiology* **15**, 234-242 (1995).

112 **Jass, J. & Lappin-Scott, H. M.** The efficacy of antibiotics enhanced by electrical currents against *Pseudomonas aeruginosa* biofilms. *Journal of Antimicrobial Chemotherapy* **38**, 987-1000 (1996).

113 **Wellman, N., Fortun, S. M. & McLeod, B. R.** Bacterial biofilms and the bioelectric effect. *Antimicrobial agents and chemotherapy* **40**, 2012-2014 (1996).

114 **Stewart, P. S., Wattanakaroon, W., Goodrum, L., Fortun, S. M. & McLeod, B. R.** Electrolytic Generation of Oxygen Partially Explains Electrical Enhancement of Tobramycin Efficacy againstPseudomonas aeruginosa Biofilm. *Antimicrobial agents and chemotherapy* **43**, 292-296 (1999).

115 **Del Pozo, J. L., Rouse, M. S., Mandrekar, J. N., Steckelberg, J. M., Patel, R.** Effect of electrical current on the activities of antimicrobial agents against *Pseudomonas aeruginosa, Staphylococcus aureus, and Staphylococcus epidermidis* biofilms. *Antimicrobial agents and chemotherapy* **53**, 35-40 (2009).

116 **Giladi, M., Porat, Y., Blatt, A., Shmueli, E., Wasserman, Y., Kirson, E. D., Palti, Y.** Microbial growth inhibition by alternating electric fields in mice with *Pseudomonas aeruginosa* lung infection. *Antimicrobial agents and chemotherapy* **54**, 3212-3218, doi:10.1128/AAC.01841-09 (2010).

117 **Blenkinsopp, S. A., Khoury, A. & Costerton, J.** Electrical enhancement of biocide efficacy against *Pseudomonas aeruginosa* biofilms. *Applied and environmental microbiology* **58**, 3770-3773 (1992).

118 **Caubet, R., Pedarros-Caubet, F., Chu, M., Freye, E., de Belem Rodrigues, M., Moreau, J. M. & Ellison, W. J.** A radio frequency electric current enhances antibiotic efficacy against bacterial biofilms. *Antimicrobial agents and chemotherapy* **48**, 4662-4664 (2004).

CHAPTER 3

CONTROLLING *PSEUDOMONAS AERUGINOSA* PERSISTER CELLS BY WEAK ELECTROCHEMICAL CURRENTS AND SYNERGISTIC EFFECTS WITH TOBRAMYCIN

This chapter has been published as below with minor modifications.
(Reproduced by permission of Elsevier)
Biomaterials 33, 7356-7365, doi:10.1016/j.biomaterials.2012.06.092 (2012).

3.1. ABSTRACT

It is well recognized that bacterial populations commonly contain a small percentage of phenotypic variants, known as persister cells, which are dormant and extremely tolerant to antibiotics. When the antibiotic treatment is stopped, surviving persister cells can regenerate the bacterial population with a similar percentage of persister cells. Such persistence presents a great challenge to curing chronic infections, such as those associated with implanted medical devices. In this study, we report that bacterial persister cells can be effectively eliminated by low-level direct currents (DCs); e.g. treatment with 70 μA/cm² DC for 1 h using stainless steel (SS) 304 reduced the number of viable planktonic persister cells of *Pseudomonas aeruginosa* PAO1 by 98% compared to the untreated control. In addition to persister killing by applying DC alone, synergistic effects were observed when treating persister cells with 70 μA/cm² DC and 1.5 μg/mL tobramycin together using SS304 electrodes. The same level of DC was also found to be cidal to biofilms-associated persister cells of *P. aeruginosa* PAO1. These results are helpful for developing more effective methods to control chronic infections associated with implanted medical devices.

3.2. INTRODUCTION

The rapid development and spreading of multidrug resistant bacteria is a major challenge to public health. Bacteria can become drug resistant through both intrinsic and acquired mechanisms. Intrinsic mechanisms are based on specific cellular structures and functions (e.g. drug extrusion by efflux pumps), which offer bacteria general protection from a variety of antibiotics and facilitate the further development of resistance through acquired mechanisms based on genetic mutations and horizontal gene transfer [1,2]. One of the major intrinsic mechanisms of resistance is biofilm formation, by which bacteria attach to surfaces and develop multicellular structures with cells embedded in an extracellular matrix [3-5]. With the high tolerance to antibiotics, biofilms cause serious medical problems. For example, biofilm formation on medical devices accounts for half of the cases of nosocomial infections in the U.S. and leads to repeated surgeries, and in more serious cases, amputations and deaths [6].

In addition to the formation of multicellular structures, it is well documented that bacterial cultures commonly contain a small fraction (0.1-1% in general) of dormant cells, known as persister cells [7-9]. Because most antibiotics are only effective against metabolically active cells, persister cells can survive the challenge of antibiotics at concentrations significantly higher than those required to lyse regular cells of the same genotype [9-11]. When the antibiotic concentration drops under a threshold after treatment, the surviving persisters can revert to an active state and regenerate the bacterial population with a similar percentage of persister cells. Persister population increases significantly when bacteria form biofilms or when a bacterial culture enters stationary

phase [10], rendering both states highly tolerant to antibiotic treatment [10,11]. In addition to dormancy, persisters embedded in biofilms are also protected from host immune systems by the polysaccharide matrix [12]. Thus, innovative technologies are needed to effectively eliminate persister cells, especially those in biofilms.

Due to the dormant nature of persister cells, antimicrobial approaches that work independently of bacterial growth phase have good potential to control bacterial persister cells. Rosenberg [13] reported that alternating electrical currents generated with platinum electrodes have bacteriostatic effects rendering *Escherichia coli* cells elongated. Later, direct currents (DCs) in the range of μA to mA/cm² and 100 kHz to 10 MHz alternating electric fields were reported for their cidal effects on bacteria after a relatively long period (several hours in most cases) of treatment [14-19]. Although the mechanism of these observations is not well understood, similar currents were also found to enhance the effects of antibiotics on biofilms, an interesting phenomenon known as bioelectric effect [18,20,21]. Consistently, a total current of 100 μA DC applied to surgical stainless steel pins has been found to prevent *Staphylococcus epidermidis* infection around percutaneous pins in goats [22].

The capability of controlling biofilm cells by DCs and alternating currents (ACs) led to our hypothesis that appropriate levels of electrochemical currents/potentials can also kill bacterial persister cells. To test this hypothesis, persister cells of the Gram-negative pathogen *Pseudomonas aeruginosa* PAO1 were challenged with 70 μA/cm^2 DC in this study. This strain was chosen because *P. aeruginosa* is one of the most important

pathogens with clinical significance including medical device-associated infections [23-25]. The effects of DC on both planktonic persister cells and those in biofilms were studied. The possible mechanisms are discussed.

3.3.MATERIALS AND METHODS

3.3.1. Bacterial strain and growth media.

The wild-type *P. aeruginosa* PAO1 was cultured in Luria-Bertani (LB) medium [26] containing 10 g/L tryptone, 5 g/L yeast extract, and 10 g/L NaCl. Each overnight culture was incubated at 37°C with shaking at 200 rpm.

3.3.2. Colony forming units.

The colony forming units (CFUs) were counted to quantify the number of viable *P. aeruginosa* PAO1 cells in planktonic cultures and in biofilms. For planktonic samples, 10 µL of each sample was diluted in a 10× series using 0.85% NaCl solution and spread on LB agar plates (1.5% agar). The CFUs were counted on the next day after incubation overnight at 37°C. The biofilm cells were collected by sonication of the biofilm samples in 0.85% NaCl solution for 1 min first [27] and then well mixed and diluted with 0.85% NaCl solution for counting CFU as described above. No significant effects of sonication on the viability of *P. aeruginosa* PAO1 was found (viability was not changed after 2 min of sonication confirmed by counting CFU).

3.3.3. Isolation of persister cells.

Previous work has demonstrated that *P. aeruginosa* persisters can be isolated by lysing the regular cells with 25 µg/mL ciprofloxacin (Cip) for 3.5 h [9]. In order to determine the sufficient Cip concentration for our strain, *P. aeruginosa* PAO1 cells were challenged with various concentrations of Cip (0 - 200 µg/mL) for 3.5 h and the killing was evaluated by counting CFU of surviving cells. Briefly, *P. aeruginosa* PAO1 was cultured in LB medium over night at 37°C. Then the cells were collected by centrifugation (Sorvall Legend RT+, Thermo scientific, Asheville, NC) at 8,000 rpm for 10 min at room temperature, and washed twice with 0.85% NaCl solution before being treated with different concentrations of Cip for 3.5 h at 37°C. After treatment, the cells were washed three times with 0.85% of NaCl solution to remove Cip and the debris of lysed cells. The number of viable persister cells was then quantified by counting CFU as described above. Five replicates were tested for each condition.

3.3.4. Growth rate measurement.

Four antibiotics were tested including tobramycin (Tob), chloramphenicol (Cm), kanamycin (Kan) and spectinomycin (Spec). An overnight culture of *P. aeruginosa* PAO1 was used to prepare subcultures in 96 well plates (Costar® No. 9017, Corning Inc, Corning, NY) with a start OD_{600} of 0.05. Each well contained 200 µL of LB medium supplemented with one of the above antibiotics at different concentrations. The concentrations tested ranged from 0 to 10 µg/mL for Tob, 0 to 40 µg/mL for Cm, 0 to 90 µg/mL for Kan and 0 to 80 µg/mL for Spec. The OD_{600} of cultures was read every hour over a period of 6 h. The growth curves were obtained to calculate the specific growth

rates and to identify the antibiotic concentrations that reduce the specific growth rate of *P. aeruginosa* PAO1 by around 50%. These reference concentrations were used to study the synergy between antibiotics and electrochemical currents (ECs).

3.3.5. Effects of DC on planktonic cells.

The susceptibility of *P. aeruginosa* PAO1 to low level DCs was investigated according to the following procedure. *P. aeruginosa* PAO1 cells in three different physiological stages were tested including persister cells isolated from stationary cultures, total cells in stationary cultures (with 99% as regular cells) and total cells in exponential cultures (with more than 99.9% as regular cells). The persister cells were isolated by treating the stationary phase cultures of *P. aeruginosa* PAO1 with 200 μg/mL Cip for 3.5 h as described above. To study the effects of DC on regular cells in stationary cultures, *P. aeruginosa* PAO1 grown overnight (99% as regular cells) were harvested by centrifugation at 8,000 rpm for 10 min at room temperature. To estimate the effects of DC on regular cells in exponential phase, overnight cultures were used to inoculate LB medium to an OD_{600} of ~0.005 and the cells were harvested by centrifugation when OD_{600} reached 0.7. The harvested cells, as described above (99.9% as regular cells), were washed twice with 0.85% NaCl solution, resuspended in 0.85% NaCl solution and treated with and without 70 $\mu A/cm^2$ DC. To deliver the DC, an electrochemical cell was constructed by inserting two SS304 electrodes along the opposite sides of a plastic cuvette (Thermo Fisher Scientific, Pittsburg, PA). A silver wire (0.015" diameter, A-M Systems, Sequim, WA) was placed in bleach for 30 min to generate an Ag/AgCl reference electrode. The reference electrode was then placed in the cuvette. A 70 $\mu A/cm^2$

DC was generated using a potentiostat (Potentiostat WaveNow, Pine Research Instrumentation, Raleigh, NC) in a 3-electrodes configuration as shown in Fig. S1. Using the AfterMath software (Potentiostat WaveNow, Pine Research Instrumentation, Raleigh, NC), a galvanostatic mode was selected to monitor the DC level and record the voltage across the system over an hour. During the treatment, 100 µL of sample was taken every 20 min to evaluate the viability of bacterial cells by counting CFU. Both SS304 and carbon electrodes were used to generate DCs. To compare the effects of electrode materials, the same conditions were also tested in the presence of 1.5 µg/mL Tob to study the synergy between DC and antibiotics.

3.3.6. Effects of DC on biofilm-associated persister cells.

P. aeruginosa PAO1 biofilms were formed on sterile SS304 coupons (3.5 cm x 0.95 cm x 0.05 cm). Briefly, an overnight culture of *P. aeruginosa* PAO1 was used to inoculate a petri dish containing 20 mL of LB medium and sterile coupons. The culture was incubated for 24 h at 37°C without shaking to allow biofilms to form on the coupons. The coupons with attached biofilms were then removed from the petri dish using sterile forceps and washed gently three times with sterile 0.85% NaCl solution. The control coupons were transferred to a 15 mL polystyrene conical tube (BD Falcon, Becton Dickinson and Company, Franklin Lakes, NJ) containing 8 mL of 0.85% NaCl solution and the biofilm cells were released from the surface by sonication for 1 min (Ultrasonic cleaner Model No B200, Sinosonic Industrial Co., Ltd, Taipei Hsien, Taiwan) to assess the total number of cells. Then the suspension was treated with 200 µg/mL Cip to count the CFU of viable persister cells. Other biofilm coupons were used either as working or

counter electrodes. According to the setup, the oxidation of the SS304 occurred at the working electrode. Therefore, a biofilm coupon was referred to as anodic biofilm (AB) electrode when it was set as the working (positively charged) electrode of the potentiostat or as cathodic biofilm (CB) electrode when the biofilm coupon was placed as the counter (negatively charged) electrode in the electrochemical cell. In either case, the biofilm was treated galvanostatically with 70 $\mu A/cm^2$ DC for 30 min in the presence and absence of 15 µg/mL Tob. Higher Tob concentration was used for biofilms due to the intrinsic tolerance of biofilms. Each coupon was then transferred to a 15 mL polystyrene conical tube containing 8 mL of 0.85% NaCl solution and the cells were removed from the surface by sonication for 1 min after treatment. The number of viable cells detached from the biofilm during DC treatments (in the 0.85% NaCl solution) was also quantified by counting the CFU in the solution. Each sample containing cells was also incubated with 200 µg/mL Cip at 37°C for 3.5 h to isolate biofilms-associated persister cells. The total numbers of cells (without Cip treatment) and persisters (with Cip treatment) were quantified by counting CFU as described above.

3.3.7. Effects of SS304 electrolytes.

To understand if the effects of DC on persister cells were due to the chemical species generated by the electrochemical reactions, 0.85% NaCl solution without bacterial cells was treated with the same level of DC (70 $\mu A/cm^2$ generated using SS304 electrodes) for 20, 40 and 60 min, respectively. Then the *P. aeruginosa* PAO1 persister cells were incubated in these pretreated 0.85% NaCl solutions for 1 h with and without 1.5 µg/mL Tob. The untreated control samples were exposed to 0.85% NaCl solution without an DC

for 1 h in the presence or absence of 1.5 μg/mL Tob. The CFU of each sample was quantified as described above after treatment. To understand if the movement of ions or some short-life chemical species are important to ECCP, *P. aeruginosa* PAO1 persister cells were resuspended in a 0.85% NaCl solution that was pretreated with 70 μA/cm^2 DC for 1 h (with SS304 in the absence of cells). Then 70 μA/cm^2 DC was applied to treat persister cells using carbon electrodes in the presence of electrolytes generated by SS304 electrodes. Samples were taken every 20 min to monitor the cell viability by counting CFU. This experiment was conducted with three replicates and consistent results were obtained.

3.3.8. Susceptibility of *P. aeruginosa* PAO1 persisters to electrochemically generated ions.

To further investigate the mechanism of the ECCP, we characterized the effects of the ions electrochemically released from SS304 on PAO1 persister cells. The elements of released ions were identified using inductively coupled plasma mass spectrometry (ICP-MS). The principle of the ICP-MS analysis is to sort the atoms of a sample based on their atom-to-charge ratio. The samples collected at several time points (20 min, 1 h and 2 h) of the DC-treated 0.85% NaCl solution were diluted by 1000 fold using 0.85% NaCl solution; and then vaporized and ionized with high temperature argon plasma in the vacuum chamber of a quadrupole mass spectrometer. The Perkin-Elmer ELAN® 6000 ICP-MS system (Perkin-Elmer, Inc., San Jose, CA) was used to determine the concentrations of the most abundant metal cations released from carbon and SS304 electrodes. To specifically study the effects of the ions identified by ICP-MS, Fe^{2+}, Fe^{3+},

Cr^{2+}, Cr^{3+}, Cr^{6+}, Mn^{2+} and Ni^{2+} ions (from Sigma) were tested against *P. aeruginosa* PAO1 persister cells. Stock solutions of these cations were prepared and diluted in a 10× series using 0.85% NaCl solution. Persister cells isolated from stationary phase cultures of *P. aeruginosa* PAO1, as described above, were washed and resuspended in 0.85% NaCl solution containing different concentrations of cations to an OD_{600} of 0.7. The persister cells were then incubated at 37°C for 1 h with shaking at 200 rpm. The CFU of each sample was quantified before and after exposure to the ions. To understand if any ions are responsible for persister control, the effects of these seven ions on persisters were also evaluated in the presence of 70 μA/cm^2 DC generated with carbon electrodes. CFU was quantified at 20 min interval over 1 h of the DC treatment to determine the cell viability.

3.3.9. Statistical analysis.

Minitab ® 16 Software was used to conduct t-test and one-way ANOVA analyses. Differences with $p < 0.05$ were considered as statistically significant.

3.4. RESULTS

3.4.1. Isolation of *P. aeruginosa* PAO1 persister cells.

An important characteristic of persister cells is their capability to survive the attack of antibiotics at concentrations well above the lethal dose for regular cells with the same genetic makeup [5]. As shown in Fig. 1, the majority of *P. aeruginosa* PAO1 cells (isolated from stationary phase cultures) were killed by less than 50 μg/mL of Cip, while a small portion (~1%) survived the challenge of Cip at concentrations up to 200 μg/mL. Thus,

200 μg/mL was chosen to ensure the complete elimination of regular cells. In the stationary phase cultures, persister cells represented around 1% of the total population under our experimental condition. This result is comparable to *P. aeruginosa* persister population (0.1 - 2.5%) reported in the literature[9,10].

3.4.2. Effects of DC on planktonic persisters and regular cells of *P. aeruginosa* PAO1.

P. aeruginosa PAO1 was found to be highly susceptible to low-level DC. Treatment with 70 μA/cm^2 DC using SS304 electrodes was found to effectively eliminate planktonic (suspended in liquid) persister cells. As shown in Fig. 2A, the viability of persister cells was reduced by ~2 logs after treatment for 60 min compared to the untreated control (one-way ANOVA, $p < 0.001$). The same current level was also found effective against planktonic regular cells in stationary phase (represented by the total stationary phase cells, 99% of which are regular cells). For example, around 2 logs of killing were achieved after treatment with 70 μA/cm^2 DC for 60 min (Fig. 2B). Compared to the regular and persister cells in stationary cultures, the treatment was found more effective against regular planktonic cells in exponential phase (represented by total cells from exponential cultures, 99.9% of which are regular cells) since no viable cells were identified after treatment for 60 min (Fig. 2C). These data suggest that low-level DCs are effective against *P. aeruginosa* PAO1 in both exponential (with rapid growth) and stationary (with no net growth but metabolically active cells) phases and in persister stage. Importantly, the above data suggest that the efficacy of DC on persister cells is comparable to that on regular cells in stationary phase. These effects are advantageous compared to antibiotics, most of which are ineffective against slow growing cells and persisters [28-30].

3.4.3. Synergistic effects between DC and Tob.

In addition to rapid elimination of persister cells by DC alone, synergistic effects were also observed between DC and the antibiotic Tob. Tob at 1.5 μg/mL was selected as it reduced specific growth rate of PAO1 by 50% (data not shown) but did not kill existing cells (regular cells in exponential & stationary phases and persister cells) significantly (Fig. 2A, B&C). This allowed us to study the synergy with DC treatment more clearly. While treatment with 1.5 μg/mL Tob alone for 1 h had no significant effect on the viability of persister cells and total cells from stationary phase cultures (Fig. 2A&B), the cidal effects of DC treatment was improved by Tob when SS304 was used to mediate the DC treatment. As shown in Fig. 2A&B, treatment with 70 $\mu A/cm^2$ DC alone for 60 min reduced the number of viable persister cells and total cells in stationary phase (99% as normal cells) by 97.7 ± 1.7% and 99.7 ± 0.0% (less than 3 logs), respectively. In comparison, treatment with 70 $\mu A/cm^2$ DC and 1.5 μg/mL Tob together caused around 5 logs of killing in both cases (one-way ANOVA, $p< 0.001$ for both cases). This 100 - 1000 times of enhancement in efficacy demonstrated a clear synergy between the DC treatment and Tob in killing PAO1 including persister cells. We named this interesting phenomenon as electrochemical control of persisters (ECCP). Synergistic effects between DC and Tob were also observed during treatment of exponential cultures. While the DC treatment exhibited rapid killing of *P. aeruginosa* PAO1 cells in exponential phase (99.9% as regular cells), the cells were eradicated 20 min sooner when treated with the same level of DC in the presence of 1.5 μg/mL Tob (Fig. 2C). Compared to Tob, however, no apparent synergy was found with the other three antibiotics tested including Cm, Kan and Spec (data not shown). In particular, it is interesting that no synergy was observed

between DC and Kan. Tob and Kan are both aminoglycosides targeting bacterial protein synthesis. These two antibiotics have similar structures but the number and position of –OH and $–NH_2$ groups vary slightly. These variations may be responsible for the difference in their antimicrobial effects against *P. aeruginosa*, difference in interaction with ions, and consequently their effects in persister control with DC. Collectively, these findings suggest that the right combination of ions and antibiotics should be used to obtain ECCP against a specific bacterial species.

3.4.4. Effects of electrode materials.

To understand if ECCP can also be achieved using other electrode materials and to understand the effects of electrochemically generated ions, the above experiments were repeated using carbon electrodes. It was found that the same DC level mediated by carbon electrodes was also effective in killing persister cells, although the effects were slightly less compared to SS304 electrodes. When treated with 70 $\mu A/cm^2$ DC using SS304 electrodes, the number of viable persister cells isolated from stationary phase cultures was reduced by about 2 logs (97.7 ± 1.7%) in 60 min (Fig. 2A); while the killing achieved with the same current density using carbon electrodes was 95.6 ± 5.4% (Fig. 3). Also, no clear synergy with antibiotics was noticed when carbon was used as the electrode material. As shown in Fig 3, DC treatment using carbon electrodes in the absence and presence of Tob exhibited 95.6 ± 5.4% and 96.0 ± 5.4% killing of persister cells, respectively (one-way ANOVA, $p = 0.43$). Different potentials were required for SS304 and carbon working electrodes to maintain the same current level (70 $\mu A/cm^2$ DC). When SS304 was used as electrodes, the voltage applied gradually decreased from 400

mV to 100 mV in 60 min. In comparison, the potential required to maintain 70 μA/cm^2 DC for carbon electrodes increased from 500 mV to 800 mV during treatment (Fig. S2). This difference is likely due to the different redox reactions that occurred at the electrode surfaces and the subsequent changes in the electrode surfaces. Such differences may cause different potencies in persister control by these two electrode materials. However, the finding that the same DC level generated with carbon electrodes was also effective in killing persister cells suggests that certain electrochemical products, such as reactive oxygen species may be important (see discussion below).

3.4.5. Effects of DC on biofilm-associated persister cells.

In addition to planktonic persisters, the effects of DC on biofilm-associated persisters were also studied. Similar to the persister population found in the stationary culture of PAO1, the persisters in our PAO1 biofilms was also found to represent around 1% of the total number of biofilm cells. This is higher than 0.1% reported in a previous study [10], presumably due to difference in culture conditions. The results shown in Fig. 4A&B indicate that the sign of the current (+: anodic; -: cathodic) plays an important role in killing biofilms-associated persisters. For the biofilms on the anodes, although the total number of PAO1 biofilm cells were reduced by 67.1 ± 5.9% (*t* test, $p = 0.001$) compared to the control, the number of persister cells were not significantly reduced by DC (*t* test, $p = 0.47$, Fig. 4A). In contrast, on the cathodic biofilm electrodes (negatively biased), the total number of biofilm cells was reduced by 85.9 ± 3.0% with the DC treatment only (*t* test, $p < 0.001$, Fig 4A), although the percentage of persister cells was not significantly reduced (*t* test, $p = 0.15$). The presence of 15 μg/mL Tob significantly increased the

efficacy of the DC (a higher concentration of Tob was used here since biofilms are more tolerant to antibiotics than planktonic cells). On the cathode, for example, the total number of biofilm cells was reduced by 97.1 ± 1.0% (*t* test, $p < 0.001$) and only 31.5 ± 10.0% of persisters survived the treatment (*t* test, $p = 0.04$) (Fig. 4B), indicating a synergy in killing biofilm-associated persister cells. Collectively, the above data suggest that the cathode was more effective than the anode in killing biofilms- associated cells (both regular and persister cells) (one-way ANOVA, $p < 0.007$ in both cases). The finding that DC is more potent against the biofilms on cathodes suggests that the presence of reduction products is important for ECCP (see Discussion section below).

To further study the effects on biofilm-associated persisters, the impact of longer DC treatment on cathodic biofilms-associated persister cells was also investigated in the absence and presence of Tob. As shown in Fig. 5A, the killing of biofilm-associated persister cells was 95.9 ± 4.0% after 2 h of DC treatment in the absence of Tob. In comparison, the DC treatments of biofilms on the cathode with 70 μA/cm^2 DC for 1 and 2 h were more effective with the addition of 15 μg/mL Tob (Fig. 5B). The viability of biofilm-associated persister cells was reduced by 99.4 ± 0.1% after 2 h of treatment (one-way ANOVA, $p < 0.006$, for both cases), consistent with the synergy observed with 30 min treatment.

3.4.6. Effects of electrolytes generated by SS304 electrodes.

As described above, the SS304 electrodes were found more effective than carbon electrodes in killing persister cells with the same level of DC. This finding led to the

question that if some of the electrochemical products generated by SS304 are highly effective in killing persister cells. To answer this question, the effects of electrochemical products were tested. As shown in Fig 6, exposure of PAO1 persister cells to SS304 ions released after 20, 40 and 60 min treatment of 0.85% NaCl solution with 70 μA/cm^2 DC did not significantly affect the viability of cells. Compared to the control sample incubated for 1 h in untreated 0.85% NaCl solution, none of the treatments with SS304 electrolytes reduced the number of viable PAO1 persister cells by more than one log. In addition, no clear synergy was observed between the pretreated 0.85% NaCl solution and 1.5 μg/mL Tob (t-test, $p > 0.17$ for all conditions). These results suggest that the electrochemical products released by SS304 alone are not sufficient to cause the same level of killing as DC exhibited. Thus, the movement of ions or the presence of some other short-life species generated by DC may be important for eradication of persister cells achieved using SS304 electrodes. To test this hypothesis, PAO1 persister cells were treated for 1 h with 70 μA/cm^2 DC using carbon electrodes in 0.85% NaCl solution pretreated with SS304 electrodes as described above. While 95.6 ± 5.4% of persister cells were eradicated by the treatment using carbon electrodes alone, 98.4 ± 2.0% (around 2 logs, one-way ANOVA, $p < 0.001$) were killed with the addition of electrolytes generated by SS304 electrodes (Fig. 3). Thus, DC treatment using carbon electrodes and a solution containing SS304 electrolyte exhibited stronger antimicrobial activities on persisters than the treatment using carbon electrodes alone. Moreover, DC treatment using carbon electrodes with SS304 electrolytes (Fig. 3) exhibited efficacy in persister killing similar to the treatment using SS304 electrodes alone (Fig. 2A) (98.4 ± 2.0% vs. 97.7 ± 1.7%), however, no synergy with Tob was observed by using carbon electrodes (Fig. 3) (one-

way ANOVA, $p = 0.31$). These results indicate that the movement of ions or other charged electrochemical products and the presence of some cathodically generated chemical species may be important for ECCP.

3.4.7. Susceptibility of *P. aeruginosa* PAO1 persisters to the electrochemically generated ions.

The data from ICP-MS analysis of 0.85% NaCl solution pretreated with 70 μA/cm^2 DC using SS304 electrodes showed that the amounts of Fe, Cr, Ni, and Mn ions released during the treatment increased over time (Fig. S3). By applying 70 μA/cm^2 DC with SS304 electrodes, 0.82 μM Fe, 0.27 μM Cr, 0.10 μM Ni and 0.02 μM Mn were released within 1 h. These concentrations of Fe, Cr, Ni and Mn represent 67.8%, 22.3%, 8.3% and 1.6%, respectively, of the amount of total ions released during the treatment using SS304. However, only trace amount of Cr, Ni and Mn (ranging from 1-10 nM) was released by 1 h of treatment mediated with carbon electrodes.

To test the effects of each ion species specifically, the PAO1 cells were exposed for 1 h to various concentrations of the ions at different oxidation states. The results showed that, without an electrical field, PAO1 persisters could tolerate at least 40.6 μM Fe^{3+}, 251.4 μM Fe^{2+}, 150.0 μM Cr^{6+}, 150.0 μM Cr^{3+}, 4.0 μM Cr^{2+}, 10 μM Ni^{2+}, 10 μM Mn^{2+} (Fig. S4). These concentrations are about 50-300, 15-560, 100 and 500 times higher than the concentrations of Fe, Cr, Ni and Mn detected in the 0.85% NaCl solution pretreated for 1 h with 70 μA/cm^2 DC, respectively. Thus, the presence of any of these ions themselves is not sufficient for killing PAO1 persister cells.

The above finding supports our hypothesis that the movement of some of these ions might be important for ECCP. To further test this hypothesis, the effects of these seven ions on persister cells were investigated in the presence of 70 μA/cm^2 DC generated with carbon electrodes. According to the results shown in Fig. 7A, Fe^{2+}, Fe^{3+}, Cr^{2+}, Cr^{3+} and Cr^{6+} ions were found more effective than Mn^{2+} and Ni^{2+} ions in killing PAO1 persister cells in the presence of 70 μA/cm^2 DC. Since treatment using anodic carbon electrodes in the absence of these ions only reduced persister viability by around 1 log and the ions were not effective without a DC, the movement of these ions or electrochemical conversion of them to a particular state and the generation of reactive oxygen species (see Discussion) may be important for ECCP.

To understand if any specific ions released from SS304 by DC may have synergy with Tob during ECCP, we repeated the above experiment in the presence of 1.5 μg/mL Tob. The data demonstrated that the activity of some ions could be altered by Tob. The most apparent effects were observed for 60 min treatments. As shown in Fig. 7B, the effects of Cr^{2+} and Cr^{6+} on killing persister cells with DC was significantly compromised by Tob (*t* test, $p < 0.001$ for both ions). In comparison, Ni^{2+}, Cr^{3+} and Fe^{2+} exhibited synergy with Tob with 84.5 ± 1.2%, 38.1 ± 5.7% and 20 ± 7.4% additional killing, respectively, compared to Tob-free samples (*t* test, $p < 0.001$ for all conditions). These results confirmed that specific interactions between ions and antibiotics could alter the efficacy of ECCP.

To understand the kinetics of release of Fe^{2+} and Fe^{3+} and their roles in the killing of persisters during DC treatment with SS304 electrodes, DC polarization curves of carbon, SS304 and Fe were recorded. Using the same electrochemical cell described in Fig. S1, anodic polarization tests of SS304, carbon and 99.5% c.p. Fe electrodes were performed in sterile 0.85% NaCl solution. A voltammogram was recorded from -2 V to 1 V (vs. Ag/AgCl potential) at a polarization scan rate of 1 mV/s to obtain the polarization curves of SS304, carbon and Fe. Under the tested condition, Fe electrodes displayed a corrosion potential (E_{corr}) of -900 mV (vs. Ag/AgCl potential). As shown in the Fig. S5, Fe underwent active corrosion for all potentials above -900 mV. This finding suggests that Fe was continuously converted to Fe^{2+} or Fe^{3+} until the anodic current density reached 10 mA/cm^2 DC. SS304 electrodes, however, displayed a double corrosion behavior separated by a passivation phase. The initial active corrosion of SS304 was short and occurred at potential comprised between the open-circuit potential (OCP, -700 mV) and -500 mV (vs. Ag/AgCl potential). The passivation of SS304 electrodes was initiated at a potential of -500 mV and was completed at -100 mV. The potentiodynamic curve (Fig. S2) of treatment with 70 $\mu A/cm^2$ DC revealed that the potential due to our DC treatment using SS304 fell in the range of passivation of the material (-500 mV to 500 mV, Fig. S5). In contrast, carbon electrode underwent anodic corrosion associated with an increased potential (E_{corr}) of -100 mV. This corroborates the finding that the voltage of DC treatment with carbon electrodes almost doubled in 1 h (increased from 500 mV to 800 mV).

3.5. DISCUSSION

Previous works proposed a few possible mechanisms by which electric currents affect bacterial cells. For instance, generation of high voltage across the cell membrane of microorganisms induced structural changes by depolarization, which can lead to cell death [31]. The diffusion of fast moving ions and antibiotics into biofilms was also suggested as a mechanism of the bioelectric effect in that the permeability of the biofilm matrix was enhanced and the most inner cells were exposed to antimicrobials [15,21]. In this study, we discovered that drug-tolerant bacterial persister cells can be eliminated by low level DCs and synergistic effects exist between DCs and certain antibiotics, e.g. Tob. We refer to this phenomenon as electrochemical control of persisters (ECCP). Although the mechanism of ECCP is not fully understood, our data suggest that the presence of certain transient reductive species including reactive oxygen species at the cathode and the movement of metal cations may be essential. We expect that electrochemical currents conducted using various materials could result in different ions released and consequently affect bacterial viability differently. Carbon and SS304 were used in this study as representative electrode materials. It is interesting to note that, while both electrodes were effective in delivering DC to kill persister cells, synergy with Tob was only observed for SS304 electrodes, but not carbon electrodes. DC treatment using SS304 was more potent than what was obtained using carbon electrodes and a lower voltage was required for maintaining the same current level (70 $\mu A/cm^2$ DC). The most abundant elements in SS304 are Cr (18-20%), Ni (8-10.5%) and Fe (~ 66%). Because carbon electrodes release only trace amounts of Cr and are also effective in killing persister cells, Cr is not necessary for ECCP. As shown in the polarization curves (Fig. S5), SS304 electrodes

displayed corrosion behavior that was different from that of carbon and pure Fe electrodes. Initially, anodic corrosion of SS304 occurs with the oxidization of Fe at low negative voltages, followed by passivation of the material at a higher potential (around -500 mV). Typically during passivation of SS304, ultra-thin films of metal oxide of Cr_2O_3, Fe_2O_3, or FeO form on its surface (between -500 mV and 400 mV), preventing further active corrosion of the metal. These thin film oxides normally provide resistance to corrosion. In our case, only SS304 exhibited a spontaneous passivation behavior. The current density associated with the formation of the passive film was 10 $\mu A/cm^2$ DC, which is lower than the 70 $\mu A/cm^2$ DC used for the ECCP experiments. This implies that the voltages needed initially were above the breakdown potential for SS304 which resulted in the induction of pitting. Once pitting is initiated, the voltage required to propagate the pits became much lower as seen in Fig. S2. These results indicate that, during the treatment of persisters, the working electrode of SS304 underwent pitting corrosion, which can possibly lead to the formation of Fe^{2+}/Fe^{3+}, Cr^{3+}, Mn^{2+}, Ni^{2+}, OH^-, and Cl^-. The natural capability of SS304 to resist to corrosion is due to the presence of Cr which forms passive films. As reported by Qiu et *al*. [32], Cr constitutes 80% of the passivation film formed in response to galvanic corrosion of SS304. On the other hand, Ni adds to the resistance of SS304 to corrosion by lowering the passive current density (like a noble material) and allowing this protection to happen at lower voltages during corrosion [32-34].

The contribution of the cathode in ECCP has also been exemplified with the enhanced cell killing in our cathodic biofilms (Figs. 4&5). The cathode (counter electrode)

attains a potential necessary to maintain the current density whenever a change occurs in the resistance of the anode. This goes along with the type of reactions that should occur on each electrode. Typically, the electrochemical reaction of iron may generate ferric cations on the anode, but reactive oxygen species (ROS) on the cathode. Some possible reactions of the electrochemical treatment of SS304 under our experimental condition are [35]:

Oxidation reaction

$$Fe \rightarrow Fe^{2+} + 2e^-$$

$$Fe^{2+} \rightarrow Fe^{3+} + e^-$$

$$2Cr + 3H_2O \rightarrow Cr_2O_3 + 6H^+ + 6e\text{-}$$

$$2H_2O \rightarrow H_2O_2 + 2H^+ + 2e^-$$

$$Fe^{2+} + H_2O_2 \rightarrow Fe^{3+} + {}^{\bullet}OH + OH^-$$

Reduction reactions

$$O_2 + H_2O + e^- \rightarrow HO_2^{\bullet} + OH^-$$

$$H_2O_2 + 2e^- \rightarrow 2OH^-$$

$$O_2 + 2H_2O + 4e^- \rightarrow 4OH^-$$

$$O_2 + 2H_2O + 2e^- \rightarrow H_2O_2 + 2OH^-$$

$$2\,Fe^{3+} + 2\,e^- \rightarrow 2\,Fe^{2+}$$

$$Fe^{3+} + H_2O_2 \rightarrow Fe^{2+} + {}^{\bullet}OOH + H^+$$

$$2\,Fe^{3+} + 2H_2O \rightarrow 2\,Fe^{2+} + H_2O_2 + 2\,H^+$$

The killing achieved with carbon electrodes, which do not release any cation significantly, suggests that the byproducts of electrochemical reactions generated at the counter electrode or cathode may be involved in the phenomenon of ECCP as well. The graphite sheet used for the carbon electrodes is made with 99.5% of very fine grains of carbon that could be released from the anode during the treatment. Also, it is well documented that at pH between 6.5 and 9, the electrolysis of graphite in water generates carbonates (HCO_3^-) at an electrode potential of 0.4V and progressively releases CO_2 when the potential approaches 1V [33]. Thus, in our 0.85% NaCl solution-electrode system, DC treatment may generate oxygen species such as hydrogen peroxide (H_2O_2), hydroxyl radical ($^{\bullet}OH$), hypochlorous acid (HOCl), and other short-live species at the cathode of both electrode materials. These agents may be the reason of the similitude in the persister killing experienced with the DC treatments using either electrode materials without an antibiotic. However, the synergistic killing effects recorded in the treatment using SS304 and Tob indicate that Fe ions may contribute to a greater extent to ECCP against *P. aerugionsa*. One interesting observation of treatment with carbon electrodes was the increase in resistance of the treated cell suspension over time (doubled progressively over one hour of experiment), which may also be due to the release of the carbon particles within the solution. This increase in resistance consequently increased the voltage required for maintaining the current level, which in turn could alter the electrochemical reactions and have an adverse effect on the synergy with antibiotics under certain conditions. On the other hand, Fe is the most abundant element released from the anode of SS304 as shown by the ICP-MS analysis (Fig. S3). The anodic breakdown of the oxide film and the pitting corrosion of SS304 induced a significant drop of the material

resistance and consequently a voltage decrease. Because the synergy with Tob is observed with SS304, but not with carbon electrode, optimization of the electrode materials is expected to further improve the efficacy of ECCP. Different bacterial species may also respond to ECCP differently and it will be interesting to test the effects of ECs on the persister cells of different bacterial species to identify the general and species-specific effects.

While persisters can tolerate very high concentrations of Cr and Fe ions, they become susceptible to low concentrations of the same ions in the presence of an electrical field (Fig. S4 & Fig. 7). The synergistic effects between DC and Tob proved that the tolerance of persisters to antibiotics can be altered by low level DC. The effects of DCs on persister cells at the genetic level are still unknown. We reported recently that similar DC treatment induced *Bacillus subtilis* genes responsible for ions transport [36]. The effects of DC on the membrane structure and function of persister cells and permeability to antibiotics, however, are yet to be explored and are part of our ongoing work. We hypothesize that certain levels of electrochemical current (EC) may positively (wakeup) or negatively (killing) affect these targets and provide new mechanisms to kill bacterial persister cells. In addition to antibiotics, DC may also have synergy with other factors. We recently discovered that the human immune factor, granulocyte-macrophage colony-stimulating factor (GM-CSF) has remarkable activities to sensitize bacterial persister cells to antibiotics (Choudhary et al. unpublished). It will be interesting to test if DC has synergy with this and other immune factors in persister control as well.

Elimination of persister cells with low-level EC and synergy with antibiotics has promising applications in infection control. Such treatments are expected to be safe to humans and the environment; e.g., longer duration of treatments at similar or higher EC levels have been shown to stimulate the proliferation of fibroblasts by increasing collagen and DNA synthesis, to trigger migration of immune cells, and to promote the healing of lower extremity wounds [37]. Further knowledge on these topics will help understand the mechanism of persister formation and associated tolerance to antimicrobials. It will also facilitate the development of more effective infection control through local delivery of low level ECs to implanted medical devices and skin. For example, by applying an appropriate EC and antibiotics through the area of skin with bacterial infection may help eliminate persister cells and promote healing. Alternatively, metallic components of an implanted medical device can be used as electrodes to help eliminate persister cells and associated biofilms.

3.6. CONCLUSIONS

Overall, this study demonstrated that bacterial persister cells can be efficiently killed with low level DCs and synergy with tobramycin. Such electrochemical control is effective against both planktonic and biofilm persisters, and only requires DCs at $\mu A/cm^2$ level and less than 60 min. Comparison between carbon and SS304 electrodes in killing persisters indicated that transient chemical species generated during reduction reaction of the electrode material may be essential for ECCP. In addition, the movement of the metal cations from the working electrodes could play an important role in the control of persisters and the synergy with antibiotics.

3.7. ACKNOWLEDGEMENTS

The authors are grateful to Blue Highway Inc. and the U.S. National Science Foundation (EFRI-1137186) for support. We also thank Dr. Thomas K. Wood at Penn State University for sharing the strain *P. aeruginosa* PAO1, and Dr. Charles Driscoll and Mario Montesdeoca at Syracuse University for helping with the ICP-MS.

3.8. REFERENCES

1 **Nikaido, H.** Prevention of drug access to bacterial targets: permeability barriers and active efflux. *Science* **264**, 382-388 (1994).

2 **Dzidic, S. & Bedeković, V.** Horizontal gene transfer-emerging multidrug resistance in hospital bacteria. *Acta Pharmacologica Sinica* **24**, 519 (2003).

3 **Elkins, J. G., Hassett, D. J., Stewart, P. S., Schweizer, H. P. & McDermott, T. R.** Protective role of catalase in *Pseudomonas aeruginosa* biofilm resistance to hydrogen peroxide. *Appl Environ Microbiol* **65**, 4594-4600 (1999).

4 **Gordon, C. A., Hodges, N. A. & Marriott, C.** Antibiotic interaction and diffusion through alginate and exopolysaccharide of cystic fibrosis-derived *Pseudomonas aeruginosa*. *J Antimicrob Chemother* **22**, 667-674 (1988).

5 **Lewis, K.** Persister cells and the riddle of biofilm survival. *Biochemistry (Moscow)* **70**, 267-274 (2005).

6 **Darouiche, R. O.** Treatment of infections associated with surgical implants. *New England Journal of Medicine* **350**, 1422-1429 (2004).

7 **Brooun, A., Liu, S. & Lewis, K.** A Dose-Response Study of Antibiotic Resistance in *Pseudomonas aeruginosa* Biofilms. *Antimicrobial agents and chemotherapy* **44**, 640-646 (2000).

8 **Lewis, K.** Persister cells, dormancy and infectious disease. *Nat Rev Microbiol* **5**, 48-56, doi:nrmicro1557 [pii] 10.1038/nrmicro1557 (2007).

9 **Moker, N., Dean, C. R. & Tao, J.** *Pseudomonas aeruginosa* increases formation of multidrug-tolerant persister cells in response to quorum-sensing signaling molecules. *J Bacteriol* **192**, 1946-1955, doi:JB.01231-09 [pii] 10.1128/JB.01231-09 (2010).

10 **Spoering, A. L. & Lewis, K.** Biofilms and planktonic cells of *Pseudomonas aeruginosa* have similar resistance to killing by antimicrobials. *J Bacteriol* **183**, 6746-6751, doi:10.1128/JB.183.23.6746-6751.2001 (2001).

11 **Keren, I., Kaldalu, N., Spoering, A.,** Wang, Y. & Lewis, K. Persister cells and tolerance to antimicrobials. *FEMS microbiology letters* **230**, 13-18 (2004).

12 **Roberts, M. E. & Stewart, P. S.** Modelling protection from antimicrobial agents in biofilms through the formation of persister cells. *Microbiology* **151**, 75-80, doi:151/1/75 [pii]10.1099/mic.0.27385-0 (2005).

13 **Rosenberg, B.** Some biological effects of platinum compounds. *Platinum Metals Review* **15**, 42–51 (1971).

14 **Bolton, L., Foleno, B., Means, B. & Petrucelli, S.** Direct-Current Bactericidal Effect on Intact Skin. *Antimicrobial agents and chemotherapy* **18**, 137-141 (1980).

15 **Costerton, J. W., Ellis, B., Lam, K., Johnson, F. & Khoury, A. E.** Mechanism of Electrical Enhancement of Efficacy of Antibiotics in Killing Biofilm Bacteria. *Antimicrobial agents and chemotherapy* **38**, 2803-2809 (1994).

16 **Del Pozo, J. L., Rouse, M. S., Mandrekar, J. N., Steckelberg, J. M. & Patel, R.** The electricidal effect: reduction of Staphylococcus and pseudomonas biofilms by prolonged exposure to low-intensity electrical current. *Antimicrob Agents Chemother* **53**, 41-45, doi:AAC.00680-08 [pii] 10.1128/AAC.00680-08 (2009).

17 **Francolini, I. & Donelli, G.** Prevention and control of biofilm-based medical-device-related infections. *FEMS Immunol Med Microbiol* **59**, 227-238, doi:FIM665 [pii]10.1111/j.1574-695X.2010.00665.x (2010).

18 **Giladi, M., Porat, Y., Blatt, A., Shmueli, E., Wasserman, Y., Kirson, E. D., Palti, Y.** Microbial growth inhibition by alternating electric fields in mice with *Pseudomonas aeruginosa* lung infection. *Antimicrob Agents Chemother* **54**, 3212-3218, doi:AAC.01841-09 [pii]10.1128/AAC.01841-09 (2010).

19 **Spadaro, J. A., Berger, T. J., Barranco, S. D., Chapin, S. E. & Becker, R. O.** Antibacterial effects of silver electrodes with weak direct current. *Antimicrob Agents Chemother* **6**, 637-642 (1974).

20 **Del Pozo, J. L., Rouse, M. S., Mandrekar, J. N., Steckelberg, J. M., Patel, R.** Effect of electrical current on the activities of antimicrobial agents against *Pseudomonas aeruginosa, Staphylococcus aureus, and Staphylococcus epidermidis* biofilms. *Antimicrob Agents Chemother* **53**, 35-40, doi:AAC.00237-08 [pii]10.1128/AAC.00237-08 (2009).

21 **Jass, J., Costerton, J. W. & Lappin-Scott, H. M.** The effect of electrical currents and tobramycin on *Pseudomonas aeruginosa* biofilms. *J Ind Microbiol* **15**, 234-242 (1995).

22 **Van der Borden, A. J., Maathuis, P. GM., Engels, E., Rakhorst, G., Van der Mei, H. C., Busscher, H. J. & Sharma, P. K.** Prevention of pin tract infection in external stainless steel fixator frames using electric current in a goat model. *Biomaterials* **28**, 2122-2126 (2007).

23 **Nordmann, P., Naas, T., Fortineau, N. & Poirel, L.** Superbugs in the coming new decade; multidrug resistance and prospects for treatment of *Staphylococcus aureus, Enterococcus spp. and Pseudomonas aeruginosa* in 2010. *Curr Opin Microbiol* **10**, 436-440, doi:S1369-5274(07)00094-X [pii] 10.1016/j.mib.2007.07.004 (2007).

24 **Navon-Venezia, S., Ben-Ami, R. & Carmeli, Y.** Update on *Pseudomonas aeruginosa* and *Acinetobacter baumannii* infections in the healthcare setting. *Curr Opin Infect Dis* **18**, 306-313, doi:00001432-200508000-00004 [pii] (2005).

25 **Doshi, H. K., Chua, K., Kagda, F. & Tambyah, P. A.** Multi drug resistant pseudomonas infection in open fractures post definitive fixation leading to limb loss: A report of three cases. *International Journal of Case Reports and Images (IJCRI)* **2**, 1-6 (2011).

26 **Sambrook, J. & Russell, D. W.** *Molecular cloning: a laboratory manual*. Vol. 3 (Cold spring harbor laboratory press, 2001).

27 **Morris, C. E., Monier, J. M. & Jacques, M. A.** A technique to quantify the population size and composition of the biofilm component in communities of bacteria in the phyllosphere. *Applied and Environmental Microbiology* **64**, 4789 (1998).

28 **Parr, T. R., Jr. & Bayer, A. S.** Mechanisms of aminoglycoside resistance in variants of *Pseudomonas aeruginosa* isolated during treatment of experimental endocarditis in rabbits. *J Infect Dis* **158**, 1003-1010 (1988).

29 **Poole, K.** Aminoglycoside resistance in *Pseudomonas aeruginosa*. *Antimicrob Agents Chemother* **49**, 479-487, doi:49/2/479 [pii]10.1128/AAC.49.2.479-487.2005 (2005).

30 **Taber, H. W., Mueller, J. P., Miller, P. F. & Arrow, A. S.** Bacterial uptake of aminoglycoside antibiotics. *Microbiol Rev* **51**, 439-457 (1987).

31 **Castro, A., Barbosa Cánovas, G. & Swanson, B.** Microbial inactivation of foods by pulsed electric fields. *Journal of food processing and preservation* **17**, 47-73 (1993).

32 **Qiu, J. H.** Passivity and its breakdown on stainless steels and alloys. *Surface and Interface Analysis* **33**, 830-833, doi:Doi 10.1002/Sia.1460 (2002).

33 **Pourbaix, M.** *Atlas of electrochemical equilibria in aqueous solutions* (Franklin, Pergamon Press, 1966).

34 **Flitt, H. J. & Schweinsberg, D. P.** A guide to polarisation curve interpretation: deconstruction of experimental curves typical of the Fe/H2O/H+/O-2 corrosion system. *Corrosion Science* **47**, 2125-2156, doi:DOI 10.1016/j.corsci.2004.10.002 (2005).

35 **Kalbacova, M., Roessler, S., Hempel, U., Tsaryk, R., Peters, K., Scharnweber, D., Kirkpatrick, J. C.,Dieter, P.** The effect of electrochemically simulated titanium cathodic corrosion products on ROS production and metabolic activity of osteoblasts and monocytes/macrophages. *Biomaterials* **28**, 3263-3272, doi:S0142-9612(07)00144-5 [pii]10.1016/j.biomaterials.2007.02.026 (2007).

36 **Szkotak, R., Niepa, T. H., Jawrani, N., Gilbert, J. L., Jones, M. B., Ren, D.** Differential Gene Expression to Investigate the Effects of Low-level Electrochemical Currents on *Bacillus subtilis*. *AMB Express* **1**, 39, doi:2191-0855-1-39 [pii]10.1186/2191-0855-1-39 (2011).

37 **Kloth, L. C.** Electrical stimulation for wound healing: a review of evidence from in vitro studies, animal experiments, and clinical trials. *Int J Low Extrem Wounds* **4**, 23-44, doi:4/1/23 [pii]10.1177/1534734605275733 (2005).

FIGURE CAPTIONS

Figure 3.1. Viability of *P. aeruginosa* PAO1 cells after 3.5 h treatment of planktonic stationary cultures with different concentrations of Cip. Five replicates were tested for each condition. Means and standard errors are shown.

Figure 3.2. Effects of DC treatment using SS 304 electrodes on planktonic *P. aeruginosa* PAO1 cells. All samples were treated with 70 μA/cm^2 DC for 1 h with and without 1.5 μg/mL Tob. (A) Planktonic persister cells. (B) Regular cells in stationary phase. (C) Regular cells in exponential phase. Four replicates were tested for each condition. Means and standard errors are shown.

Figure 3.3. Effects of DC treatment using carbon electrodes on planktonic *P. aeruginosa* PAO1 persister cells. Addition of SS 304-electrolytes from DC-treated 0.85% NaCl solution enhanced the killing of persister cells by 70 μA/cm^2 DC mediated with carbon electrodes. The electrolytes were generated by treating 0.85% NaCl solution with 70 μA/cm^2 DC for 1 h using SS 304 electrodes. Six replicates were tested for each condition. Means and standard errors are shown.

Figure 3.4. Effects of DC on persisters and regular cells in biofilms. Cathodic and anodic *P. aeruginosa* PAO1 biofilms were formed on SS 304 coupons (with 24h incubation) and treated with 70 μA/cm^{2}DC for 30 min in the presence or absence of 15 μg/mL Tob. The cells were collected from the coupons by sonication and the persister population was isolated after treatment with 200 μg/mL Cip for 3.5 h. The viability of the cathodic and anodic biofilm cells

was compared to the untreated control. (A) DC treatment only. (B) DC treatment with 15 µg/mL Tob. Four replicates were tested for each condition. Means and standard errors are shown.

Figure 3.5. Effects of longer EC treatment on persisters and regular cells in cathodic biofilms. Cathodic *P. aeruginosa* PAO1 biofilms were formed on SS 304 coupons and treated with 70 µA/cm^2 DC for 1 and 2 h in the presence or absence of 15 µg/mL Tob. The cells were collected from the coupons by sonication and the persister population was isolated after treatment with 200 µg/mL Cip for 3.5 h. The viability of the cathodic and anodic biofilm cells was compared to the untreated control. (A) DC treatment only. (B) DC treatment with 15 µg/mL Tob. Two replicates were tested for each condition. Means and standard errors are shown.

Figure 3.6. Effects of SS 304-generated electrolytes on *P. aeruginosa* PAO1 persister cells. Sterile 0.85% NaCl solution was pretreated for 20, 40 or 60 min with 70 µA/cm^2 EC and the persister cells were exposed to the electrolytes for 1 h in the presence or absence of 1.5 µg/mL Tob. The untreated control sample was exposed to 0.85% NaCl solution only for 1 h in the presence or absence of 1.5 µg/mL Tob. The number of viable cells was quantified by counting by CFU. Three replicates were tested for each condition. Means and standard errors are shown.

Figure 3.7. Effects of metal cations at different oxidation states on PAO1 persister cells during EC treatment mediated with carbon electrodes. PAO1 persisters were resuspended in 0.85% NaCl solution containing Fe2+, Fe3+, Cr2+, Cr3+,

Cr6+, Ni2+, Mn2+ at the same concentrations released after 70 µA/cm2 DC treatment for 1 h using SS 304 electrodes. (A) DC treatment only. (B) DC treatment with 1.5 µg/mL Tob. At least two replicates were tested for each condition. Means and standard errors are shown.

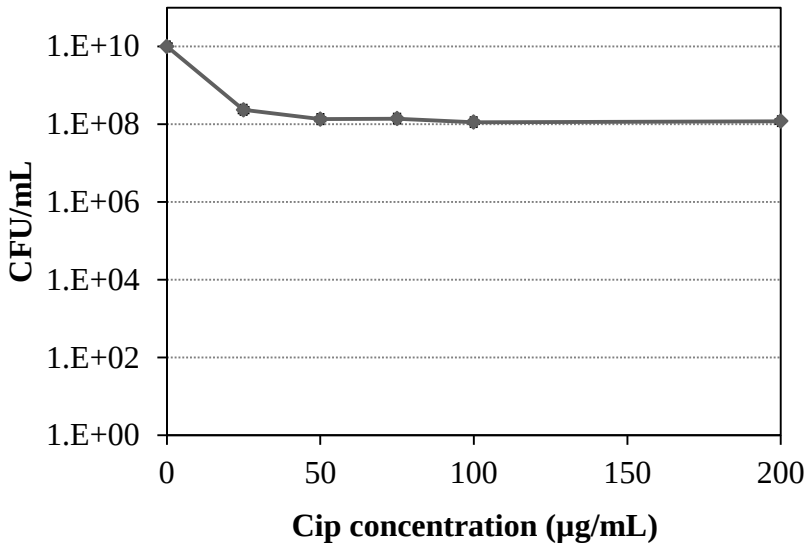
1.E+10
1.E+08
1.E+06
1.E+04
1.E+02
1.E+00
CFU/mL
0
50
100
150
200
Cip concentration (µg/mL)

Figure 3.1

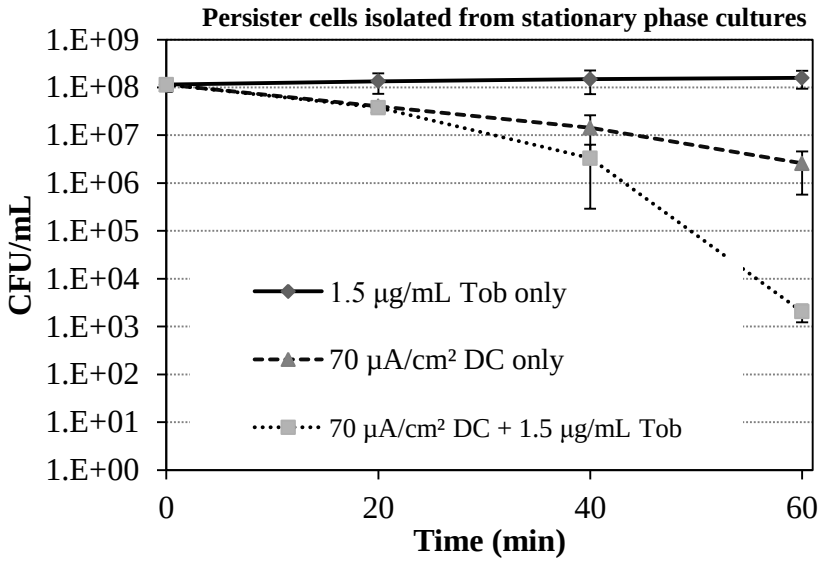
Persister cells isolated from stationary phase cultures
1.E+09
1.E+08
1.E+07
1.E+06
1.E+05
1.E+04
1.E+03
1.E+02
1.E+01
1.E+00
CFU/mL
1.5 µg/mL Tob only
70 µA/cm² DC only
70 µA/cm² DC + 1.5 µg/mL Tob
0
20
40
60
Time (min)

(A)

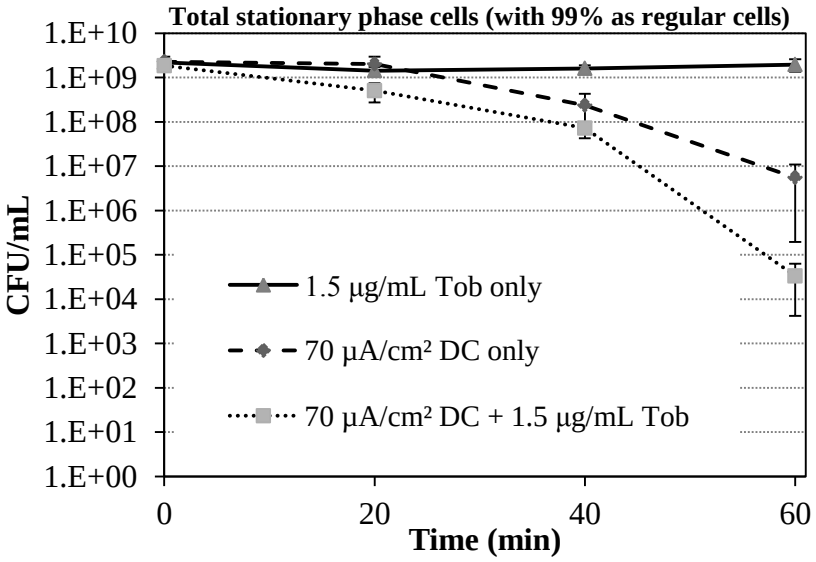
Total stationary phase cells (with 99% as regular cells)
1.E+10
1.E+09
1.E+08
1.E+07
1.E+06
1.E+05
1.E+04
1.E+03
1.E+02
1.E+01
1.E+00
CFU/mL
1.5 µg/mL Tob only
70 µA/cm² DC only
70 µA/cm² DC + 1.5 µg/mL Tob
0
20
40
60
Time (min)

(B)

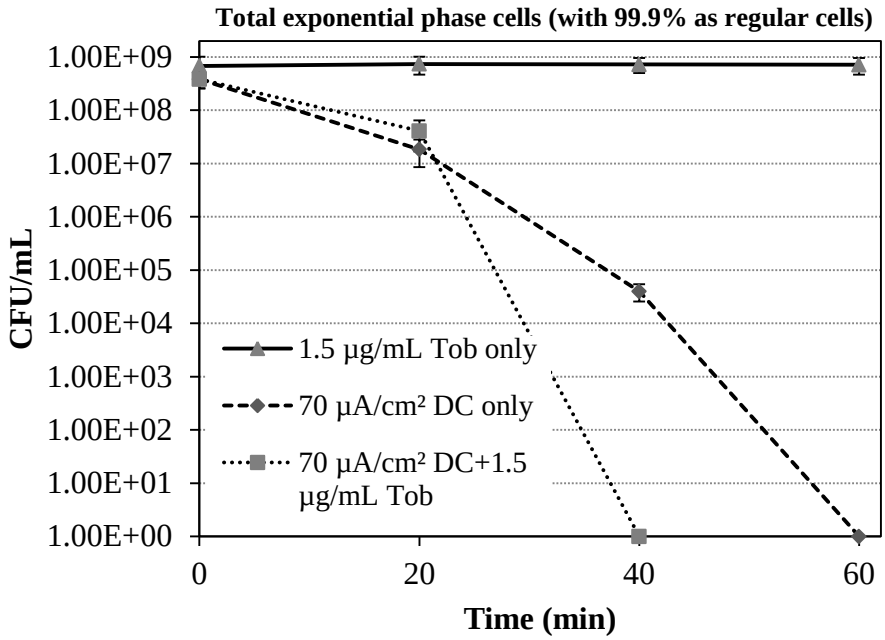
Total exponential phase cells (with 99.9% as regular cells)
1.00E+09
1.00E+08
1.00E+07
1.00E+06
1.00E+05
1.00E+04
1.00E+03
1.00E+02
1.00E+01
1.00E+00
CFU/mL
1.5 µg/mL Tob only
70 µA/cm² DC only
70 µA/cm² DC+1.5 µg/mL Tob
0
20
40
60
Time (min)

(C)

Figure 3.2

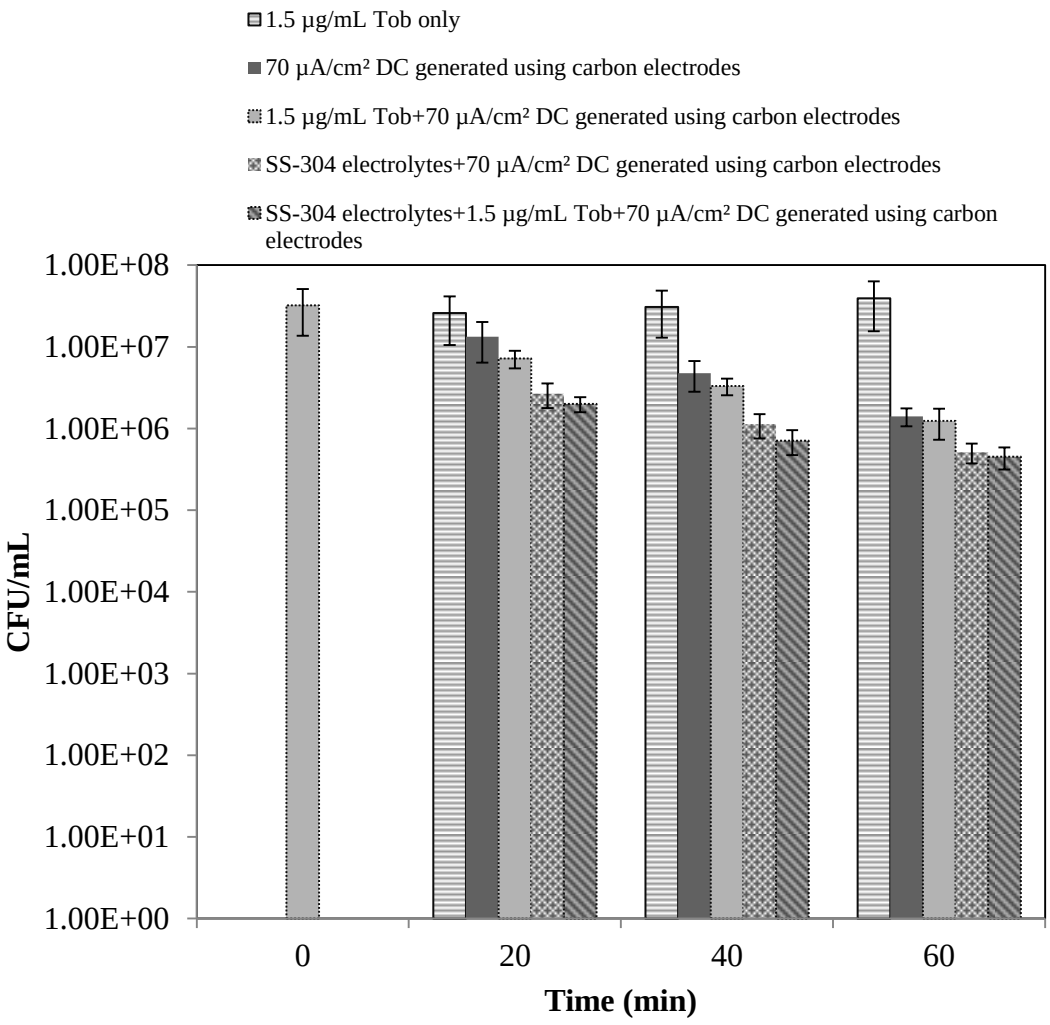
1.5 µg/mL Tob only
70 µA/cm² DC generated using carbon electrodes
1.5 µg/mL Tob+70 µA/cm² DC generated using carbon electrodes
SS-304 electrolytes+70 µA/cm² DC generated using carbon electrodes
SS-304 electrolytes+1.5 µg/mL Tob+70 µA/cm² DC generated using carbon electrodes
1.00E+08
1.00E+07
1.00E+06
1.00E+05
1.00E+04
1.00E+03
1.00E+02
1.00E+01
1.00E+00
CFU/mL
0
20
40
60
Time (min)

Figure 3.3

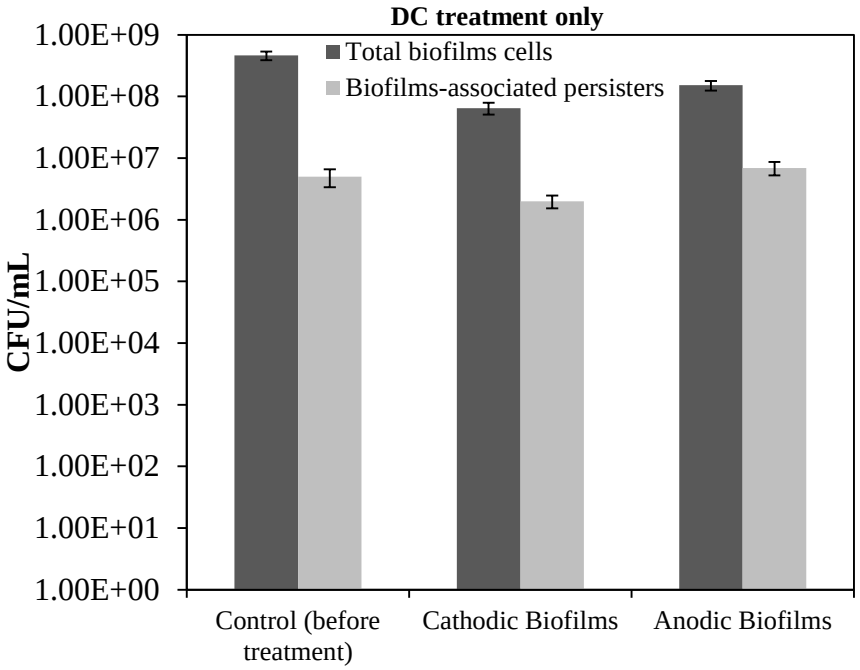
DC treatment only
Total biofilms cells
Biofilms-associated persisters
CFU/mL
1.00E+09
1.00E+08
1.00E+07
1.00E+06
1.00E+05
1.00E+04
1.00E+03
1.00E+02
1.00E+01
1.00E+00
Control (before treatment)
Cathodic Biofilms
Anodic Biofilms

(A)

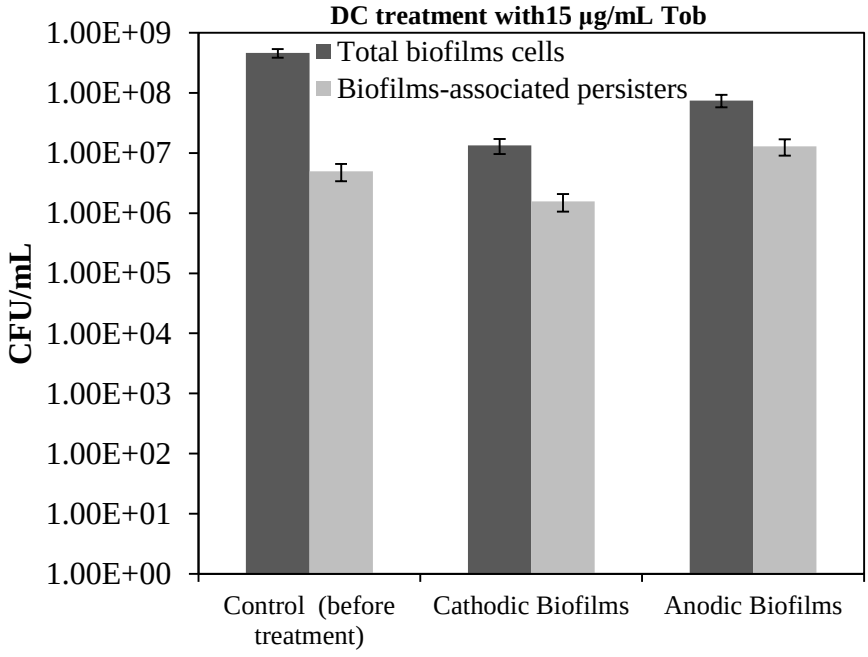
DC treatment with15 µg/mL Tob
Total biofilms cells
Biofilms-associated persisters
CFU/mL
1.00E+09
1.00E+08
1.00E+07
1.00E+06
1.00E+05
1.00E+04
1.00E+03
1.00E+02
1.00E+01
1.00E+00
Control (before treatment)
Cathodic Biofilms
Anodic Biofilms

(B)

Figure 3.4

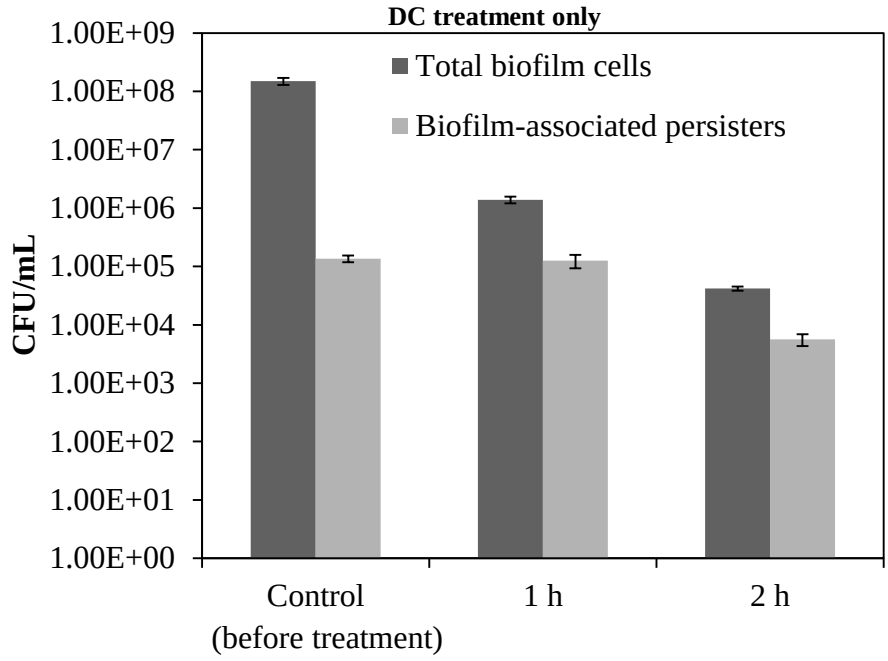
DC treatment only
Total biofilm cells
Biofilm-associated persisters
CFU/mL
1.00E+09
1.00E+08
1.00E+07
1.00E+06
1.00E+05
1.00E+04
1.00E+03
1.00E+02
1.00E+01
1.00E+00
Control
(before treatment)
1 h
2 h

(A)

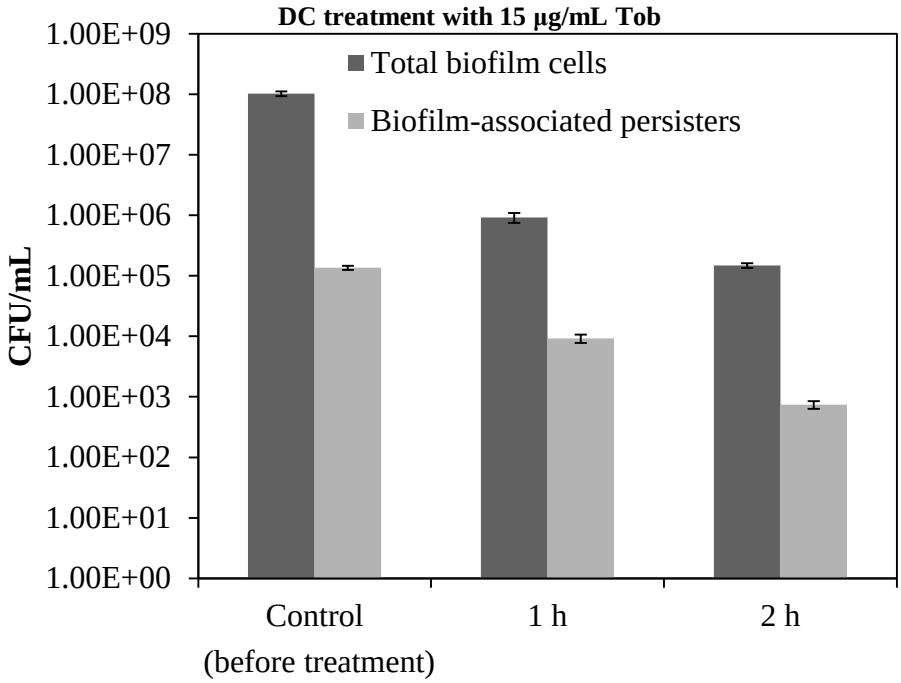
DC treatment with 15 µg/mL Tob
Total biofilm cells
Biofilm-associated persisters
CFU/mL
1.00E+09
1.00E+08
1.00E+07
1.00E+06
1.00E+05
1.00E+04
1.00E+03
1.00E+02
1.00E+01
1.00E+00
Control
(before treatment)
1 h
2 h

(B)

Figure 3.5

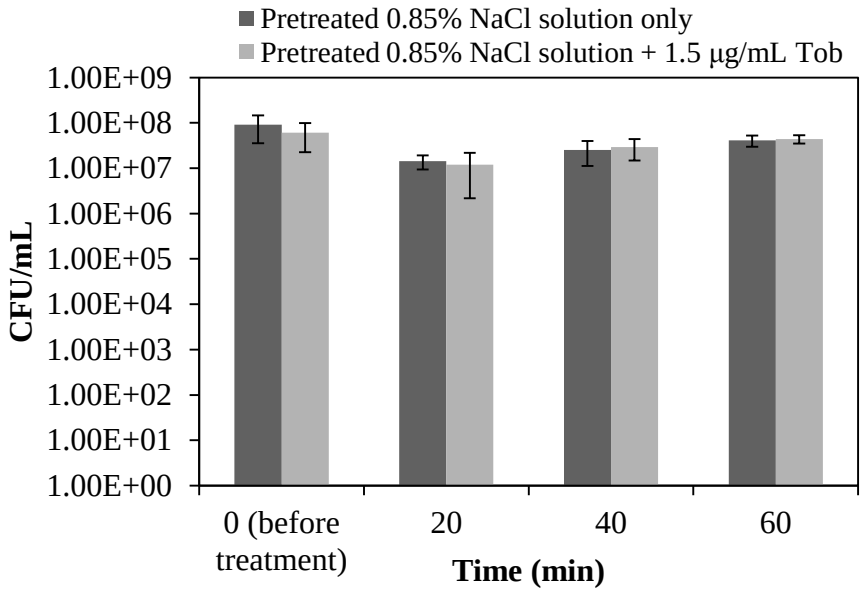
Pretreated 0.85% NaCl solution only
Pretreated 0.85% NaCl solution + 1.5 μg/mL Tob
1.00E+09
1.00E+08
1.00E+07
1.00E+06
1.00E+05
1.00E+04
1.00E+03
1.00E+02
1.00E+01
1.00E+00
CFU/mL
0 (before treatment)
20
40
60
Time (min)

Figure 3.6

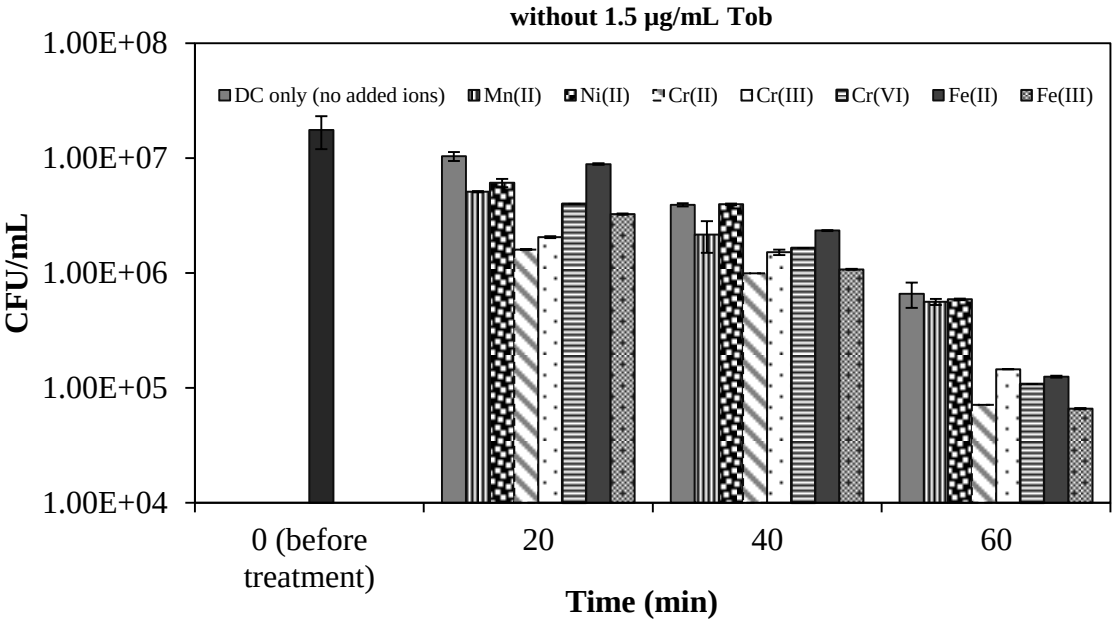
without 1.5 µg/mL Tob
1.00E+08
1.00E+07
1.00E+06
1.00E+05
1.00E+04
CFU/mL
DC only (no added ions)
Mn(II)
Ni(II)
Cr(II)
Cr(III)
Cr(VI)
Fe(II)
Fe(III)
0 (before treatment)
20
40
60
Time (min)

(A)

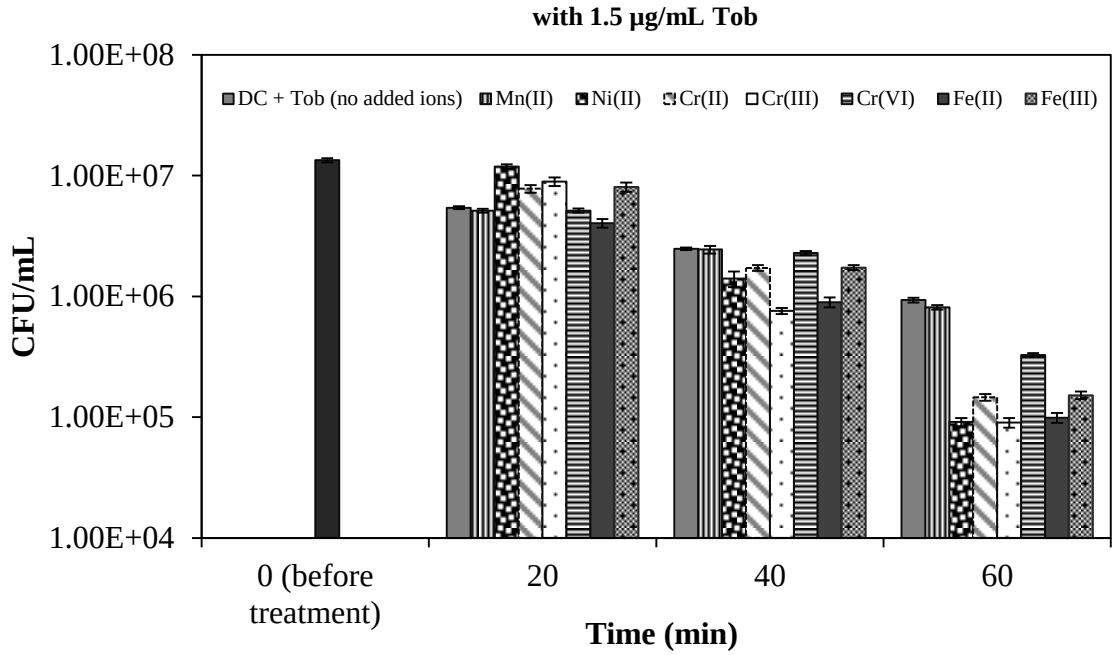
with 1.5 µg/mL Tob
1.00E+08
1.00E+07
1.00E+06
1.00E+05
1.00E+04
CFU/mL
DC + Tob (no added ions)
Mn(II)
Ni(II)
Cr(II)
Cr(III)
Cr(VI)
Fe(II)
Fe(III)
0 (before treatment)
20
40
60
Time (min)

(B)

Figure 3.7

CHAPTER 4

PERSISTER CONTROL USING TGON 805 IN SINGLE AND DUAL CHAMBER SYSTEMS

4.1. ABSTRACT

Electrochemical treatment of bacteria is a promising approach since it is effective in killing both the normal and persister cells. To further develop this technology for possible medical applications, it is important to understand the killing mechanisms of the electrochemical currents. In this chapter, the activity of the electrical field/potential, currents density and electrochemically-generated ions were investigated to determine how the electrochemical factors could be optimized to improve persister control. Electrode materials including stainless steel (SS) 304 and TGON 805 (a graphite-based material with electrochemical property similar to carbon electrode) were employed to develop various electrochemical systems, and to test their effects on *Pseudomonas aeruginosa* persister cells. Our findings demonstrated that the increase of the current density from 35 $\mu A/cm^2$ DC to 70 $\mu A/cm^2$ DC using TGON 805 resulted in persister killing from 65% to 100%; however, no killing was observed when the TGON 805 electrodes were separated in two individual chambers connected with a salt bridge. Under similar setting, the electrochemical species generated at cathodic SS 304 electrodes with 70 $\mu A/cm^2$ DC reduced the viability of persister cells by 99.6%.

4.2. INTRODUCTION

Control of microorganisms with electrochemical factors has been of a great interest to the field of bioelectrochemistry, and has led to the development of novel strategies for sterilization[1,2] and bioremediation[3,4]. However, the implementation of these techniques to control antibiotic-resistant bacterial infections remains challenging, in part due to the limited understanding of the electrophysiology of living cells, and lack of information regarding the electrochemical factors that affect cells.

The improved understanding of bacterial biofilms and the discovery of the persister cells, a dormant and antibiotic-tolerant microbial subpopulation, have contributed to the development of novel approaches to control multi-drug resistance and chronic infections *in vitro* and *in vivo*. For instance, treatment of *P. aeruginosa* biofilm with 70 $\mu A/cm^2$ DC can sensitize the treated cells to commonly used antibiotics such as Tob, Cip. DC was also found to enhance the activity of antibiotics on biofilm-embedded cells, a phenomenon referred to as bioelectric effects[5-7]. Moreover, metal cations in the mM range have been found to kill biofilm and persister cells. This is intriguing because DC treatment can also generate metal cations. However, as described in chapter 3, the metal ions alone (without DC) are not effective against persister cells, emphasizing on the importance of DC current. DC treatment of the persister cells of *P. aeruginosa* PAO1 using carbon and SS 304 electrodes resulted in the killing of 95.6 ± 5.4% and 97.7 ± 1.7%, respectively[9]. Under these conditions, the effects of the DC treatments were attributed to the electrochemical properties of the electrode materials and to the

movement of the electrochemical species and SS304-released cations generated during the treatments.

The control of the Gram-positive and Gram-negative bacteria with direct or alternating electric currents and potentials has been demonstrated in many *in vitro* studies. For instance, electric field comprised between 1V to 4V and generated with silver-nylon material [10] or gold electrodes [11] exhibited antibacterial activities against *P. aeruginosa, Staphylococcus aureus,* and *Escherichia coli*. In studies focusing on direct currents (DC) at μA to mA levels, the cidal[12] or inhibitory[13] effects on bacterial cells have been demonstrated using platinum, gold, stainless steel (SS) electrodes. However, in the most experimental systems, the effects of electric current, electric potential and electrochemical products are mixed; it is challenging to determine what factors are the most important. In Chapter 3, we demonstrated that carbon electrodes can generate low level DC and kill PAO1 persister cells. However, we found that carbon electrode could also release carbon particles that hinder the study of the effects of carbon-mediated DC at the cellular level. Meanwhile, we learned that TGON was made out of graphite fibers, which could be convenient for further study. In this chapter, the response of persister cells to electrochemical currents and fields generated with SS304 and TGON 805 (a carbon-based electrode) was investigated in a single and dual chamber systems to study the electrochemical factors separately.

4.3. MATERIALS AND METHODS

4.3.1. Bacterial strain and growth media.

The wild-type *P. aeruginosa* PAO1 was cultured in Luria-Bertani (LB) medium [15] containing 10 g/L tryptone, 5 g/L yeast extract, and 10 g/L NaCl. All overnight cultures were incubated at 37°C with shaking at 200 rpm.

4.3.2. Colony Forming Units (CFUs).

The colony forming units (CFUs) were counted to quantify the number of viable *P. aeruginosa* PAO1 cells before and during the electrochemical treatments. A volume of 20 μL of each sample was diluted in a 10× series using 0.85% NaCl solution and 10 μL of the last 6 dilutions was plated on LB agar plates (1.5% agar). The CFUs were counted on the next day after incubation overnight at 37°C.

4.3.3. Electrochemical properties of TGON 805

TGON 805 was purchased from Laird Technologies (Schaumburg, IL, USA). The manufacturer describes TGON 805 as a material made with more than 98% carbon. Before the material was used for the study, the electrochemical properties of TGON 805 were investigated. First, the composition of TGON 805 was examined using SEM with energy dispersive spectroscopy (SEM-EDS) (Joel 5600, Joel, Japan). To verify that the electrochemical properties of TGON 805 are similar to that of carbon, a polarization curve of TGON 805 was recorded over the range of -2 V to 1V, and compared to that of carbon, as reported in Chapter 3 (Fig. S3.5-Appendix I).

4.3.4. Effects of the DC treatment using TGON 805

The persister cells of *P. aeruginosa* PAO1 were isolated by treating the stationary phase cultures for 3.5 h with 200 µg/mL Cip. The harvested cells were washed twice with 0.85% NaCl solution, resuspended in 0.85% NaCl solution and treated with 35, 52.5 or 70 µA/cm^2 DC for 1 h. To deliver DC, an electrochemical cell was constructed by inserting two TGON 805 electrodes along the opposite sides of a plastic cuvette (Thermo Fisher Scientific, Pittsburg, PA). A silver wire (0.015" diameter, A-M Systems, Sequim, WA) was placed in bleach for 30 min to generate an Ag/AgCl reference electrode, which was then placed in the cuvette. DC was generated using a potentiostat (Potentiostat WaveNow, Pine Research Instrumentation, Raleigh, NC) in a 3-electrodes configuration as shown in Fig. 4.1. Using the AfterMath software (Potentiostat WaveNow, Pine Research Instrumentation, Raleigh, NC), a galvanostatic mode was selected to monitor the DC level and record the voltage across the electrochemical cell during the 1 h treatment. The cathodic potential was recorded using a voltmeter, while the anodic potential was recorded directly by the potentiostat. During the treatment, 100 µL of sample was taken every 20 min to evaluate the viability of PAO1 persister cells by counting CFU.

4.3.5. Effects of TGON 805 –released ions

In Chapter 3, we demonstrated that the electrochemical products generated by 70 µA/cm^2 DC using SS 304 did not affect the viability of PAO1 persister cells in the absence of DC[9]. To understand if the killing of the persister cells under DC using TGON were due to the chemical species generated by DC treatment using TGON 805, 0.85% NaCl solution without bacterial cells was treated with 70 µA/cm^2 DC generated using TGON 805

electrodes for 20 min, 40 min and 60 min, respectively. Then the PAO1 persister cells were incubated in these pretreated 0.85% NaCl solutions for 1 h to evaluate the effects of electrochemical species generated by TGON 805. The untreated 0.85% NaCl solution was used as a control. Viability of PAO1 cells was determined by counting CFU as described above.

4.3.6. Effects of electric field/potential

According to our electrochemical setup in this thesis research, the oxidizing currents were generated by the working electrodes. To more specifically evaluate how the electric potential and the electrochemical species generated at the working and counter electrodes affect the viability of PAO1 persister cells, a 2-chamber electrochemical cell connected by a salt bridge was constructed (Fig. 4.2). The counter electrodes were introduced in one chamber (counter chamber) of the electrochemical cell, while working and the Ag/AgCl electrode were placed in the other chamber (working chamber). Three milliliters of the PAO1 persister cell suspensions (OD_{600} of 0.7) were introduced in the chambers to treat the cells in the galvanostatic mode with 70 $\mu A/cm^2$ DC using SS304 and TGON 805 for 60 min. The number of viable cells present in each chamber was quantified by counting CFU in the solution as described above. This configuration provided different set of parameter to evaluate the effects of the treatments on the persisters. Under this condition, the salt bridge had a resistance of 22 kΩ. Because of the high resistance of the salt bridge connecting the chambers, only local fields that were determined by the anodic electrode potential (Ep_a) or cathodic electrode potential (Ep_c) were present in each corresponding chamber. The current profiles in both the working and the counter chambers were the

same; however, different electrochemical gradients were established in the two chambers due to the specific types of species generated in each chamber.

4.3.7. Statistical analysis.

SAS Software was used to conduct t-test and one-way ANOVA. Differences with $p < 0.05$ were considered as statistically significant.

4.4. RESULTS

4.4.1. Effects of DCs generated using TGON 805 in the single chamber system

The electrochemical analysis of TGON 805 using SEM-EDS showed that 99.9% of TGON is made up of carbon. In contrast to previously used graphite electrodes (Chapter 3), TGON exhibits interesting electrical properties because of its conductivity. The oxidation of TGON is initiated with a potential of -0.33 V vs. -0.07 V for carbon electrodes (Fig. 4.2), which suggests that TGON 805 could conduct electric current at lower potentials compared to carbon electrodes. To test the effects of the electrochemical currents generated using TGON 805 electrodes on PAO1 persister cells, the electrochemical cell shown in Fig. 4.1 was constructed to deliver different levels of DC and monitor the killing of PAO1 persister cells by counting CFUs. As shown in Fig. 4.3A, treatment of the persister cells with 70 $\mu A/cm^2$ DC for 40 min resulted in eradication of PAO1 persister cells corresponding to 7 logs of killing. In comparison, treatment with 52.5 $\mu A/cm^2$ and 35 $\mu A/cm^2$ DC for 60 min kill persister cells by 99.7 ± 0.0% (3 logs) and 65.1 ± 3.1 %, respectively. Although, similar electric fields were established under the current levels tested, the killing effects were highly different between 40 min and 60

min of treatment. Though, the killing effects were significantly different among three current levels, the electric potential varied very little (2.4 V – 2.7 V) and the electric potential during the treatment with 70 μA/cm^2 DC was not significantly different from that with 52.5 μA/cm^2 DC (one-way ANOVA, p=0.09).

4.4.2. Effects of TGON 805-released electrochemical species

To evaluate if the electrochemical products generated with the 70 μA/cm^2 DC treatment using TGON 805 had bactericidal effects on the cells, the persister cells were exposed for 1 h to 0.85% NaCl solutions pre-treated with 70 μA/cm^2 DC using TGON 805 for 20 min, 40 min and 60 min respectively. Fig. 4.4 shows that the exposure of PAO1 persister cells to 0.85% NaCl solutions pretreated with DC using TGON 805 significantly reduced the viability of the cells. The cell viability decreased by 61.4 ± 10.1% (one-way ANOVA, p=0.009) after 1 h incubation in the 20 min DC-treated 0.85% NaCl solution. No significant difference was found between the samples treated for 20 min, 40 min and 60 min (one-way ANOVA, p>0.13). These results justified that some species generated during the treatment with 70 μA/cm^2 DC using TGON 805 have cidal effects on PAO1 persister cells.

4.4.3. Effects of the electric potential

To understand the importance of electric field in ECCP, the PAO1 persister cells were introduced in an electrochemical cell comprising counter and working chambers connected with a high resistance salt bridge. The persister cells were treated with 70 μA/cm^2 DC and the number of viable cells in the chambers was quantified over 1 h. As

shown in Fig. 4.5A, the level of killing previously achieved in the single chamber system (with all three electrodes) with 70 μA/cm^2 DC using TGON was not attained in the 2-chamber system, suggesting that current density and the electrode potential were not enough for the complete eradication of the persister cells. However, more cells were found in the working chamber containing a positively charged anode, compared to the counter chamber with negatively charged cathode. The number of cells in the counter chamber was reduced by 47.7 ± 18.4% after 60 min of treatment, while the number of persister cells in the working chamber increased by 55.3 ± 18.7% during the same time period. However, the field profile of the chambers illustrated in Fig. 4.5B demonstrated that the Ep_a was stronger than the Ep_c. This led us to speculate if the persister response under this condition was linked to a galvanotaxic behavior or to the electrochemical species generated of in each chamber.

To comprehend if the electrochemical species or the field profile was the most determining factors for persister control under this condition, the persister cells of PAO1 were treated in the similar configuration using 70 μA/cm^2 DC mediated using SS 304. As shown in Fig. 4.6A, the DC treatment resulted in persister cell killing, in both the working and the counter chambers. The number of viable persister cells in the counter chamber was 99.6 ± 0.3%, corresponding to 3 logs reduction in cell viability. In contrast, the number of persister cells in the working chamber was reduced by 73.8 ± 2.5%. Consistent with the treatment of the PAO1 persister cells with 70 μA/cm^2 DC using TGON 805 in the 2-chamber system, improved killing activity was observed in the counter chamber. Unlike the treatment with TGON, however, the electric potential profile

of the electrodes showed that Ep_a was 10-15 times lower than the than Ep_c. The potential at the cathode was maintained as 1V, while the potential at the anode decreased from 0.2 V to 0.05 V. The results suggest that the reduction of persister cell viability in the working chamber was not caused by the electric potential, but instead by the electrochemical products moved across the electrochemical cell.

4.5. DISCUSSION

This study investigated the response of PAO1 persister cells to electrochemical stresses generated under various settings. To comprehend the effects of some electrochemical factors on ECCP, two electrochemical cells were constructed, and the effects of electric field, electric potential, current density and generated electrochemical species were examined. Our results demonstrated that the control of the persister cells by low-level electrochemical currents is the most effective when all electrodes where inserted on a single chamber. By varying the current density between 35 and 70 $\mu A/cm^2$ DC, dose dependent killing of PAO1 persister cells was observed in TGON 805-mediated treatments. However, such changes in current density led to little variation in the electric field suggesting that the rate of the electrochemical reaction at the electrodes may be a determining factor in ECCP. In the dual chamber system, the oxidation of TGON 805 occurred at the anode in the working chamber, while the generation of the reactive oxygen species (ROS), known for inducing cell killing through oxidative damage of the DNA[17,18], occurred at the cathode. Consistently, more killing was observed for the cells in the counter chamber. The finding that 61% PAO1 persister cells were killed by TGON treated 0.85% NaCl solutions in the absence of DC suggests that ROS may play a role.

However, the electrochemical properties of electrode materials have a great impact on the persister cells. The anodic current density of 70 μA/cm^2 DC generated with SS304 in the presence of a minimal electric potential comprised between 0.2 V and 0.05 V resulted in 73.8 ± 2.5% decreased viability of the persister cells that are located in the working chamber. In contrast, a higher electric potential of 1V was generated in the working chamber during the 70μA/cm^2 DC treatment using TGON 805. Under the latter condition, however, the anodic current density of 70 μA/cm^2 DC failed to reduce the viability of persister cells. These results suggest that the movement of the metal cations resulting from the oxidation of SS304 may disrupt the integrity of the cells membrane and cause cells death, consistent with our previous finding (Chapter 4). In fact, intracellular accumulation of metal cations, such as those derived from iron or chromium elements, is well known to induce oxidation damage and cell killing[19-21]. Our data provide evidence that the rate of generation of specific cationic species (moving from the anode towards the cathode), instead of the difference in potential across of working chamber, controls the fate of PAO1 persister cells under these conditions.

It is interesting that the electric potential of cathodic SS 304 and TGON electrodes were comparable (1V vs. 0.9V) to each other and the current density in both conditions was similar. However, the viability of the persister cells after the treatment with cathodic SS 304 electrode was reduced by 99.6 ± 0.3%, while the number of viable persisters under treatment with TGON electrodes was reduced by 55.3 ± 18.7%. Further study will help understand if the TGON 805-treated cells found in the counter chamber were killed or moved to the working chamber by galvanotaxis.

Understanding the effects of the electrical potential, electric current and electrochemical products on the viability of bacteria is important for designing the *in vivo* study. Treatments of persister cells in the 2-chamber system provided valuable information for the design of *in vivo* model of electrochemical treatment. A major challenge in delivering appropriate levels of currents to deep tissue is linked to the resistance of skin and tissues. The 2-chamber configuration presents an interesting model to evaluate the effectiveness of an electrochemical treatment while accounting for the resistance in the path of the ionic flow. Our results revealed that the cathodic electrode potential and the related electrochemical species of SS304 contributed to the effectiveness of the treatment. Although TGON 805 was also very effective in 1-chamber configuration, the potency of the treatment was diminished in the 2-chamber system, suggesting that this material may perform poorly *in vivo* due to the impedance of animal tissues. In comparison, the effects of the electrochemical cationic species generated with SS304-mediated were significant. The findings of this study indicate that persister cells could be effectively controlled with cathodic current/potential, and suggest that SS 304 may be appropriate for *in vivo* control of bacterial infections.

4.6. CONCLUSIONS

The comparative study of the effects of the electrochemical agents on the viability of persister cells had demonstrated that DC, electrical field/potential and the related electrochemical species contribute differently to the potency of the electrochemical systems. While the density at current flow and the type of ions moving across an

electrochemical cell directly impact the viability of cells, their effects could be enhanced in the presence of cathodic oxidative stress, and in the presence of a greater electric field. The 2-chamber electrochemical system revealed that effective control of persister cells could be achieved in spite of a high resistance in the path of the electrochemical flow, which could be experimented in infection models *in vivo*.

4.7. ACKNOWLEDGEMENTS

We are grateful to Blue Highway Inc. for supporting the project. We thank Dr. Thomas K. Wood at Penn State University for sharing the strain *P. aeruginosa* PAO1. We appreciate Dr. Jeremy L. Gilbert (Syracuse Biomaterial Institute) for his insightful contribution to the understanding of the electrochemical systems.

4.8. REFERENCES

1 **Jayaram, S. H.** Sterilization of liquid foods by pulsed electric fields. *Electrical Insulation Magazine, IEEE* 16, 17-25 (2000).

2 **Zhang, Q., Barbosa-Cánovas, G. V. & Swanson, B. G.** Engineering aspects of pulsed electric field pasteurization. *Journal of Food Engineering* 25, 261-281 (1995).

3 **Park, J.-C., Lee, M. S., Lee, D. H., Park, B. J., Han, DW., Uzawa, M., Takatori, K.** Inactivation of bacteria in seawater by low-amperage electric current. *Applied and environmental microbiology* 69, 2405-2408 (2003).

4 **Wick, L. Y., Shi, L. & Harms, H.** Electro-bioremediation of hydrophobic organic soil-contaminants: A review of fundamental interactions. *Electrochimica Acta* 52, 3441-3448 (2007).

5 **Costerton, J. W., Ellis, B., Lam, K., Johnson, F. & Khoury, A. E.** Mechanism of electrical enhancement of efficacy of antibiotics in killing biofilm bacteria. *Antimicrobial agents and chemotherapy* 38, 2803-2809 (1994).

6 **Del Pozo, J. L., Rouse, M. S. & Patel, R.** Bioelectric effect and bacterial biofilms. A systematic review. *International Journal of Artificial Organs* 31, 786-795 (2008).

7 **Szkotak, R., Niepa, T. H., Jawrani, N., Gilbert, J. L., Jones, M. B., Ren, D.** Differential Gene Expression to Investigate the Effects of Low-level

Electrochemical Currents on *Bacillus subtilis*. *AMB Express* 1, 39, doi:10.1186/2191-0855-1-39 (2011).

8 **Harrison, J. J., Turner, R. J. & Ceri, H.** Persister cells, the biofilm matrix and tolerance to metal cations in biofilm and planktonic *Pseudomonas aeruginosa*. *Environmental microbiology* 7, 981-994 (2005).

9 **Niepa, T. H., Gilbert, J. L. & Ren, D.** Controlling *Pseudomonas aeruginosa* persister cells by weak electrochemical currents and synergistic effects with tobramycin. *Biomaterials* 33, 7356-7365, doi:10.1016/j.biomaterials.2012.06.092 (2012).

10 **Marino, A. A., Deitch, E. A., Albright, J. A. & Specian, R. D.** Electrical augmentation of the antimicrobial activity of silver-nylon fabrics. *Journal of Biological Physics* 12, 93-98 (1984).

11 **Zituni, D., Schütt-Gerowitt, H., Kopp, M., Krönke, M., Addicks, K., Hoffmann, C., Hellmich, M., Faber, F., Niedermeier, W.** The growth of *Staphylococcus aureus* and *Escherichia coli* in low-direct current electric fields. *International journal of oral science* (2013).

12 **Del Pozo, J. L., Rouse, M. S., Mandrekar, J. N., Steckelberg, J. M. & Patel, R.** The electricidal effect: reduction of Staphylococcus and pseudomonas biofilms by prolonged exposure to low-intensity electrical current. *Antimicrobial agents and chemotherapy* 53, 41-45, doi:10.1128/AAC.00680-08 (2009).

13 **Falcone, A. E. & Spadaro, J. A.** Inhibitory effects of electrically activated silver material on cutaneous wound bacteria. *Plastic and reconstructive surgery* 77, 455-458 (1986).

14 **Rowley, B. A.** Electrical Current Effects on E. coil Growth Rates. *Experimental Biology and Medicine* 139, 929-934 (1972).

15 **Sambrook, J. & Russell, D. W.** *Molecular cloning: a laboratory manual*. Vol. 3 (Cold spring harbor laboratory press, 2001).

16 **Chen, C.-Y., Nace, G. W. & Irwin, P. L.** A 6× 6 drop plate method for simultaneous colony counting and MPN enumeration of *Campylobacter jejuni, Listeria monocytogenes,* and *Escherichia coli*. *Journal of microbiological methods* 55, 475-479 (2003).

17 **Keyer, K., Gort, A. S. & Imlay, J. A**. Superoxide and the production of oxidative DNA damage. *Journal of bacteriology* 177, 6782-6790 (1995).

18 **Wu, Y., Vulic, M., Keren, I. & Lewis, K.** Role of oxidative stress in persister tolerance. *Antimicrobial agents and chemotherapy* 56, 4922-4926, doi:10.1128/AAC.00921-12 (2012).

19 **Miller, R. A. & Britigan, B. E.** Role of oxidants in microbial pathophysiology. *Clinical Microbiology Reviews* 10, 1-18 (1997).

20 **McCormick, M. L., Buettner, G. R. & Britigan, B. E.** Endogenous superoxide dismutase levels regulate iron-dependent hydroxyl radical formation in *Escherichia coli* exposed to hydrogen peroxide. *Journal of bacteriology* 180, 622-625 (1998).

21 **Chang, W., Small, D. A., Toghrol, F. & Bentley, W. E.** Microarray analysis of *Pseudomonas aeruginosa* reveals induction of pyocin genes in response to hydrogen peroxide. *BMC genomics* 6, 115 (2005).

FIGURE CAPTIONS

Figure 4.1. Schematic representation of the electrochemical cell system for generating electric currents in this study. The single chamber electrochemical cell (A) was constructed by inserting two electrodes (4.5 cm x 0.95 cm x 0.05 cm) in a plastic cuvette. The working, counter and reference electrodes were connected to a potentiostat to deliver the desired current. In the 2-chamber electrochemical cell (B) the working and the Ag/AgCl reference electrode were placed in the working chamber, while the counter electrode was introduced in the counter chamber. The chambers were connected by a salt bridge.

Figure 4.2. SEM-EDS was performed to determine the composition of TGON. A representative SEM image (A) shows that TGON 805 is composed of graphite fibers. The polarization curve of TGON 805 electrodes is also shown (B). Voltages ranging from -2V to 1V (vs. Ag/AgCl potential) were generated across sterile 0.85% NaCl solution using TGON 805 electrodes. Voltammograms were recorded at a polarization scan rate of 1 mV/s.

Figure 4.3. Effects of DC treatment on *P. aeruginosa* PAO1 planktonic persister cells. All samples were treated in the 1-chamber electrochemical cell with 70 $\mu A/cm^2$ DC using TGON 805 for 1 h (A). The electric field of the treatment was recorded (B).

Figure 4.4. The effects of TGON 805-generated electrolytes on *P. aeruginosa* PAO1 persister cells. Sterile 0.85% NaCl buffer was pretreated for 0, 20, 40 or 60 min with 70 $\mu A/cm^2$ DC and the persister cells were exposed to the electrolytes for 1

h in the absence of Tob or electrical current/field. The number of viable cells was quantified by counting CFU.

Figure 4.5. Effects of DC treatment on *P. aeruginosa* PAO1 planktonic persister cells. All samples were treated in a 2-chamber electrochemical cell with 70 μA/cm^2 DC using TGON 805 for 1 h (A). The electric field of the treatment was recorded (B).

Figure 4.6. Effects of DC treatment on *P. aeruginosa* PAO1 planktonic persister cells. All samples were treated in the 2-chamber electrochemical cell with 70 μA/cm^2 DC using SS 304 for 1 h (A). The electric field of the treatment was recorded (B).

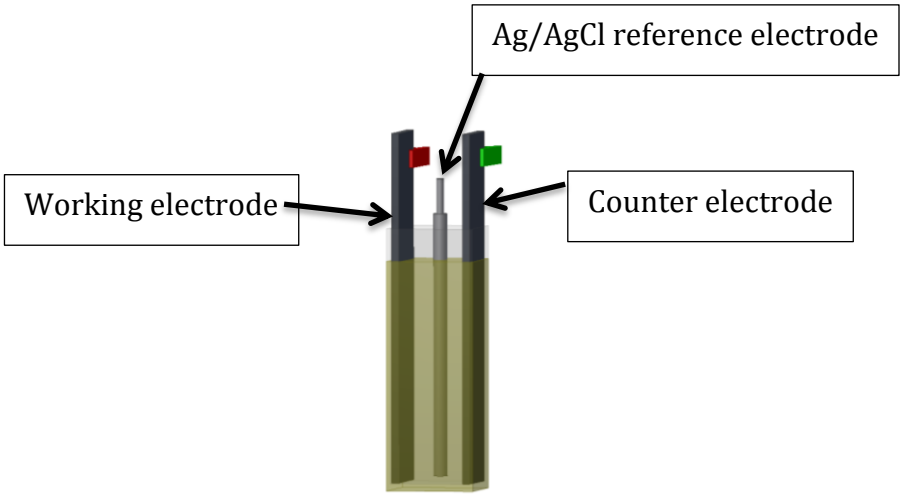
Ag/AgCl reference electrode
Working electrode
Counter electrode

(A)

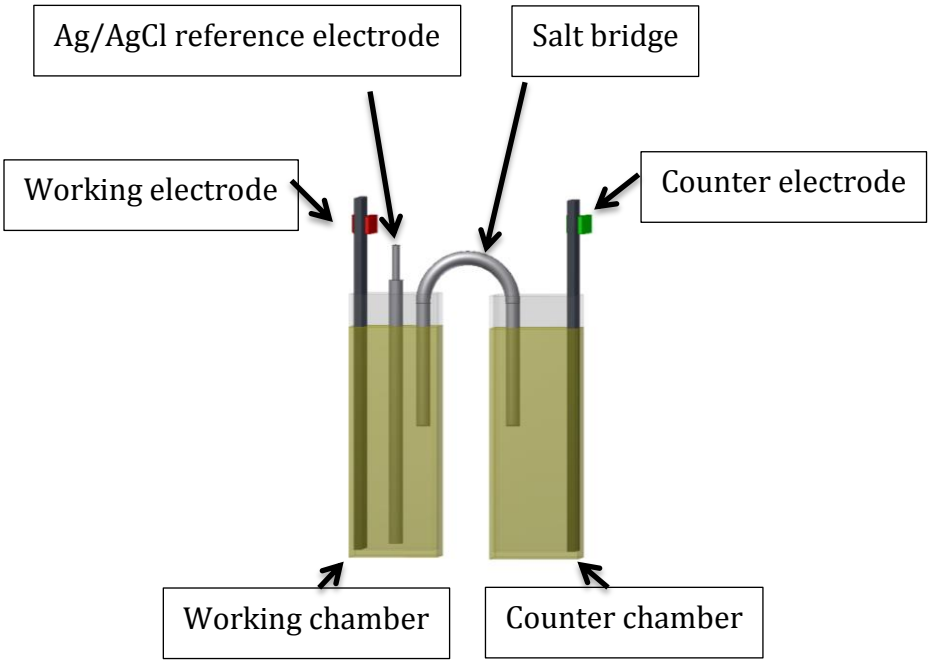
Ag/AgCl reference electrode
Salt bridge
Working electrode
Counter electrode
Working chamber
Counter chamber

(B)

Figure 4.1

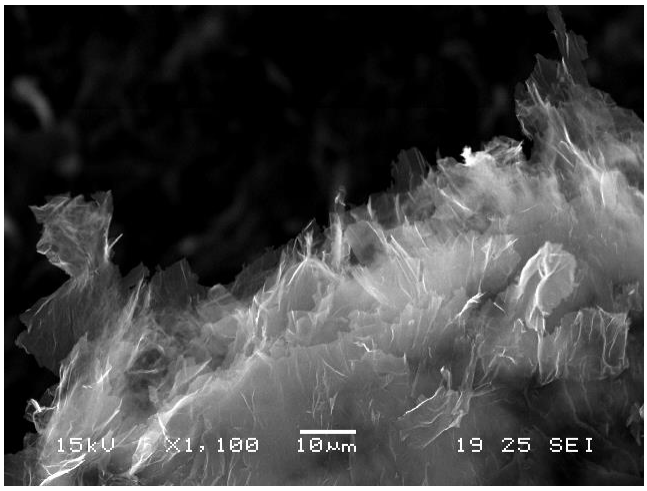
15kV X1,100 10µm 19 25 SEI

(A)

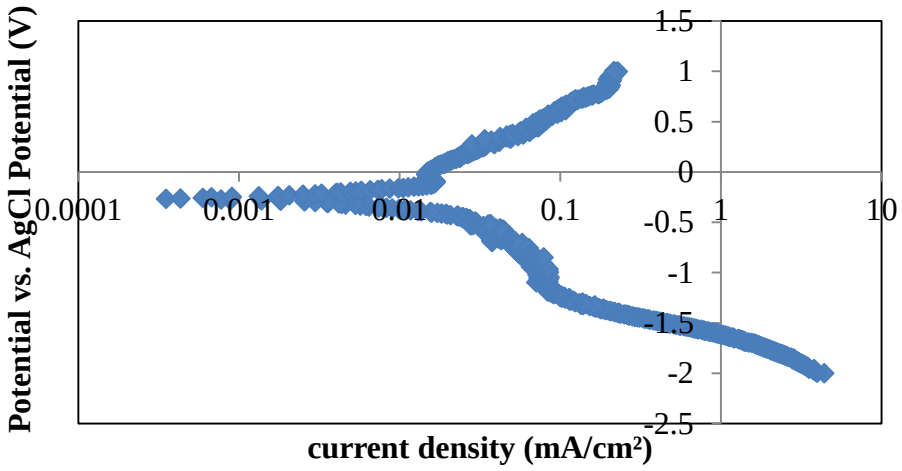
Potential vs. AgCl Potential (V)
1.5
1
0.5
0
-0.5
-1
-1.5
-2
-2.5
0.0001
0.001
0.01
0.1
1
10
current density (mA/cm²)

(B)

Figure 4.2

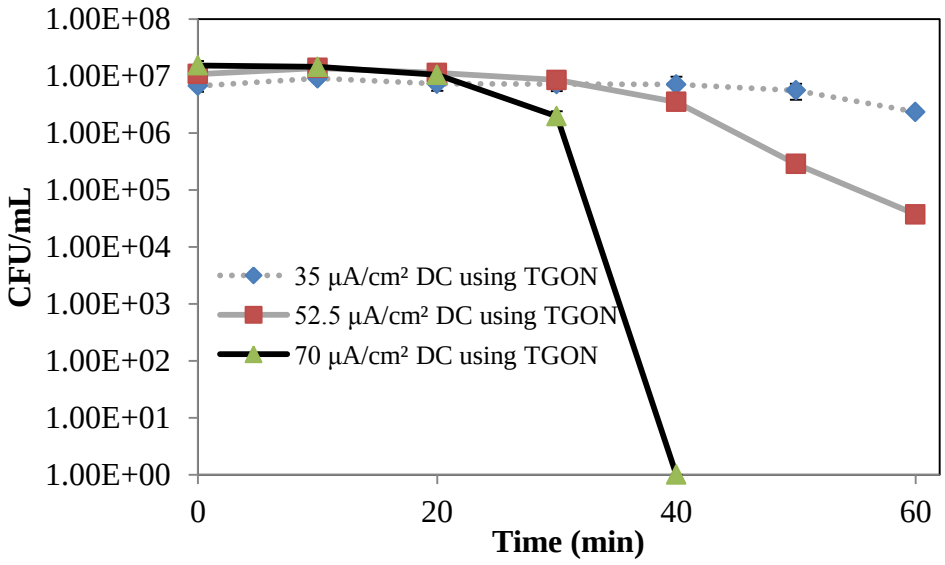

(A)

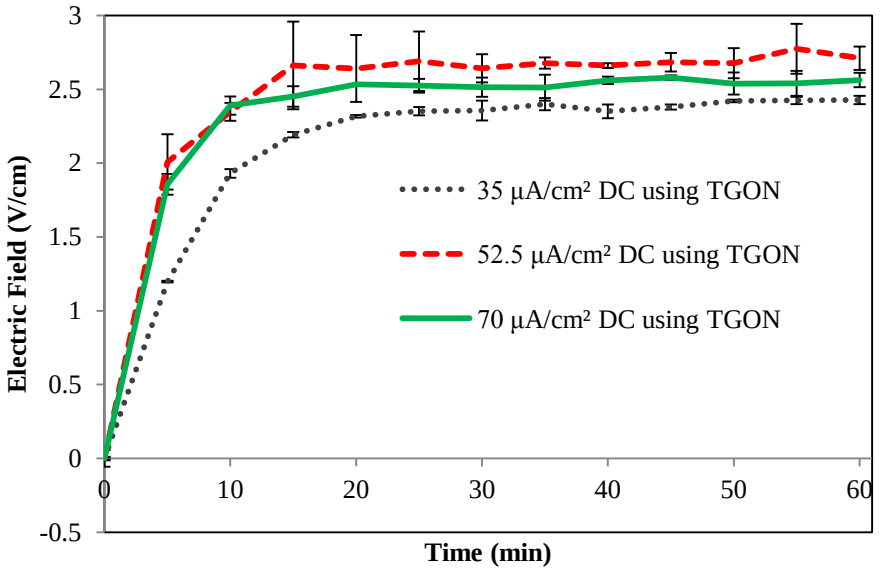

Dose dependent voltage picture with SS

(B)

Figure 4.3

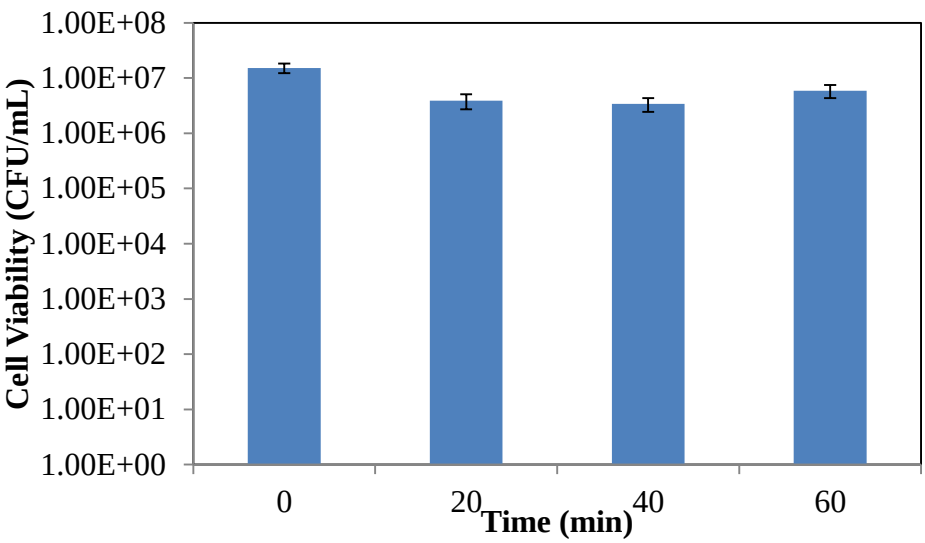
1.00E+08
1.00E+07
1.00E+06
1.00E+05
1.00E+04
1.00E+03
1.00E+02
1.00E+01
1.00E+00
Cell Viability (CFU/mL)
0
20
40
60
Time (min)

Figure 4.4

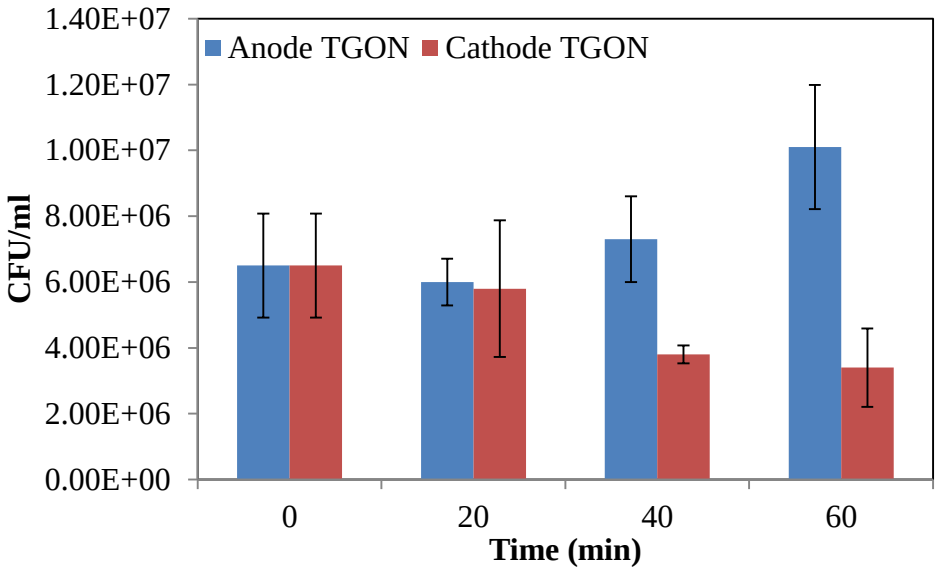
1.40E+07
1.20E+07
1.00E+07
8.00E+06
6.00E+06
4.00E+06
2.00E+06
0.00E+00
CFU/ml
Anode TGON
Cathode TGON
0
20
40
60
Time (min)

(A)

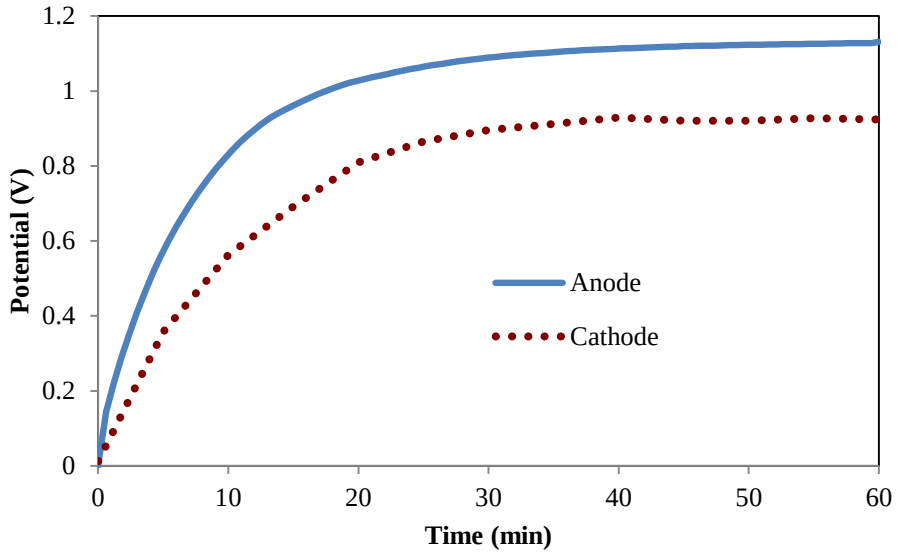
1.2
1
0.8
0.6
0.4
0.2
0
Potential (V)
Anode
Cathode
0
10
20
30
40
50
60
Time (min)

(B)

Figure 4.5

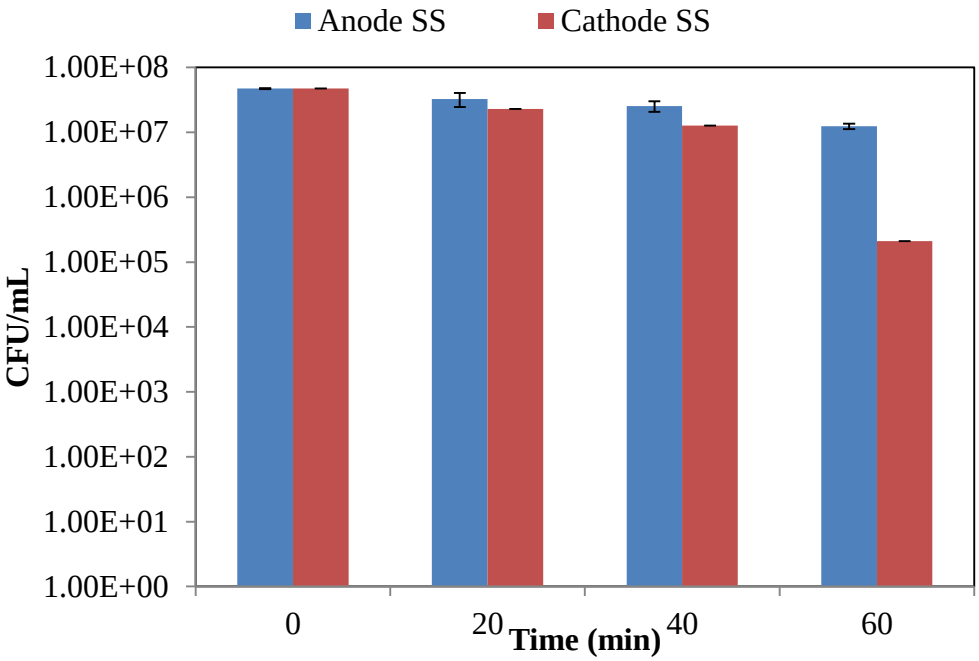
Anode SS
Cathode SS
1.00E+08
1.00E+07
1.00E+06
1.00E+05
1.00E+04
1.00E+03
1.00E+02
1.00E+01
1.00E+00
CFU/mL
0
20
40
60
Time (min)

(B)

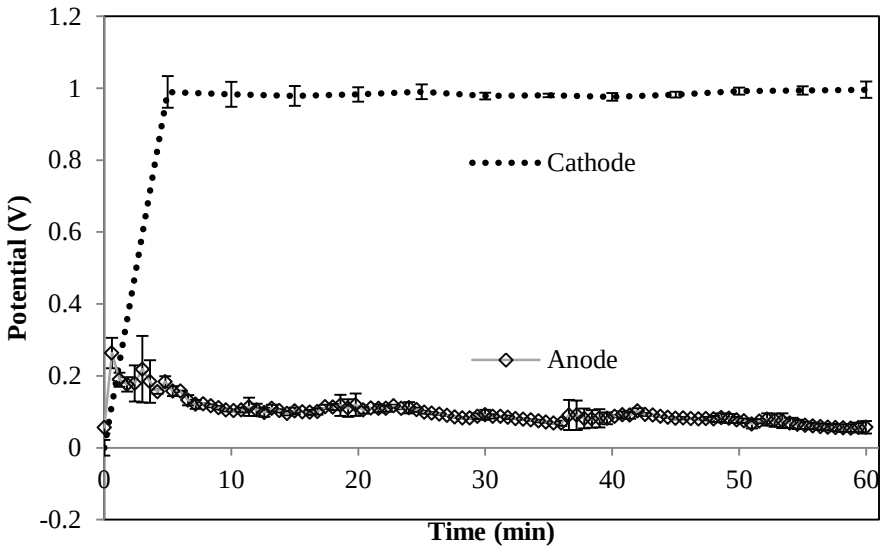
1.2
1
0.8
0.6
0.4
0.2
0
-0.2
Potential (V)
Cathode
Anode
0
10
20
30
40
50
60
Time (min)

(B)

Figure 4.6

CHAPTER 5

SENSITIZING *PSEUDOMONAS AERUGINOSA* CELLS TO ANTIBIOTICS BY ELECTROCHEMICAL DISRUPTION OF MEMBRANE FUNCTIONS

Henry Lars Peterson contributed to the study of the protein expression of *P. aeruginosa* cells treated with direct current using SS 304 electrodes. Shiril Sivan contributed to the nanoindentation of the cells using AFM.

5.1 ABSTRACT

The increasing prevalence of antibiotic-resistant bacteria referred to as ESKAPE pathogens (*Enterococcus faecium, Staphylococus aureus, Klebsiella pneunomoniae, Acinetobacter baumanii, Pseudomonas aeruginosa,* and *Enterobacteriaceae*) has presented a great challenge to infection control. *P. aeruginosa* in particular, in addition to its intrinsic multi-drug resistance, develop community protection mechanisms by forming multicellular structures, known as biofilms, which harbor a subpopulation of dormant cells such as the persister cells. Conventional methods of antibacterial treatment involving high doses of antibiotics or surgical interventions have proven insufficient for eradicating persistent infections associated with these structures. Recently, we reported that bacterial persister cells can be eliminated through synergistic effects between low-level electric current and antibiotics, a phenomenon we named electrochemical control of persister cells (ECCP). To understand the mechanism of ECCP, the electrophysiological changes in *P. aeruginosa* cells induced by DC treatment were characterized at the cellular and genetic levels. TEM and SEM-EDS analyses revealed that DC treatments affected membrane integrity and functions of *P. aeruginosa,* owing to the increase in cellular concentration of metal ions and a subsequent change in the cell surface charge. DC treatments also led to the compartmentalization of cellular contents, release of outer membrane vesicles, and cell lysis. Moreover, electrochemical treatments mediated via carbon electrodes provoked the permeabilization of the cells, increased their susceptibility to antibiotics, and led to complete eradication of the persisters. These results provide new insight for designing novel systems to effectively control infections associated with biofilms and persister cells.

5.2. INTRODUCTION

Each year, millions of medical devices with various complexities are implanted in humans to palliate failing body components. The implantation of biomaterials can lead to recurrent complications associated with the adherence of microbial pathogens on these devices and the development of chronic infections in the surrounding tissues. Such implant-associated infections account for around half of the cases of hospital-acquired infections. In the U.S. alone, 5% of the 2 million individuals receiving fracture fixation each year are infected with bacteria adhering to the implants. The incidence is even higher when it comes to ventricle-assisted heart implants, which have a 40% infection rate [1]. According to the Center of Diseases Control, $45 billion was spent in 2007 to cover the inpatient services associated with infections acquired in US hospitals [2]. This constitutes a high burden for the healthcare system and seriously affects the life quality of these patients [3].

Chronic and drug-tolerant infections remain as major challenge for modern medicine. In recent years, few antibiotics have been developed and approved by the U.S. Food and Drug Administration (FDA). In the past three decades (1980-2009), 29, 23 and 9 antibiotics were approved, respectively [4]. However, 26 among the antibiotics approved between 1980 and 1999 have been withdrawn already [4], an alarming decline that raises calls for more action toward the development of new therapeutics [5]. In comparison, new antibiotic-resistant bacteria are emerging with an increasing frequency [6].

Multiple intrinsic and acquired mechanisms of bacterial cells provide them with

remarkable resistance against antibiotics. It is well documented that bacteria can obtain resistance by degrading antibiotics or modifying their cellular targets[7]. Bacteria can also regulate their membrane properties to selectively control nutrient up-take while extruding antibiotics using efflux pumps [8,9]. In addition to these mechanisms, the failure of antibiotics in curing chronic infections is also partially due to the ineffectiveness of these drugs against dormant or slow growing cells. In general, antibiotics corrupt the major growth-related pathways, such as DNA replication, by interacting with cellular targets [10]. Increasing evidence indicates that bacterial populations contain a small percentage of phenotypic variants, known as persister cells, which are dormant and extremely tolerant to antibiotics. Although persister cells represent less than 1% of the total population [11], they can wake up from their dormant state after antibiotic treatment, and regenerate a new bacterial population with similar percentage of persister cells. Such persistence presents a great challenge to treatment of chronic infections [12,13]. Beyond these intrinsic capabilities of individual persister cells to survive the attack of the antibiotics, bacteria can also obtain high-level tolerance to antibiotics by attaching to surfaces and forming biofilms, a condition that is very common with implant-associated infections and cystic fibrosis [1,13,14]. Biofilm cells are embedded in an extracellular matrix produced by attached cells and comprised of polysaccharides, proteins, and extracellular DNA. Biofilms also harbor many slow growing cells including persister cells. Consequently, a large number of biofilm-associated cells can tolerate antibiotics at concentrations up to 1000 times higher than those required to kill their planktonic (free swimming) counterparts [15]. These challenges emphasize the need for novel techniques that could eradicate bacterial infections involving persister cells and biofilms.

To control biofilm formation, antifouling and antimicrobial surfaces are being developed with topographic modification and antimicrobial coatings. However, these surfaces are not ideal for long-term prevention against bacterial colonization and cannot treat existing biofilms. Other approaches involving physical, chemical and electrical factors may be advantageous. Recently, we introduced a novel method for controlling bacterial persistence based on a phenomenon we named electrochemical control of persister cells (ECCP). We reported that persister cells isolated from *Pseudomonas aeruginosa* could be killed by 98% using low-level direct current (70 μA/cm^2 DC) for 1 h. Also, DC was found to enhance the killing activities of Tob in a combined treatment, showing an interesting synergy equivalent to 5-log killing[11]. To understand the mechanism of ECCP, we use complementary approaches to systematically characterize the electrophysiological changes in *P. aeruginosa* induced by the electrochemical treatments at the cellular levels. The data will help better understand the mechanism of ECCP and design novel therapeutic systems against chronic infections associated with biofilms and persister cells.

5.3. MATERIALS AND METHODS

5.3.1. Bacterial strain and Persister isolation

The wild-type *P. aeruginosa* PAO1 (henceforth PAO1) was cultured in Luria-Bertani (LB) medium [16] containing 10 g/L tryptone, 5 g/L yeast extract, and 10 g/L NaCl. Each overnight culture was incubated at 37°C with shaking at 200 rpm. To isolate persister cells, the cells from overnight cultures were harvested by centrifugation (Sorvall Legend RT, Thermo Scientific, Asheville, NC) at 8000 rpm for 10 min, washed twice with 0.85%

NaCl, and treated with 200 μg/mL Cip for 3.5 h at 37°C with gyratory rotation (200 rpm). Finally, the cells were washed three times with 0.85% NaCl to remove the antibiotic and the debris of lyzed cells.

5.3.2. Synergy between DC and antibiotics: sequential treatment

To understand the mechanism of electrochemical control of persister cells (ECCP), the efficacy of the antibiotics in killing persister cells was evaluated following DC treatment. To evaluate the ability of DC alone to reduce bacterial persistence, DC treatment was performed before persister isolation. Thus, stationary phase PAO1 cells were collected from overnight cultures by centrifugation and washed twice with 0.85% NaCl. The cells were then resuspended in 0.85% NaCl to reached OD_{600} of 0.9. A 3 mL cell suspension was transferred to a polystyrene electrochemical cell to perform DC treatment as previously described [11]. Using either carbon or SS 304 electrodes, a current density of 70 $\mu A/cm^2$ DC was generated across the electrochemical cell to treat the samples for 60 min. Immediately after the DC treatment, the samples were well-mixed and 1 mL of the samples was diluted in 10× series using 0.85% NaCl, spread on LB agar (1.5% agar) and cultured at 37ºC for 16 h to quantify the total number of viable cells by counting colony-forming units (CFUs). Similarly the total number of viable cells within the untreated samples was quantified. However, to determine the number of cells that remain as persister cells, the DC-free and the DC-treated samples were introduced in microcentrifuge tubes and treated for persister isolation as described above. Then the samples were resuspended in 0.85% NaCl, and 10× serial dilutions were performed to

culture the viable persister cells on LB agar plates (1.5% agar) overnight. Finally, CFU were counted to evaluate the change in the persister level.

The ability of DC to sensitize PAO1 persister cells to various antibiotics was also investigated on PAO1 persister cells isolated from overnight culture. The persister cells were first resuspended in 0.85% NaCl at OD_{600} of 0.6 and then, treated with 70 $\mu A/cm^2$ DC using carbon or SS 304 electrodes for 1 h. Immediately thereafter, the DC-treated persister cells were further challenged with 1.5 µg/mL Tob, 60 µg/mL kanamycin (Kan), or 60 µg/mL spectinomycin (Spec) for 1 h. To evaluate if the cells could recover cellular functions after DC treatment is stopped, the antibiotics were added to the suspensions of DC-treated persister cells 15 or 30 min following DC treatments. The viability of persister cells was assessed after the sequential treatments by plating the samples on LB agar plates in a 10× serial dilution and counting CFU. Furthermore, to assess if cell recovery was dependent on nutrient availability, PAO1 persisters were challenged with 70 $\mu A/cm^2$ DC using either carbon or SS 304 electrodes for 60 min. Immediately after DC treatments, the cells were introduced in 96 well plate containing LB medium with or without antibiotics to an OD_{600} of 0.05. The cells were incubated at 37° C in the presence or absence of 1.5 µg/mL Tob, 60 µg/mL Spec, and 60 µg/mL Kan for 6 h and the growth curves were recorded by reading OD_{600} using a fluorescence microplate reader (Biotek, VT, USA).

5.3.3. Membrane integrity of *P. aeruginosa* PAO1 cells

First, propidium iodine (PI), a membrane impermeable dye, was used to evaluate

membrane integrity. The stationary phase cells of PAO1 were resuspended in 0.85% NaCl to OD_{600} of 1.5 and treated with DC using carbon or SS 304 electrodes, as described above. Immediately and at 15 and 30 min after DC treatment, 1.5 µL PI was added in 1 mL sample to stain the cells for 15 min. The cells were then washed using 0.85% NaCl to remove non-specifically bound dye and the absorbance of PI by the cells was determined using a fluorescence plate-reader at excitation and emission wavelength of 530/25 and 590/35 nm, respectively (Synergy 2 Multi-Mode Microplate Reader, Biotek, VT)

A complementary approach using Transmission electron microscope (JEOL 2000EX, JOEL, Japan) was used to examine the membrane integrity of the treated and untreated cells. One hundred µL of the samples was fixed in 400 µL of 2.5% glutaraldehyde. The cells were attached to a copper grid (T400H-Cu, Electron Microscopy Science, PA) and allowed to fully dry at room temperature. Different staining methods have been tested to optimize imaging quality. Initially, the samples were stained with methylamine vanadium (NanoVan®, Nanoprobes Inc., NY) to observe the morphology of cells through TEM. To acquire a well-defined contrast among cellular features such as intracellular compartments, a complementary approach was taken to stain the DC-treated cells for 15 s with uranyl acetate, which heavy metal elements provides better contrast agents compared to methylamine vanadium. The staining was followed by three successive washes with HPLC grade water, drying of the grid at room temperature, and TEM imaging. To investigate the effects of DC on the membrane integrity of the cells, further analysis was performed to acquire transections of the cells

and examine the structural changes in the cell membranes at 20, 40 and 60 min of the DC treatments. To achieve this, PAO1 cells in stationary phase were treated with DC using carbon or SS 304 electrodes for 20, 40 and 60 min; and all the samples, including the untreated cells, were collected by centrifugation at 5000 g for 5 min. After fixing cells in 2.5% glutaraldehyde for 1 h, the cells were collected by centrifugation and treated with 2% osmium for 1 h to cross-link the lipid molecules in cell membrane. The cell pellets were then dehydrated with increasing content of ethanol e.g. 50, 70, 80, 90 and 100% (dehydration in 100% ethanol was repeated three times). Then, the cell pellets were rinsed three times with a solution of propylene oxide (100 %), and gradually embedded in increasing concentration (50%, 75%, and 100%) of Araldite 502 epoxy resin (Electron Microscopy Sciences, PA) prepared with propylene oxide. After the third embedment in 100% epoxy resin, the samples were incubated overnight in a 60º C oven to allow the resin to polymerize. Using the MT2-8 ultra-microtome (Sorvall Porter-Blum), the resin-embedded samples were cut into 80 nm thin sections and were successively stained for 30 s with 2% uranyl acetate and Sato's lead citrate [17] before imaging with TEM.

5.3.4. Ion accumulation in *P. aeruginosa* PAO1 cells

Recently, we proposed that the generation and the movement of metal ions are important to ECCP[11]. To investigate how DC-induced movement of metal ions affect bacterial cells, the intracellular accumulation of the ions was investigated. PAO1 cells in the stationary phase were collected from an overnight culture, washed twice with 0.85% NaCl, and resuspended in 0.85% NaCl to an OD_{600} of 1.5. The cells were introduced to an electrochemical cell as described above, and a current density of 70 $\mu A/cm^2$ DC was

maintained across the samples for 1 h using carbon and SS 304 electrodes, respectively. The DC-treated samples and the untreated control were deposited on a gold-coated glass slides. The samples were vacuumed for 24h before they were examined using SEM with energy dispersive spectroscopy (SEM-EDS) (Joel 5600, Joel, Japan) to determine the relative cellular concentration C, P, N, O, Fe, Cr, Mn, and Ni.

5.3.5. Surface charge of *P. aeruginosa* PAO1 cells

To evaluate the cellular activity of the DC treatments, the surface charge of treated cells were assessed and compared with untreated control. Following previous protocols [18,19] with slight modifications, the interaction between cells and charged particles (e.g. ions) were characterized by measuring the Zeta (ζ) Potential. In principle, the ζ-Potential device utilizes a light scattering technique to measure the electrophoretic mobility of particles of a specific size within the electric field. To investigate how the change in surface properties relates to cellular activity and the accumulation of extracellular materials, such as metal ions, PAO1 cells in stationary growth phases were washed and resuspended in 0.85% NaCl to OD_{600} of 0.6 and DC treatment (70 μA/cm^2 DC) using carbon and SS 304 was performed for 1 h. DC-treated cells, untreated control, and cells exposed to electrochemical byproducts of the DC treatments for 1 h were collected in 15 mL conical tubes and stored on ice before the ζ-potential measurement. Finally, 200 μL of cell suspension was transferred into a BI-SCP polystyrene cuvette (Brookhaven Instruments, NY) containing 2800 μL of distilled water (resulting in 10 mM NaCl solution) to measure the ζ-Potential using the Zeta 90 PLUS potential analyzer (Brookhaven Instruments, Holtsville, NY).

5.3.6. Mechanical properties of *P. aeruginosa* PAO1 cells

To understand if DC treatment affects membrane integrity and associated mechanical properties of the cells, the elastic property of the cell membrane were characterized through measurement of the young's modulus and the hardness of the cells using atomic force microscopy (AFM) (Digital Instruments Nanoscope III, Veeco, NY). Stationary phase cells of PAO1 were treated for 1 h with or without DC using carbon and SS 304 electrodes, respectively, as described above. The DC-treated cells and the untreated control cells were fixed with 2.5% glutaraldehyde in PBS for 1 h and washed twice with Millipore water. The samples were allowed to dry on gold-coated glass coupons, which were previously cleaned with 190 proof ethanol. NSC14/AIBS probe (MikroMasch, CA, USA), with a force constant of 5.7 N/m, was used in tapping mode to locate the bacterial cells. Once the coordinates of the cells were recorded, the device was switched to the contact mode to perform nanoindentation on the cells (an indent on a sterile substrate was made first to set the deflection sensitivity of the tip). Then, a series of single indents on the cells was performed to acquire all the force curves by following a protocol described previously [20].

5.3.7. Statistical analysis.

SAS Software was used to conduct t-test and one-way ANOVA analyses. Differences with $p < 0.05$ were considered as statistically significant.

5.4. RESULTS

5.4.1. DC treatment reduced persistence in PAO1 stationary phase cells

Recently, we reported that co-treatment of PAO1 persister cells with DC and Tob exhibited synergistic effects in killing PAO1 persister cells. To reveal the mechanism ECCP, we were interested in understanding the effects of DC on the electrophysiology of the persister cells. In this study, we first tested if DC treatment alone can reduce persistence. Thus, planktonic PAO1 cells were treated with 70 μA/cm^2 DC using carbon or SS 304 electrodes, and the numbers of viable persister cells were determined. As shown in Fig. 5.1, the electrochemical treatment reduced the original level of persistence. For example, when the 70 μA/cm^2 DC was delivered using carbon electrodes, 74.0±3.1 % stationary phase cells was killed. In comparison the number of the persister cells was reduced by 92.5 ±1.0 % (one-way ANOVA, p=0.0025), a decreased of more than 1 log. The effects were even greater when the DC treatment was performed with SS 304. Under this condition, 99.2±0.1% stationary phase cells were eliminated. However, 95.5±0.6% of the persister cells become susceptible to 200 μg/mL Cip (one-way ANOVA, p=0.0022). Overall, these results demonstrate that the susceptibility of the persister cells to Cip was increased following the DC treatment, suggesting that DC could reduce persistence.

5.4.2. Sequential treatment with DC followed by Tob led to complete eradication of persister cells.

Persistence reduction through DC treatment led to speculating on the ability of DC to alter membrane property of PAO1 cells and increase their permeabilization to antibiotics. To test this hypothesis, we first treated the PAO1 persister cells with 70 μA/cm^2 DC

using SS 304 or carbon electrodes for 1 h. Then the tolerance of the persister cells to antibiotics Tob, Kan and Spec was investigated immediately after the DC treatments. According to the results shown in Fig. 5.2A, pre-treatment of persister cells with 70 $\mu A/cm^2$ DC using carbon electrodes significantly improved killing by 1.5 µg/mL Tob. No viable persister cells were found after the treatment, corresponding to a 7-log reduction in persistence (one-way ANOVA, p=0.0004). This is 2-log more than the killing achieved by co-treatment with DC & 1.5 µg/mL Tob[11]. Interestingly, sequential treatment with DC followed by Kan and Spec did not exhibit the same effects (Fig. 5.2A). In fact, persister killing after pre-treatment with DC was not significantly enhanced with 60 µg/mL Kan (one-way ANOVA, p=0.08) and with 60 µg/mL Spec (one-way ANOVA, p=0.6). Similar results were also obtained for Kan and Spec when DC was applied using SS 304 electrodes; e.g. no further enhancement of persister killing was observed with subsequent treatment using 60 µg/mL Kan (one-way ANOVA, p=0.5), and 60 µg/mL Spec (insignificant increase, one-way ANOVA, p=0.054). Interestingly, sequential treatment with DC using SS 304 followed by 1.5 µg/mL Tob (one-way ANOVA, p=0.52) did not exhibit synergy either (Fig. 5.2B). This sequential treatment only showed killing by 2 logs, which is similar to the killing achieved with DC alone using SS 304.

To understand if DC treatment can cause irreversible damage to the viability functions of the persister cells, a 15 or 30 min recovery time was given between DC and antibiotic treatments. In all tested conditions, the recovery did not improve the antibiotic tolerance of persister cells pretreated with DC. These findings demonstrated that DC might induce long-lasting damage, which could hinder the persisters' ability to maintain

cellular and membrane functions, and properly respond to subsequent antibiotic attacks. To confirm this analysis, the conditions following the DC treatments were adjusted to allow PAO1 persister cells to recover in LB medium and evaluate the ability of the DC-treated cells to replicate in the presence of nutrients with and without antibiotics. As shown in Fig. 5.3A, the growth rate of cells treated with carbon electrodes declined during the 6 h incubation in LB, even in the absence of antibiotics. However, no significant increase in the viability of the persister cells treated with SS 304 was recorded in the presence and absence of antibiotic. The cell density remained constant in the presence and the absence of antibiotics (Fig. 5.3B). The above findings strongly support that PAO1 persister response to DC treatments varies according to the carbon and SS 304 electrodes.

5.4.3. DC treatment affected the mechanical properties of *P. aeruginosa* PAO1.

DNA microarray analysis revealed major differences between the treatments mediated with carbon and SS 304 electrodes, and demonstrated that genetic pathways such as protein secretion, transport of small molecules, SOS response, and pyocin-related genes of PAO1 persister cells were significantly affected by DC treatment. To understand if DC treatments affect the membrane integrity and permeability of PAO1, DC-treated PAO1 cells were stained with PI, a membrane impermeable dye that stains DNA, and the membrane integrity of the cells was measured using the Synergy 2 Multi-Mode Microplate Reader (Biotek, VT, USA). As shown in Fig. 5.4, PAO1 cells were more permeable to PI after DC treatment using carbon electrodes than the untreated control or DC treatment with SS 304. Overtime, however, the permeability of the cells treated with

DC using carbon decreased once the treatment is stopped. This observation was not recorded with cells treated using SS 304, which permeability was lower and remained constant after the treatment was interrupted. These findings suggest that DC may affect membrane integrity of PAO1, and the damage due to the treatments appeared to irreversibly lead to the failure of the cell to recover completely in LB medium over 6h, as shown in Fig. 5.3A,B.

These findings are corroborated with TEM analysis, which was used as a complementary approach for the assessment of the membrane integrity and morphology of PAO1 cells following DC treatment. The stationary phase PAO1 cells were treated with DC using SS 304 or carbon electrodes and the cells were imaged using TEM. Significant, but different, morphological changes were observed for PAO1 cells treated with carbon and SS 304 electrodes. Compared to the untreated PAO1 cells (Fig. 5.5A), the cells treated with 70 $\mu A/cm^2$ DC mediated with carbon electrodes showed two main configurations: dark areas near the poles of these treated cells (Fig. 5.5B2), which were more apparent when the samples were stained with uranyl acetate (Fig. 5.5B3, B4), and disintegrated cell membrane suggesting loss of membrane integrity (Fig. 5.5B1). In contrast, the cells treated using SS 304 electrodes exhibited more membrane damage leading to the release of cellular contents (Fig. 5.5C1). Interestingly, it appears that DC treatment of PAO1 using SS 304 electrodes for 1 h resulted in the release of OMVs (see Fig. 5.5C2), which confirms secretion of extracellular proteins or that the cells subjected to the SS 304 mediated treatment underwent loss of the membrane integrity and functions under DC using SS 304.

To further investigate these differences, TEM analysis was performed on cross-sections of stationary PAO1 cells treated with DC for 20, 40 or 60 min. Compared to the untreated control (Fig. 5.6A1, A2), compartmentalization of intracellular materials is visible at 20 min of DC treatment using carbon electrodes (Fig. 5.6B1). At 40 min of the treatment, the size of the inclusion body increased and the cells experienced some morphological deformations around the cell membrane (Fig. 5.6B2). The deformation of the cell membrane was more apparent at 60 min of the DC treatment using carbon, during which the intracellular features of the cells became less visible and some cells ruptured (Fig. 5.6B3). Under this condition, intact cells were barely seen. The effects of SS 304-DC on the membrane of the treated cells were different than that on the cells treated using carbon. As shown in Fig. 5.6C1, intracellular changes were observed after the first 20 min of the DC treatment. After 40 min of the treatment, the outer membrane of the cells treated using SS 304 became loose and localized accumulation of inner material around the inner cell membrane was observed (Fig. 5.6C2). More membrane damage was noticed at 60 min of the DC treatment, which may have led to cell lysis as shown in Fig. 5.6C3.

Since DC treatments induced morphological changes and altered the integrity of PAO1 cells, we expected that DC treatment may affect the mechanical properties of these cells. To test this, nanoindentation was performed on DC-treated cells and the untreated control, which were previously fixed in 2.5% gluteraldehyde and allowed to dry on gold-coated substrates before the test. The force curves of the cell membranes were recorded and the slope of the linear region (k) of the unload curve (Supplementary data Fig. 5.S2)

was used to derive the mechanical properties including the stiffness (Young's modulus), and the hardness of the cell membranes. The mechanical properties of the cells were determined according to the theory defined by Sneddon *et al*. [21] and based on the Hertz model [22,23]. For our condition, the modulus was defined as:

$$\text{Modulus: } E = \frac{3\,F(1-\nu^2)}{4\ R^{0.5}\ I^{1.5}};\ \text{with Poisson ratio } \nu = 0.5$$

$$\text{Hardness: } H = \frac{Fmax}{A_i}$$

Based on the characteristics of the probes suggested by the manufacturer such as the radius of curvature "R" of the tip and the depth of the indent "I" (nm) performed on the sample, the contact area "Ai" (nm^2) between the tip and the sample was computed according to the following:

$$\text{Area of indentation: } A_i = \left[\pi * I * \frac{\tan(15^\circ)}{\cos(15^\circ)}\right] + 541.17\ (nm^2)$$

In our conditions, the Young's modulus of the control sample of PAO1 cells was found to be 0.39±0.05 GPa (Table 2). Compared to the untreated control, DC treatment applied for 1 h at 70 $\mu A/cm^2$ using SS 304 did not cause significant change in the stiffness of the PAO1 cells (0.36±0.17 GPa, one-way ANOVA, p=0.95). The average indent performed on the cells treated with SS 304 was 36.0±14.4 nm, compared to 28.9±3.6 nm for the untreated control. However, significant change in the cell stiffness was recorded after DC treatment with 70 $\mu A/cm^2$ DC using carbon electrodes for 1 h. Due to the effects of the treatment using carbon electrodes, the modulus of the PAO1 cells reached 3.0±1.5 GPa (one-way ANOVA, p=0.001), corresponding to a maximum indent of 11.9±0.5 nm. The comparison of the DC treatments showed major differences in the cell stiffness or

hardness. The cells treated with carbon electrodes were 8 times harder than those treated with SS 304 electrodes (3.08±0.0 GPa vs. 0.36±0.1 GPa; one-way ANOVA, $p<0.0001$). This finding correlated with large difference in the maximum force of the indents. Under DC treatment using carbon, PAO1 cells withstood a maximum load of 391.8±16.6 nN vs. 276.1±8.0 for the cells treated with 70 $\mu A/cm^2$ DC using SS 304 (one-way ANOVA, $p=0.008$), suggesting an impediment of the mechanical properties of the cell membrane due to the carbon treatment. As described previously, the inner compartmentalization of the cells occurring under DC using carbon electrodes and the loosening of the outer membrane under DC using SS 304 might explain these differences in the hardening and the softening of the cells. These results strongly supported that the electrochemical treatments had variable effects on the membrane function of the cells.

5.4.4. Electrically-induced interaction of *P. aeruginosa* PAO1 with metal ions results in surface charge disruption

To determine the origin of polar compartmentalization within the cells and to understand the localized accumulation around the cell inner membrane as observed on the TEM images, further study was conducted on the chemical composition and the surface charge of the DC-treated and untreated cells. Stationary phase PAO1 cells were treated for 1 h with 70 $\mu A/cm^2$ DC using carbon and SS 304 electrodes, and the concentration of SS 304-relevant metal ions (e.g. Fe, Cr, Ni, Mn), as well as the content of some organic elements such as C, O, K and S were investigated to study how the electrode materials affect the chemical composition of the cells. The SEM-EDS data shown in Fig. 5.7 revealed that DC treatment of PAO1 cells in the presence of SS 304-releasedmetal ions

resulted in the cellular accumulation of Fe and Cr ions. The weight percentage of Fe and Cr was 23.9±9.2% and 5.0±1.8%, respectively, in the cellular composition of the cells treated with DC using SS 304 electrode. However, the relative concentration of P and N in the cells treated with DC using SS 304 was lower compared to the control. However, the difference was only significant when DC treatments using SS 304 was compared to that using carbon electrodes, as cells treated with carbon contained 2.9% and 8.2% more P and N elements, respectively, compared to the cells treated with SS 304 (one-way ANOVA, p=0.046 for P, and p=0.0499 for N); This may suggest that DC treatment induced the release of cellular proteins from cells treated with SS 304. This finding led to the hypothesis that electrically-induced movement of charged elements or interactions between cells membrane and metal ions may affect the surface properties of the cells, and consequently their membrane functions. To test this hypothesis, the net surface charge of the stationary phase cells previously treated with 70 $\mu A/cm^2$ DC using carbon or SS 304 were measured using the Zeta 90 PLUS potential analyzer (Brookhaven Instruments, Holtsville, NY). Under our conditions, stationary PAO1 cells maintained a ζ-Potential of -27.6±1.3 mV in 10 mM of NaCl solution (Fig. 5.8). However, the net charge of the cells was different in the presence of DC-generated ions. The stationary phase cells treated with DC using SS 304 electrodes became less negatively charged (-23.4±0.9 mV; one-way ANOVA, p=0.013), presumably due to the accumulation of the metal ions. However, the cells were more negatively charged than when they are resuspended in SS 304-electrolyte only (-19.5±1.5; one-way ANOVA, p<0.0001), which may be explained by the fact that the intact cells have better interaction with the positively charged metal ions (see Discussion).

In contrast, no significant change in the chemical composition of the PAO1 cells was found after DC treatment using with carbon electrodes. This suggests that the dark areas shown in the SEM images of DC-treated cells were primarily due to the accumulation of intracellular materials, instead of the intracellular accumulation of carbon particles. Therefore, the polar compartmentalization of proteins could have originated from inclusion bodies formed under the DC condition using carbon, which were confirmed by SDS-PAGE gel and shown in the supplementary data. Contrary to the treatment using SS 304, DC treatment using carbon electrodes did not affect the net charge of the cells. The surface charge of the DC-free cells remained unchanged in the presence of carbon-released particles, and when the cells were treated with 70 $\mu A/cm^2$ DC using carbon electrodes. The net surface charge of the cells in the presence of carbon only was -27.3±1.0 (one-way ANOVA, p=0.84) and that in the presence of DC was -28.7±0.8 (one-way ANOVA, p=0.53). These results showed that DC generated by carbon electrodes have less effect on the surface charge of the cells compared to the treatment using SS 304.

5.5. DISCUSSION

The study of the electrical properties of bacterial cell has contributed to the understanding that net electrical forces (current or field resulting from the membrane potential) are required to facilitate the permeation of chemical compounds across the cell membrane. Recent interests in bioelectrochemistry and electrophysiology have demonstrated that the permeability of the bacterial cell membrane could be effectively controlled by the means a small electrical pulses, presenting great opportunities to better characterize the affinity

between antibiotics and their cellular targets, or design new strategies to improve the availability of biocides and antimicrobials within the pathogens [24]. Today, many techniques are being developed, which could track and measure electrophysiological changes induced by the cross-membrane transport of small molecules in bacterial cells [25-27]. Our goal is to characterize the properties of the persister cells to understand how electrical field and currents could be applied towards impairing their defense mechanisms, and reducing drug tolerance. Recently, we have developed novel systems to control antibiotic-resistant bacterial subpopulation, known as persister cells, with weak electrochemical currents, a phenomenon that we called ECCP. We have demonstrated that the viability of persister cells following treatment with 70 $\mu A/cm^2$ DC using SS 304 electrodes for 1 h was reduced by ~2 logs compared to the untreated control. Synergistic effects were recorded when 1.5 µg/mL Tob was supplied to the treatment with 70 $\mu A/cm^2$ DC using SS 304. For example, around 5 logs of killing of the persisters were achieved after 60 min of co-treatment with 70 $\mu A/cm^2$ DC using SS 304 and 1.5 µg/mL Tob[11]. Similarly, the treatments were effective on biofilm-associated persister cells. The synergy between DC and some antibiotics during ECCP revealed that the movement of some ions could have a direct impact on the cells. These findings led us to hypothesize and test several possible mechanisms to explain the killing of the persister cells with electrochemical treatments.

In this study, we expand our understanding of the electrophysiology of persisters to their response to electrochemical stresses generated by carbon or SS-304 mediated DC treatments and antibiotics. Firstly, we found that DC alone could reduce persistence in

PAO1 cultures and alter the defense system of the persister cells against certain antibiotics. The sequential DC-Tob treatments provided new evidence that DC sensitizes persister cells to antibiotics. For instance, 92.5% of the persisters that tolerate Cip-treatment (200 µg/mL Cip) become susceptible to the same concentration of Cip following a preliminary DC treatment using carbon electrodes. Moreover, all the persisters could be eradicated with 1.5 µg/mL Tob after the electrochemical sensitization using carbon electrodes. Such susceptibility of the persister cells to Tob remains constant even 30 min after the treatment, indicating that DC using carbon could engender permanent damage to the cellular functions of the persister cells. The discoveries that synergy and complete killing were achieved in sequential treatments of DC using carbon and Tob suggest that, in this condition, the antibiotics became more available to the cells or were more effective in reducing the viability of the persisters. This could elucidate our previous understanding of ECCP, in which no clear synergy was found during co-treatments of the PAO1 persister cells with DC using carbon and Tob [11]. Thus, it appears that DC using carbon electrodes could increase the permeability of the persister cells and facilitate the transportation of toxic materials (e.g. reactive oxygen species or ROS, antibiotics) within the cells only if the bactericides are not denatured by some adverse electrochemical reactions.

To prove that transport and accumulation of charged elements within PAO1 cells could disrupt the membrane functions of the cells, we sought electrochemical conditions to investigate the ability of PAO1 cells to uptake extracellular electrode materials. The SEM-EDS analysis of PAO1 cells indicated that DC treatments enable the interaction

between metal ions and cells, with subsequent effects varying upon the physiological states of the cells (intact vs. treated cells). The accumulation of Fe, and Cr, in particular, was observed for the cells treated with SS 304-mediated DC, and appeared to change the surface charge of the PAO1 cells. Like many Gram-negative bacteria, PAO1 have a net negative charge due to negatively charged molecules such as alginate, and phosphorylated polysaccharides, which are present on the outer membrane of the cells [28]. The presence of the metal ions decreased the surface charge of the untreated cell, which is consistent with report suggesting that increase of the ionic strength is inversely proportional to change in the bacterial zeta potential and electrophoretic mobility [19]. Because the bacterial cell membrane is exposed to the surrounding environment and thus experiences the flows of ions during the electrochemical treatments, it was of interest to understand how the mode of transportation and the accumulation of extracellular materials impair the ability of the cells to control their surface properties, including the surface charge. Our experimental results reveal that the surface charge of the cells varies not only as function of ionic strength of the cell surrounding, but also as a function of the cell physiology. It was found that PAO1 cells experiencing DC treatment were more negatively charged than the untreated cells resuspended in the same ionic solution. One explanation for this observation could be the fact that the electrically-induced flow of SS 304-associated ions might denature the chemical configuration of the cell membrane, which in turn reduced the level of interaction between the cells and the metal ions. The chemical alteration of the cell surface was reported to have variable disruptive effects on the surface charge of PAO1 [29]. In contrast to untreated cells exposed to SS 304 released ions, the cells resuspended in carbon electrolytes maintained the same surface charge as

the untreated PAO1 cells. Similarly, the surface charge of the cells treated with DC using carbon electrodes remained unchanged. Although the cells experienced the 70 $\mu A/cm^2$ DC current flow, they did not accumulate extracellular carbon. Instead, the carbon-treated cells appeared to accumulate intracellular materials. The polar compartmentalization of cellular materials might indicate that the electrical field generated by the treatment may cause a certain alignment of charged molecules (intracellular proteins, or DNA) and result in bacteriostatic effects [30], which need to be further studied. With no doubt, such change might affect the physiological properties the cells.

The membrane functions were further impaired in that, the electrochemical currents generated via carbon electrodes increased their permeability and resulted in the hardening of the cell membrane. Although fixed with 2.5% gluteraldehyde, the stiffness of the untreated PAO1 cells was comparable to bacterial membrane stiffness reported. Eaton *et al.* [31] reported a value of 0.221 GPa for *Escherichia coli* cells, which were also air-dried on a solid substrate, but without previous treatment with gluteraldehyde. After DC treatment using carbon electrodes, the elasticity of the cell membrane of PAO1, in our experimental condition, became about 8 times stiffer than the 0.39 GPa of the untreated cells. This change in the membrane properties may suggest that mechanical properties of the cell membrane were impaired.

Physical damage of the PAO1 cell membrane was not only induced by DC using carbon but DC treatment using SS 304 also affected the membrane configuration of PAO1. In response to the electrochemical stress, the cells secreted various proteins.

During the treatments, the cells lost their membrane integrity, resulting in the separation of the outer membrane from the inner membrane, and finally in cell lysis. Consistently, these morphological changes corroborated with the effects of DC on the mechanical properties of the PAO1 cells. Compared to the carbon-treated cells that harden under DC treatment, PAO1 cells treated with DC using SS 304 experienced greater physical deformation represented by large indent and major decrease in the stiffness of the cell membrane. Similar effects of the metal ion on the stiffness of bacterial cells were previously reported. Kumar *et al*. [32] described that the membrane elasticity of Gram-positive *Brevibacterium casei* (original Young's Modulus=0.769 GPa) decreases as a results of 0-72 h incubation in Co^{2+} solution, attributing the effects to biochemical interactions between the cell membrane components and the cations. Hence, the change in the membrane properties of the cells could affect the physiological response of the persister to DC and antibiotic treatments.

5.6. CONCLUSIONS

Overall, our findings reveal that the electrochemical treatment of bacterial cells disrupts the membrane properties of the cells. Depending on the electrode material, various effects were recorded. While treatment with SS 304 was more effective in synergy with antibiotics Tob, the sequential treatment using carbon and Tob resulted in the highest killing of the persister cells. Our data provide strong evidence that the DC affect the cellular and intracellular properties of the cells. Both the membrane activity and the intracellular organization of the cells were altered due to the DC treatments. This technology demonstrates that the activity of DC on the persister cells must be link to

physical damage. However, because the persisters maintain a certain level of metabolic activity, appropriate antibiotic should be used to enhance the efficacy of the treatment.

5.7. ACKNOWLEDGEMENTS

The authors are grateful to Blue Highway Inc. and the U.S. National Science Foundation (EFRI-1137186) for support. We also thank Dr. Thomas K. Wood at Penn State University for sharing the strain *P. aeruginosa* PAO1, Robert P. Smith at SUNY ESF for helping with the TEM, and Charles Driscoll and Mario Montesdeoca at Syracuse University for helping with the ICP-MS. We also thank Henry L. Peterson for his contribution in the proteomic study, Shiril Sivan and, Jeremy L. Gilbert for helping with the study of the mechanical properties of the cells.

5.8. REFERENCES

1 **Darouiche, R. O.** Treatment of infections associated with surgical implants. *The New England journal of medicine* **350**, 1422-1429, doi:10.1056/NEJMra035415 (2004).

2 Scott, R. (2009).

3 **Doshi, H. K., Chua, K., Kagda, F. & Tambyah, P. A.** Multi drug resistant pseudomonas infection in open fractures post definitive fixation leading to limb loss: A report of three cases. *International Journal of Case Reports and Images (IJCRI)* **2**, 1-6 (2011).

4 **Outterson, K., Powers, J. H., Seoane-Vazquez, E., Rodriguez-Monguio, R. & Kesselheim, A. S.** Approval and Withdrawal of New Antibiotics and Other Antiinfectives in the US, 1980–2009. *The Journal of Law, Medicine & Ethics* **41**, 688-696 (2013).

5 **Spellberg, B., Guidos, R., Gilbert, D., Bradley, J., Boucher, H. W., Scheld, W. M., Bartlett, J. G., Edwards, J.** The epidemic of antibiotic-resistant infections: a call to action for the medical community from the Infectious Diseases Society of America. *Clinical Infectious Diseases* **46**, 155-164 (2008).

6 **Taubes, G.** The bacteria fight back. *Science* **321**, 356-361, doi:10.1126/science.321.5887.356 (2008).

7 **Walsh, C. & Wright, G.** Introduction: antibiotic resistance. *Chemical reviews* **105**, 391-394 (2005).
8 **Lewis, K.** Persister cells, dormancy and infectious disease. *Nature reviews. Microbiology* **5**, 48-56, doi:10.1038/nrmicro1557 (2007).
9 **Nikaido, H.** Prevention of drug access to bacterial targets: permeability barriers and active efflux. *Science* **264**, 382-388 (1994).
10 **Kohanski, M. A., Dwyer, D. J. & Collins, J. J.** How antibiotics kill bacteria: from targets to networks. *Nature Reviews Microbiology* **8**, 423-435 (2010).
11 **Niepa, T. H., Gilbert, J. L. & Ren, D.** Controlling *Pseudomonas aeruginosa* persister cells by weak electrochemical currents and synergistic effects with tobramycin. *Biomaterials* **33**, 7356-7365, doi:10.1016/j.biomaterials.2012.06.092 (2012).
12 **Lewis, K.** Persister cells. *Annual review of microbiology* **64**, 357-372, doi:10.1146/annurev.micro.112408.134306 (2010).
13 **Mulcahy, L. R., Burns, J. L., Lory, S. & Lewis, K.** Emergence of *Pseudomonas aeruginosa* strains producing high levels of persister cells in patients with cystic fibrosis. *Journal of bacteriology* **192**, 6191-6199, doi:10.1128/JB.01651-09 (2010).
14 **Fux, C., Costerton, J., Stewart, P. & Stoodley, P.** Survival strategies of infectious biofilms. *Trends in microbiology* **13**, 34-40 (2005).
15 **Costerton, J. W., Ellis, B., Lam, K., Johnson, F. & Khoury, A. E.** Mechanism of electrical enhancement of efficacy of antibiotics in killing biofilm bacteria. *Antimicrobial agents and chemotherapy* **38**, 2803-2809 (1994).
16 **Sambrook, J. & Russell, D. W.** Molecular cloning: a laboratory manual. third. *Cold pring Harbor Laboratory Press, New York* (2001).
17 **Hanaichi, T., Iwamoto, T., Malavasi-Yamashiro, J., Hoshino, M. & Mizuno, N. A** stable lead by modification of Sato's method. *Journal of electron microscopy* **35**, 304-306 (1986).
18 **Soni, K. A., Balasubramanian, A. K., Beskok, A. & Pillai, S. D.** Zeta potential of selected bacteria in drinking water when dead, starved, or exposed to minimal and rich culture media. *Current microbiology* **56**, 93-97 (2008).
19 **Tourney, J. & Ngwenya, B. T.** The effect of ionic strength on the electrophoretic mobility and protonation constants of an EPS-producing bacterial strain. *Journal of colloid and interface science* **348**, 348-354, doi:10.1016/j.jcis.2010.04.082 (2010).
20 **Velegol, S. B. & Logan, B. E.** Contributions of bacterial surface polymers, electrostatics, and cell elasticity to the shape of AFM force curves. *Langmuir : the ACS journal of surfaces and colloids* **18**, 5256-5262 (2002).
21 **Sneddon, I. N.** The relation between load and penetration in the axisymmetric Boussinesq problem for a punch of arbitrary profile. *International Journal of Engineering Science* **3**, 47-57 (1965).
22 **Barber, J. R.** *Elasticity*. Vol. 172 (Springer, 2009).
23 **Lin, D. C., Dimitriadis, E. K. & Horkay, F.** Robust strategies for automated AFM force curve analysis—I. Non-adhesive indentation of soft, inhomogeneous materials. *Journal of biomechanical engineering* **129**, 430-440 (2007).

24 **Schulz, P., Garcia-Celma, J. J. & Fendler, K.** SSM-based electrophysiology. *Methods* **46**, 97-103, doi:10.1016/j.ymeth.2008.07.002 (2008).

25 **Strahl, H. & Hamoen, L. W.** Membrane potential is important for bacterial cell division. *Proceedings of the National Academy of Sciences of the United States of America* **107**, 12281-12286, doi:10.1073/pnas.1005485107 (2010).

26 **Ohmizo, C., Yata, M. & Katsu, T.** Bacterial cytoplasmic membrane permeability assay using ion-selective electrodes. *Journal of microbiological methods* **59**, 173-179, doi:10.1016/j.mimet.2004.06.008 (2004).

27 **Harris, H. W., El-Naggar, M. Y., Bretschger, O., Ward, M. J., Romine, M. F., Obraztsova, AY., Nealson, K. H.** Electrokinesis is a microbial behavior that requires extracellular electron transport. *Proceedings of the National Academy of Sciences of the United States of America* **107**, 326-331, doi:10.1073/pnas.0907468107 (2010).

28 **Jiang, W., Saxena, A., Song, B., Ward, B. B., Beveridge, T. J., Myneni, S. CB.** Elucidation of functional groups on gram-positive and gram-negative bacterial surfaces using infrared spectroscopy. *Langmuir : the ACS journal of surfaces and colloids* **20**, 11433-11442 (2004).

29 **Bruinsma, G. M., Rustema-Abbing, M., van der Mei, H. C. & Busscher, H. J.** Effects of cell surface damage on surface properties and adhesion of *Pseudomonas aeruginosa*. *Journal of microbiological methods* **45**, 95-101 (2001).

30 **Rosenberg, B.** Some biological effects of platinum compounds. *Platinum Metals Rev* **15**, 42-51 (1971).

31 **Eaton, P., Fernandes, J. C., Pereira, E., Pintado, M. E. & Xavier Malcata, F.** Atomic force microscopy study of the antibacterial effects of chitosans on *Escherichia coli* and *Staphylococcus aureus*. *Ultramicroscopy* **108**, 1128-1134 (2008).

32 **Kumar, U., Vivekanand, K. & Poddar, P.** Real-Time Nanomechanical and Topographical Mapping on Live Bacterial Cells *Brevibacterium casei* under Stress Due to Their Exposure to Co2+ Ions during Microbial Synthesis of Co3O4 Nanoparticles. *The Journal of Physical Chemistry B* **113**, 7927-7933 (2009).

FIGURE CAPTIONS

Figure 5.1. Sensitization of *P. aeruginosa* PAO1 persister cells by DC treatment. Stationary phase cells of *P. aeruginosa* PAO1 (OD_{600} of 0.9) were treated with 70 μA/cm^2 DC for 1 h using Carbon and SS 304 electrodes. After the DC treatment, the cells were exposed to ciprofloxacin (Cip) for 3.5 h to isolate the persister cells. The viable (regular and persister) cells were quantified by counting CFUs. The means and standard deviations are shown. (* $p \leq 0.05$, and ** $p \leq 0.01$)

Figure 5.2. Sequential treatment of *P. aeruginosa* PAO1 persister cells using 70 μA/cm^2 DC followed with antibiotics. The persister cells were treated for 1 h with DC using carbon and SS 304 electrodes. Subsequently to the DC treatment, the cells were exposed to antibiotics, including 1.5 μg/mL Tob, 60 μg/mL Kan, and 60 μg/mL Spec immediately, 15 and 30 min after the treatment for 1 h. The viable cells were quantified by CFUs count. Three replicates were tested for each condition. The means and standard deviations are shown.

Figure 5.3. Recovery of *P. aeruginosa* PAO1 persister cells following treatment with 70 μA/cm^2 DC. The persister cells were treated for 1 h using carbon (A) and SS 304 (B) electrodes. Subsequently to the DC treatment, the cells were resuspended in LB medium with or without antibiotics, including 1.5 μg/mL Tob, 60 μg/mL Kan, and 60 μg/mL Spec. The growth curve of the cell was recorded by measuring OD600 using a microplate reader. The means and standard deviations are shown.

Figure 5.4. Permeability of *P. aeruginosa* PAO1 to Propidium Iodide (PI) following DC treatments. The cells were treated with 70 μA/cm^2 DC using carbon or SS 304 electrodes for 1 h. After the treatment, DC treated cells, as well as the untreated control cells were exposed to PI for 15 min.

Figure 5.5. Representative TEM images of planktonic *P. aeruginosa* PAO1 cells control (A) vs. cells treated with 70 μA/cm^2 DC. (B) DC using carbon electrodes for 1 h and the cells were stained with vanadium oxide (Top) vs. uranyl acetate (bottom). Intracellular compartmentalization occurred after DC for 1 h. (C) DC using SS 304 electrodes for 1 h was performed and the cells were briefly stained with vanadium oxide. The treatment resulted in cells damage and in secretion of outer membrane vesicles (B).

Figure 5.6. Representative TEM images of untreated planktonic *P. aeruginosa* PAO1 cell. The cells were embedded in resin, stained with uranyl acetate and lead citrate. To performed TEM the cells were sectioned in 80 nm thin slides. (A) Untreated control *P. aeruginosa* PAO1 cells. PAO1 cells treated with 70 μA/cm^2 DC using carbon electrodes (B1) for 20 in resulted in initiation dark compartment within the cells. (B2) The accumulation increased after 40 min and (B3) DC treatment for 60 min resulted in the misshaping of the cell membrane. In all the cases, no major protein secretion was observed. The cells were treated with 70 μA/cm^2 DC using SS 304 electrodes (C1) for 20 min resulting in the protein secretion around the cells membrane, and (C2) Bulging of the cell membrane occurred at 40 min of the DC treatment; (C3) At 60 min of

the treatment, cells with a loose cells membrane were observed. Protein secretion became more significant with increasing treatment time.

Figure 5.7. Effects of DC treatment on the cellular accumulation of metal cations by *P. aeruginosa* PAO1 cells. Stationary phase cells were treated with 70 μA/cm^2 DC using carbon or SS 304 electrodes for 1 h. SEM-EDS analysis was performed to quantify the relative cellular concentration of the metal or organic elements. At least four replicates were tested for each condition. The means and standard errors are shown. (* $p \leq 0.05$, and ** $p \leq 0.01$)

Figure 5.8. Effects of DC on the surface charge of *P. aeruginosa* PAO1 cells. Stationary l phase cells were treated with 70 μA/cm^2 DC using carbon and SS 304 for 1 h or were resuspended in electrolytes generated for the DC treatments. The samples were resuspended in a solution of 10 μM of NaCl and the zeta-potential of the cells was measured. (* $p \leq 0.05$, and ** $p \leq 0.01$)

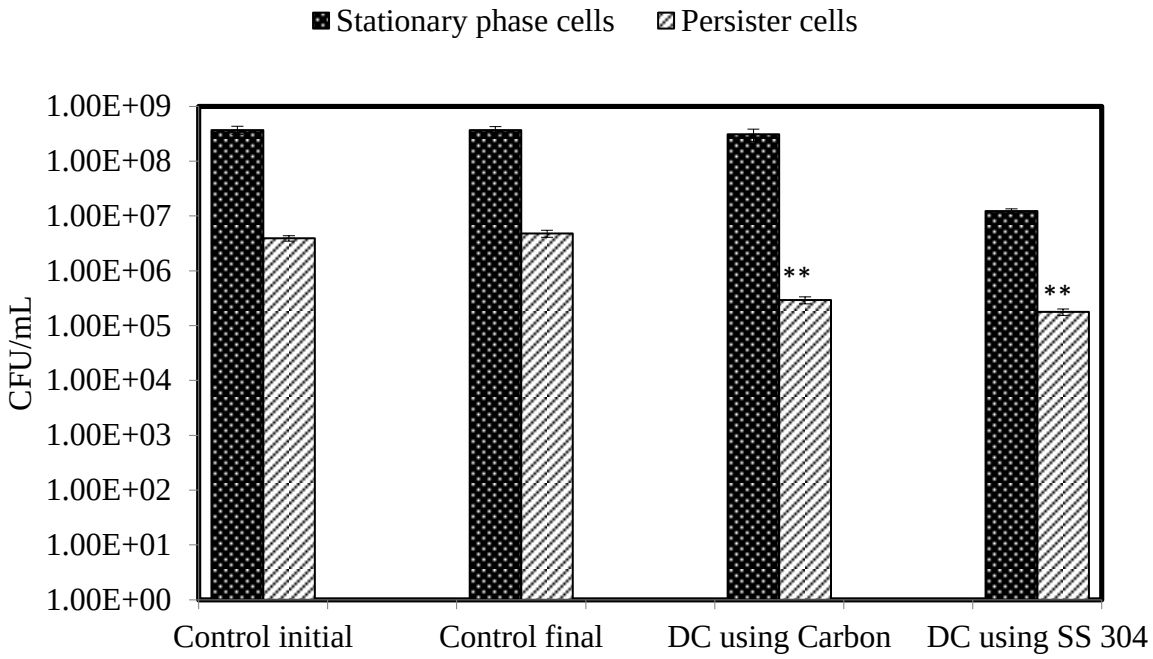
Stationary phase cells
Persister cells
1.00E+09
1.00E+08
1.00E+07
1.00E+06
1.00E+05
1.00E+04
1.00E+03
1.00E+02
1.00E+01
1.00E+00
CFU/mL
**
**
Control initial
Control final
DC using Carbon
DC using SS 304

Figure 5.1

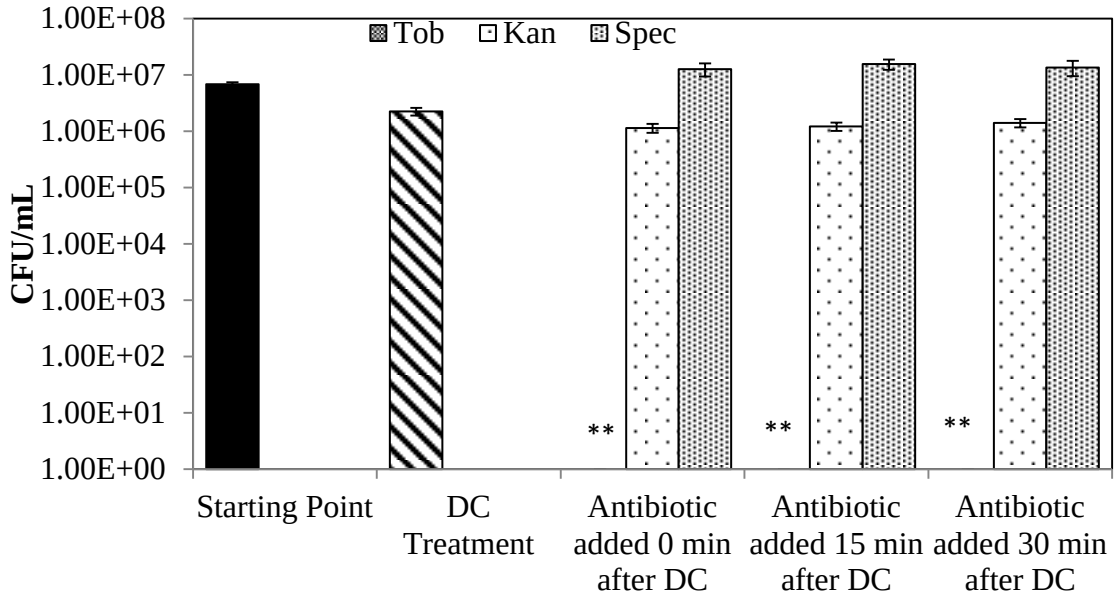
1.00E+08
1.00E+07
1.00E+06
1.00E+05
1.00E+04
1.00E+03
1.00E+02
1.00E+01
1.00E+00
CFU/mL
Tob
Kan
Spec
**
**
**
Starting Point
DC Treatment
Antibiotic added 0 min after DC
Antibiotic added 15 min after DC
Antibiotic added 30 min after DC

(A)

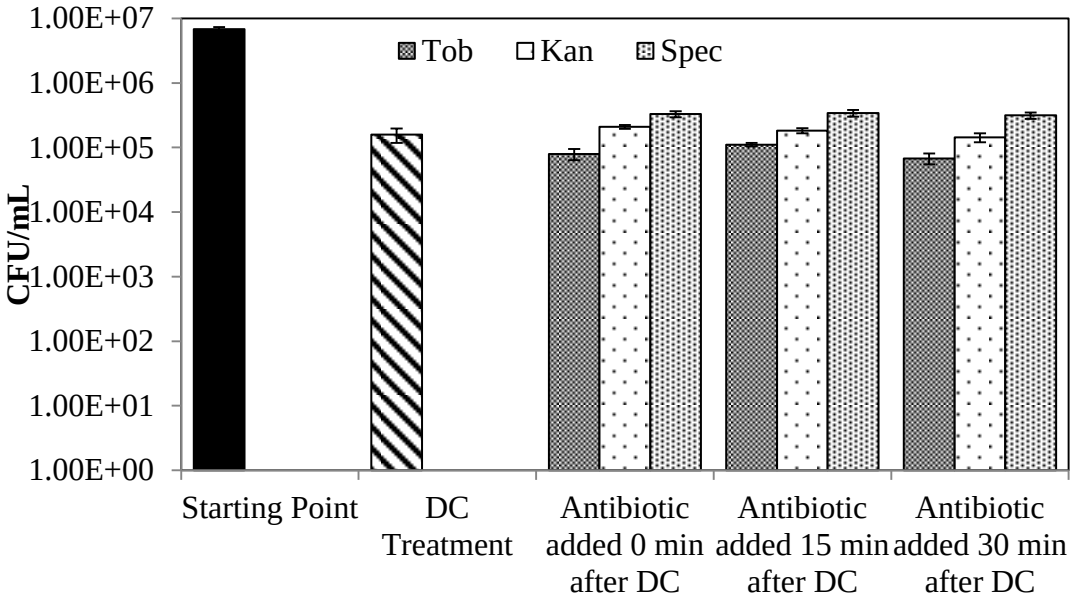
1.00E+07
1.00E+06
1.00E+05
1.00E+04
1.00E+03
1.00E+02
1.00E+01
1.00E+00
CFU/mL
Tob
Kan
Spec
Starting Point
DC Treatment
Antibiotic added 0 min after DC
Antibiotic added 15 min after DC
Antibiotic added 30 min after DC

(B)

Figure 5.2

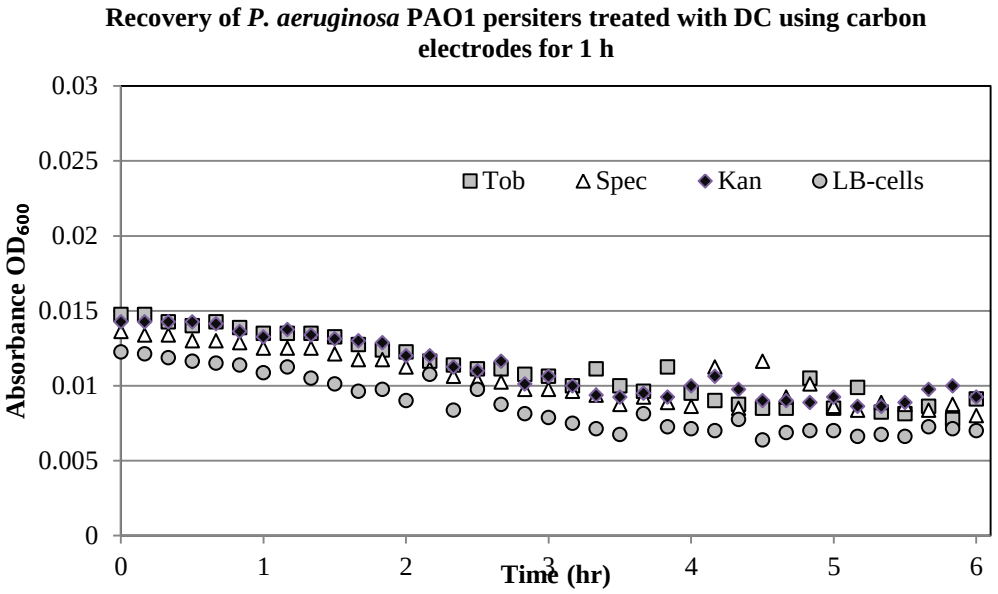
Recovery of P. aeruginosa PAO1 persiters treated with DC using carbon electrodes for 1 h
Absorbance OD600
Time (hr)
Tob
Spec
Kan
LB-cells
0.03
0.025
0.02
0.015
0.01
0.005
0
0
1
2
3
4
5
6

(A)

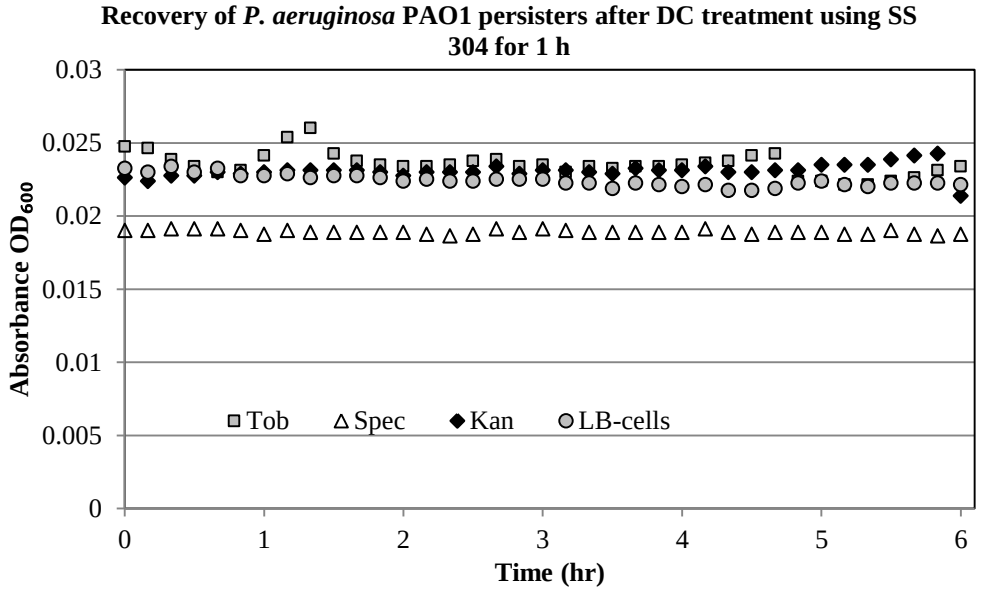
Recovery of P. aeruginosa PAO1 persisters after DC treatment using SS 304 for 1 h
Absorbance OD600
Time (hr)
Tob
Spec
Kan
LB-cells
0.03
0.025
0.02
0.015
0.01
0.005
0
0
1
2
3
4
5
6

(B)

Figure 5.3

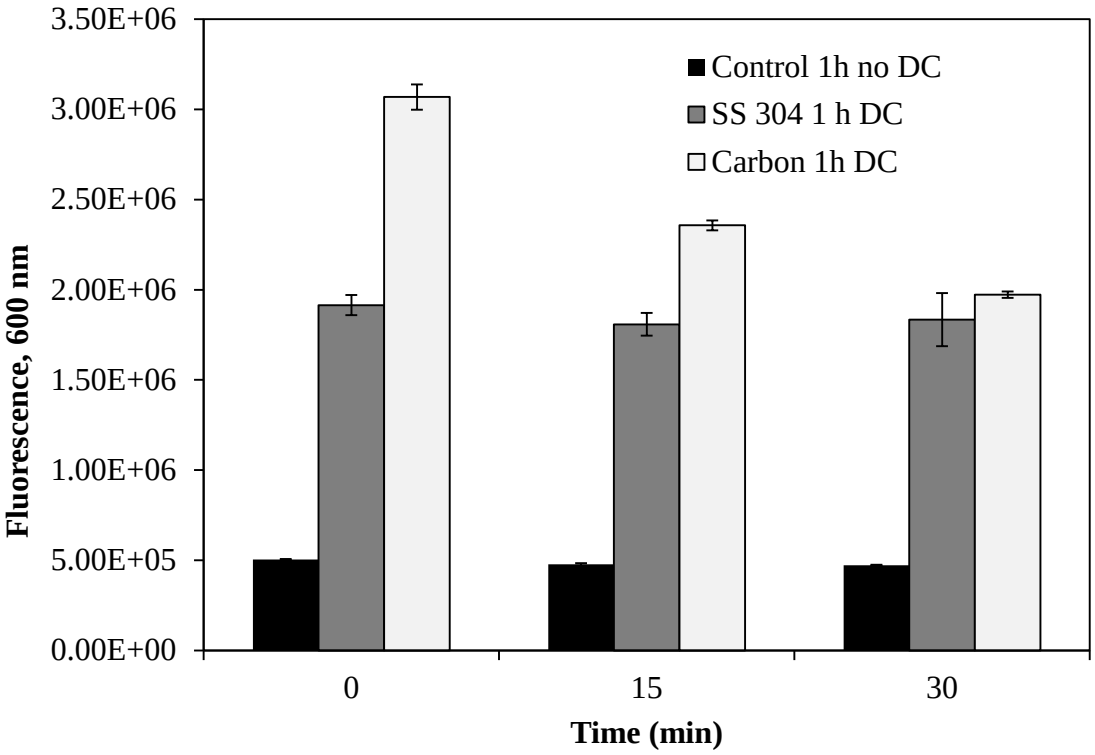
3.50E+06
3.00E+06
2.50E+06
2.00E+06
1.50E+06
1.00E+06
5.00E+05
0.00E+00
Fluorescence, 600 nm
Control 1h no DC
SS 304 1 h DC
Carbon 1h DC
0
15
30
Time (min)

Figure 5.4

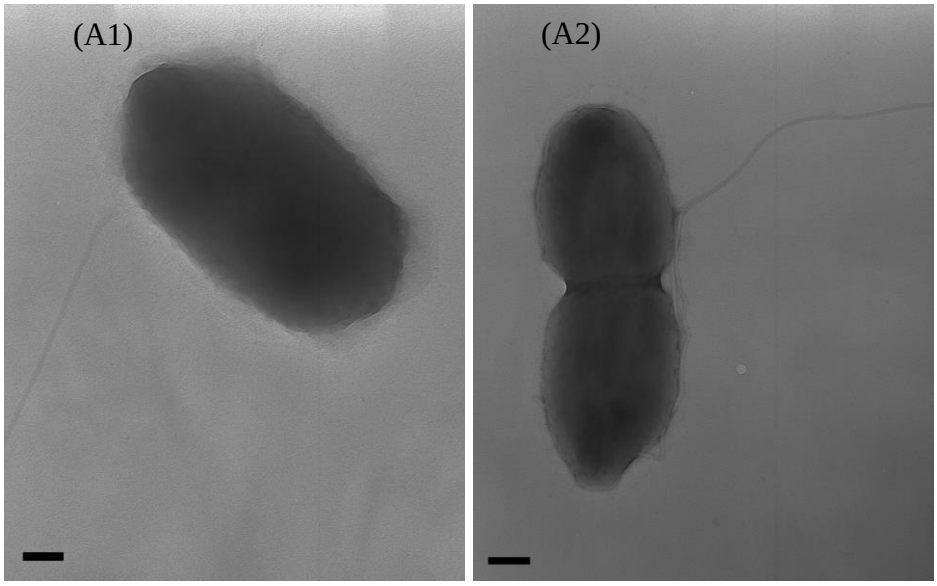
(A1)
(A2)

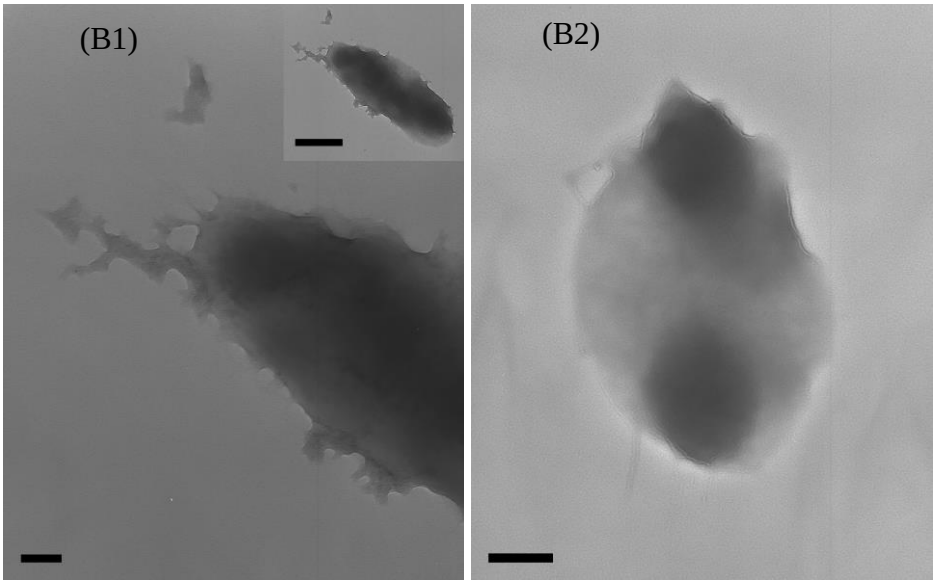
(B1)
(B2)

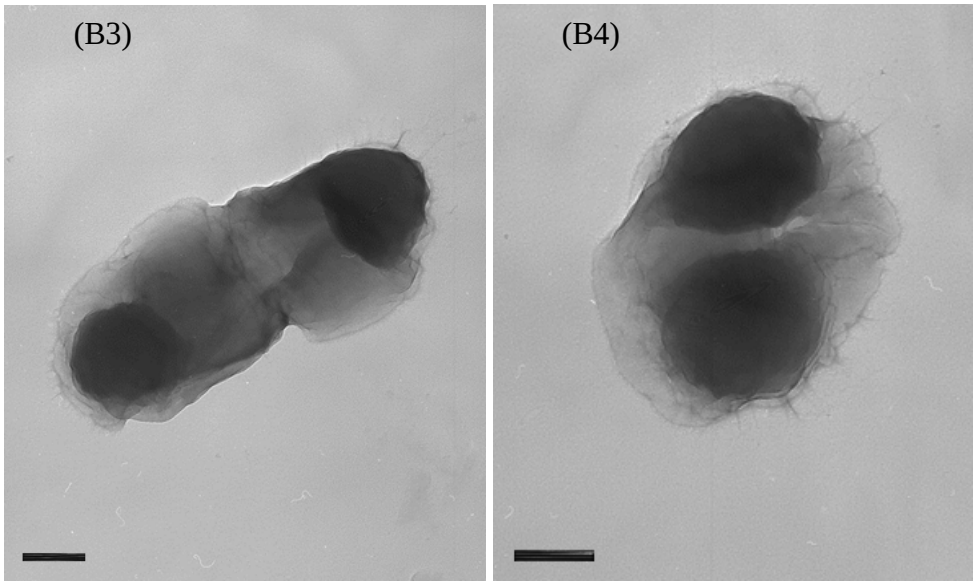
(B3)
(B4)

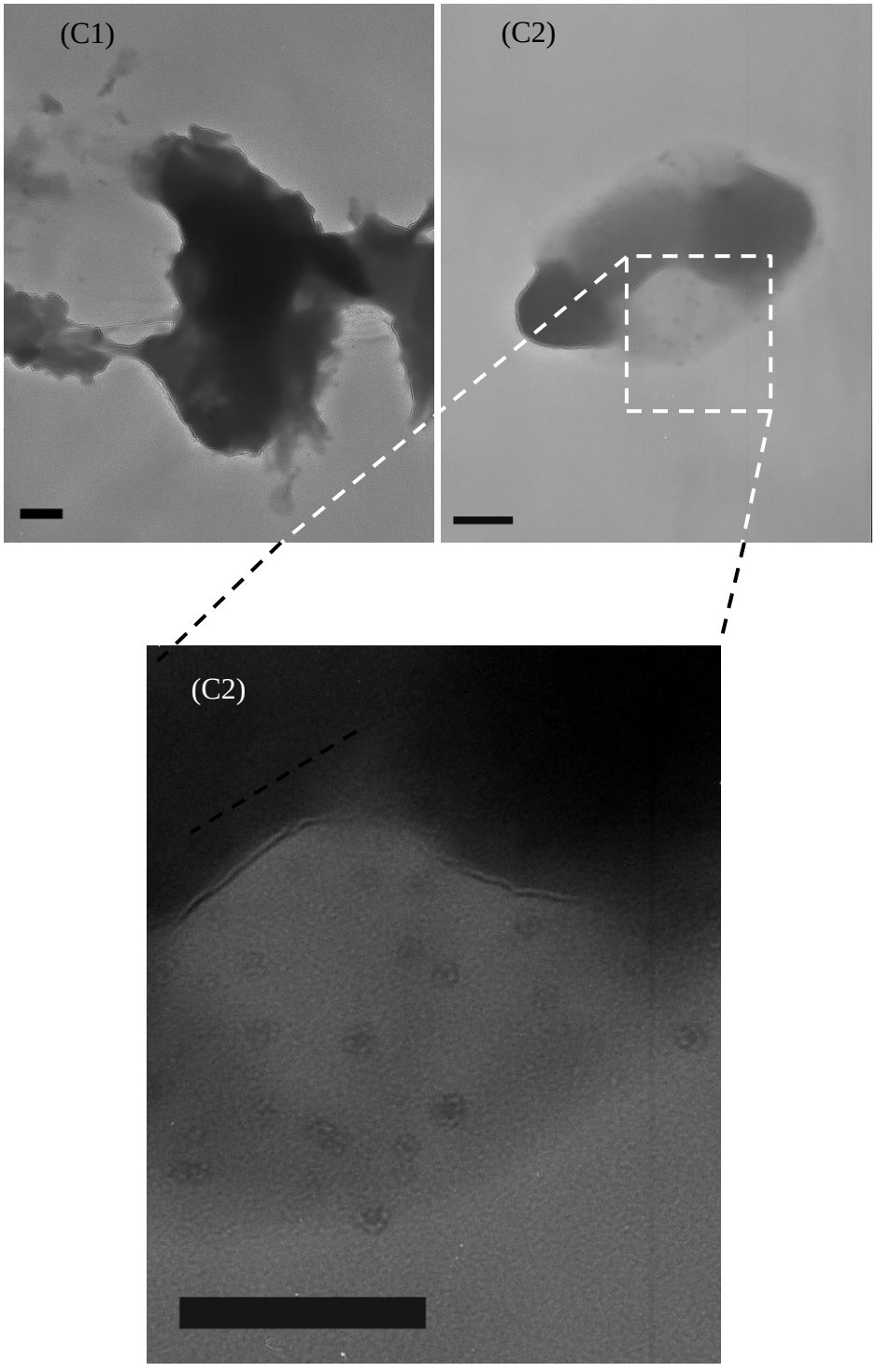

Figure 5.5

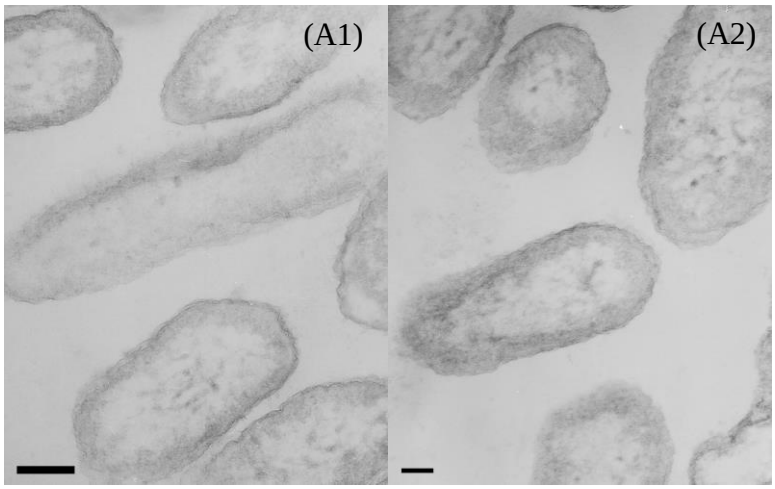
(A1)
(A2)

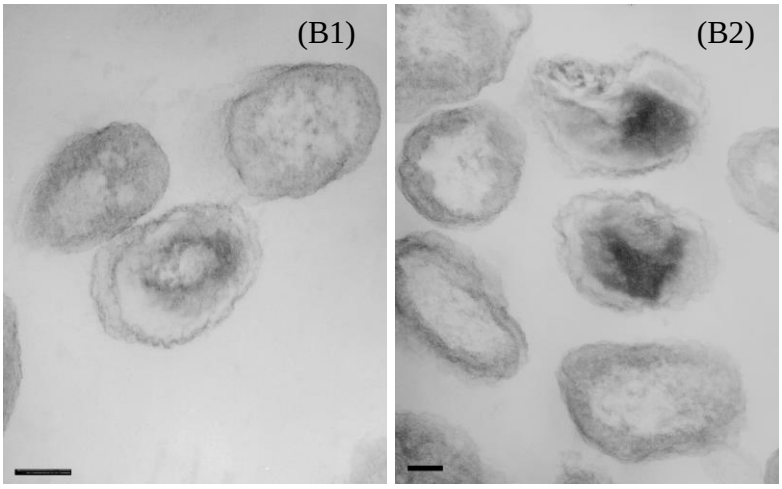
(B1)
(B2)

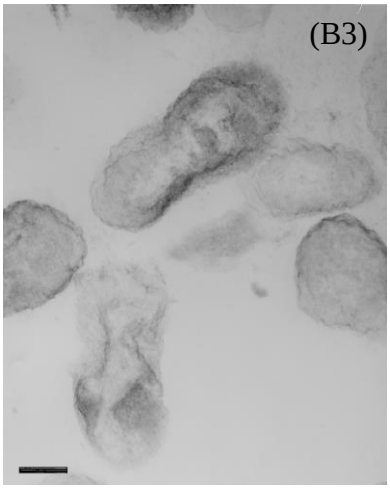
(B3)

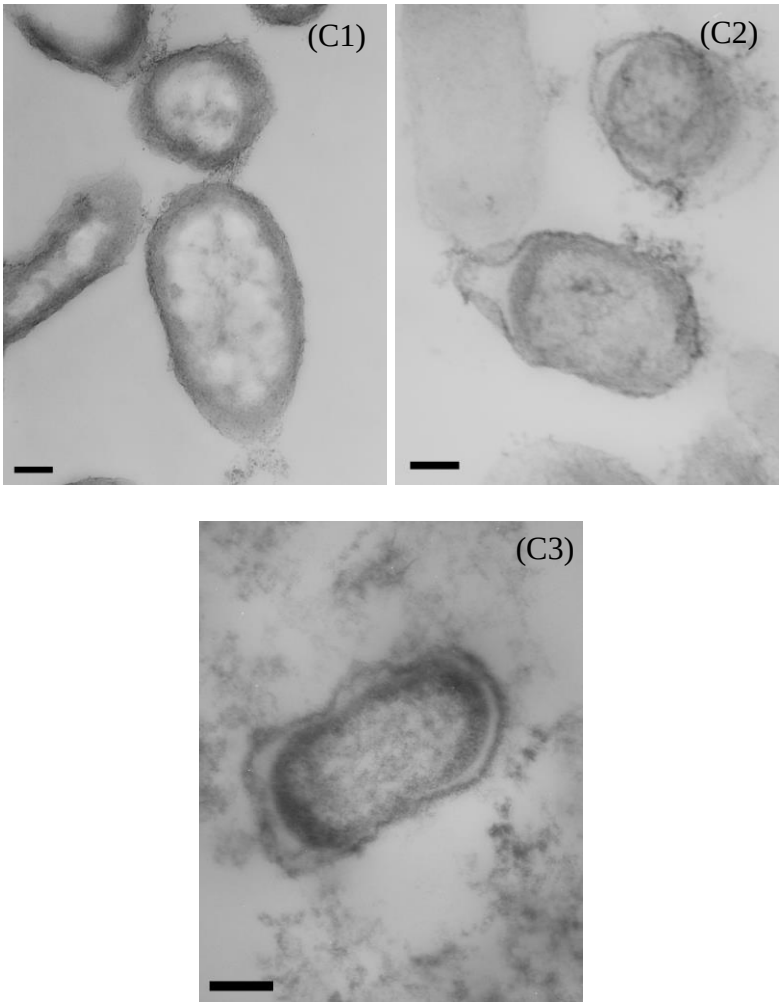

Figure 5.6

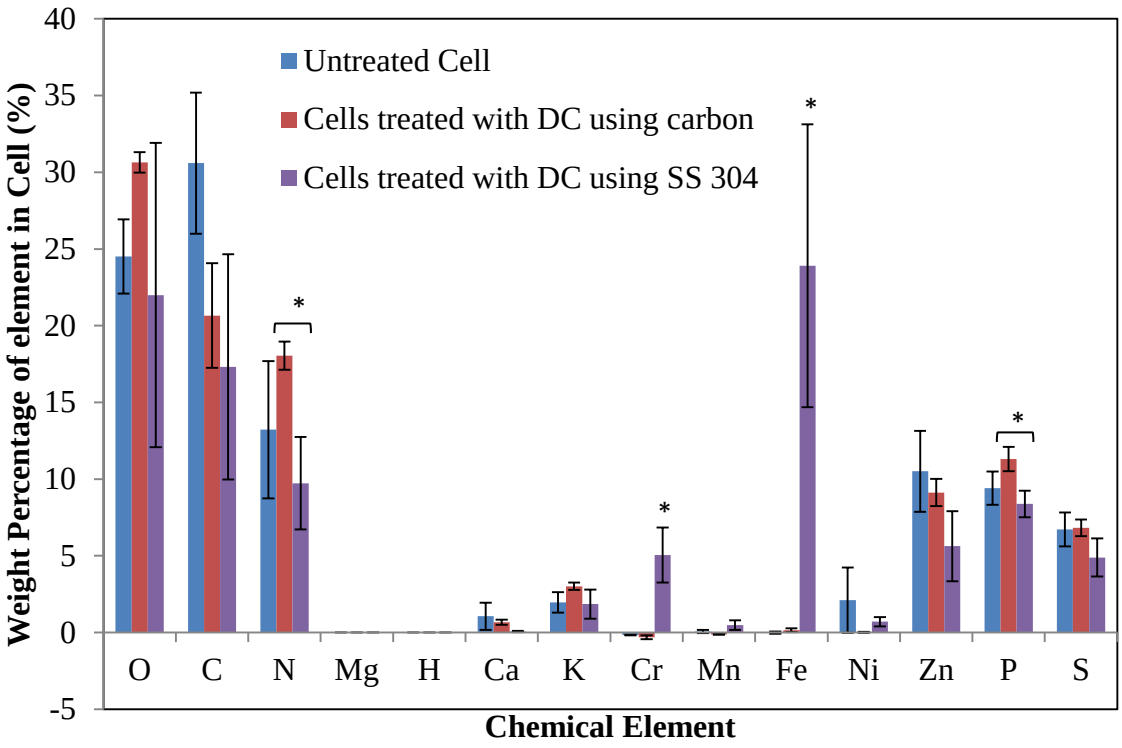
Untreated Cell
Cells treated with DC using carbon
Cells treated with DC using SS 304
Weight Percentage of element in Cell (%)
40
35
30
25
20
15
10
5
0
-5
O
C
N
Mg
H
Ca
K
Cr
Mn
Fe
Ni
Zn
P
S
*
*
*
*
Chemical Element

Figure 5.7

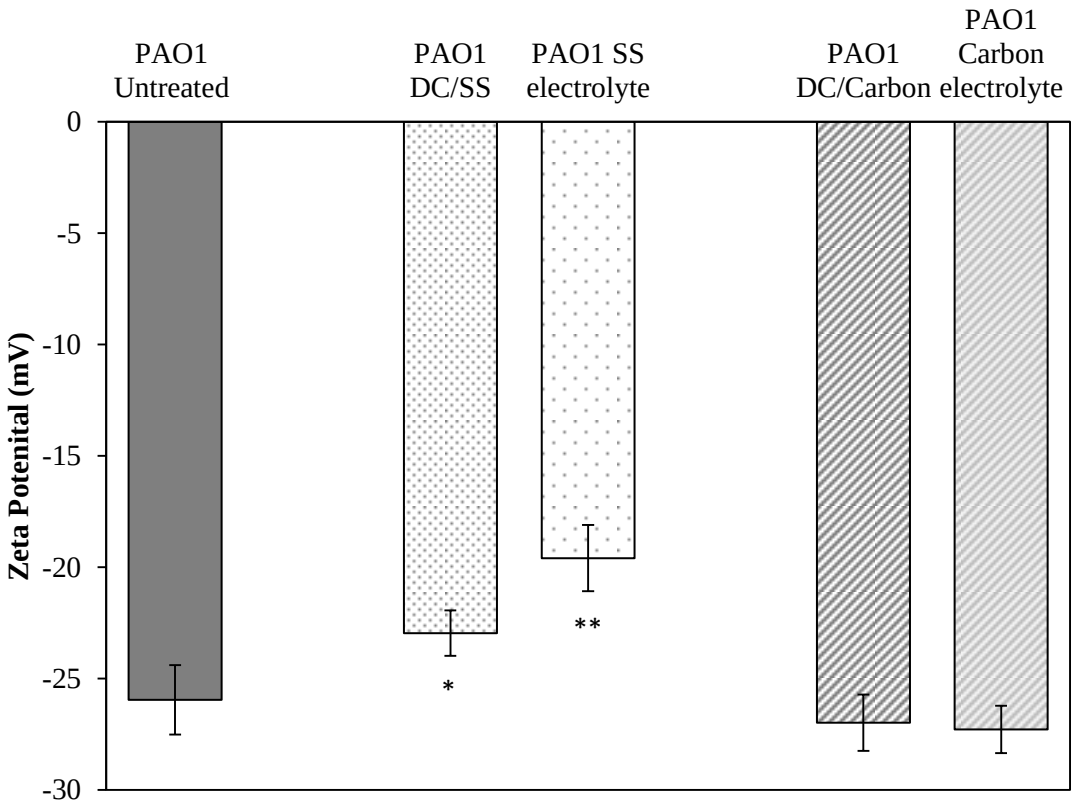
PAO1
Untreated
PAO1
DC/SS
PAO1 SS
electrolyte
PAO1
DC/Carbon
PAO1
Carbon
electrolyte
Zeta Potenital (mV)
0
-5
-10
-15
-20
-25
-30
*
**

Figure 5.8

Table 5.1

Mechanical properties of stationary phase cells of *P. aeruginosa* showing the effects of treatments with 70 µA/cm^2 DC using SS 304 or carbon electrodes.

	Untreated PAO1 (control)	**PAO1 treated with DC/ SS 304**	**PAO1 treated with DC/Carbon**
	Average ± SD	*Average ± SD*	*Average ± SD*
Maximum indent (nm)	***28.9 ± 3.6***	***36.0 ± 14.4***	***11.9 ± 0.5***
Maximum Load (nN)	***398.9 ± 78.6***	***376.1 ± 8.0***	***391.8 ± 16.6***
Area in contact with Samples (nm²)	***3536.5 ± 717.3***	***5712.4 ± 4551.7***	***1044.5 ± 46.5***
Slope of linear range (nN/nm)	***32.1 ± 1.1***	***32.9 ± 12.1***	***135.8 ± 67.8***
Modulus (GPa or nN/nm²)	***0.39 ± 0.05***	***0.36 ± 0.17***	***3.0 ± 1.5***
Hardness (GPa or nN/nm²)	***0.11 ± 0.01***	***0.09 ± 0.04***	***0.38 ± 0.0***

CHAPTER 6

EFFECTS OF LOW-LEVEL ELECTRIC CURRENT ON GENE EXPRESSION OF *PEUDOMONAS AERUGINOSA* PERISTER CELLS

The DNA microarray analysis described in this Chapter was collaborative work performed with Marcus Jones. Laura M Shepenger contributed to the testing of *P. aeruginosa* PAO1 mutants with antibiotics and DC.

6.1. ABSTRACT

Electrochemical control of antibiotic-tolerant bacteria presents a potential opportunity to eradicate bacterial infections involving biofilms and persister cells. In Chapter 5, it was demonstrated that *Pseudomonas aeruginosa* PAO1 cells respond differently to electrochemical treatments mediated with various electrode materials. For instance, direct current (DC) treatment of PAO1 using carbon electrodes resulted in intracellular accumulation of proteins, while the DC treatment using stainless steel (SS) 304 caused cell lysis and release of intracellular proteins. To understand these differences at the genetic level and correlate the results with those from electrochemical treatments of the persister cells, DNA microarray analysis was conducted on *P. aeruginosa* PAO1 persister cells. The findings from this study revealed that DC treatments have profound effects on the physiology of PAO1 persister cells. For instance, genes involved in pyocin-related functions and SOS response were induced by the DC treatments with carbon and SS304, respectively, and genes for antibiotic tolerance were differentially expressed. To corroborate the results, ten mutants were tested with the same electrochemical treatments. The results demonstrated that *pqsB, pvcA* and *PA1897* may contribute to the response of PAO1 to DC treatment.

6.2. INTRODUCTION

The metabolic versatility of *Pseudomonas aeruginosa* provides this opportunistic pathogen with a remarkable level of adaptability to survive in different environments, and causes chronic infections in patients with compromised immune systems such as those associated with medical implants, cystic fibrosis and burns. . The ability of *P. aeruginosa* to form bacterial biofilms, which embed sub-population of persister cells, creates an increasing challenge to curing *P. aeruginosa* infections with conventional antibiotics

Since antibiotics target biological processes such as DNA, protein, and cell wall synthesis, alternative approaches that target the physical properties of microorganisms have good potential to eradicate antibiotic-resistant bacterial infections. The finding that bacterial biofilms could be eliminated through synergistic effects with DC and antibiotics has led to the testing of the bioelectric effects on bacterial cells *in vivo*[1-3]. Our study conducted on the regular and persister cells of *P. aeruginosa* PAO1 demonstrated that the response of the cells is dependent upon the type of electrode material used to mediate the DC treatment. As shown in Chapter 3, DC treatment using SS304 led to the killing of PAO1 persister cells by 98% and 5 logs through synergy with tobramycin[4]. However, the same level of DC with carbon electrodes was less effective in killing PAO1 persister cells and the co-treatment with DC and Tob did not exhibit synergistic effects. Interestingly, complete eradication of the PAO1 persister cells was achieved, when Tob treatment was performed after the DC treatment. These findings corroborated the data reported in Chapter 5 that carbon and SS304 electrodes affected the cell morphology differently, resulting in intracellular accumulation of protein and cell lysis, respectively. We thus

hypothesize that electrochemical killing of *P. aeruginosa* using carbon and SS304 electrodes is based on different mechanisms, which could be further investigated through analysis of the transcriptomes of PAO1 persister cells.

Chang *et al.* [5] reported that *P. aeruginosa* responds to oxidative stress with induction of pyocin genes, and downregulation of intracellular transport genes, such as those controlling iron uptake. Also, it is well known that aminoglycoside uptake can be affected by changes in the membrane potential of bacteria cells[6,7]. This inspired us to investigate if DC treatment may influence the antibiotic uptake by *P. aeruginosa* and the antibiotic susceptibility of treated cells. In this chapter, DNA microarrays were used to investigate the response of the PAO1 persister cells to DC treatments. The transcriptional profiles of the cells before and after the treatment with both carbon and SS304 electrodes were compared to identity the genes involved in response to each treatment.

6.3. MATERIALS AND METHODS

6.3.1. Bacterial strain and growth media

The wild-type *P. aeruginosa* PAO1 was cultured in Luria-Bertani (LB) medium[8] containing 10 g/L tryptone, 5 g/L yeast extract, and 10 g/L NaCl. Each overnight culture was incubated at 37°C with shaking at 200 rpm. PAO1 mutants carrying ISlacZ/hah or ISphoA/hah were acquired from the *Pseudomonas aeruginosa* PAO1 transposon mutant library (UW-Genome Sciences , University of Washington, WA, USA) and cultured in LB medium with or without 10 μg/mL tetracycline (Tet). The mutants PW4389 (PA1939-G06::ISlacZ/hah), PW10231 (PA5461-A02::ISlacZ/hah), PW2800 (pqsB-

B05::ISlacZ/hah), PW8462 (PA4430-C09::ISphoA/hah), PW4830 (pvcA-F05::ISlacZ/hah), PW4567 (fusA2-F06::ISlacZ/hah), PW7877 (oprG-A04::ISphoA/hah), PW6348 (glk-C11::ISphoA/hah), PW3811 (aer-B08::ISlacZ/hah), and PW4324 (PA1897-B09::ISphoA/hah)[9] were grown in LB with 10 µg/mL tetracycline (Tet).

6.3.2. Colony Forming Units (CFUs)

The colony forming units (CFUs) were counted to quantify the number of viable *P. aeruginosa* PAO1 cells. Briefly 10 µL of each sample was diluted in a 10× series using 0.85% NaCl solution and spread on LB agar plates (1.5% agar). The CFUs were counted the next day after incubation overnight at 37°C.

6.3.3. DC treatment of persister cells

The PAO1 persister cells were isolated by treating the stationary phase cultures for 3.5 h with 200 µg/mL Cip, as described in Chapter 3. The harvested cells were washed twice with 0.85% NaCl solution, resuspended in 0.85% NaCl solution and treated with 70 µA/cm^2 DC for 20, 40 or 60 min. To deliver the DC, an electrochemical cell was constructed by inserting two SS304 or two carbon electrodes along the opposite sides of a plastic cuvette (Thermo Fisher Scientific, Pittsburg, PA) as shown in Figure 4.1A. A silver wire (0.015" diameter, A-M Systems, Sequim, WA) was placed in bleach for 30 min to generate an Ag/AgCl reference electrode. The reference electrode was then placed in the cuvette. DC was generated using a potentiostat (Potentiostat WaveNow, Pine Research Instrumentation, Raleigh, NC) in a 3-electrodes configuration. Using the AfterMath software (Potentiostat WaveNow, Pine Research Instrumentation, Raleigh,

NC), a galvanostatic mode was selected to monitor the DC level for 1 h. During DC treatments of the PAO1 mutants, 100 μL of sample was taken every 20 min to evaluate the viability of bacterial cells by counting CFU.

6.3.4. DNA microarray analysis

In order to understand the effects of DC on PAO1 persister cells at the genetic level, DNA microarray analysis was performed to determine the transcriptional profiles of the persister cells after various levels of DC treatment. Seven samples of PAO1 persister cells were isolated from overnight cultures (50 mL each), as described above. The cells were resuspended in 3 mL 0.85% NaCl and treated with 70 μA/cm^2 DC. Both carbon and SS304 electrodes were tested for 20 min and 40 min treatments. A DC-free sample was used as control. Immediately after each treatment, the cell pellet was collected by centrifugation at 15,000 g for 2.5 min at 4 ºC, frozen in dry-ice immediately and stored at -80°C until RNA extraction. The total RNA was extracted from the cells using RNeasy Mini Kit (Qiagen) as described previously[10], and sent to J. Craig Venter Institute for DNA microarray analysis.

6.3.5. Q-PCR analysis

To confirm the results of the microarray analysis, 10 representative genes including *PA0647, PA4430, PA4614, PA0166, pscF* (for DC treatment using SS304), *PA1032, PA4067, PA0633, PA0640, pscF* (for DC treatment using carbon) and the housekeeping gene *pbpA* (penicillin-binding protein 2) were selected to perform quantitative PCR (qPCR). Corresponding sets of primers (forward and reverse) were designed for the

selected genes (Table 1). The gene expression profile of PAO1 persister cells treated with 70 μA/cm^2 DC for 20 min or 40 min using carbon or SS304 electrodes was compared to that of the untreated control sample. The iScript cDNA synthesis kit (Bio-Rad, Hercules, CA, USA) was used to synthesize cDNA templates based on 200 ng total RNA. Following the manufacturer's protocol, primer mix (containing the forward and reverse primers) and Syber green mix (including the Syber green dye and cDNA templates) were prepared to quantify the relative expression ratios of the gene of interest by running qPCR using a Eppendorf Realplex Mastercycler (Eppendorf North America, Inc., Westbury, NY).

6.3.6. Susceptibility of *P. aeruginosa* PAO1and selected mutants to tobramycin

To understand the mechanism of ECCP, the function of a set of PAO1 genes identified from microarray study was investigated under the electrochemical treatment mediated using carbon and SS304. Mutants of *PA1939, PA5461, pqsB, PA4430, pvcA, fusA2, oprG, glk, aer, and PA1897* were acquired from the *Pseudomonas aeruginosa* PAO1 transposon mutant library (UW Genome Sciences) [9] to study the role of the corresponding genes in the response of the *P. aeruginosa* persister cells to the treatment with 70 μA/cm^2 DC. To evaluate the effects of the mutants on the susceptibility of PAO1 to Tob, the mutants were grown overnight in LB supplemented with 10 μg/mL Tet. Then, the cells were sub-cultured at an initial OD_{600} of 0.05 in 200 μL LB contained in 96 well plates (Costar ® No. 9017, Corning, NY) in the presence or absence of 1.5 μg/mL Tob. The wild type PAO1 was also grown in a 96 well-plate and all the samples were tested with 8 replicates

at 37 °C for 7h. Growth curves were recorded by measuring OD_{600} every hour using an ELx808 Absorbance Microplate Reader (Biotek, Winooski, VT).

6.3.7. Effects of gene mutation on persister formation

Previous work[11] has demonstrated that *P. aeruginosa* persisters can be isolated by lysing the regular cells with 25 μg/mL ciprofloxacin (Cip) for 3.5 h. In order to determine the sufficient Cip concentration for our strain, *P. aeruginosa* PAO1 and mutant cells were challenged with various concentrations of Cip (0 - 200 μg/mL) for 3.5 h and the killing was evaluated by counting CFUs of surviving cells. Briefly, the cells were cultured in LB medium over night at 37°C. Then the cells were collected by centrifugation (Sorvall Legend RT+, Thermo scientific, Asheville, NC) at 8,000 rpm for 10 min at room temperature, and washed twice with 0.85% NaCl solution before being treated with different concentrations of Cip for 3.5 h at 37°C. After treatment, the cells were washed three times with 0.85% of NaCl solution to remove residual Cip and the debris of lysed cells. The number of viable persister cells was then quantified by counting CFU as described above. Two replicates were tested for each condition.

6.3.8. Effects of DC on PAO1 mutants

Based on the transcriptional profiles of the DC treated PAO1 persister cells, the mutants of *PA1939, PA5461, pqsB, PA4430, pvcA* were selected to further study the function of the corresponding genes in DC treatments mediated with SS304; while mutants of *fusA2, oprG, glk, aer,* and *PA1897* were tested with DCs generated with carbon electrodes. The mutants were cultured overnight in LB medium supplemented with 10 μg/mL Tet. The

persister cells were isolated with 200 μg/mL Cip and treated with 70 μA/cm^2 DC for 1 h, as described above. During the treatment, 100 μL of sample was taken every 20 min to evaluate the viability of bacterial cells by counting CFU.

6.3.7. Statistical analysis

SAS Software was used to conduct t-test and one-way ANOVA analyses. Differences with $p < 0.05$ were considered as statistically significant.

6.4. RESULTS

6.4.1. Genes that were consistently changed by carbon and SS304 mediated treatments

To understand what genes and pathways in PAO1 persister cells are affected by DC, persister cells harvested from 50 mL cultures of PAO1 were treated with 70 μA/cm^2 DC using carbon or SS304 electrodes for 20 min and 40 min. The total RNA was isolated for microarray analysis, and the transcriptional profiles were validated with qPCR analysis of 10 representative genes (Table 1). Gene expression with a 2 fold or higher change ratio was considered significant. As shown in Table 2, the DC treatment resulted in the expression of a common set of genes induced or repressed by the electrochemical currents generated by carbon and SS304 electrodes. For instance, genes including *PA4623, PA4140, PA2756, PA2484, PA2313, PA09075* ("hypothetical, unclassified, unknown"), *PA0616, PA0639, PA0644* ("related to phage, transposon, or plasmid"), and *rpsP, glk, PA0206, PA4786* involved in "Translation, post-translational modification, degradation", "Carbon compound catabolism", "Transport of small molecules", and

"Putative enzymes", respectively, were commonly induced in DC treatments mediated with both carbon and SS304 electrodes. The genes that were repressed under all conditions include *PA0317, PA4319, PA4347, PA4894* ("hypothetical, unclassified, unknown"), *panB, PA2324, pscF, PA1600* and *PA0322.* The five latter genes are involved in "Biosynthesis of cofactors, prosthetic groups and carriers", "Putative enzymes", "Protein secretion/export apparatus", "Energy metabolism", and "Transport of small molecules", respectively.

6.4.2. Effects of carbon electrode-mediated DC on gene expression in PAO1 persister cells

Treatment with 70 μA/cm^2 DC for 20 min using carbon electrodes induced 51 genes and repressed 32 genes consistently in duplicated experiments (Fig. 6.1A). In comparison, the same treatment condition for 40 min induced 139 genes and repressed 47 genes (Fig. 6.1B). A total of 23 genes were induced by both 20 min and 40 min treatments, including *ribH* (involved in the "biosynthesis of cofactors, prosthetic groups and carriers"), *glk* (involved in "carbon compound catabolism"), *PA4010, PA0612, PA1042, PA1913, PA1967, PA2613, PA3205,* and *PA3320* (all of "hypothetical, unclassified, unknown" functions), *PA1897* and *oprG* (encoding "membrane proteins"), *PA1470* (encoding for a "putative enzyme"), *PA0617, PA0627, PA0628, PA0629, PA0633,* and *PA0636* ("pyocin-related genes"), *fusA1* and *fusA2* (elongation factors involved in "translation, post-translational modification, and degradation") and *fruK* and *ccmA* (involved in the "transport of small molecules").

Our findings also suggest that DC treatment using carbon electrodes may affect multi-drug resistance, and pyocin-related functions and biosynthesis in PAO1 cells. For example, *mexA, OprM, OprG, PA1032* and *PA4375*, which are involved in antibiotics resistance and bacterial efflux systems, were induced by the 40 min DC treatment using carbon. Strikingly, 17 out of 18 phage-related genes that were induced by 40 min DC treatment using carbon electrodes are known to be involved in pyocin production, which include *PA0616, PA0617, PA0619, PA0622, PA0623, PA0624, PA0626, PA0627, PA0628, PA0629, PA0633, PA0636, PA0637, PA0638, PA0639, PA0640,* and *PA0644*. Finally, the induction of 13 genes (3 genes at 20 min, 11 at 40 min and 2 at both conditions) involved in 'translation, post-translational modification, and degradation' suggests that DC treatment may affect the biosynthesis in treated cells. These genes include *lexA* (encoding for LexA repressor induced by 1.9 fold at 40 min), the ribosomal genes *rpsB, rpsL, rpsO, rpsP, rpsS,* and *fusA1*, and *fusA2* (encoding for elongation factors). Also, three genes for DNA repair were repressed, including *PA2138, ogt* (at 20 min) and *recR* (at 40 min). Energy metabolism related genes such as *cyoD, PA1600, PA0510* (at 20 min), *ccmH, nirJ, PA2716* (at 40 min), together with some genes encoding putative enzymes associated with oxido-reduction (*PA0237, PA4621, PA5327*) were also repressed. The downregulation of *PA1600, cyoD* and *ccmH* (which encode for cytochromes) suggest that DC might also affect cell respiration through oxido-reduction reactions and therefore the membrane functions of persister cells.

6.4.3. Effects of SS304-mediated DC on gene expression in PAO1 persister cells

Compared to the data of PAO1 cells treated with carbon electrodes, DC treatments of PAO1 persister cells using SS304 electrodes affected the physiological status of the persisters to a greater extent. A total of 250 genes were induced and 244 genes were repressed by the SS-mediated DC treatment for 20 min (Fig. 6.1A); while 135 genes were induced and a total of 95 genes were repressed by DC treatments using SS304 for 40 min in duplicated experiments (Fig. 6.1B). Overall, 74 genes and 35 genes were commonly induced and repressed, respectively, by both 20 min and 40 min DC treatments using SS304 (See supplementary data-Appendix II). The top 10 induced genes at both conditions include *sdhD* ("energy metabolism"), *PA1939*, *PA5461*, *PA1057*, *PA1343* ("hypothetical, unclassified, unknown"), *pqsB* ("biosynthesis of cofactors, prosthetic groups and carriers"), *secE* ("protein secretion/export apparatus"), *pvcA* ("secreted factors, toxins, enzymes, alginate"), *PA0810* ("carbon compound catabolism"), and *leuA* ("amino acid biosynthesis and metabolism"). The 10 most repressed genes by SS304-mediated DC treatments include *cysH* ("amino acid biosynthesis and metabolism"), *PA2768* and *PA1972* ("hypothetical, unclassified, unknown"), *pscQ* and *pscF* ("protein secretion/export apparatus"), *PA3630* ("transcriptional regulators"), *PA0345* ("membrane proteins"), *lasB* ("translation, post-translational modification, degradation"), *PA0600* ("two-component regulatory systems"), and *PA0240* ("transport of small molecules").

Some pathways, including protein secretion and export apparatus, energy-related functions, and SOS response, were among the features of the SS-mediated DC treatment, along with the antibiotic resistance functions, which were downregulated. For instance,

genes involved in “transport of small molecules” (23 genes), “energy metabolism” (14 genes), “transcriptional regulators” (13 genes), “biosynthesis of cofactors, prosthetic groups and carriers” (12 genes) and “putative enzymes” (11 genes) are among the most represented groups of genes induced by SS304 mediated DC for 20 min. The most significant functions of the repressed genes include “transport of small molecules” (26 genes), “transcriptional regulators” (25 genes), and “putative enzymes” (24 genes) groups. Seven genes involved in “energy metabolism”, including *snr1, cycH, PA2165, nirN, PA0509, PA0521, PA1600,* and *PA2417,* were repressed by 20 min DC treatment using SS304. DC treatment using SS304 for 40 min resulted in the induction of fewer genes compared to carbon, including 11 genes for “transport of small molecules” and “transcriptional regulators”, respectively. The most representative categories of genes repressed by 40 min of SS304 treatment are also involved in “transport of small molecules” (10 genes) and “transcriptional regulators” (10 genes). Among the “transport of small molecules” genes repressed under both conditions of DC using SS304, 5 are identified as probable major facilitator superfamily (MFS) genes and 9 are related to the ATP-binding cassette (ABC) transporters. These two major types of transporters regulate bacterial response to chemiosmotic ion gradients and the cross-membrane transport of large molecules, including antibiotics [12,13]. ABC transporters are required when energy is needed to perform cellular functions such as DNA repair [14]. Under our conditions, 6 genes involved in the translation or the repair of DNA were also found induced at 20 min or 40 min, which are *ruvB* and *ruvC* (encoding for holliday junction enzymes), *uvrB* (encoding for excinuclease ABC subunit B), *ihf* (encoding for integration host factor beta unit), *gyrA* (encoding for DNA gyrase subunit A), and *PA5348* (encoding a probable

DNA-binding protein). The induction of these genes by SS304-mediated DC suggests that the treatment might cause DNA damage. Moreover, genes encoding "protein secretion/export apparatus" were repressed by SS304-mediated DC treatment for 20 min (*hasE, pscK, pcrV*), 40 min (*xcpX*), and in both conditions (*PA2673, pcrG, pscF, pscQ*), or induced at 20 min (*popD, secE, SecG*) and 40 min (*xcpS, PA3404, secE*). Finally, DC treatment using SS304 induced 24 genes involved in synthesis of outer membrane vesicles (OMV) (see Table 3), which indicates potential changes in membrane integrity and functions.

6.4.4. Susceptibility of selected *P. aeruginosa* mutants to antibiotics including Tob and Cip

The analysis of the transcriptional profiles of PAO1 persister cells before and after the DC treatment performed with carbon or SS304 electrodes revealed that some genes may be important to the response of the persisters to the electrochemical treatments. Based on the microarray analysis, a total of 10 genes that were highly induced by the DC treatment using carbon and SS304 electrodes were selected for further investigation (Table 4). These strains have mutations in *PA1939, PA5461, pqsB, PA4430* and *pvcA* (induced by SS304-mediated treatment) as well as *fusA2, oprG, glk, aer* and *PA1897* (induced by carbon electrode mediated DC).

To determine if there is any difference in antibiotic susceptibility among these mutants, the cells were grown in LB medium in the presence or absence of 1.5 μg/mL Tob for 7 h. As shown in Fig. 6.2A, most mutants have normal growth except that the

mutant of *oprG* grew slowly in LB medium, compared to the wild-type and the other mutants. However, the growth of all the mutant strains in the presence of 1.5 μg/mL Tob was similar or slightly higher than the growth of the wild-type PAO1 (Fig. 6.2B). To further test the susceptibility of the mutants to antibiotics, all the strains were exposed to increasing concentration of Cip. The results of this test are shown in Fig. 6.3 demonstrating that the concentration of 200 μg/mL Cip was also appropriate for the isolation of persister cells from these mutant strains. However, the exact number of persisters isolated varied depending on the mutated genes. The number of persisters within stationary culture of mutants including *pqsB, fusA2, PA4430, glk,* and *oprG* represented 1% of the total cells found within the stationary cultures, which was similar to the level of persister cells in the wild-type PAO1[4]. The number of persister cells in stationary cultures of *pvcA, PA1939, PA5461*, and *aer* mutants represented between 0.1 to 1% of the total population. However, the stationary cultures of mutant of *PA1897* harbored the lowest number of persisters, representing only 0.01% of the overall population.

6.4.5. Effects of DC on the persister cells of selected mutants

To evaluate the roles of the genes that were differentially expressed to electrochemical treatments, the selected mutant strains were cultured and the persister populations were isolated as described in the Method section. The cells were washed with 0.85% NaCl solution and resuspended in the same at OD_{600} of 0.8 to perform DC treatments. Mutants including *PA1939, PA5461, pqsB, PA4430,* and *pvcA* were treated with 70 μA/cm^2 DC using SS304 electrodes, while the remaining mutants (*fusA2, oprG, glk, aer,* and *PA1897*)

were treated with 70 μA/cm^2 DC using carbon electrodes for 1 h. The response of the mutants to the electrochemical treatments demonstrated that some gene might be very important to PAO1 persisters. As shown in Fig. 6.4A, DC treatment using carbon electrodes resulted in more killing of the persister cells of PA1897 mutant. Compared to the wild-type PAO1, the persisters of mutant of *PA1897* were killed by 1.7 log after DC for 60 min (vs. 1.1 log for the wild type, one-way ANOVA, $p<0.0001$), suggesting that this mutation may affect the resistance of the *P. aeruginosa* cells to the DC treatment. The DC treatment did not significantly affect the viability of mutants of *oprG* (Two-way ANOVA, $p=0.8$) and *aer* (one-way ANOVA, $p=0.5$. Also mutants of *fusA2* (one-way ANOVA, $p=0.001$) and *glk* (one-way ANOVA, $p=0.02$) were less susceptible to DC treatment compared to the wild type. This suggests that there are redundancies in the functions of the genes involved in the response of PAO1 persisters to DC treatment.

DC treatment using SS304 highlighted more genetic functions, which could be interesting for the persister control using electrochemical treatments (Fig. 6.4B). For instance, while the persister cells of wild-type PAO1 were killed by 1.6 log with 70 μA/cm^2 DC using SS304 electrodes, the persisters collected from the mutants of *pqsB, pvcA* and *PA4430* were killed by 2.8 logs (one-way ANOVA, $p<0.0001$), 2.8 logs (one-way ANOVA, $p<0.0001$) and 2.1 logs (one-way ANOVA, $p=0.04$), respectively. These results suggest that *psqB, pvcA* and *PA4430* might constitute important targets of the electrochemical treatment. No clear difference was found in the killing effect of the DC treatment of the persisters of PAO1 vs. those of mutant of *PA5461* (one-way ANOVA, $p=0.6$). Interestingly, deletion of *PA1939* rendered the persister cells less susceptible to

the treatment of 70 μA/cm^2 DC using SS304. These mutants were killed 1 log less than the wild type PAO1 (one-way ANOVA, p<0.0001).

6.5. DISCUSSION

The electrophysiological properties of the persister cells were investigated using DNA microarrays. Under our experimental condition, DC treatments were performed for 20 min and 40 min only, since strong killing effects were observed in the 1 h treatments [4]. The differentially expressed genes provide important information for understanding the effects of DC on persister cells. A common feature of the DC treatment using both carbon and SS304 is the generation of ROS due to the oxido-reduction reactions occurring at the electrodes. Oxygen radicals generated through the electrolysis of water, or Fenton reaction in the presence of Fe, has been widely reported as a cause of DNA damage [15,16] [17]. The DC treatment in our system provides an exogenous source of Fe, which may increase the concentration of free Fe ions within the cells, and results in more oxidative stress as previously reported [18]. Our microarray data analysis confirmed that SOS response to oxidative stress was more prevalent in DC treatments performed with SS304, compared to that performed with carbon electrodes. Some more genes involved in the DNA repair were induced by the SS mediated treatments. The induction of *lexA*, a SOS regulon repressor of DNA damage, escalated from 2 to 6-fold with the 20 min and 40 min treatments using SS304 (Table 3). DC treatment using SS304 also induced the lexA gene 3 times more than the treatment using carbon electrodes (at 40 min). The finding that 17 pyocin-related genes were induced by the treatment with DC using carbon electrodes confirmed that pyocin production may be a result of oxidative stress in persister cells[5].

The DC treatments stimulated variable responses associated with drug resistance. Previously, we discovered that the co-treatment of the persister cells with antibiotics and DC using carbon electrodes did not show any synergistic killing activity[4]. However, synergistic effects were achieved during sequential treatment with DC for 1 h, followed with 1.5 μg/mL Tob for 1 h. The microarray analysis of cells treatment with carbon electrodes showed that the genes associated with drug resistance were affected during the treatment. For instance, *mexA* and *oprM* that encode efflux systems involved in multidrug resistance were induced by 40 min treatment with DC using carbon electrodes. Thus we hypothesize that such synergistic effects from sequential treatment with DC and Tob may be partially caused by the effect of DC and its electrochemical byproducts on membrane functions of the cells. Similarly, DC treatment using SS304 also affected genes associated with antibiotic resistance. For instance many genes associated with protein secretion and export apparatus, transport of small molecules, and energy metabolism were either induced or repressed. Several genes involved in response to antibiotics were repressed at 20 min by the DC treatment using SS304, such as *PA1129, PA1237* and *PA2018*. It will be interesting to further investigate if such effects contribute to the synergistic killing during co-treatment with DC and Tob.

The test of selected mutants with DC treatment has revealed that some genes are indeed involved in bacterial response to DC. For instance, the increased sensitivity of *PA1897* to DC suggests that a hypothetical protein encoded by this gene may contribute to the response of persister cells to electrochemical current mediated with carbon electrodes. It was also discovered that some mutations led to an altered level of

persistence. This finding suggests that some genes involved in persister formation may also be involved in response to electrochemical stresses. Interestingly, mutation of *fusA* and *glk* genes, encoding for elongation factor G and glucokinase, respectively, rendered the persister cells less susceptible to DC. Further studies on gene regulation are required to better understand the functions of these genes and their roles in bacterial response to DC.

6.6. CONCLUSIONS

In this study, the response of the *P. aeruginosa* PAO1persister cells to the DC treatments were investigated to understand the differences in persister killing by DC mediated with carbon vs. SS304 electrodes. The results revealed that pyocin production and SOS response were induced by DC treatments using carbon and SS304, respectively. The microarray results were validated by qPCR. Furthermore, some mutants of selected genes exhibited altered susceptibility to DC treatment. Overall, this study provided additional information for understanding the mechanism of ECCP and for designing more effective controls.

6.7. ACKNOWLEDGEMENTS

The authors are grateful to Blue Highway Inc. for supporting the project. We thank Dr. Thomas K. Wood at Penn State University for sharing the strain *P. aeruginosa* PAO1. The PAO1 mutants were acquired from the *Pseudomonas aeruginosa* PAO1 transposon mutant library (UW Genome Sciences). We also like to thank Marcus Jones for performing microarrays and Laura Shepenger for helping with mutant testing.

6.8. REFERENCES

1 **Del Pozo, J. L., Rouse, M. S., Euba, G., Kang, C., Mandrekar, J. N., Steckelberg, J. M., Patel, R.** The electricidal effect is active in an experimental model of *Staphylococcus epidermidis* chronic foreign body osteomyelitis. *Antimicrobial agents and chemotherapy* **53**, 4064-4068 (2009).

2 **Van der Borden, A. J., Maathuis, P. GM., Engels, E., Rakhorst, G., van der Mei, H. C., Busscher, H. J., Sharma, P. K.** Prevention of pin tract infection in external stainless steel fixator frames using electric current in a goat model. *Biomaterials* **28**, 2122-2126 (2007).

3 **Rowley, B. A., McKenna, J. M., Chase, G. R. & Wolcott, L. E.** The influence of electrical current on an infecting microorganism in wounds. *Annals of the New York Academy of Sciences* **238**, 543-551 (1974).

4 **Niepa, T. H., Gilbert, J. L. & Ren, D.** Controlling *Pseudomonas aeruginosa* persister cells by weak electrochemical currents and synergistic effects with tobramycin. *Biomaterials* **33**, 7356-7365, doi:10.1016/j.biomaterials.2012.06.092 (2012).

5 **Chang, W., Small, D. A., Toghrol, F. & Bentley, W. E.** Microarray analysis of *Pseudomonas aeruginosa* reveals induction of pyocin genes in response to hydrogen peroxide. *BMC genomics* **6**, 115 (2005).

6 **Damper, P. D. & Epstein, W.** Role of the membrane potential in bacterial resistance to aminoglycoside antibiotics. *Antimicrobial agents and chemotherapy* **20**, 803-808 (1981).

7 **Taber, H. W., Mueller, J., Miller, P. & Arrow, A.** Bacterial uptake of aminoglycoside antibiotics. *Microbiological reviews* **51**, 439 (1987).

8 **Sambrook, J. & Russell, D. W.** *Molecular cloning: a laboratory manual*. Vol. 3 (Cold spring harbor laboratory press, 2001).

9 **Bassetti, M., Merelli, M., Temperoni, C. & Astilean, A.** New antibiotics for bad bugs: where are we? *Ann. Clin. Microbiol. Antimicrob* **12**, 1186 (2013).

10 **Szkotak, R., Niepa, T. H., Jawrani, N., Gilbert, J. L., Jones, M. B., Ren, D.** Differential Gene Expression to Investigate the Effects of Low-level Electrochemical Currents on *Bacillus subtilis. AMB Express* **1**, 39, doi:10.1186/2191-0855-1-39 (2011).

11 **Moker, N., Dean, C. R. & Tao, J.** *Pseudomonas aeruginosa* increases formation of multidrug-tolerant persister cells in response to quorum-sensing signaling molecules. *J Bacteriol* **192**, 1946-1955, doi:JB.01231-09 [pii] 10.1128/JB.01231-09 (2010).

12 **Van Bambeke, F., Balzi, E. & Tulkens, P. M.** Antibiotic efflux pumps. *Biochemical pharmacology* **60**, 457-470 (2000).

13 **Pao, S. S., Paulsen, I. T. & Saier, M. H.** Major facilitator superfamily. *Microbiology and Molecular Biology Reviews* **62**, 1-34 (1998).

14 **Doolittle, R., Johnson, M. S., Husain, I., Van Houten, B., Thomas, D. C., Sancar, A.** Domainal evolution of a prokaryotic DNA repair protein and its relationship to active-transport proteins. *Nature* **323**, 451-453 (1986).

15 **Miller, R. A. & Britigan, B. E.** Role of oxidants in microbial pathophysiology. *Clinical Microbiology Reviews* **10**, 1-18 (1997).

16 **Keyer, K., Gort, A. S. & Imlay, J. A.** Superoxide and the production of oxidative DNA damage. *Journal of bacteriology* **177**, 6782-6790 (1995).
17 **Imlay, J. A.** Pathways of oxidative damage. *Annual Reviews in Microbiology* **57**, 395-418 (2003).
18 **Keyer, K. & Imlay, J. A.** Superoxide accelerates DNA damage by elevating free-iron levels. *Proceedings of the National Academy of Sciences* **93**, 13635-13640 (1996).

FIGURE CAPTIONS

Figure 6.1. Transcriptional profile of *P. aeruginosa* PAO1 persister cells treated with 70 μA/cm^2 DC using carbon or SS304 electrodes for (A) 20 min, and (B) 40 min.

Figure 6.2. Growth curves of the wild-type *P. aeruginosa* PAO1 and mutants in LB medium in the absence (A) or presence (B) of 1.5 μg/mL Tob.

Figure 6.3. Viability of *P. aeruginosa* PAO1 and mutants after a 3.5-h treatment of planktonic stationary cultures with different concentrations of Cip.

Figure 6.4. Effects of DC treatment of cultures of *P. aeruginosa* PAO1 and mutants of planktonic persister cells in stationary phase. The persister cells were treated with 70 μA/cm^2 DC for 1 h using carbon (A) or SS304 (B) electrodes.

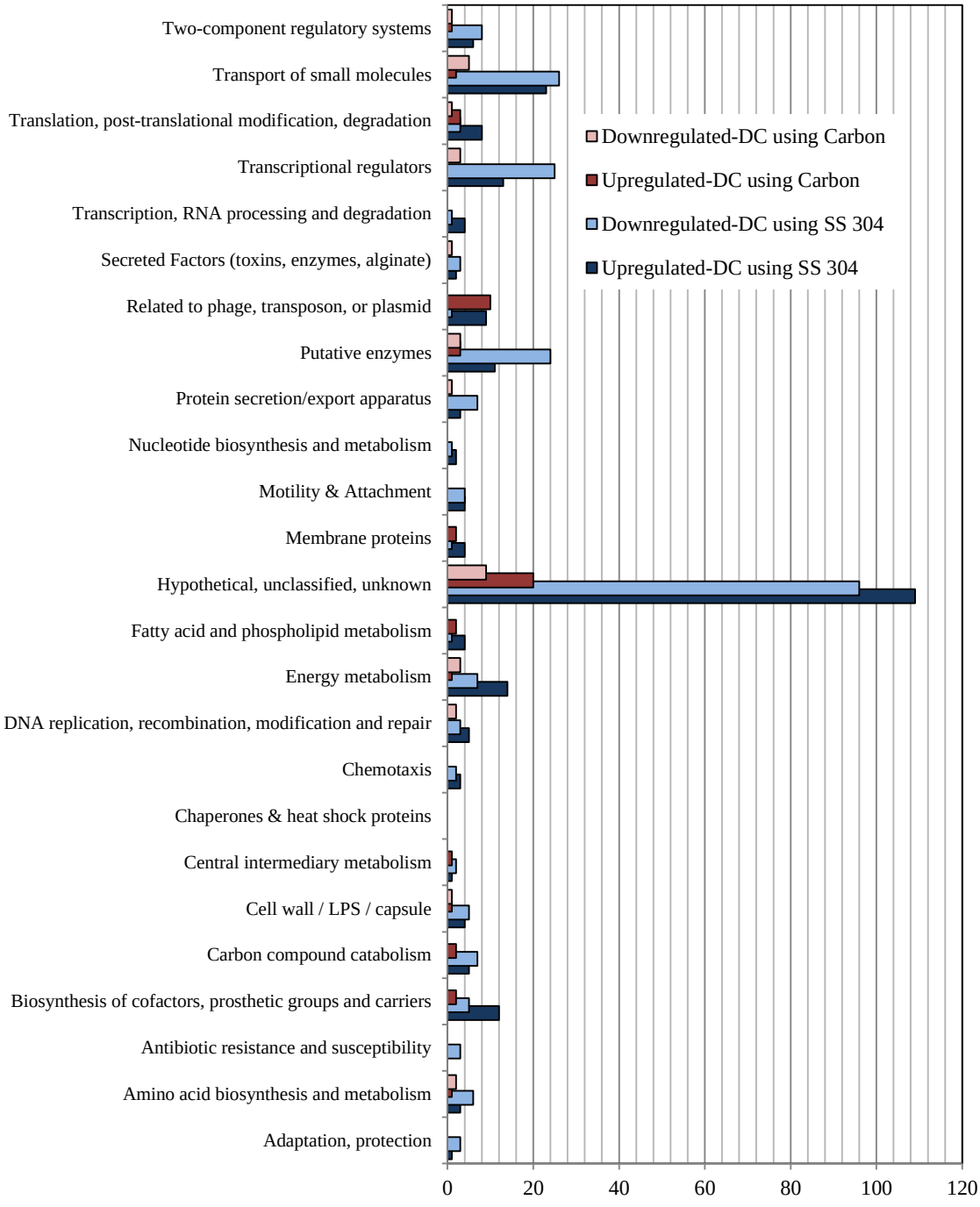
Two-component regulatory systems
Transport of small molecules
Translation, post-translational modification, degradation
Transcriptional regulators
Transcription, RNA processing and degradation
Secreted Factors (toxins, enzymes, alginate)
Related to phage, transposon, or plasmid
Putative enzymes
Protein secretion/export apparatus
Nucleotide biosynthesis and metabolism
Motility & Attachment
Membrane proteins
Hypothetical, unclassified, unknown
Fatty acid and phospholipid metabolism
Energy metabolism
DNA replication, recombination, modification and repair
Chemotaxis
Chaperones & heat shock proteins
Central intermediary metabolism
Cell wall / LPS / capsule
Carbon compound catabolism
Biosynthesis of cofactors, prosthetic groups and carriers
Antibiotic resistance and susceptibility
Amino acid biosynthesis and metabolism
Adaptation, protection
Downregulated-DC using Carbon
Upregulated-DC using Carbon
Downregulated-DC using SS 304
Upregulated-DC using SS 304
0
20
40
60
80
100
120

(A)

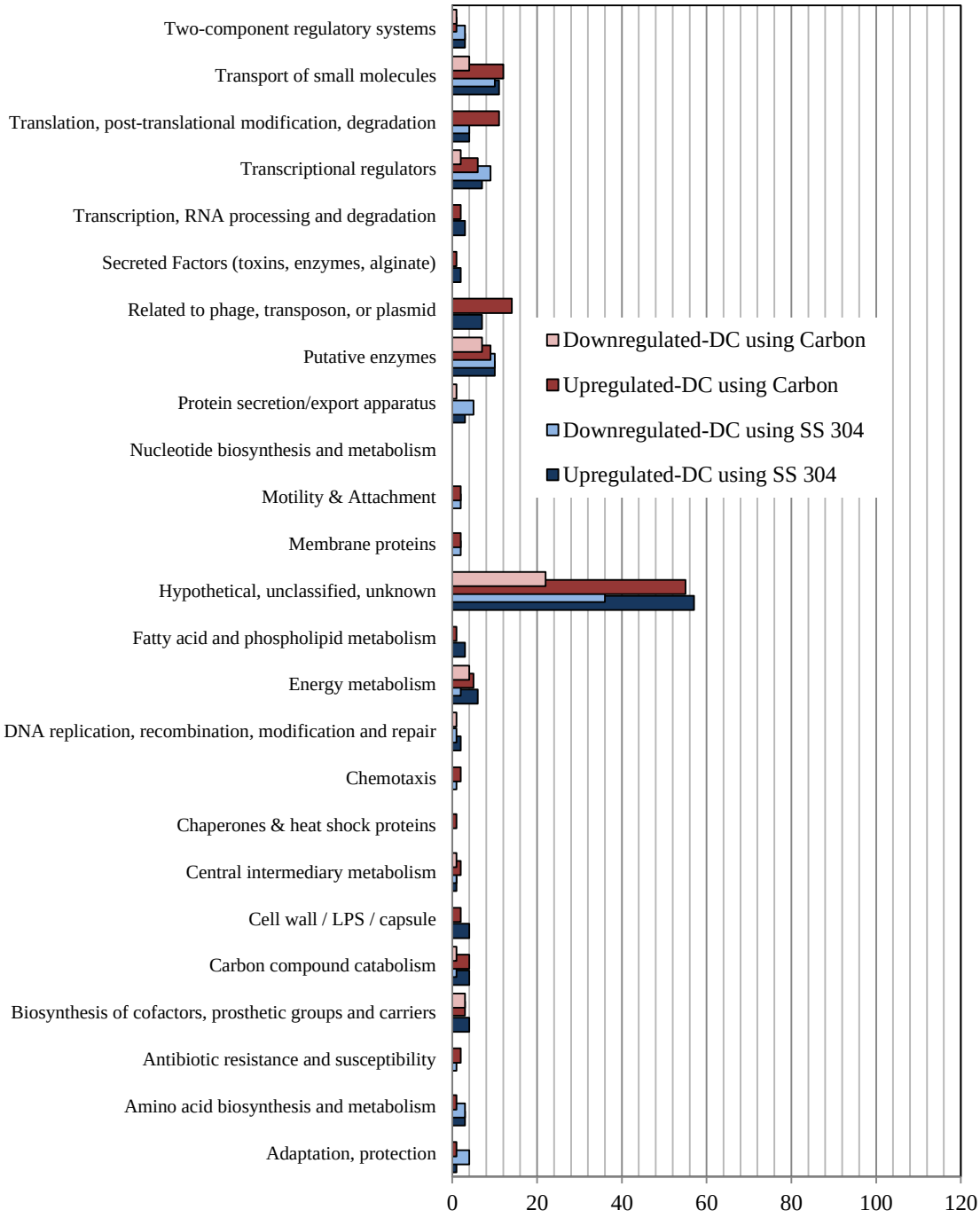
Two-component regulatory systems
Transport of small molecules
Translation, post-translational modification, degradation
Transcriptional regulators
Transcription, RNA processing and degradation
Secreted Factors (toxins, enzymes, alginate)
Related to phage, transposon, or plasmid
Putative enzymes
Protein secretion/export apparatus
Nucleotide biosynthesis and metabolism
Motility & Attachment
Membrane proteins
Hypothetical, unclassified, unknown
Fatty acid and phospholipid metabolism
Energy metabolism
DNA replication, recombination, modification and repair
Chemotaxis
Chaperones & heat shock proteins
Central intermediary metabolism
Cell wall / LPS / capsule
Carbon compound catabolism
Biosynthesis of cofactors, prosthetic groups and carriers
Antibiotic resistance and susceptibility
Amino acid biosynthesis and metabolism
Adaptation, protection
Downregulated-DC using Carbon
Upregulated-DC using Carbon
Downregulated-DC using SS 304
Upregulated-DC using SS 304
0
20
40
60
80
100
120

(B)

Figure 6.1

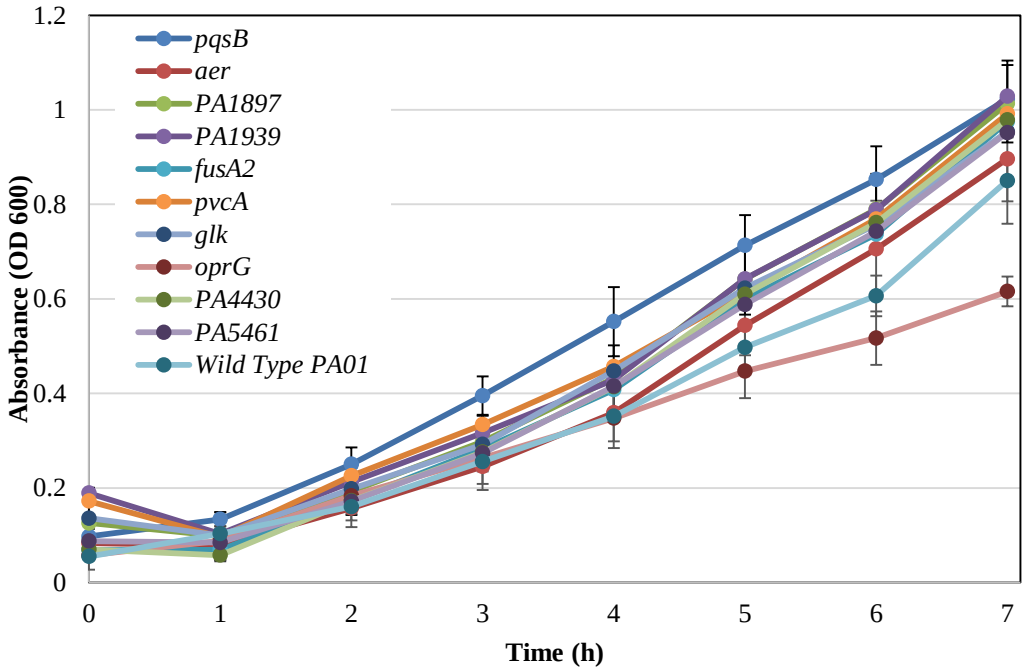
1.2
1
0.8
0.6
0.4
0.2
0
Absorbance (OD 600)
0
1
2
3
4
5
6
7
Time (h)
pqsB
aer
PA1897
PA1939
fusA2
pvcA
glk
oprG
PA4430
PA5461
Wild Type PA01

(A)

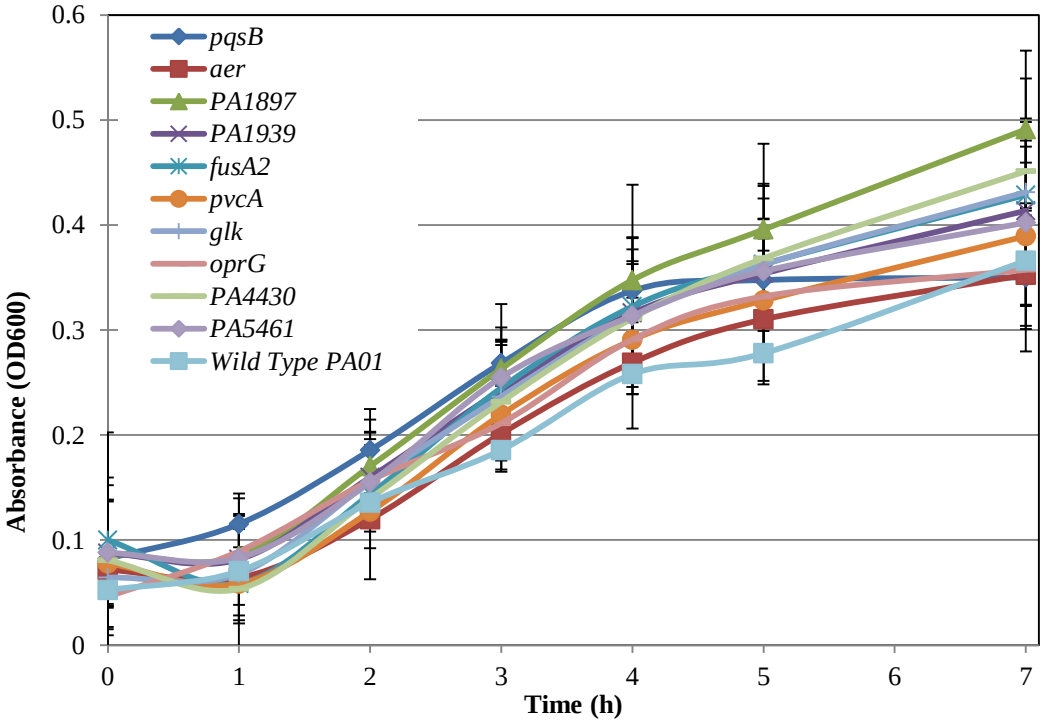
0.6
0.5
0.4
0.3
0.2
0.1
0
Absorbance (OD600)
0
1
2
3
4
5
6
7
Time (h)
pqsB
aer
PA1897
PA1939
fusA2
pvcA
glk
oprG
PA4430
PA5461
Wild Type PA01

(B)

Figure 6.2

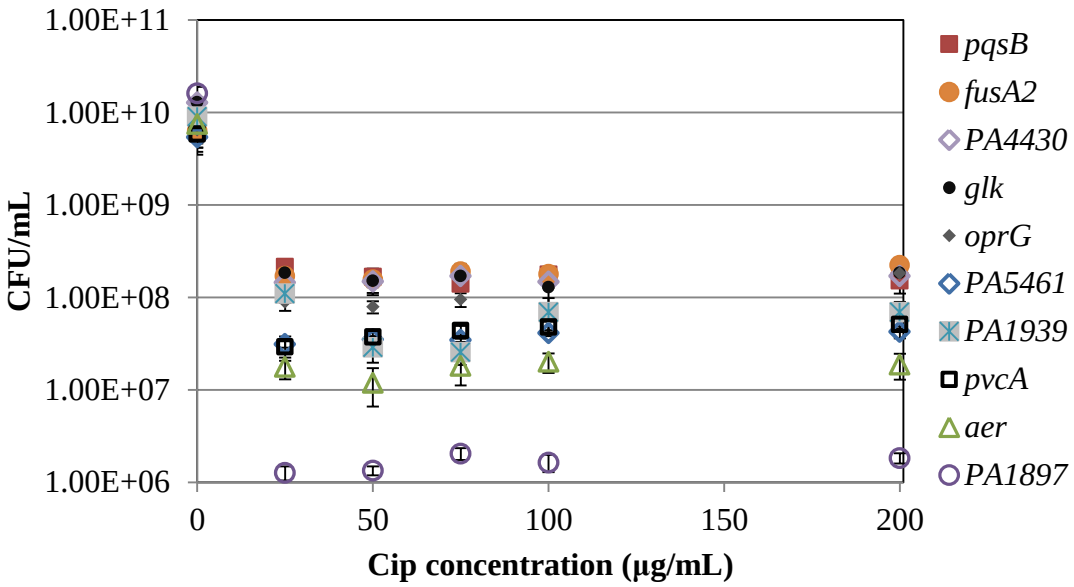
1.00E+11
1.00E+10
1.00E+09
1.00E+08
1.00E+07
1.00E+06
CFU/mL
0
50
100
150
200
Cip concentration (µg/mL)
pqsB
fusA2
PA4430
glk
oprG
PA5461
PA1939
pvcA
aer
PA1897

Figure 6.3

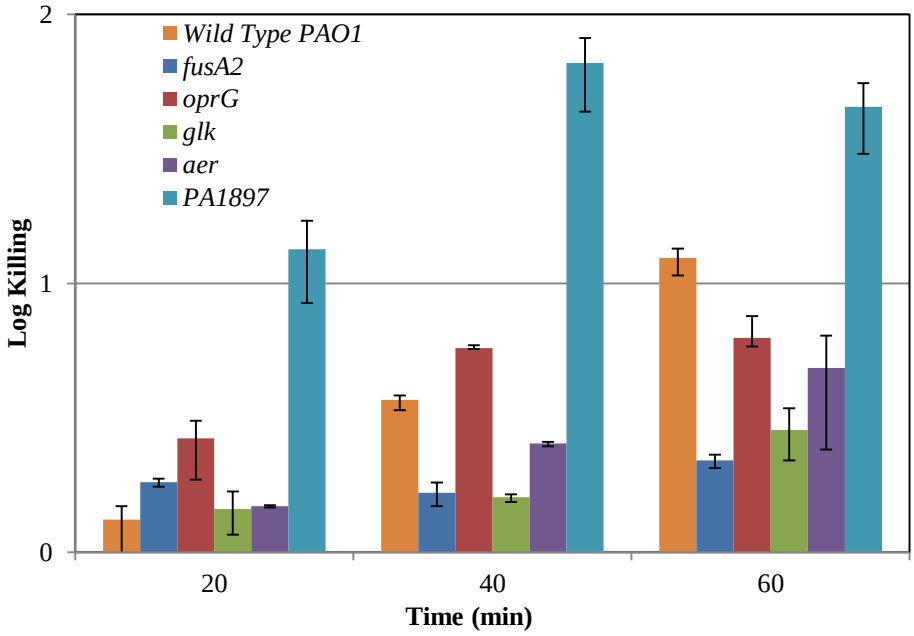
Wild Type PAO1
fusA2
oprG
glk
aer
PA1897
Log Killing
2
1
0
20
40
60
Time (min)

(A)

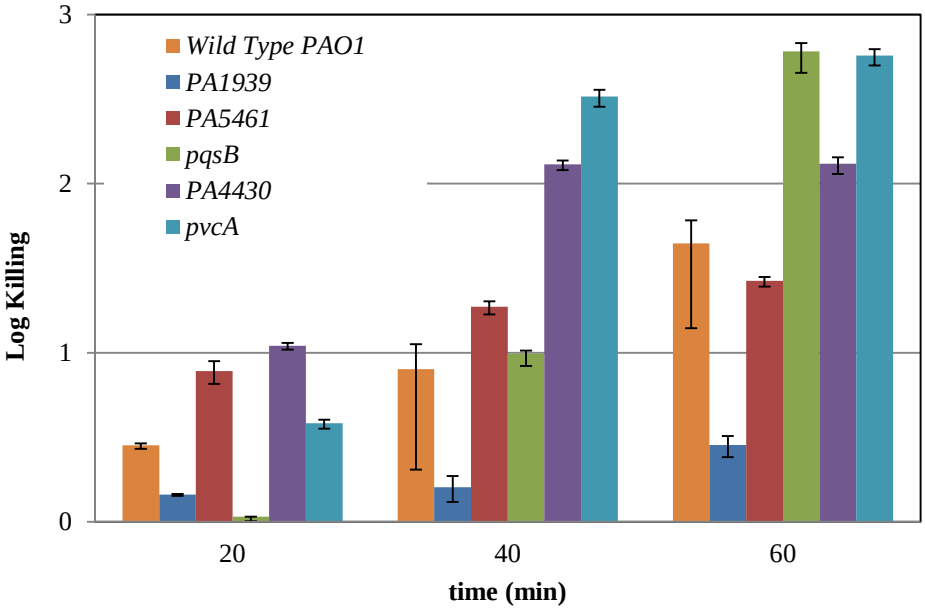
Wild Type PAO1
PA1939
PA5461
pqsB
PA4430
pvcA
Log Killing
3
2
1
0
20
40
60
time (min)

(B)

Figure 6.4

Table 6.1

Comparison of transcriptional profile of selected genes expressed during

DC treatment mediated with carbon and SS304 for 20 and 40 min using DNA microarray and q-PCR analysis

Target	Forward primer (5'-3')	Reverse primer (5'-3')	Fold change in mRNA level			
			Microarray		*Quantitative PCR*	
			20 min	40 min	20 min	40 min
	Housekeeping gene					
pbpA	CCACAAATAGTCCCCAGTCCC	TTGCGGTCGAAGATGATCCC				
	DC using SS304					
PA0647	GAGATTCGATAGCCGTCTCGG	TCGATCACTTGGGCAACTCC	3.2	2.3	38.1	21.5
PA4430	CTTCGAGATGGCCAACCAGT	GTAGCCGAGGATCACGAAGG	3.1	16.9	1.3	12.9
PA4614	GAGTCGACTTCTCCGACCTG	TCACGACTTGTTCTGCTGGG	2.0	2.3	2.7	11.2
PA0166	GGTGGCGCTGATCTACCTG	GATATAGATCCCGACGTGCCG	-2.4	-2.0	-2.4	-1.3
pscF	GGCATTCTTTCGCAGCTCAC	ACCGACCACTTGTTGATCTTGT	-3.1	-2.4	-3.2	-8.0
	DC using carbon					
PA1032	ACGTTAGCTTCCCGTTCCAG	AGATCAGTTCGATCCCGTGC	1.8	3.5	6.8	31.6
PA4067	AGCATGAAGCTGCAGGACTC	CGCGACAGTCTACGACTCAG	4.5	2.4	1.4	2.8
PA0633	CAGATCTACGCCCTGGTTCC	TCGTCTCGCCATCTTTCTCG	2.4	2.8	1.2	17.2
PA0640	CGACATATTCAAGCGAGCCG	AGGTCAGCCCTTTCGATTCC	2.6	1.7	1.9	2.4
pscF	GGCATTCTTTCGCAGCTCAC	ACCGACCACTTGTTGATCTTGT	-2.5	-1.4	-1.4	-1.7

Table 6.2
List of genes common to the DC treatments using carbon and SS304 electrodes

genes		carbon		SS304	
		20 min	40 min	20 min	40 min
	Common genes induced				
PA4786	short-chain dehydrogenase	1.1	3.5	2.2	1.0
PA4623	hypothetical protein	1.0	3.4	1.4	2.1
PA4140	hypothetical protein	1.6	2.1	3.1	2.9
rpsP	30S ribosomal protein S16	1.3	2.8	3.0	2.4
glk	glucokinase	3.2	8.5	3.7	0.9
lexA	LexA repressor	1.5	1.9	1.8	6.0
PA2756	hypothetical protein	0.6	6.6	2.3	5.9
PA2484	hypothetical protein	2.6	1.3	1.3	2.9
PA2313	hypothetical protein	1.0	4.3	1.0	2.0
PA0907	hypothetical protein	0.9	2.8	4.8	1.0
PA0644	hypothetical protein	0.9	2.0	1.8	2.1
PA0639	hypothetical protein	1.4	2.2	2.0	2.1
PA0616	hypothetical protein	0.7	2.5	2.2	2.0
PA0206	probable ATP-binding component of ABC transporter	1.1	7.3	3.0	1.8
	Common genes repressed				
PA4894	hypothetical protein	-1.2	-2.8	-1.8	-2.2
panB	3-methyl-2-oxobutanoate hydroxymethyltransferase	-1.0	-2.0	-2.0	-1.1
PA4347	hypothetical protein	-1.3	-2.1	-2.3	-2.3
PA4319	hypothetical protein	-2.1	-0.6	-2.5	-0.9
PA2324	hypothetical protein	-2.8	-1.5	-3.0	-1.4
pscF	type III export protein PscF	-2.5	-1.4	-3.1	-2.4
PA1600	probable cytochrome c	-2.3	-0.9	-2.2	-1.6
PA0322	probable transporter	-2.5	-1.7	-1.3	-2.7
PA0317	hypothetical protein	-1.0	-2.0	-1.5	-2.3

Table 6.3

List of genes for outer membrane vesicle regulation after 70 μA/cm^2 DC using SS304 electrodes

		fold change	
gene	**description**	**20 min**	**40 min**
PA4623	hypothetical protein	1.36	2.14
PA1526	probable transcriptional regulator	2.98	6.43
PA0647	hypothetical protein	3.21	2.32
PA4638	hypothetical protein	3.04	0.79
PA2885	probable transcriptional regulator	2.08	1.17
PA4451	hypothetical protein	2.44	3.86
PA0631	hypothetical protein	2.27	1.72
PA0648	hypothetical protein	1.24	2.25
xylZ	toluate 1,2-dioxygenase electron transfer component	1.39	2.28
PA2479	probable two-component response regulator	3.20	2.98
PA2135	probable transporter	2.53	5.12
hepA	ATP-dependent helicase HepA	2.95	2.38
PA1895	hypothetical protein	1.91	2.49
PA3330	probable short chain dehydrogenase	2.94	1.41
PA0368	hypothetical protein	3.77	2.04
rpsI	30S ribosomal protein S9	3.04	1.95
PA4372	hypothetical protein	2.27	2.11
PA3517	probable lyase	2.17	2.39
PA0616	hypothetical protein	2.22	2.02
PA0206	probable ATP-binding component of ABC transporter	3.02	1.79
PA5380	probable transcriptional regulator	3.36	1.12
PA0779	probable ATP-dependent protease	1.50	3.27
PA1504	probable transcriptional regulator	0.59	3.95
PA0308	hypothetical protein	2.69	1.76

Table 6.4

List of mutants selected to study the gene function under DC treatments

Condition	Gene	Description	Fold Change 20 min	Fold Change 40 min
DC using SS304 electrode	*pqsB*	beta-keto-acyl-acyl-carrier protein synthase-like protein	7.0	2.1
	pvcA	pyoverdine biosynthesis protein PvcA	6.2	2.4
	PA1939	hypothetical protein	10.5	3.5
	PA4430	probable cytochrome b	3.1	16.9
	PA5461	hypothetical protein	9.7	12.5
DC using carbon electrode	*aer*	aerotaxis receptor Aer	1.5	4.0
	glk	glucokinase	3.2	8.5
	fusA2	elongation factor G	4.7	6.1
	oprG	Outer membrane protein OprG precursor	4.5	2.4
	PA1897	hypothetical protein	2.3	4.1

CHAPTER 7

PROBING THE SYNERGY BETWEEN TOBRAMYCIN AND CHROMIUM (III) IN THE ELECTROCHEMICAL TREATMENTS OF BACTERIAL CELLS

7.1. ABSTRACT

The ability of the aminoglycosides to eliminate antibiotic-resistant bacteria can be enhanced by means of several physicals factors. For example, tobramycin (Tob) exhibited synergistic killing effects with direct currents (DC) in the electrochemical control of bacterial cells. As described in Chapter 3, the treatment of *Pseudomonas aeruginosa* persister cells with 70 μA/cm^2 DC mediated with stainless steel 304 and 1.5 μg/mL Tob resulted in 5-log reduction of the persister cell viability vs. 2-log in the absence of this antibiotic, and killing by Tob alone. Supplementation of the metal ions, e.g. Ni^{2+}, Cr^{2+} and Fe^{2+}, to carbon-mediated DC treatment was also found to increase persister killing in the presence of Tob, leading to our hypothesis that the interactions between Tob and metal ions could contribute to the synergy. To better understand these interactions and their effects on the cells, the electrochemical properties of the aminoglycosides, including Tob and a similar molecule, kanamycin (Kan), were investigated. The results of Nuclear Magnetic Resonance (NMR) analysis demonstrated that, unlike Kan, increase in the concentration of Cr^{3+} caused a shift in the HSQC peak of Tob, suggesting the formation Cr^{III}(Tob) complexes under DC treatment. The stability of the complexes was further studied using UV-visible spectroscopy and cyclic voltammetry, which demonstrated that the configuration of the Cr^{III}(Tob) complexes under the electrochemical treatment conditions could enhance the affinity between the complexes and negatively charged cellular components such as DNA or RNA. These findings are helpful for developing more effective approaches for improving the bioactivity of aminoglycosides and treat antibiotic-resistant bacteria more effectively.

7.2. INTRODUCTION

The transport of aminoglycoside antibiotics across bacterial membranes consisting of lipid bilayers and complex transmembrane porins and channels is an energy-demanding process. This process is affected by many factors such the membrane potential of targeted cells, ionic strength and pH of the medium for treatment, and the electrochemical gradient of compounds in the vicinity of the cells[1]. Upon entering the cells, aminoglycosides bind to the ribosomal RNA[2,3]. Such interactions interrupt the function of the translational machinery, leading to protein mistranslation, SOS response and eventually cell death [4]. Thus, the bactericidal effects of aminoglycosides are dependent upon their strong affinity with the cellular targets, which could be affected not only by the structure of the antibiotic itself but also by external physicochemical factors that can affect the transport of aminoglycosides.

In contrast to other aminoglycosides such as gentamycin (Gen), amikacin (Amk), streptomycin (Strep) and kanamycin (Kan), Tob has an excellent bioactivity in the treatment of bacterial infections. *In vitro* and *in vivo* models of infections have demonstrated that Tob is very effective in killing multidrug-resistant pathogens including *P. aeruginosa*, *Staphylococcus aureus* and some *Enterobacteriaceae*. Tob differs structurally from Kan in that the later compound possesses an additional hydroxyl (OH) group (Fig. 7.1). This slight modification is believed to lower the basicity of Kan, weakening its electrostatic interaction with 16S ribosomal RNA, and consequently contributing to its low bioactivity[3]. In addition to these electrostatic considerations inherent to the antibiotics, the affinity between an aminoglycosides and its cellular target

could also be affected by the ionic strength of the solution [5].Interactions between positively charged ions and aminoglycosides have been documented. Specifically, the susceptibility of *P. aeruginosa* to Strep, Gen, Amk and Tob decreased when the cells were grown on Mueller-Hinton Agar containing divalent cations such as Mg^{2+} or Ca^{2+} [6-9]. However, some reports present clear evidence that longer exposure of bacteria to metal cations alone including Co^{2+}, Ni^{2+}, Cu^{2+}, Zn^{2+}, Al^{3+} and Pb^{2+} in the mM range could reduce the number of viable *P. aeruginosa* cells by 3 logs [10]. Interestingly, in a model of cystic fibrosis on epithelial cells, the bioactivity of Tobramycin against *P. aeruginosa* biofilm was found enhanced with the supplementation of iron chelators including deferoxamine and deferasirox [11], suggesting some rather synergistic effects between Tob and Fe.

The synergistic killing of bacterial biofilm with DC, aminoglycosides and metal ions is a well-known phenomenon, referred to as bioelectric effects[12-14]. Recently, we have demonstrated synergistic killing of *P. aeruginosa* PAO1 persister cells can be achieved with low-level DC and 1.5 μg/mL Tob using SS 304 electrodes containing Fe, Cr, Mn an Ni. However, no synergy was found when Tob was added subsequently to the DC treated PAO1 persister cells. Also, the supplementation of 0.1 μM Ni^{2+}, 0.27 μM Cr^{3+}, or 0.82 μM Fe^{2+} to the carbon mediated-DC treatment in the presence of 1.5 μg/mL Tob improved the killing of persister cells by 84.5 ± 1.2%, 38.1 ± 5.7%, and 20 ± 7.4%, respectively, compared to the treatment without ion supplementation. These findings led us to hypothesize that possible interaction between the SS-released metal cations and Tob could be beneficial to the control of bacterial persister cells, which could guide the design

of new therapeutics. Thus, the study in this chapter aims to characterize the electrochemical properties of Tob and metal cations, and their synergistic activities in killing *P. aeruginosa* cells.

7.3. MATERIALS AND METHODS

7.3.1. Chemicals and reagents

Nickel (II) Chloride ($NiCl_2$), Chromium (II) Chloride ($CrCl_2$), Chromium (VI) oxide (CrO_3), Chromium (III) chloride hexahydrate ($CrCl_3.6H_2O$) were purchased from Acros Organics (Thermo Fisher Scientific, Waltham, MA). Iron (II) chloride tetrahydrate ($FeCl_2.4H_2O$) was purchased from Sigma-Aldrich (St. Louis, MO). Ferric chloride anhydrous ($FeCl_3$) and Manganese Chloride ($MnCl_2(H_2O)_x$) were purchased from Fisher scientific (Waltham, MA). Tobramycin was purchased from TCI America (Portland, OR). Stock solutions for these chemicals were prepared with Milli-Q water.

7.3.2. Electrochemical treatments

To investigate the interaction between metal ions and aminoglycosides including Tob and Kan, an electrochemical cell as described in chapter 3 was constructed using TGON 805, a carbon-based material, as working and counter electrodes. An Ag/AgCl electrode was used as a reference electrode. Tob and Kan was diluted in Milli-Q water at the concentration of 9 mM and was supplemented with 10 μM Fe^{2+}, Fe^{3+}, Cr^{2+}, Cr^{3+}, Cr^{6+}, Mn^{2+}, or Ni^{2+}. Three milliliters of each mixture were treated with 70 $\mu A/cm^2$ DC for 1 h using TGON 805, and the untreated sample was used as a control. After DC was

performed, both the untreated samples and the DC-treated samples were stored one ice till NMR was performed.

7.3.3. Effects of Tob and Cr^{3+} on PAO1 without DC

As mentioned in Chapter 3, we found that supplementation of Cr^{3+} to DC treatment of PAO1 mediated with carbon electrodes and in the presence of 1.5 μg/mL Tob resulted in improved killing of the persister cells. To understand if Cr^{III}(Tob) complexes exhibit agonist or antagonist effects outside of the electric field, the wild-type *P. aeruginosa* PAO1 was cultured overnight in 25 mL Luria-Bertani (LB) medium [15] containing 10 g/L tryptone, 5 g/L yeast extract, and 10 g/L NaCl. Each overnight culture was incubated at 37°C with shaking at 200 rpm. The next day, the cells were sub-cultured at an initial OD_{600} of 0.05 in 200 μL LB contained in 96 well plates (Costar ® No. 9017, Corning, NY) in the presence or absence of 3.2 μM of Tob (~1.5 μg/mL Tob), 3.2μM Cr^{3+} in the presence of 3.2 μM Tob, and 3.2 μM Cr^{III}(Tob), the DC-treated Cr^{3+}-Tob mixture generated under electrochemical condition described above. PAO1 without treatment was used as a control and all the samples were grown with 8 replicates at 37 °C for 7h. Growth curves were recorded by measuring OD_{600} every hour using the ELx808 Absorbance Microplate Reader (Biotek, Winooski, VT).

7.3.4. Nuclear magnetic resonance spectroscopy

Sensitivity-enhanced $^{1\,h}$-^{13}C HSQC-NMR experiment was performed on DC-free or DC-treated ion-aminoglycoside mixtures using the Bruker Avance 500 MHz NMR (Bruker BioSpin Corporation, Billerica, MA). All experiments were conducted using a Bruker 5

mm QXI gradient probe at 25 ºC, with a 2 s relaxation delay. The delay for the INEPT transfer was determined based on the coupling constant of 155 Hz. The samples were scanned 32 times with a proton sweep width of 4005.4 Hz (equivalent to 8 ppm) and the carbon sweep width was 22638.2 Hz (equivalent to 180 ppm). To establish the heteronuclear correlation, 1024 points were collected for proton and 256 points for carbon, and the spectra were processed with 1024 points in both dimensions.

7.3.5. UV-Vis Spectroscopy

To study electrochemical properties of Cr^{III}(Tob) complexes, solutions of 15 mM Cr^{3+} solutions were prepared by dissolving 4.096 g $CrCl_3.6H_2O$ in 1 L Milli-Q water. Cr^{III}(Tob) complexes were formed by adding 7.2 g/L, 14.4 g/L or 21.6 g/L Tob to 15 mM Cr^{3+} solutions, resulting to a molar Tob:Cr^{3+} ratio of 1:1, 2:1 and 3:1, respectively (state final concentrations 15mM Tob and 15 µM Cr^{3+}, 30 mM Tob and 15 µM Cr^{3+} for the 2:1, and 45 mM Tob and 15 µM Cr^{3+} for 3:1 mixtures. The cell path length was 1 cm). The pH of the solutions was adjusted to 1, 2, 4, 6, 8 and 10 using 12N HCl or 10N NaOH. To induce the deprotonation of Tob (Isoelectric point Ip=11.11) and the formation of Cr^{III}(Tob) complex, the pH was also adjusted to 12. Using the Evolution™ 201-UV-Visible Spectrophotometer (ThermoFisher Scientific, Waltham, MA), UV-visible spectra were recorded immediately after mixing the Tob and Cr^{3+} solutions, and 2.5 h later to evaluate the shift in the absorbance peaks.

7.3.6. Cyclic Voltammetry (CV)

To evaluate the stability of the interaction between the aminoglycosides and ions, cyclic voltammetry was performed. A working gold electrode was used as the inert electrode to study the reversibility of the binding between Tob and Cr^{3+}. TGON 805 and Ag/AgCl electrodes were used as counter and reference electrodes, respectively. First, the redox behavior of reference solution containing 15 mM Iron (II) ammonia sulfate ($(NH_4)_2Fe(SO_4)_2 \cdot 6H_2O$), 15 mM Iron (III) chloride ($FeCl^3$), and 15 mM $CrCl_3.6H_2O$ were evaluated. A sweep voltage was applied at a scan rate of 100 mV/s between -1 V and 1 V, and a cyclic voltammogram was recorded. To evaluate the redox properties of the Tob-Cr^{3+} complexes, the cyclic voltammograms of Tob alone, and complexes formed between 15 mM Tob and 15 mM Cr^{3+} were recorded following the same procedure.

7.4. RESULTS

7.4.1. Antagonist effects of Tob and Cr^{3+} on the cells in absence of DC

The interaction between Tob and Cr^{3+} have been shown to contribute to the killing of PAO1 persister cells under DC conditions in chapter 3 [16]. To better understand the effects of the interaction between Tob and Cr^{3+}, and the role of such interaction in the synergistic killing of the PAO1 cells, the bioactivity of the complexes were investigated outside of an electric field. A subculture of PAO1 was grown in LB in the presence or absence of Tob, and mixtures of Tob and Cr^{3+} (molar ratio of 3.2 μM: 3.2 μM) pre-treated with or without 70 $\mu A/cm^2$ DC using TGON 805. As shown in Fig. 7.2, the growth curve of the PAO1 cells demonstrated that the presence of Cr^{3+} affected the bioactivity of Tob. The cell density of PAO1 reached OD_{600} of 0.4 after 4 h of incubation

at 37º C with 3.2 μM Tob alone. However, compared to the growth with 3.2 μM (1.5 μg/mL) Tob alone, the inhibitory activity of Tob on PAO1 cells was lost in the presence Cr^{3+}. The growth of PAO1 in the presence of 3.2 μM Tob and 3.2 μM Cr^{3+} (Tob/Cr^{3+}), or 3.2 μM Cr^{III}(Tob) or Tob-Cr^{3+} complex generated electrochemically was similar to that of PAO1 cells culture in LB alone. All the cultures reached OD_{600} of 1 after 7 h of growth.

7.4.2. Formation of Cr^{III}(Tob) under DC treatment.

To evaluate if electrochemical treatments facilitate the interaction between the aminoglycosides and metal ions, 10 μM of the metal ions were supplemented to 9 mM Tob or Kan in Milli-Q water and the mixtures were treated with 70 $\mu A/cm^2$ DC using TGON 805 electrodes. As shown in Fig 7.3, no chemical shift was observed in the NMR-HSQC spectra of Tob treated with DC compared to the untreated samples, suggesting that DC treatment in the presence of Ni^{2+}, Fe^{3+}, Fe^{2+}, Cr^{2+}, Cr^{6+} and Mn^{2+} did not induce any structural change to Tob or Kan. However, DC treatment of Tob-Cr^{3+} mixtures followed by analysis using ^{1}H-^{13}C HSQC-NMR showed changes in the chemical shifts of both ^{1}H and ^{13}C resonances of Tob as a function of the concentration of Cr^{3+} initially added to the system. Since the peaks in the 2D NMR spectrum are well defined and are not greatly shifted relative to the free antibiotic, they cannot be due to direct binding of mononuclear Cr^{3+} to Tob. Chromium (III) has a $3d^3$ electronic configuration with $S = 3/2$ in an octahedral crystal field (Table 2). This property of the ion produces long spin-lattice relaxation times for protons on attached ligands causing resonances to be highly shifted and broad effectively rendering them unobservable in the NMR spectrum [17]. Since combining more than one Cr^{3+} ion to form di or polynuclear complexes can reduce the

effective electronic spin of the system through anti-ferromagnetic coupling mechanisms, it is possible that the chromium species produced upon the application of DC current is a polynuclear complex low net spin leading to narrow and only modestly shifted $^{1\,h}$ and ^{13}C resonances [18-20]. Clearly additional work will be needed to identify the structure of this complex and how it is produced in the presence of the electric field. As shown in Fig. 7.4, the increase in the concentration of Cr^{3+} correlates with the shift of the peaks, confirming that Cr^{III}(Tob) complex formation occurred under DC treatment. Six major H chemical shifts were recorded and the relative value of the shift in comparison to the DC-free sample is reported in Table 1. The most significant H chemical shifts (shift 4 and 5) were generated by the hydrogen of the $-CH_2-$ bound group to the primary amine group ($-CH_2-NH_2$). While the positions of peaks 4 and 5 for the DC-free control sample made of 9 mM Tob and 10 μM Cr^{III} were located at 3.069 ppm and 2.812 ppm respectively, they shifted to 3.193 ppm and 2.939 ppm, respectively, after DC treatment.

7.4.3. Interaction between Tob and Cr^{3+}.

The strength of interaction between Tob and Cr^{3+} was further investigated using UV-visible spectroscopy. Tob and Cr^{3+} were mixed at equal concentration of 15 mM and the pH of the mixtures was adjusted to 1-12 using HCl to observe the interaction in acidic pH or NaOH to induce the deprotonation of Tob and facilitate its binding to Cr^{3+}. As shown in Fig 7.5, the UV-Vis spectra of the samples, which were acquired immediately after samples were mixed, show that representative sifts occurred at pH lower than 6 and great than 10, and the sample precipitated at pH between 6 and 10. However, to insure that complex formation occur, the rest of the experiment was conducted at pH 12, to insure

deprotonation of Tob (Ip=11.11). The samples were mixed and collected after equilibrium was reached, which occurred after 2.5 h. As shown in Fig. 7.5, the solution of $CrCl_3.6H_2O$ exhibits 3 peaks, which are located at 300.02 nm, 425.27 nm and 588.87 nm, with a respective intensity of 0.539, 0.416 and 0.357, respectively. However, the gradual addition of Tob to Cr^{3+} solutions at pH 12 resulted in increase in the absorbance energy, broadening of the absorbance band and chemical shift (Fig. 7.6). The mixture of Tob and Cr^{3+} at a ratio of 1:1 generated peaks at 298.89 nm, 423.16 nm and 588.7 nm. The 2:1 Cr^{III}(Tob) mixture further increased the shift in the absorbance band, resulting in peaks at 289.99 nm, 422.05 nm and 585.48 nm. Finally, the addition of the third volume of Tob to the Cr^{3+} solution resulted on absorbance peak at 289.56 nm, 421.23 nm and 584.75 nm. The shift intensity of the peak under this condition was 0.35, 0457 and 0.385, respectively. These results suggested that the binding of Tob to Cr^{3+} might increase the energy state of Cr^{3+}.

To further evaluate the stability of the Cr^{III}(Tob) complexes, CV experiments using a working gold electrode were performed and compared to other metal-ligand complexes involving amine groups. Thus, $(NH_4)_2Fe(SO_4)_2 \cdot 6H_2O$ was used as a control solution. Other solutions including metal cation solutions ($FeCl_3$, $CrCl_3.6H_2O$) and Tob, were also used as references. The cyclic voltammogram for the solutions of $FeCl_3$ is shown in Fig. 7.7A, and demonstrated that Fe^{3+} is oxidized reversibly and reduced with peaks 490.95 mV and 310.3 mV. Similarly, the redox behavior of $(NH_4)_2Fe(SO_4)_2 \cdot 6H_2O$ showed that Fe^{2+} was oxidized and reduced at working electrode potentials of 580.42 mV

and -63.84 mV, respectively, suggesting a reversible reactions between Fe^{2+} and its amine or sulfate ligand.

The cyclic voltammetric response of $CrCl_3.6H_2O$ demonstrated that no electron was generated from Cr^{3+}, corroborating with the absence of the oxidation peak. Instead, a reduction peak was recorded at 536.22 mV. Also, the cyclic voltammogram of Tob illustrated in Fig. 7.7B supports that the antibiotic did not lose electron over the range of -0.5 V to 0.75 V. The CV plot of the mixture of Tob and Cr^{3+} at pH 5.8 (Fig. 7.7C) showed that the complex was not oxidized nor reduced over the voltage range tested, suggesting a stable interaction at pH 5.8. Similarly, the redox properties of the Cr^{III}(Tob) complexes was tested at pH 12, and showed that the complexes did not oxidize (Fig. 7.7D). However, a reduction peak became more apparent with the increase in the amount of Tob in the solutions (Fig. 7.7D), suggesting a loss of stability with the increase of Tob.

7.5. DISCUSSION

The electrical enhancement of antibiotic activity in killing cell associated with bacterial biofilms is well-known phenomena known to as bioelectric effects[12,14,21]. Recently, this finding has inspired our study on the persister cells' response to electrochemical stress and led to the conclusion that similar technology could be employed to target recalcitrant bacterial infections associated with biofilms and persister cells, a phenomenon we named ECCP or electrochemical control of bacterial persister cells[16]. This interesting discovery led to hypothesize that the DC contributes to the electrochemical disruption of the membrane of the persister cells and facilitates the transport of the antibiotics through

interaction with electrochemical byproducts. Because electrochemical treatment mediated with SS304 electrodes generates metal cations including Fe, Cr, Mn, and Ni ions with various oxidation states, we proposed that the synergistic effects of the antibiotic Tob and DC in killing persister cells occurred in combination with the metal cations. This hypothesis was verified during the treatment of PAO1 persisters with 70 $\mu A/cm^2$ DC using carbon electrodes in the presence of Tob and Ni^{2+}, Cr^{3+} or Fe^{2+} (Chapter 3).

In this Chapter, the interaction between Tob and the metal cations was further investigated. Different metal cations formed with SS-released elements were treated with DC in the presence of Tob to induce the interactions such as those occurring under the conditions of ECCP. Using NMR analysis, it was found that the interaction between Cr^{3+} and Tob caused by DC resulted in H chemical shifts, suggesting that DC might induce structural change in Tob, which could be relevant to the synergy. The ^{1}H-^{13}C chemical shifts were analyzed based on previous study [22]. It occurred that Cr^{3+} may bind to the free primary methylamine group ($-CH_2-NH_2$) or to a free primary amine of the cyclohexane group of Tob.

To understand the roles of interaction between Tob and the SS-released cations in the synergistic control of the *P. aeruginosa* cells, PAO1 cells were grown in LB medium in the presence or absence of the Tob and the Cr^{3+}. The results of this test confirmed that the interactions between Tob and Cr^{3+} still occurred without DC. However outside of the electrical field, such interactions were detrimental, as the bioactivity of Tob was found lower compared to Tob alone without Cr^{3+}. To further understand between Tob and Cr^{3+},

additional tests were performed to determine the electrochemical properties of the complex. First, the ability of Tob and Cr^{3+} to form conjugated species was evaluated over a range of pH varying from 1 to12. The UV-visible spectra show clearly that Cr^{3+} and Tob interact at pH lower than 6 and higher than 10, which might explain the finding that Cr^{3+} interfered with the bioactivity of Tob during the growth in LB solution. In effect, the redox properties of Cr^{III}(Tob) at a 1: 1 molar ratio and at pH of 5.8 also showed no redox properties, suggesting the formation of stable complexes.

To further investigate the nature of the interactions, the mixed solution of Tob and Cr^{3+} were adjusted to pH 12 to induce deprotonation, as DC treatment using carbon electrode induced local pH change. Thus, Cr^{III}(Tob) complexes were formed at different molar ratio to study the electrochemical properties of the complexes. The cyclic voltammetric response of the complexes to forward and reverse voltage scan ranging from -500 to 600 mV demonstrated that the complex was not oxidized, and was stable, unless more Tob molecules were interaction with Cr^{3+} (e.g. Tob:Cr^{3+} mixture with a molar ratio of 3:1). Then, a reduction peak, similar to that of Tob alone, was observed, suggesting that Cr^{3+} could become less stable with increasing interactions with Tob molecules. The UV-visible spectra of the complexes showed an increase in shift with the increase in Tob concentration. In addition, a third absorbance peak was recorded at ~290nm, which suggests that Cr^{3+} might display a hydration isomery comparable to $[Cr(H_2O)_6].Cl_3$ as reported by Barbier *et al*[23].

The study of the electrochemical properties of Tob and Cr^{3+} could help understand the interaction between the aminoglycosides and the positively charged ions during the electrochemical control of bacterial cells. This interaction could be advantageous in the case of electrically induced disruption of the membrane functions. Thus, the movement of the complex under the DC condition may facilitate the transport of Tob and Cr^{3+}, which could contribute to synergistic killing of bacterial cells. In effect, Cr^{3+} alone is known to cause oxidative damage of the DNA[24-26]. Due to its high electropositivity, Cr^{3+} interacts well with negatively charged molecules, including DNA [27]. Hence, the binding of Cr^{3+} to Tob could increase the overall charge of Tob, which is positivily charged at pH below 11.11 (pI of Tob), and could favor the electrostatic binding interaction between the Cr^{III}(Tob) complex and ribosomal RNA in the presence of DC. In the absence of DC, the Tob- Cr^{3+} interactions could exhibit adverse effects due to the binding of the complex to negatively-charged bacterial cells, and lead to the inability of Cr^{III}(Tob) complex to cross the membrane barrier.

7.6. CONCLUSIONS

The interaction of Cr^{3+} and Tob was investigated in this study. The interaction between Cr^{3+} and Tob was hypothesized believe to contribute to the synergistic killing of PAO1 cells during the electrochemical treatments. However, adverse effects were also recorded in the absence of DC, suggesting that the synergy between Cr(III) and Tob may be caused by electrically induced trans-membrane transport of Tob in the cells toward their negatively charged cellular target. However, DC treatment did not stimulate the formation of Cr^{III}(Kan) complex. This finding demonstrates that the effectiveness of the

electrochemical treatment relies on the specific nature of the electrochemical agents exposed to the cells.

7.7. ACKNOWLEDGEMENTS

The authors are grateful to Blue Highway Inc. for supporting the project. We are grateful to Dr. Thomas K. Wood at Texas A&M University for sharing the strain *P. aeruginosa* PAO1. We are grateful to Dr. James Dabrowiak for providing invaluable insights on UV-visible spectroscopy and NMR study, and Dr. Deborah Kerwood for helping with the NMR analysis. Finally, we thank Dr. Jeremy Gilbert for his insightful remarks on the cyclic voltammetry experiments.

7.8. REFERENCES

1 **Taber, H. W., Mueller, J., Miller, P. & Arrow, A.** Bacterial uptake of aminoglycoside antibiotics. *Microbiological reviews* **51**, 439 (1987).

2 **Kohanski, M. A., Dwyer, D. J. & Collins, J. J.** How antibiotics kill bacteria: from targets to networks. *Nature Reviews Microbiology* **8**, 423-435 (2010).

3 **Wang, H. & Tor, Y.** Electrostatic interactions in RNA aminoglycosides binding. *Journal of the American Chemical Society* **119**, 8734-8735 (1997).

4 **Jana, S. & Deb, J.** Molecular understanding of aminoglycoside action and resistance. *Applied microbiology and biotechnology* **70**, 140-150 (2006).

5 **Beggs, W. H. & Andrews, F. A.** Role of ionic strength in salt antagonism of aminoglycoside action on *Escherichia coli* and *Pseudomonas aeruginosa*. *Journal of Infectious Diseases* **134**, 500-504 (1976).

6 **Davis, S. D. & Iannetta, A.** Antagonistic effect of calcium in serum on the activity of tobramycin against Pseudomonas. *Antimicrobial agents and chemotherapy* **1**, 466-469 (1972).

7 **Washington, J. A., Snyder, R. J., Kohner, P. C., Wiltse, C. G., Ilstrup, D. M., McCall, J. T.** Effect of cation content of agar on the activity of gentamicin, tobramycin, and amikacin against *Pseudomonas aeruginosa*. *Journal of Infectious Diseases* **137**, 103-111 (1978).

8 **Kenny, M. A., Pollock, H. M., Minshew, B. H., Casillas, E. & Schoenknecht, F. D.** Cation components of Mueller-Hinton agar affecting testing of

Pseudomonas aeruginosa susceptibility to gentamicin. *Antimicrobial agents and chemotherapy* **17**, 55-62 (1980).

9 **Davis, S. D. & Iannetta, A.** Antagonistic effect of calcium in serum on the activity of tobramycin against Pseudomonas. *Antimicrobial agents and chemotherapy* **1**, 466-469 (1972).

10 **Harrison, J. J., Turner, R. J. & Ceri, H.** Persister cells, the biofilm matrix and tolerance to metal cations in biofilm and planktonic *Pseudomonas aeruginosa*. *Environmental microbiology* **7**, 981-994 (2005).

11 **Moreau-Marquis, S., O'Toole, G. A. & Stanton, B. A.** Tobramycin and FDA-approved iron chelators eliminate *Pseudomonas aeruginosa* biofilms on cystic fibrosis cells. *American journal of respiratory cell and molecular biology* **41**, 305 (2009).

12 **Wellman, N., Fortun, S. M. & McLeod, B. R.** Bacterial biofilms and the bioelectric effect. *Antimicrob Agents Chemother* **40**, 2012-2014 (1996).

13 **del Pozo, J. L., Rouse, M. S. & Patel, R.** Bioelectric effect and bacterial biofilms. A systematic review. *International Journal of Artificial Organs* **31**, 786-795 (2008).

14 **Costerton, J. W., Ellis, B., Lam, K., Johnson, F. & Khoury, A. E.** Mechanism of electrical enhancement of efficacy of antibiotics in killing biofilm bacteria. *Antimicrobial agents and chemotherapy* **38**, 2803-2809 (1994).

15 **Sambrook, J. & Russell, D. W.** *Molecular cloning: a laboratory manual*. Vol. 3 (Cold spring harbor laboratory press, 2001).

16 **Niepa, T. H., Gilbert, J. L. & Ren, D.** Controlling *Pseudomonas aeruginosa* persister cells by weak electrochemical currents and synergistic effects with tobramycin. *Biomaterials* **33**, 7356-7365, doi:10.1016/j.biomaterials.2012.06.092 (2012).

17 **Watson, H., Hatfield, J. & Vincent, J. B.** ^{1}H NMR studies of Cr (III)–imidazole complexes: can ^{1} H NMR be used as a probe of Cr–guanine DNA adducts? *Inorganica chimica acta* **344**, 265-269 (2003).

18 **Glass, M., Belmore, K. & Vincent, J.** Nuclear magnetic resonance studies of multinuclear chromium assemblies. *Polyhedron* **12**, 133-140 (1993).

19 **Belmore, K., Madison, X., Harton, A. & Vincent, J.** Carbon-13 NMR studies of oxo-centered trinuclear chromium (III) complexes of the general formula $[Cr_3O(O_2CR)_6(L)_3]^+$(R= Me, Ph; L= H_2O, py). *Spectrochimica Acta Part A: Molecular Spectroscopy* **50**, 2365-2370 (1994).

20 **Harton, A., Nagi, M. K., Glass, M. M., Junk, P. C., Atwood, J. L., Vincent, J. B.** Synthesis and characterization of symmetric and unsymmetric oxo-bridged trinuclear chromium benzoate complexes: Crystal and molecular structure of $[Cr_3O(O_2CPh)_6(py)_3]ClO_4$. *Inorganica chimica acta* **217**, 171-179 (1994).

21 **Del Pozo, J. L., Rouse, M. S. & Patel, R.** Bioelectric effect and bacterial biofilms. A systematic review. *Int J Artif Organs* **31**, 786-795 (2008).

22 **Eneva, G. I., Spassov, S. L. & Haimova, M. A.** Complete 1H and 13C NMR Chemical Shift Assignments for Some N-Polyformylated Aminoglycoside Antibiotics. *Spectroscopy Letters* **28**, 69-79 (1995).

23 **Barbier, J., Kappenstein, C. & Hugel, R.** The hydration isomers of chromium (III) chloride. *Journal of Chemical Education* **49**, 204 (1972).

24 **Speetjens, J. K., Collins, R. A., Vincent, J. B. & Woski, S. A.** The nutritional supplement chromium (III) tris (picolinate) cleaves DNA. *Chemical research in toxicology* **12**, 483-487 (1999).

25 **Sugden, K., Geer, R. & Rogers, S.** Oxygen radical-mediated DNA damage by redox-active chromium (III) complexes. *Biochemistry* **31**, 11626-11631 (1992).

26 **Voitkun, V., Zhitkovich, A. & Costa, M.** Cr (III)-mediated crosslinks of glutathione or amino acids to the DNA phosphate backbone are mutagenic in human cells. *Nucleic acids research* **26**, 2024-2030 (1998).

27 **Santonen, T.** *Inorganic chromium (III) compounds*. Vol. 76 (World Health Organization, 2009).

FIGURE CAPTIONS

Figure 7.1. Structure of Tobramycin (A) and Kanamycin (B)

Figure 7.2. Growth curve of PAO1 in the presence or absence of Tob and Cr^{III}. Tob/Cr3+ represent the growth in the presence of Tob and Cr^{3+}, and [Tob-Cr^{3+}] represents the growth in the presence of the DC-treated Tob-Cr^{3+} complex.The cells were subcultured at OD_{600} of 0.05 and the growth curve was recorded for 7h.

Figure 7.3. HSQC-NMR of a mixed solution of 9mM Tob and 10 µM Cr^{3+} (purple peaks), 9mM Tob and 50 µM Cr^{3+} (blue peaks), 9mM Tob and 100 µM Cr^{3+} (green peaks) treated with 70 µA/cm^2 DC using TGON vs. untreated control (red peaks). δ F1 corresponds to δ ^{13}C (in ppm) and δ F2 to δ ^{1}H (in ppm).

Figure 7.4. UV-visible spectra of Cr^{III}(Tob) complexes at pH 1 to 12. The samples were allowed to reached equilibrium after 2.5h and the spectra were recorded.

Figure 7.5. UV-visible spectra of Cr^{III}(Tob) complexes at pH 12. The samples were allowed to reached equilibrium after 2.5h and the spectra were recorded

Figure 7.6. Cyclic voltammogram of (A) $(NH_4)_2Fe(SO_4)_2 \cdot 6H_2O$, $FeCl_3$ and $CrCl_3.6H_2O$ solutions, (B) Tobramycin and Cr^{III}-Tob complexes at (C) pH 5.8 and (D) pH 12.

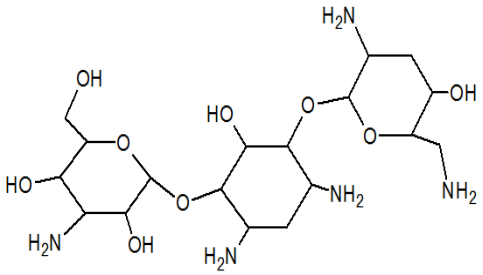
H2N
OH
HO
O
O
HO
O
OH
NH2
NH2
H2N
OH
H2N

(A)

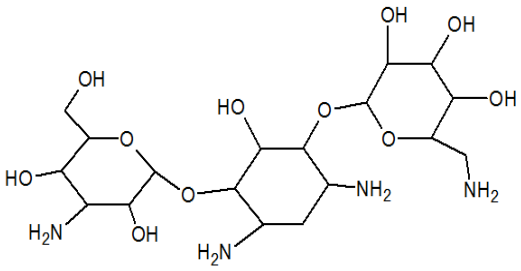
OH
OH
OH
HO
O
O
OH
HO
O
NH2
NH2
H2N
OH
H2N

(B)

Figure 7.1

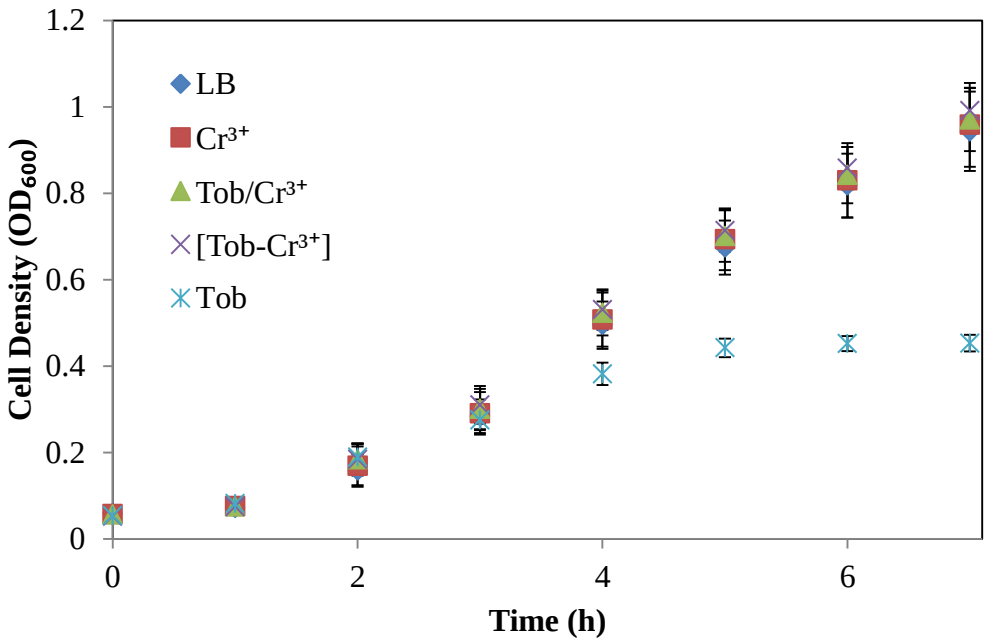
1.2
1
0.8
0.6
0.4
0.2
0
0
2
4
6
Cell Density (OD600)
Time (h)
LB
Cr3+
Tob/Cr3+
[Tob-Cr3+]
Tob

Figure 7.2

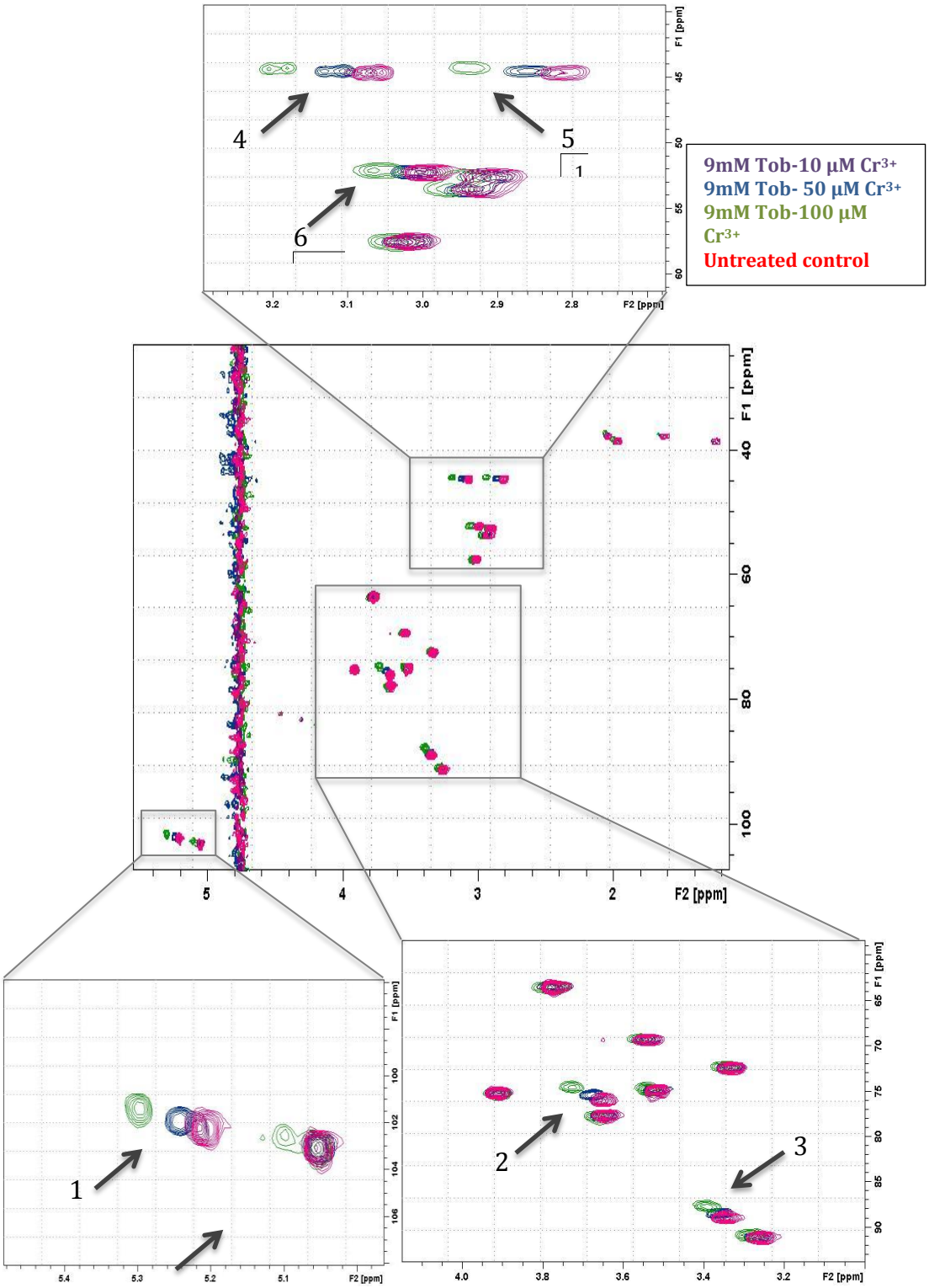
9mM Tob-10 µM Cr3+
9mM Tob- 50 µM Cr3+
9mM Tob-100 µM Cr3+
Untreated control
F1 [ppm]
F2 [ppm]
1
2
3
4
5
6

Figure 7.3

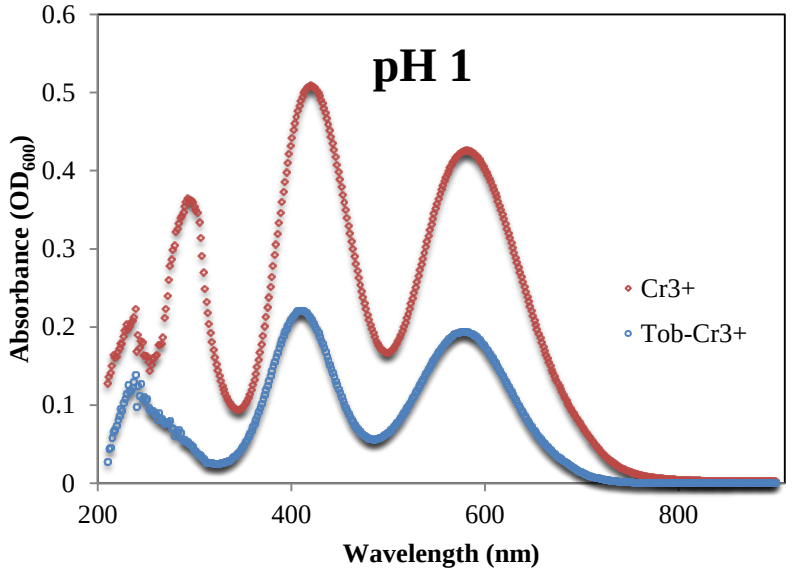
pH 1
Absorbance (OD600)
0.6
0.5
0.4
0.3
0.2
0.1
0
200
400
600
800
Wavelength (nm)
Cr3+
Tob-Cr3+

(A)

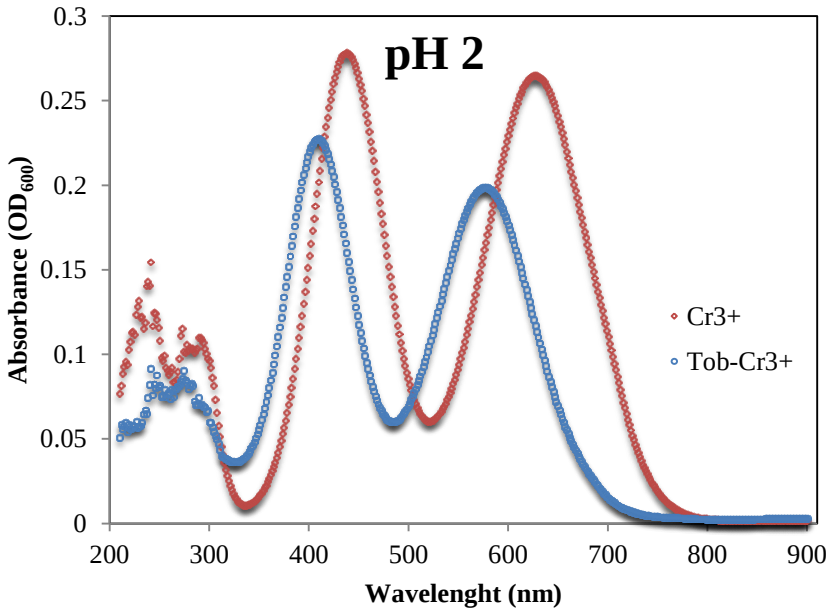
pH 2
Absorbance (OD600)
0.3
0.25
0.2
0.15
0.1
0.05
0
200
300
400
500
600
700
800
900
Wavelenght (nm)
Cr3+
Tob-Cr3+

(B)

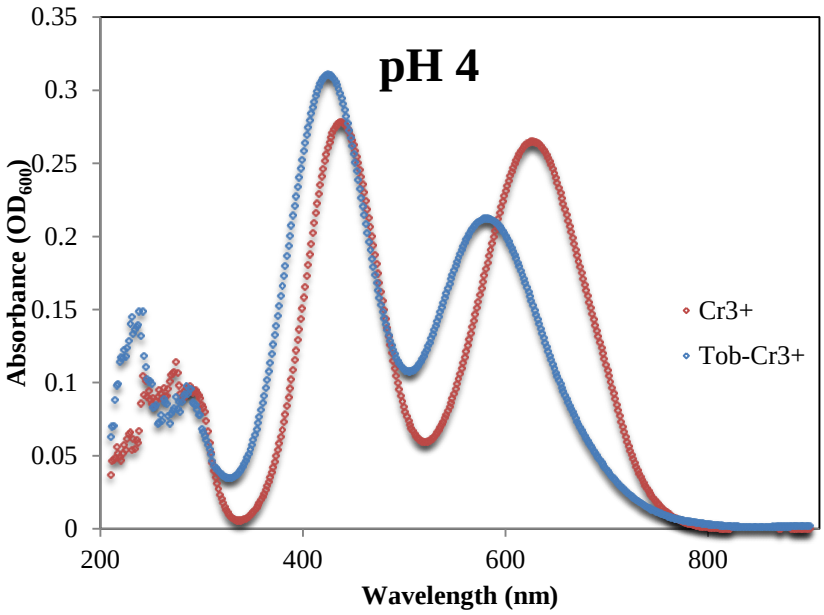
pH 4
Absorbance (OD600)
Wavelength (nm)
Cr3+
Tob-Cr3+
0.35
0.3
0.25
0.2
0.15
0.1
0.05
0
200
400
600
800

(C)

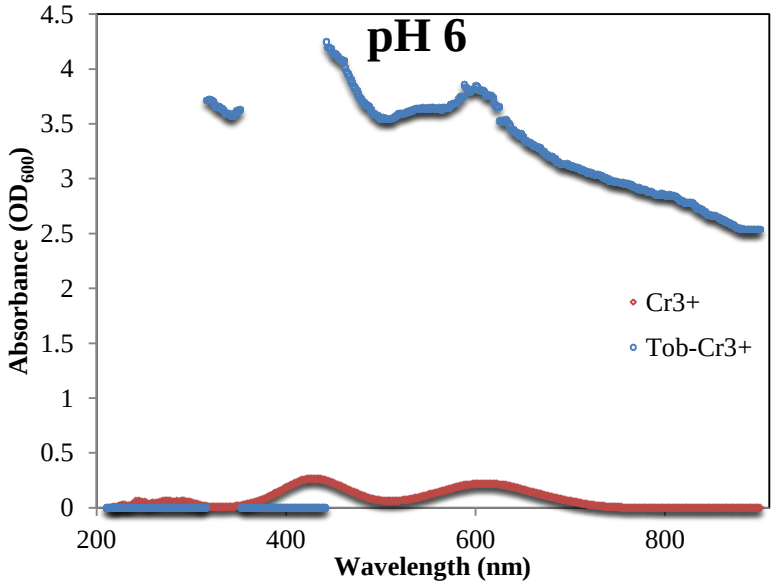
pH 6
Absorbance (OD600)
Wavelength (nm)
Cr3+
Tob-Cr3+
4.5
4
3.5
3
2.5
2
1.5
1
0.5
0
200
400
600
800

(D)

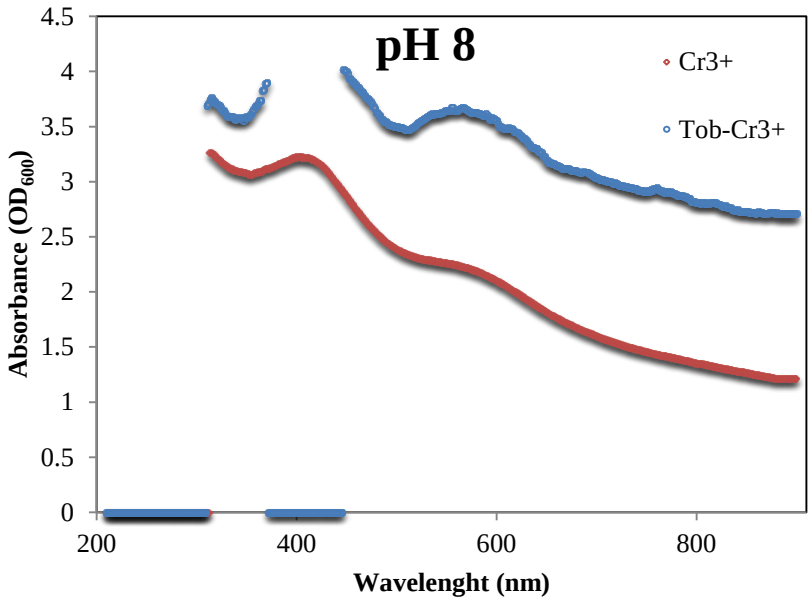
pH 8
Cr3+
Tob-Cr3+
Absorbance (OD600)
Wavelenght (nm)
4.5
4
3.5
3
2.5
2
1.5
1
0.5
0
200
400
600
800

(E)

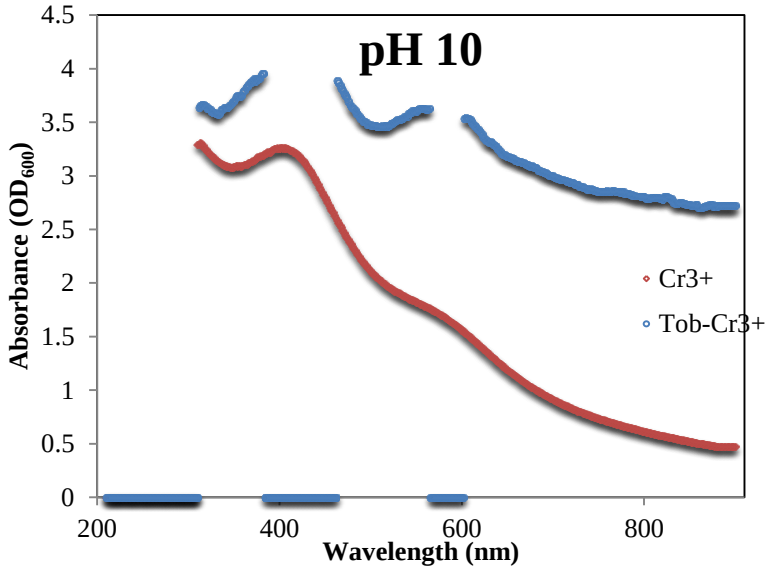
pH 10
Cr3+
Tob-Cr3+
Absorbance (OD600)
Wavelength (nm)
4.5
4
3.5
3
2.5
2
1.5
1
0.5
0
200
400
600
800

(F)

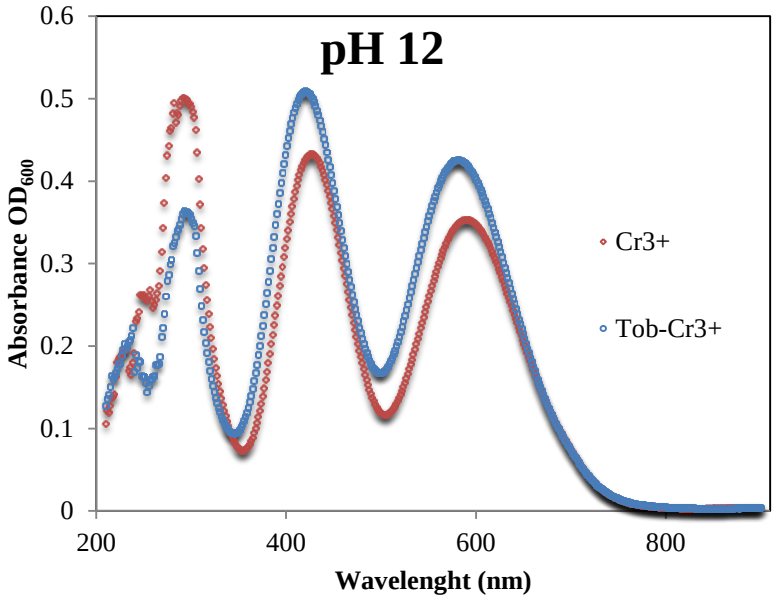
pH 12
Absorbance OD600
Wavelenght (nm)
Cr3+
Tob-Cr3+
0.6
0.5
0.4
0.3
0.2
0.1
0
200
400
600
800

(G)

Figure 7.4

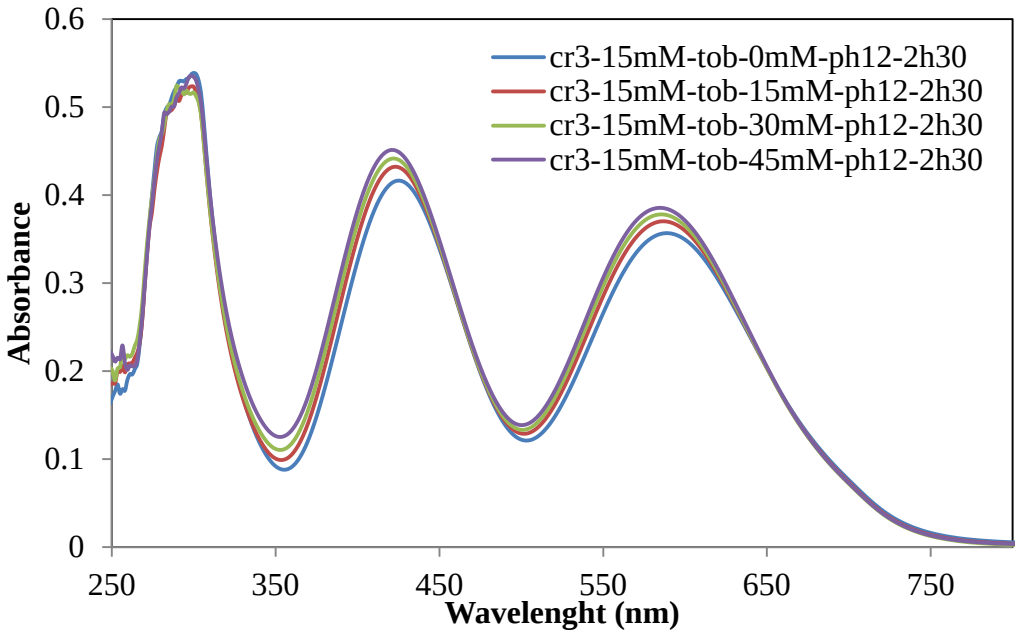
0.6
0.5
0.4
0.3
0.2
0.1
0
Absorbance
250
350
450
550
650
750
Wavelenght (nm)
cr3-15mM-tob-0mM-ph12-2h30
cr3-15mM-tob-15mM-ph12-2h30
cr3-15mM-tob-30mM-ph12-2h30
cr3-15mM-tob-45mM-ph12-2h30

Figure 7.5

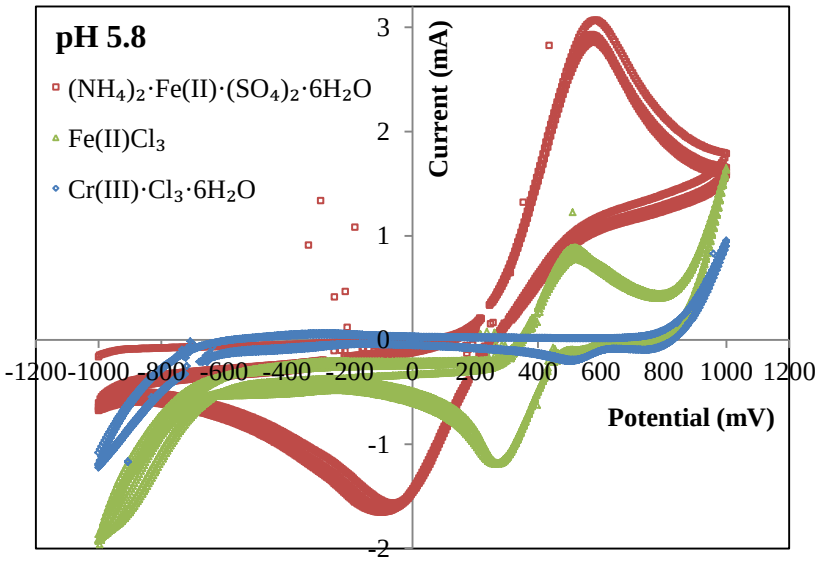
pH 5.8
(NH4)2·Fe(II)·(SO4)2·6H2O
Fe(II)Cl3
Cr(III)·Cl3·6H2O
Current (mA)
Potential (mV)
3
2
1
0
-1
-2
-1200 -1000 -800 -600 -400 -200 0 200 400 600 800 1000 1200

(A)

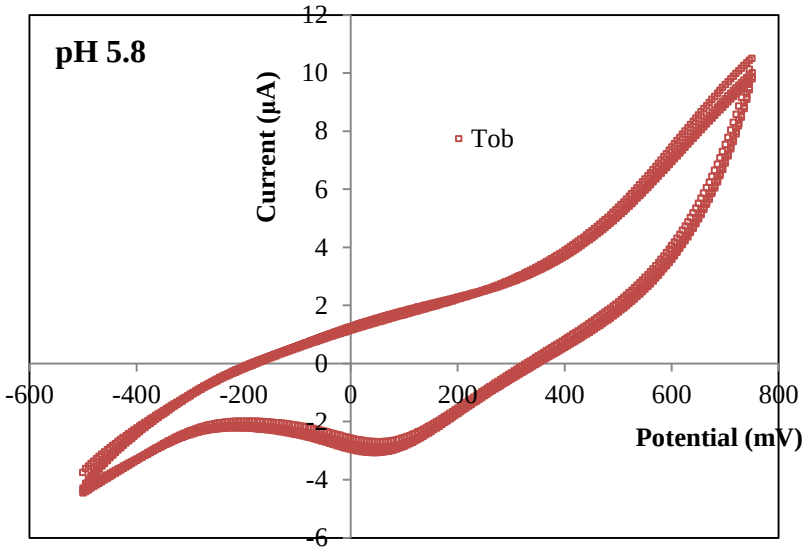
pH 5.8
Tob
Current (µA)
Potential (mV)
12
10
8
6
4
2
0
-2
-4
-6
-600 -400 -200 0 200 400 600 800

(B)

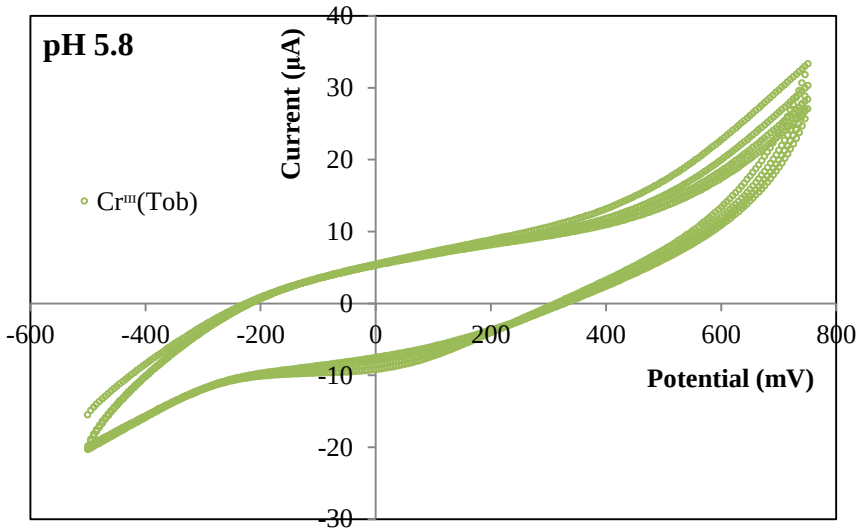
pH 5.8
Current (µA)
Potential (mV)
Cr^{III}(Tob)
40
30
20
10
0
-10
-20
-30
-600
-400
-200
0
200
400
600
800

(C)

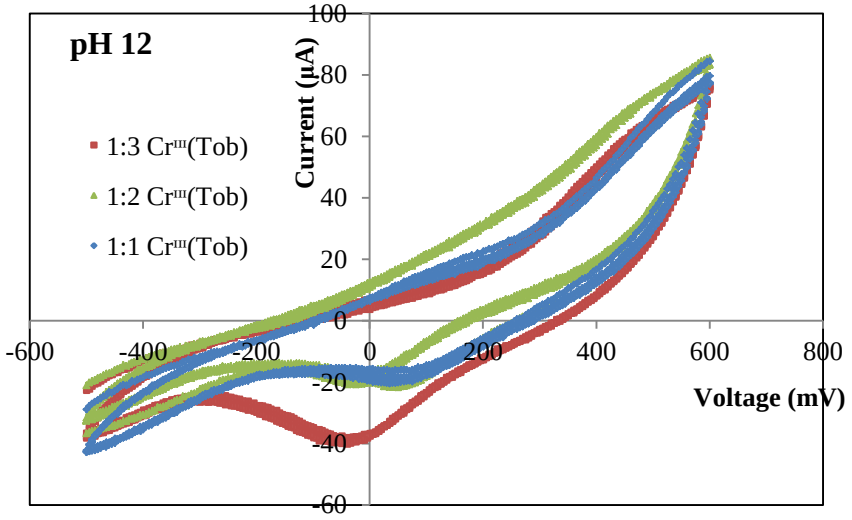
pH 12
Current (µA)
Voltage (mV)
1:3 Cr^{III}(Tob)
1:2 Cr^{III}(Tob)
1:1 Cr^{III}(Tob)
100
80
60
40
20
0
-20
-40
-60
-600
-400
-200
0
200
400
600
800

(D)

Figure 7.6

Table 7.1 : Relative value of the H chemical shifts (in ppm) with the increasing concentration of Cr^{3+} and assignement of the H chemical shifts

Peak	1	2	3	4	5	6
Untreated control sample	5.2075	3.647	3.3446	3.0688	2.8122	2.9965
DC_9mM Tob-10μM Cr^{3+}	5.219	3.6601	3.3564	3.0845	2.831	3.0035
DC_9mM Tob-50μM Cr^{3+}	5.2423	3.678	3.3629	3.1063	2.8599	3.0147
DC_9mM Tob-100 μM Cr^{3+}	5.2999	3.7288	3.3943	3.1926	2.9386	3.0595

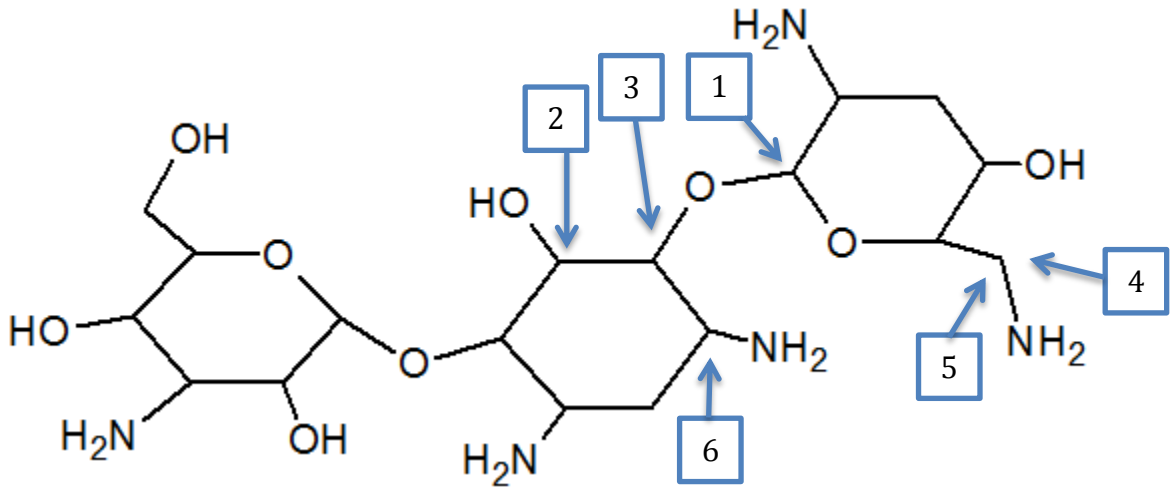

Table 7.2 : Cristal field effects of Cr(III)

		$^4A_2$ (Ground State)	State in the crystal field)				
	pH	$^4T_2(F)$ (nm)	$^4T_2(F)$ (cm^{-1})	$^4T_1(F)$ (nm)	$^4T_1(F)$ (cm^{-1})	$^4T_1(P)$ (nm)	$^4T_1(P)$ cm^{-1})
Cr(III) in water	1	590	16949	426	23474	300	33333
	2	636	15723	444	22523	295	33898
	4	634	15773	444	22523	289	34602
	12	600	16667	434	23041	300	33333
Cr(III)/Tob 1:1	1	577	17331	409	24450		
	2	574	17422	405	24691		
	4	591	16920	432	23148	294	34014
	12	582	17182	423	23641	292	34247

Average crystal field increases in the presence of Tob
Conclusion: The amino groups of Tob are binding to Cr(III)

CHAPTER 8

SELECTIVE CONTROL OF *P. AERUGINOSA* CELLS BY ELECTROCHEMICAL TREATMENT OF CO-CULTURES INVOLVING HUMAN EPITHELIAL CELLS

8.1. ABSTRACT

The implantation of artificial materials can encounter recurring complications due to surface colonization by multi-drug resistant microorganisms. The formation of microbial communities known as biofilms on contaminated biomaterials and the presence of biofilm associated persister cells present a great challenge for controlling device-associated infections. As described in previous chapters, in vitro studies on *Pseudomonas aeruginosa*, a model of Gram-negative pathogen, have demonstrated that the electrochemical agents including direct current (DC) can improve the killing activities of antibiotics such as Tobramycin against the biofilm cells and persister cells. This approach holds to control potential chronic infections associated with implanted medical devices. To evaluate the safety of this technology and to help design *in vivo* studies, the effects of DC treatments on bacterial cells were further investigated in a co-culture model involving four human epithelial cell lines. The results show that 68.1% human cells can survive the treatment with 70 $\mu A/cm^2$ DC using stainless steel (SS) 304 electrodes for 1 h, while 90% *P. aeruginosa* cells were eliminated in the co-culture with epithelial cells. An additional 2-log killing of *P. aeruginosa* was achieved by augmenting the current density to 84 $\mu A/cm^2$ DC or through synergistic effects with Tob.

8.2. INTRODUCTION

Infection with opportunistic pathogens is a major risk factor associated with implantation of medical devices, on medical equipment and devices has increased the risk of acquiring and developing chronic infections during or after major surgeries[1], intubation procedure[2], and treatment of burn patients[3]. In the last two decades, *Pseudomonas aeruginosa* has emerged as one of the leading nosocomial pathogens for which novel strategies of control are urgently needed[4-6]. Owing to inherent abilities such as efflux pumps, this Gram-negative bacterium can extrude antibiotics that are commonly used to treat infection, or adopt a different lifestyle allowing it to colonize surfaces of tissues of biomaterials and develop sessile communities known as biofilms. The extracellular polymeric substances of biofilms provide the embedded cells with extra layers of protection against the host immune system and limit flow across the biofilms, rendering the diffusion of antibiotics. Consequently, *P. aeruginosa* can escape from the treatment of many antibiotics such as β-lactam[7], fluoroquinolones[8], carbapenems[9] and aminoglycosides[10,11], and cause to persistent infections.

The mechanisms of antibiotic resistance rely on the ability of the cells to control membrane permeability, modify the cellular targets of antibiotics or enzymatically degrade antibiotic compounds. Given the rapid increase in antibiotic resistant infection, other approaches, such as those involving physical or electrochemical factors, are being pursued. Among these non-conventional methods, low direct currents (DCs), alternating currents (ACs), and electric fields have been proven to kill bacteria[12,13]. Recently, we reported that persister cells isolated from *P. aeruginosa* PAO1 can be effectively killed

(by about 2 logs) with low-level DC (70 μA/cm^2). Also, synergistic effects were observed when persister cells were treated with DC and Tob together.

Although the safety of such DC treatment has not been tested, certain electrical currents and potentials are known to be beneficial to mammalian cells and could promote the migration of macrophages, neutrophils[14], fibroblasts[15] and epithelial cells[16,17] engaged in inflammatory response, and thus improve wound repair [18-20]. Thus, we hypothesize that selective killing of bacterial cells can be achieved by applying low-level DC to co-cultures of mammalian and bacterial cells. In the study outlined in this chapter, different human epithelial cancer cell lines were utilized in a model of infection with PAO1 to test the efficacy of the DC treatment using SS 304 in killing bacterial cells and evaluate the cytotoxicity of this treatment. The effects of antibiotic (Tob) and electric currents on the viability of both bacterial and human cells were investigated.

8.3. MATERIALS AND METHODS

8.3.1. Bacterial cell and culture condition

The wild-type *P. aeruginosa* PAO1 was cultured in Luria-Bertani (LB) medium[21] containing 10 g/L tryptone, 5 g/L yeast extract, and 10 g/L NaCl. Each overnight culture was incubated at 37°C with shaking at 200 rpm.

8.3.2. Human cell lines and culture condition

Human epithelial lung cancer cells CRL-5907 (NCI-H1944), CRL-5908 (NCI-H1975), CLR-5803 (NCI-H1299), and human epithelial breast cancer cell MDA-MB-231

(ATCC® HTB-26 ™) were generously provided by Dr. Jing An at SUNY Upstate Medical University. The epithelial cells were grown in RPMI medium supplemented with 10% Fetal Bovine Serum (FBS) and 1% of Penicillin-Streptomycin-Glutamine (PSG).

8.3.3. Effects of low-level DCs on human epithelial cells.

To test the effects of DC on adherent cells, human epithelial cells (NCI-H1944) were grown for 8 days on collagen-coated 12 well-plate inserts in the presence of 2 mL of RPMI medium supplemented with 10% FBS and 1% PSG; and the medium was replenished after the fourth day of the culture. The cells attached on the insert were washed with Hank's balanced salt solution (HBSS), and the insert was transferred to an electrochemical cell with of HBSS buffer to investigate the effects of electrochemical currents on mammalian cells. The electrochemical cell was constructed by inserting two flexible sheets of SS 304 in a well of a 12 well-plate, above and below the sample, respectively. An Ag/AgCl-reference electrode was prepared by dipping a silver wire into a solution of sodium hypochlorite for 30 min. All the electrodes were introduced in the well in the 3-configuration system, as depicted on Fig. 8.1. Using a potentiostat, Total DC level of 500 μA was delivered to the cells for 30 min. In this experiment, the cells were tested under three conditions: (1) The untreated control sample was exposed to HBSS solution only without DC treatment; (2) The sample treated using cathodic current had the cells exposed to the counter electrode while the working electrode was separated from the cells by the permeable membrane of the insert; (3) The sample treated using anodic current had the cells directly exposed to the working electrode. The viability of

cells was evaluated by imaging after staining with Live/dead Cell-Mediated Cytotoxicity Kit (Life Technologies, NY).

To test the effects of DC on suspended cells, human epithelial cells NCI-H1299, NCI-H1975 and ATCC® HTB-26 ™ were grown in a T-flask containing 25mL of RPMI supplemented with 10% FBS and 1% PSG. The cells were incubated for 4 days in the presence of 5% CO_2 at 37 °C. To release the adherent cells in the suspension, the cells were treated with TE buffer containing 0.25% Trypsin and 0.53 mM EDTA. After re-suspension in RPMI, the cells were washed and re-suspended in HBSS buffer to perform DC treatment. An electrochemical cell was constructed by inserting two SS 304 coupons along the opposite sides of a cuvette. An Ag/AgCl electrode was also inserted into the cuvette to establish the 3 electrodes system. To investigate the effects of electrochemical currents on epithelial cells, 70 μA/cm² DC was supplied to the cells for 1 h in the absence of antibiotic. Using the trypan blue exclusion method, the cell viability was evaluated every 20 min.

8.3.4. Determination of Tob concentration for testing the synergy with DC

To determine what concentration of Tob is appropriate for testing the synergy with DC in co-culture, NCI-H1299, and NCI-H1975 were allowed to adhere on the surface of a 12-well plate after 4 days of incubation at 37°C in a 5% CO_2 incubator. The medium was then decanted and the cells were washed with PBS buffer. The adherent mammalian cells were infected with PAO1 cells with a cell density at OD_{600} equals to 0.5. Concentrations of Tob varying from 0-120 μg/mL were used to treat the co-cultures for 1 h and 2h. The

cells were incubated at 37°C without shaking. To understand whether or not the adherence of the mammalian cells to surfaces affected the susceptibility of the bacterial cells to Tob, another experiment was performed, in which human epithelial cells NCI-H1299, and NCI-H1975 were re-suspended in PBS buffer and infected with the same density of *P. aeruginosa* PAO1 cells (OD_{600}= 0.5) in 24-well plate. Finally, the cells were treated with 0-120 µg/mL Tob for 1 and 2 h and were incubated at 37°C with shaking to prevent the adherence of the mammalian cells. In both conditions, the viability of bacterial cells was determined by counting colony-forming unit (CFU).

To test the effects of Tob on *P. aeruginosa* PAO1, NCI-H1299 cells re-suspended at a density of $1.5x10^5$ cells/mL were infected with PAO1 cells at OD_{600} of 0.15, resulting to a bacteria/NCI-H1299 ratio of 100-1000/1. The co-culture of NCI-H1299-PAO1 was treated with 3 µg/mL Tob (without DC) and compared with the Tob free co-culture controls. The viability of the mammalian cells during treatment was determined using trypan Blue exclusion assay. The number of viable bacterial cells was quantified by counting CFU.

8.3.5. Effect of DC and Tob on the viability of *P. aeruginosa* PAO1 in co-cultures

NCI-H1975 cells were collected after treatment of a 4-day culture with TE buffer and centrifugation at 1000 rpm for 3 min. The NCI-H1975 cells were then re-suspended in 0.85% NaCl solution. Meanwhile, *P. aeruginosa* PAO1 cells were collected from an overnight culture and the cells were washed and re-suspended in 0.85% NaCl solution. Initially, NCI-H1975 cells were introduced in the electrochemical cell with *P. aeruginosa*

PAO1 cells at OD_{600} of 0.15. DC with a current density of 70 μA/cm^2 DC was supplied for 1 h using SS 304 electrodes in the presence and absence of Tob to challenge the co-culture of bacterial and human cells. The viability of human cells was investigated after 1 h of DC treatment using Trypan Blue exclusion assay. The number of viable bacterial cells was quantified by counting CFU.

8.4. RESULTS

8.4.1. Effects of DC treatment on epithelial cells.

Human epithelial cells NCI-H1944 were successfully grown on collagen-coated 12 well-plate inserts. The cells were seeded for 8 days at a density of 60,000 cells/insert and treated with 500 μA of total DC for 30 min. The results revealed that less than 50% of the cells treated with the cathodic currents for 30 min were viable (Fig. 8.2). However, cells treated using anodic current were less affected than those treated with the cathodic current. To test if the low survival rate of the cells exposed to cathodic currents was the result of high current density delivered to each individual cell, the cell density was doubled to $1.3x10^5$ cells/insert in order to improve the confluence of the cells and therefore their tolerance of the current density. These cells were also treated with a total DC of 500 μA for 30 min using SS 304. As shown in Fig. 8.3, the treatment was slightly improved in that condition. The cells displayed a higher survival rate during the treatment administered using anodic currents. On the other hand, the viability of cells treated with cathodic currents was lower, and most dead cells were found near the center of insert.

To investigate the effects of electrochemical currents on suspended mammalian cells, planktonic suspensions of NCI-H1944 cells were treated with current levels ranging between 35 and 70 µA/cm² DC. Fig. 8.4A shows that the viability of the planktonic suspension of human epithelial cells was reduced by 26.8%, with 35 µA/cm² DC using SS 304. Similar level of killing was observed for all three conditions (one-way ANOVA, p =0.17). The viability of NCI-H1299, NCI-H1975 and ATCC® HTB-26 ™ cells tested with 500 µA or 70 µA/cm² DC for 1 h was also evaluated. Fig. 8.4B demonstrates that low-level DC treatment had cidal effects on the tested epithelial cancer cells. In particular, ATCC® HTB-26 ™ epithelial breast cells was severely affected by the treatment with 70 µA/cm² DC, which resulted in the decrease of the cell viability by 69.0%. The NCI-H1975 cells, which are epithelial cells derived from the lung cancer, were more resistant to 70 µA/cm² DC. Only 43.9% NCI-H1975 were eliminated by DC treatment. Among the epithelial cancer cells, NCI-H1299 tolerated the most the DC treatment. Only 35.7% of the cells were killed by the DC treatment (one-way ANOVA, p =0.057), suggesting that NCI-H1299 might have a greater resistance to the electrochemical currents.

8.4.2. Effects of antibiotics on cell viability in a co-culture model

To determine a concentration of Tob that has minor effects on the viability of bacterial cells in the co-culture model, suspensions of NCI-H1299 and NCI-H1975 were infected with *P. aeruginosa* PAO1 cells (OD_{600}= 0.15) and treated with 0-120 µg/mL Tob. The viability of *P. aeruginosa* PAO1 cells in the co-cultures was significantly reduced by the antibiotic treatment after 1 h and 2 h, compared to the Tob free control sample. As shown in Fig. 8.5A, incubation of PAO1 with 120 µg/mL Tob reduced the number of viable

PAO1 cells by 2 logs, while the cells incubated with the epithelial cells were killed by 3 logs by Tob. Fig. 8.5B demonstrates that this difference increases overtime. After 2 h of (120 μg/mL) Tob treatment, the number of viable PAO1 cells incubated with the epithelial cells decreased by 4.5 logs (one way ANOVA, p <0.001 for all conditions). However, the survival of bacteria was not significantly affected by Tob with a concentration lower than 3 μg/mL. To determine if attachment of the mammalian cells affects the susceptibility of the bacterial cell to Tob, NCI-H1299 and NCI-H1975 were also tested by allowing these cells to adhere to the surface of a 12-well plate and were infected with *P. aeruginosa* PAO1 cells at OD_{600} equals to 0.15. The cells were incubated with Tob for 1 h. As shown in Fig. 8.6, PAO1 cells incubated with NCI-H1975 was more susceptible to the antibiotic treatment compared to those incubated with NCI-H1299 (one-way ANOVA, p=0.001 for both conditions). In the presence of 120 μg/mL Tob, the bacteria were killed by 5 logs when they were incubated with NCI-H1975. In contrast, the PAO1 cells in co-culture with NCI-H1299 were killed by 3 logs (one-way ANOVA, p =0.001 for both conditions). This finding suggests that both physiological state (attached vs. suspended) affect the interaction with bacteria and thus the efficacy of antibiotic treatments.

To confirm that 3 μg/mL Tob alone has minimal effect on *P. aeruginosa* in our co-culture model, mixed suspension of PAO1 and NCI-H1299 cells was treated with 3 μg/mL Tob (without DC) for 4 h and the cell viability was compared to that of the Tob-free control. The viability of *P. aeruginosa* PAO1 cells was reduced by about 1 log after 4 h treatment of the co-culture with 3 μg/mL Tob (Fig. 8.7A). On the other hand, the

viability of the NCI-H1299 cells did not decrease (Fig. 8.7B) even after 16 h treatment of the co-culture with 3 μg/mL Tob (t-test, p =0.901). These results indicate that Tob levels between 1.5 and 3 μg/mL are appropriate for testing the synergistic effects of DCs and antibiotics in the co-culture model.

8.4.3. Viability of the bacterial cells during DC treatment.

To evaluate the effects of electrochemical currents in a co-culture model, NCI-H1299 cells prepared as described above were mixed with stationary phase PAO1 cells with an inoculation OD_{600} of 0.15. Then, 70 μA/cm^2 DC was delivered to the co-cultures for 1 h in the presence and absence of 1.5 or 3μg/mL Tob. It was found that the viability of the NCI-H1299 cells was not significantly reduced (Fig. 8.8A). In contrast, 70 μA/cm^2 DC treatment mediated with SS 304 electrodes killed PAO1 by more than 1 log and synergy was observed with increasing level of Tob (t-test, p <0.025 for all conditions, Fig. 8.8B). The killing was found to be dependent on both the concentration of Tob and the dose of DC delivered to the cells. Increasing Tob concentration from 3 to 12 and 30 μg/mL resulted in increased killing of PAO1 cells (Fig. 8.8B). Furthermore, by augmenting the current density from 70 μA/cm^2 to 84 μA/cm^2, the DC treatment became more effective in selective killing of PAO1 cells. One additional log killing was achieved by increasing DC level from 7 to 84 μA/cm^2 (Fig. 8.8B). The results suggest that selective killing of the bacterial cells could be achieved by means of the electrochemical treatments.

8.5. DISCUSSION

The bioactivity of the DC and electric fields on mammalian cells is well documented and has demonstrated that the cells react differently to various levels of currents[22]. In the medical field, low-level direct currents and electric fields has been utilized both to promote the growth of normal cells during wound healing[19,20,23] and to eliminate tumor cell[24-27], which is referred to as electrochemical cancer therapy (ECT). Because the electrophysiological properties of cancer cells is lower than that of normal cells[28], it was beneficial for us to develop a model of infection with epithelial cancer cells to study the selectivity of the DC treatments, not only because the cancer cells are more susceptible to electrical treatments compared to normal cells, but also because they replicate faster compared to the normal epithelial cells, offering convenience for experiments. Furthermore, the cancer cells can be suspended allowing us to compare the killing in a well-mixed co-culture, to develop an in vitro model of bacterial infection with epithelial cells, four epithelial cell lines were used, including NCI-H1944, NCI-H1299, NCI-H1975, and ATCC® HTB-26 ™. The epithelial cancer cell lines were tested with 70 $\mu A/cm^2$ DC using SS 304 electrodes to evaluate the cytotoxicity of the electrochemical treatments. The results show that the epithelial cells were more susceptible to the treatments when exposed to cathodic currents instead of anodic currents. The increase in cell density enhanced the tolerance of epithelial cells to anodic current, which may better represent the tissues with multiple layers and high density of mammalian cells. In addition, our results showed that these cell lines have different levels of tolerance to the electrochemical currents, and that NCI-H1299 withstood better the effects of DC than the other three cell lines tested.

After the initial tests, the co-cultures were used to simulate infections; it was found that PAO1 cells become more sensitive to Tob in the presence of epithelial cells, which may be due to the secretion of different factors by the human cells. The treatment of the mixed cultures revealed that the *P. aeruginosa* PAO1 cells were significantly killed after treatment with high level of antibiotic and long exposure to antibiotics. At concentration lower than 3 μg/mL Tob, however, no major killing effects were recorded. Therefore, the concentration of 3 μg/mL Tob was retained to test the synergy with 70 $\mu A/cm^2$ DC and Tob in killing bacteria in the mixed cultures. The results of the DC treatment revealed that DC was more effective in killing PAO1 cells compared to epithelial cells under the selected condition, and synergistic effects between DC and Tob were observed. The extent of the bacterial killing under this condition was about 3 logs, which is lower than the 5 logs achieved in the DC treatment of *P. aeruginosa* PAO1 cells using SS 304 electrodes and 1.5 μg/mL Tob in the absence of human cells.

The mechanism of the selective killing of bacterial cells by the low-level currents is unknown. In Chapter 3, it was demonstrated that the metal ions released from SS 304 (Fe, Cr, Ni and Mn) during the DC treatment play an important role in bacterial killing [29]. It is well documented that the high chloride concentration can induce pitting corrosion of stainless steel and the subsequent release of Fe, Cr and Ni ions among many others [30].Hence, from these results, it is tempting to postulate that cathodic current affect the cells in a way that the accumulation of positive charges at this electrode and around negatively charged cells affect the membrane properties of the cells. Also, the generation

of cathodic electrochemical byproducts such as reactive oxygen species (ROS) has been proposed as one of the reasons why treatment of the cells with cathodic current was more potent [31]. The results described in this chapter suggest that this technology may be extended to chronic infections associated with deep tissue or medical implants.

The results also provide guidance for testing of safety and efficacy of the electrochemical treatments in animal models and the development of an electrochemical technology for infection control. The preliminary data collected in this chapter show that the delivery of appropriate level of electric current density at the infection site could result in the selective killing of bacterial cells [29].

8.6. CONCLUSIONS

Electrochemical treatments generated with 70 μA/cm^2 DC using SS 304 electrodes were found to effectively kill PAO1 cells in co-cultures involving human epithelial cells. *P. aeruginosa* PAO1 cells can be selectively eliminated with appropriate level of current density. While anodic currents were found safer for epithelial cells, the cathodic current presents a greater advantage compared to the anodic current in killing bacterial cells. Also, synergistic killing of *P. aeruginosa* PAO1 cells was achieved between and 3 μg/mL Tob. Overall, this study demonstrated that electrochemical treatments using DC and antibiotics have potential to eliminate bacterial cells attached to medical devices or attached to epithelial cells.

8.7. ACKNOWLEDGEMENTS

The authors are grateful to Blue Highway Inc. and the U.S. National Science Foundation (EFRI-1137186) for support. We also thank Dr. Thomas K. Wood at Penn State University for sharing the strain *P. aeruginosa* PAO1, and Dr. Jing An at SUNY Upstate Medical University for providing epithelial cell lines.

8.8. REFERENCES

1 **Darouiche, R. O.** Treatment of infections associated with surgical implants. *The New England journal of medicine* **350**, 1422-1429, doi:10.1056/NEJMra035415 (2004).

2 **Husni, R. N., Goldstein, L. S., Arroliga, A. C., Hall, G. S., Fatica, C., Stoller, J. K., Gordon, S. M.** Risk factors for an outbreak of multi-drug-resistant Acinetobacter nosocomial pneumonia among intubated patients. *CHEST Journal* **115**, 1378-1382 (1999).

3 **Pruitt Jr, B. A., McManus, A. T., Kim, S. H. & Goodwin, C. W.** Burn wound infections: current status. *World journal of surgery* **22**, 135-145 (1998).

4 **Zavascki, A. P., Carvalhaes, C. G., Picão, R. C. & Gales, A. C.** Multidrug-resistant Pseudomonas aeruginosa and *Acinetobacter baumannii*: resistance mechanisms and implications for therapy. *Expert review of anti-infective therapy* **8**, 71-93 (2010).

5 **Aloush, V., Navon-Venezia, S., Seigman-Igra, Y., Cabili, S. & Carmeli, Y.** Multidrug-resistant *Pseudomonas aeruginosa*: risk factors and clinical impact. *Antimicrobial agents and chemotherapy* **50**, 43-48 (2006).

6 **Boucher, H. W., Talbot, G. H., Bradley, J. S., Edwards, J. E., Gilbert, D., Rice, L. B., Scheld, M., Spellberg, B. & Bartlett, J.** Bad bugs, no drugs: no ESKAPE! An update from the Infectious Diseases Society of America. *Clinical Infectious Diseases* **48**, 1-12 (2009).

7 **Li, X.-Z., Ma, D., Livermore, D. M. & Nikaido, H.** Role of efflux pump (s) in intrinsic resistance of *Pseudomonas aeruginosa*: active efflux as a contributing factor to beta-lactam resistance. *Antimicrobial agents and chemotherapy* **38**, 1742-1752 (1994).

8 **Michéa-Hamzehpour, M., Auckenthaler, R., Regamey, P. & Pechere, J.** Resistance occurring after fluoroquinolone therapy of experimental *Pseudomonas aeruginosa* peritonitis. *Antimicrobial agents and chemotherapy* **31**, 1803-1808 (1987).

9 **Pai, H., Kim, JW., Kim, J., Lee, J. H., Choe, K. W., Gotoh, N.** Carbapenem resistance mechanisms in *Pseudomonas aeruginosa* clinical isolates. *Antimicrobial agents and chemotherapy* **45**, 480-484 (2001).

10 **Aires, J. R., Köhler, T., Nikaido, H. & Plésiat, P.** Involvement of an active efflux system in the natural resistance of *Pseudomonas aeruginosa* to aminoglycosides. *Antimicrobial agents and chemotherapy* **43**, 2624-2628 (1999).
11 **Westbrock-Wadman, S., Sherman, D. R., Hickey, M. J., Coulter, S. N., Zhu, Y. Q., Warrener, P., Nguyen, L.Y., Shawar, R. M., Folger, K. R., Stover, C. K.** Characterization of a *Pseudomonas aeruginosa* efflux pump contributing to aminoglycoside impermeability. *Antimicrobial agents and chemotherapy* **43**, 2975-2983 (1999).
12 **Costerton, J. W., Ellis, B., Lam, K., Johnson, F. & Khoury, A. E.** Mechanism of electrical enhancement of efficacy of antibiotics in killing biofilm bacteria. *Antimicrobial agents and chemotherapy* **38**, 2803-2809 (1994).
13 **Del Pozo, J. L., Rouse, M. S. & Patel, R.** Bioelectric effect and bacterial biofilms. A systematic review. *International Journal of Artificial Organs* **31**, 786-795 (2008).
14 **Kohanski, M. A., Dwyer, D. J. & Collins, J. J.** How antibiotics kill bacteria: from targets to networks. *Nature Reviews Microbiology* **8**, 423-435 (2010).
15 **Nishimura, K. Y., Isseroff, R. R. & Nuccitelli, R.** Human keratinocytes migrate to the negative pole in direct current electric fields comparable to those measured in mammalian wounds. *Journal of Cell Science* **109**, 199-207 (1996).
16 **Nuccitelli, R. & Erickson, C. A.** Embryonic cell motility can be guided by physiological electric fields. *Experimental cell research* **147**, 195-201 (1983).
17 **McCaig, C. D., Rajnicek, A. M., Song, B. & Zhao, M.** Controlling cell behavior electrically: current views and future potential. *Physiological Reviews* **85**, 943-978 (2005).
18 **Stromberg, B. V.** Effects of electrical currents on wound contraction. *Annals of Plastic Surgery* **21**, 121 (1988).
19 **Kloth, L. C.** Electrical stimulation for wound healing: a review of evidence from in vitro studies, animal experiments, and clinical trials. *The international journal of lower extremity wounds* **4**, 23-44 (2005).
20 **Kloth, L. C. & McCulloch, J. M.** Promotion of wound healing with electrical stimulation. *Advances in Skin & Wound Care* **9**, 42&hyhen (1996).
21 **Sambrook, J. & Russell, D. W.** *Molecular cloning: a laboratory manual*. Vol. 3 (Cold spring harbor laboratory press, 2001).
22 **Balint, R., Cassidy, N. J. & Cartmell, S. H.** Electrical stimulation: a novel tool for tissue engineering. *Tissue Engineering Part B: Reviews* **19**, 48-57 (2012).
23 **Cutting, K. F.** Electric stimulation in the treatment of chronic wounds. *Wounds UK* **2**, 62-71 (2006).
24 **Breton, M. & Mir, L. M.** Microsecond and nanosecond electric pulses in cancer treatments. *Bioelectromagnetics* **33**, 106-123 (2012).
25 **Sree, V. G., Udayakumar, K. & Sundararajan, R.** Electric Field Analysis of Breast Tumor Cells. *International journal of breast cancer* **2011** (2011).
26 **Xin, Y.-L.** Advances in the treatment of malignant tumours by electrochemical therapy (ECT). *The European journal of surgery. Supplement.: = Acta chirurgica. Supplement*, 31-35 (1993).
27 **Xin, Y. l., Xue, FZ., Ge, BS., Zhao, FR., Shi, B., Zhang, W.** Electrochemical treatment of lung cancer. *Bioelectromagnetics* **18**, 8-13 (1997).

28 **Levin, M. & Stevenson, C. G.** Regulation of cell behavior and tissue patterning by bioelectrical signals: challenges and opportunities for biomedical engineering. *Annual review of biomedical engineering* **14**, 295-323 (2012).

29 **Niepa, T. H., Gilbert, J. L. & Ren, D.** Controlling *Pseudomonas aeruginosa* persister cells by weak electrochemical currents and synergistic effects with tobramycin. *Biomaterials* **33**, 7356-7365, doi:10.1016/j.biomaterials.2012.06.092 (2012).

30 **Cruz, R., Nishikata, A. & Tsuru, T.** AC impedance monitoring of pitting corrosion of stainless steel under a wet-dry cyclic condition in chloride-containing environment. *Corrosion science* **38**, 1397-1406 (1996).

31 **Pourbaix, M.** *Atlas of electrochemical equilibria in aqueous solutions*. 1st English edn, (Pergamon Press, 1966).

FIGURE CAPTIONS

Figure 8.1. Electrochemical cell used for DC treatment of epithelial cells adhered to a well-insert. The epithelial cells were attached to the well-insert and sandwiched between the working and the counter electrode to perform DC treatment.

Figure 8.2. DC treatment of epithelial NCI-H1944 cells (60,000 cells/insert) seeded for 8 days on collagen-coated inserts. The samples were treated without (A1, A2) or with 500 μA total DC of cathodic (B1, B2) or anodic (C1, C2) DC for 30 min using SS 304.

Figure 8.3. DC treatment of epithelial NCI-H1944 cells (130,000 cells/insert) seeded for 7 days film on collagen-coated inserts. The samples were treated (A1, A2) without or with 500 μA total DC of (B1, B2) cathodic or (C1, C2) anodic DC for 30 min using SS 304.

Figure 8.4. Viability of the epithelial cells after the electrochemical treatment of cells in suspension. (A) viability of the NCI-H1944 cells reported as a function of current level. (B) viability of different human epithelial cell lines including NCI-H1975, NCI-H1299, and ATCC® HTB-26 ™ after treatment with 70 $\mu A/cm^2$ DC using SS 304.

Figure 8.5. Viability of the PAO1 cells in the co-culture model after 1 h (A) or 2 h (B) treatment using Tob. The PAO1 cells were treated with 0-120 μg/mL Tob in the presence of NCI-H1975 or NCI-H1299 epithelial cells. The number of viable PAO1 cells was quantified by counting CFU.

Figure 8.6. Viability of the PAO1 cells in the co-culture model after 1 h treatment using Tob. The PAO1 cell suspension was added to adherent culture of NCI-H1975

and NCI-H1299 epithelial cells and treated with 0-120 μg/mL Tob. The number of viable PAO1 cells was quantified by counting CFU.

Figure 8.7. Viability of PAO1 cells (A) and that of NCI-H1299 (B) in the co-culture model treated with 3μg/mL Tob only. The number of viable PAO1 cells was quantified by counting CFU, and that of the NCI-H1299 cell was quantified using the trypan blue exclusion method.

Figure 8.8. Viability of PAO1 cells treated with different levels of DCs and antibiotics. The number of viable PAO1 cells was quantified by counting CFU, and that of the NCI-H1299 cell was quantified using the trypan blue exclusion method.

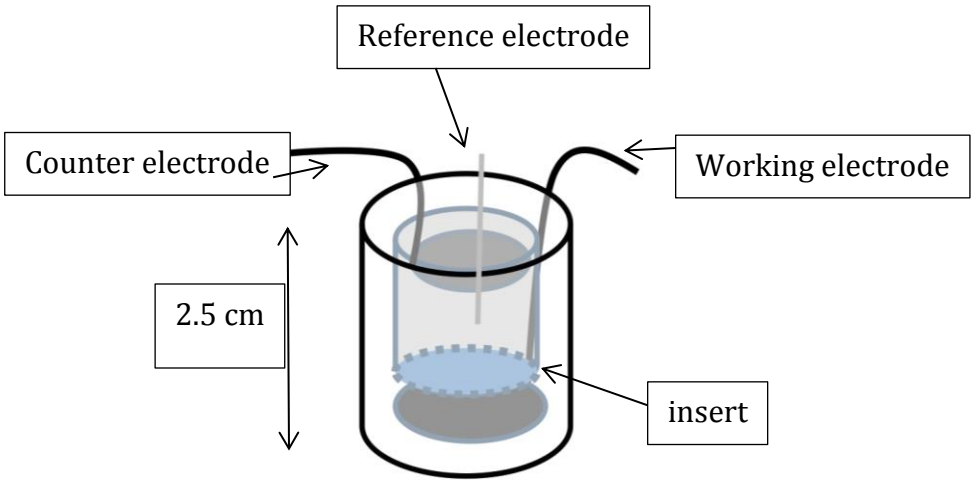
Reference electrode
Counter electrode
Working electrode
2.5 cm
insert

Figure 8.1

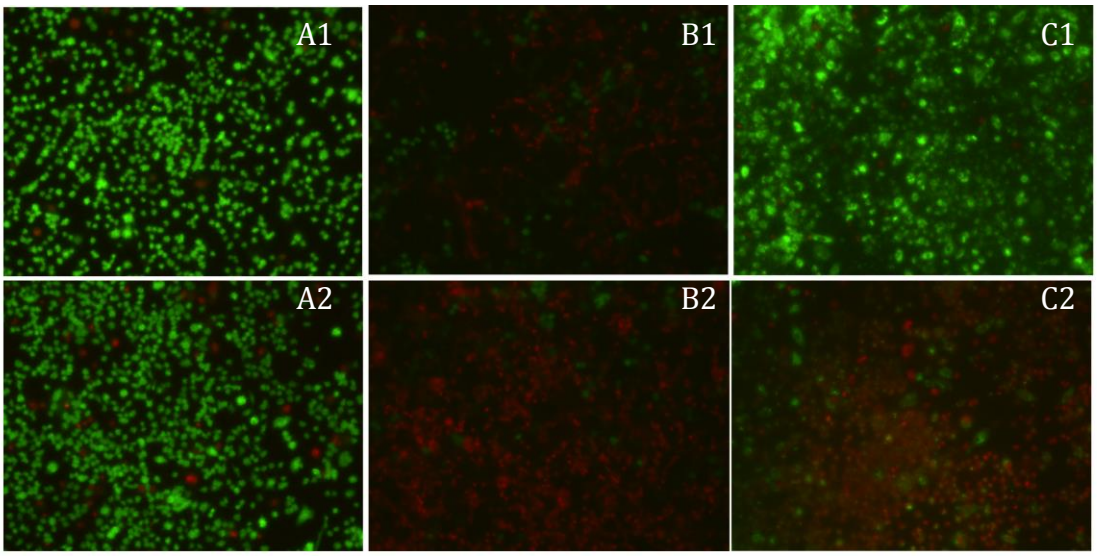

Figure 8.2

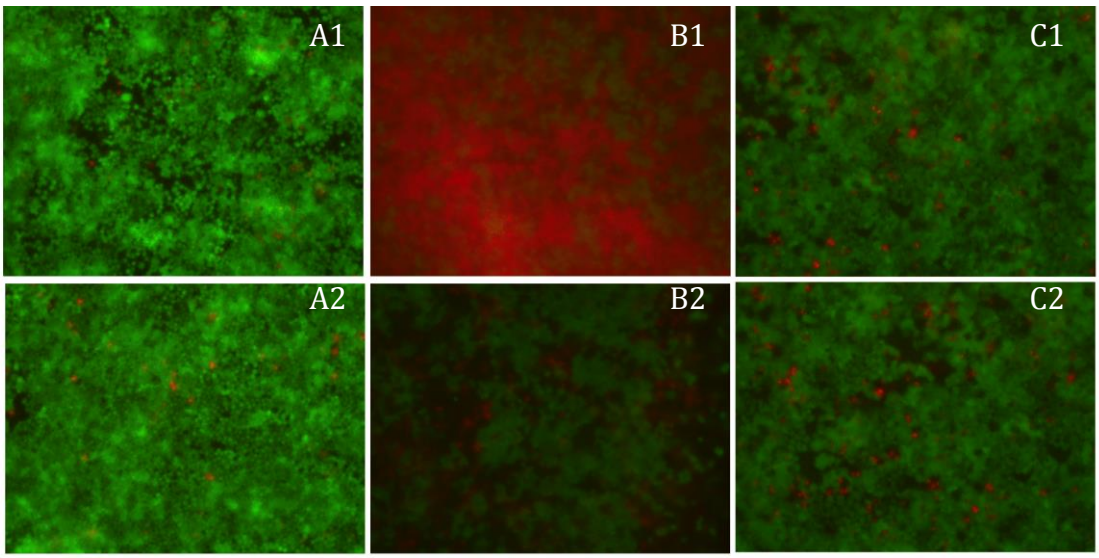

Figure 8.3

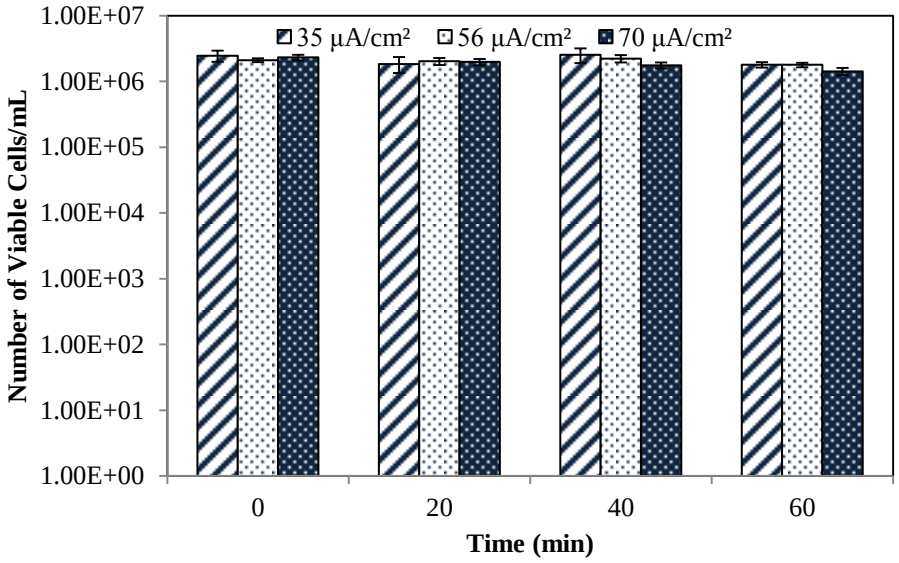
35 µA/cm²
56 µA/cm²
70 µA/cm²
Number of Viable Cells/mL
1.00E+07
1.00E+06
1.00E+05
1.00E+04
1.00E+03
1.00E+02
1.00E+01
1.00E+00
0
20
40
60
Time (min)

(A)

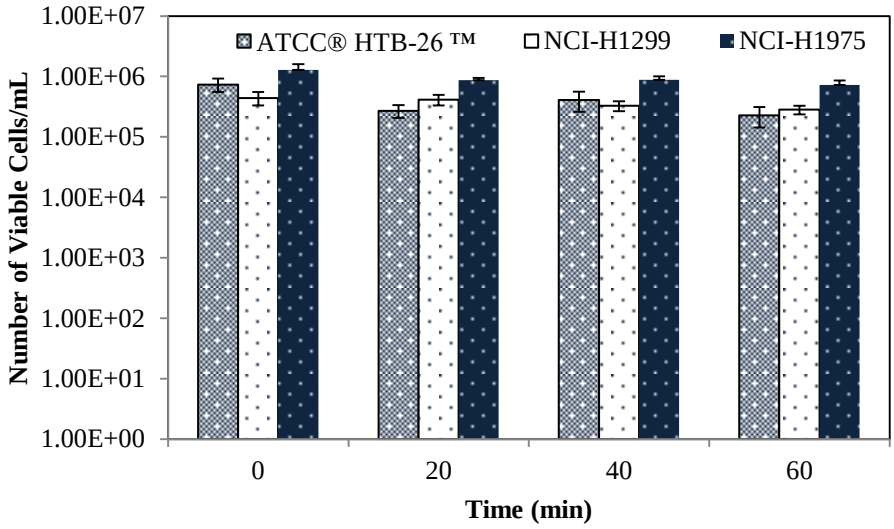
ATCC® HTB-26 ™
NCI-H1299
NCI-H1975
Number of Viable Cells/mL
1.00E+07
1.00E+06
1.00E+05
1.00E+04
1.00E+03
1.00E+02
1.00E+01
1.00E+00
0
20
40
60
Time (min)

(B)

Figure 8.4

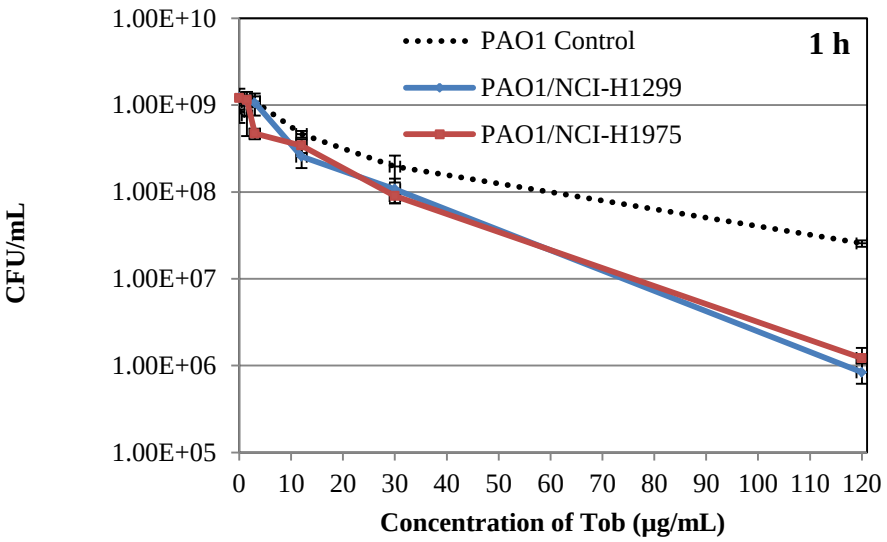
1.00E+10
1.00E+09
1.00E+08
1.00E+07
1.00E+06
1.00E+05
CFU/mL
PAO1 Control
PAO1/NCI-H1299
PAO1/NCI-H1975
1 h
0 10 20 30 40 50 60 70 80 90 100 110 120
Concentration of Tob (µg/mL)

(A)

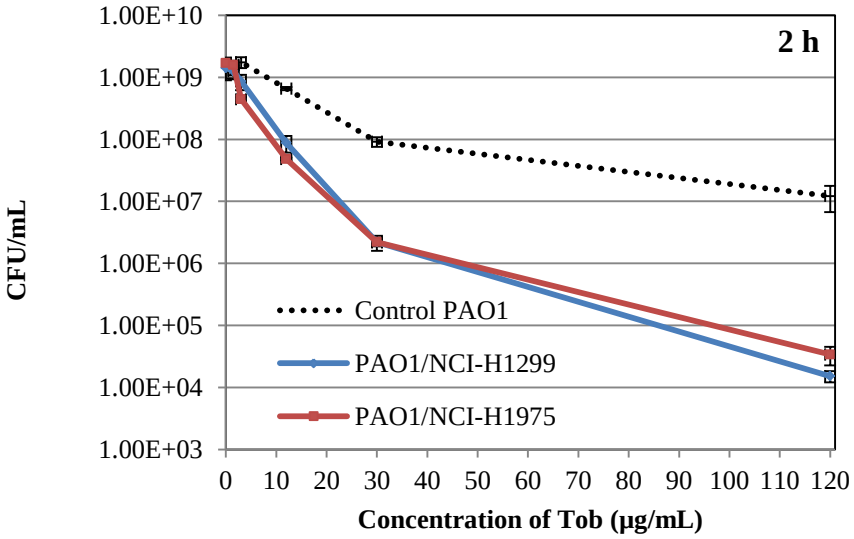
1.00E+10
1.00E+09
1.00E+08
1.00E+07
1.00E+06
1.00E+05
1.00E+04
1.00E+03
CFU/mL
2 h
Control PAO1
PAO1/NCI-H1299
PAO1/NCI-H1975
0 10 20 30 40 50 60 70 80 90 100 110 120
Concentration of Tob (µg/mL)

(B)

Figure 8.5

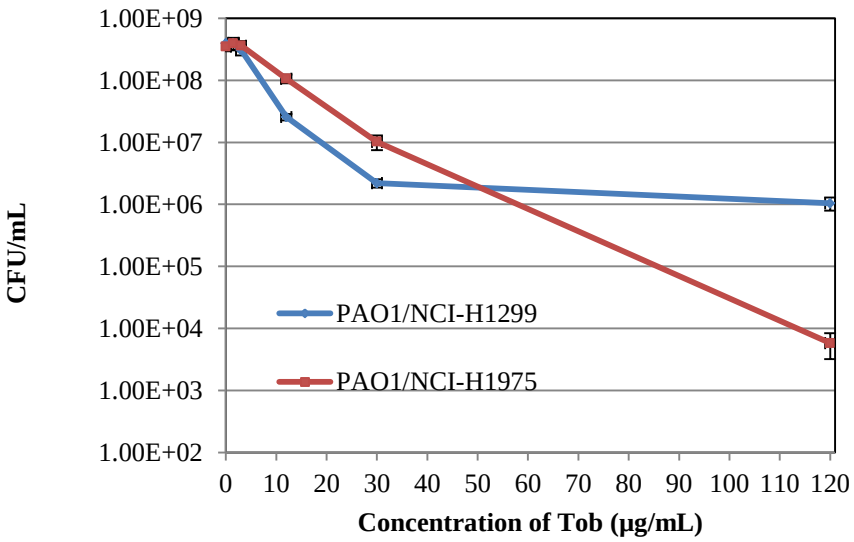
1.00E+09
1.00E+08
1.00E+07
1.00E+06
1.00E+05
1.00E+04
1.00E+03
1.00E+02
CFU/mL
PAO1/NCI-H1299
PAO1/NCI-H1975
0 10 20 30 40 50 60 70 80 90 100 110 120
Concentration of Tob (µg/mL)

Figure 8.6

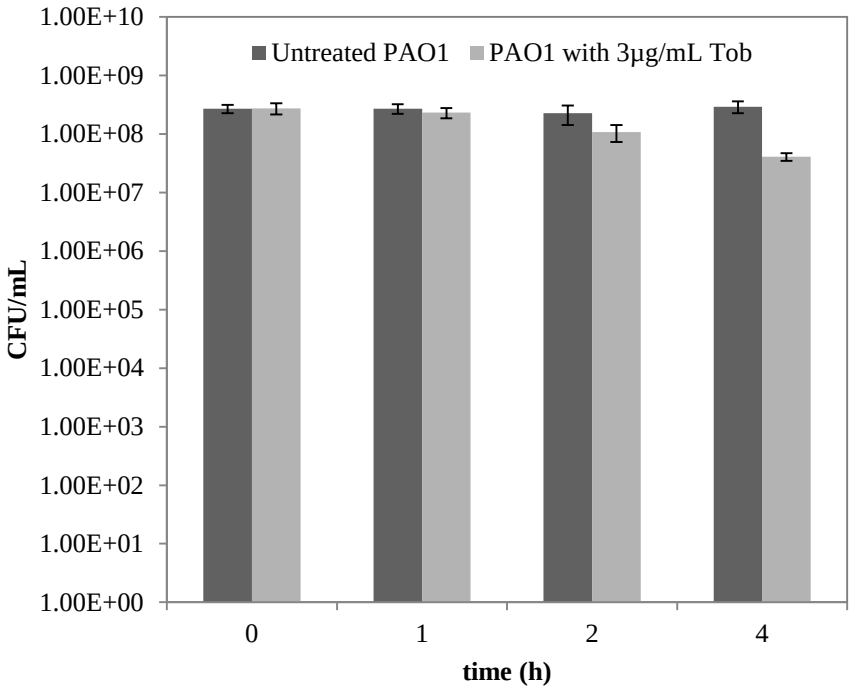
1.00E+10
1.00E+09
1.00E+08
1.00E+07
1.00E+06
1.00E+05
1.00E+04
1.00E+03
1.00E+02
1.00E+01
1.00E+00
CFU/mL
Untreated PAO1
PAO1 with 3µg/mL Tob
0
1
2
4
time (h)

(A)

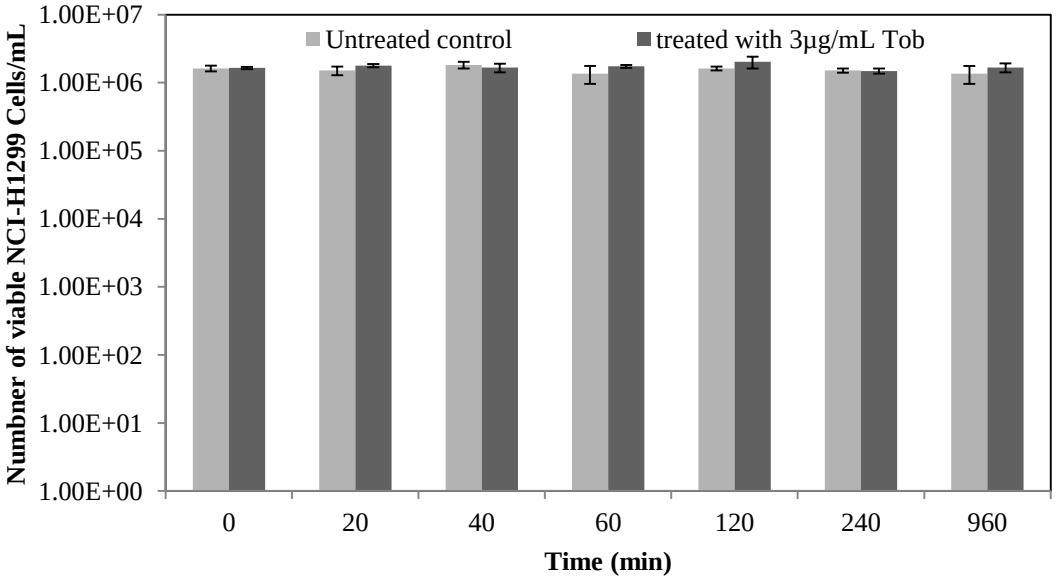
1.00E+07
1.00E+06
1.00E+05
1.00E+04
1.00E+03
1.00E+02
1.00E+01
1.00E+00
Numbner of viable NCI-H1299 Cells/mL
Untreated control
treated with 3µg/mL Tob
0
20
40
60
120
240
960
Time (min)

(B)

Figure 8.7

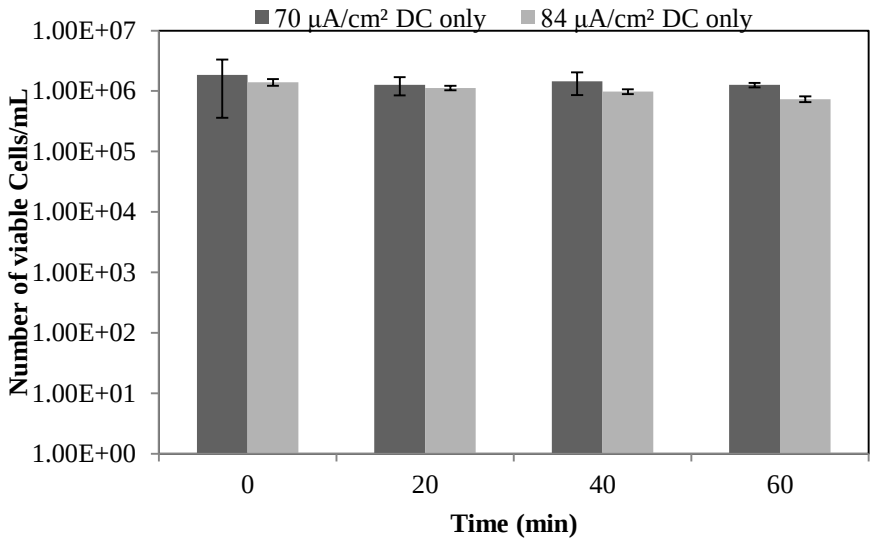
70 µA/cm² DC only
84 µA/cm² DC only
1.00E+07
1.00E+06
1.00E+05
1.00E+04
1.00E+03
1.00E+02
1.00E+01
1.00E+00
Number of viable Cells/mL
0
20
40
60
Time (min)

(A)

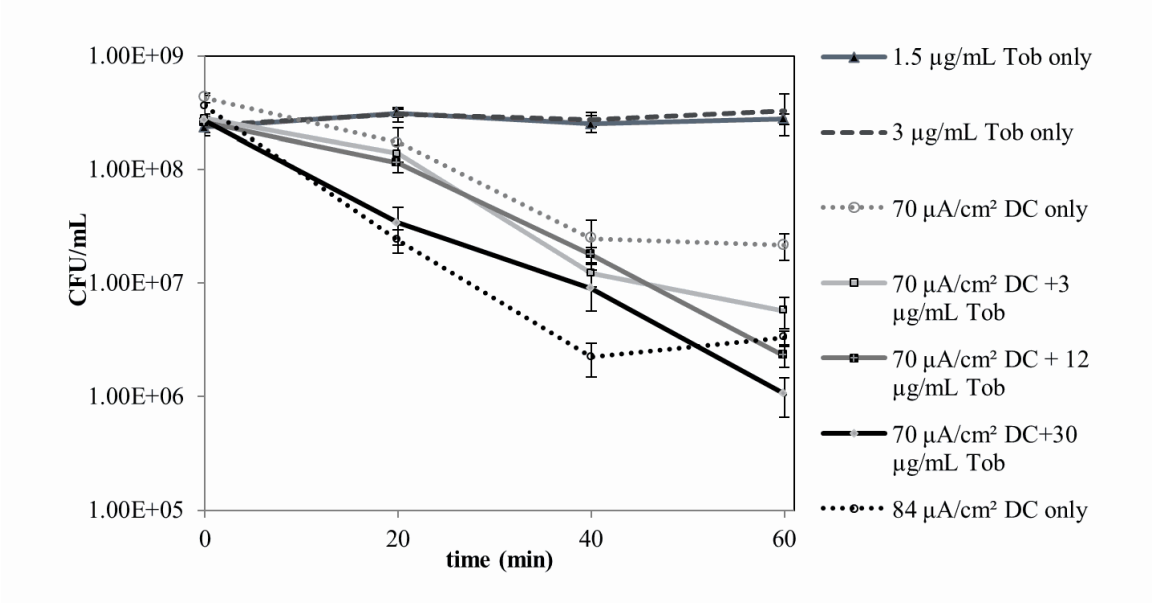
1.00E+09
1.00E+08
1.00E+07
1.00E+06
1.00E+05
CFU/mL
0
20
40
60
time (min)
1.5 µg/mL Tob only
3 µg/mL Tob only
70 µA/cm² DC only
70 µA/cm² DC +3 µg/mL Tob
70 µA/cm² DC + 12 µg/mL Tob
70 µA/cm² DC+30 µg/mL Tob
84 µA/cm² DC only

(B)

Figure 8.8

CHAPTER 9

ELECTROCHEMICAL TREATMENT OF *PSEUDOMONAS AERUGINOSA* IN A RABBIT MODEL OF SINUSITIS

The animal surgery described in this Chapter was conducted by Dr. Parul Goyal and Dr. Greg Haveman (SUNY Upstate Medical University).

9.1. ABSTRACT

Sinusitis is a common medical condition related to the inflammation of sinuses. The presence of bacterial biofilms on the sinus mucosa renders antibiotic treatments ineffective, and contributes to the recurrence of infections. The potent activities of direct current (DC) to effectively kill the biofilm cells, or enhance the susceptibility of the embedded bacterial cells to antibiotics, have attracted increasing interest recently. In chapter 3, we have demonstrated that such synergistic effects could also be extended to eradicate drug tolerant persister cells. In this chapter, the effects of electrochemical currents were further tested on an *in vivo* model of sinus infection. A model of sinusitis in rabbits was induced with *Pseudomonas aeruginosa*, and the infection was treated for 1 h with 15 μg/mL Tob in the presence or absence of a total direct current (DC) of 1mA. Compared to the untreated controls, treatment with Tob alone reduced the total number of cells within the pus by 88.3%, but failed to prevent the proliferation of biofilm cells. Co-treatment of the infections with 1 mA DC and 15 μg/mL Tob had more profound effects, reducing the cells count in pus by 3 logs and the biofilm cells by 58.0%, compared to the treatment with Tob alone. These results corroborated with SEM analysis showing the presence of lyzed *P. aeruginosa* cells on mucosal specimen of sinus treated with both DC and Tob. In addition, histological analysis of the specimen validated the effectiveness and the safety of electrochemical treatments in reducing biofilms and eradicating planktonic cells of *P. aeruginosa* in rabbit model.

9.2. INTRODUCTION

Rhinosinusitis constitutes a significant health care burden in the U.S. and worldwide. It is estimated that over 30 million Americans are affected by sinusitis annually, leading to $5.8 billion cost in health care, and loss of productivity of affected individuals. In addition, many of the sinusitis patients suffer from persistent symptoms despite antimicrobial and surgical treatments [1,2]. Biopsies of sinus tissues from patients with recalcitrant sinusitis have been found to harbor bacterial biofilms[3], which are multicellular structures of bacteria embedded in a matrix with self-secreted proteins and extracellular DNA. The protection of the extracellular matrix enables the cells to escape from host immune response and antibiotics. These microbial aggregates play a major role in a wide range of infections, particularly in chronic disease processes, and those associated with medical implants. In fact, bacterial biofilms are involved in up to two thirds of human infections[4], such as head and neck infections, chronic otitis media[5], and chronic tonsillitis[6].

It is well established that bacteria in biofilms are highly resistant to antibiotics, and require concentrations 500 to 5,000 times higher than those needed to treat free swimming cells[7]. Multiple therapies have been developed in the hope to weaken or eradicate sinus biofilms. These methods involve high concentration antibiotics, various surfactants, and techniques to physically remove the biofilms. However, no treatment method has been proven effective to treat biofilms without causing excessive damage to sinus mucosa [8].

In the early 90's, several studies showed that the killing effects of antibiotics could be dramatically enhanced when given in the presence of a mild electrical field[9,10]. These findings have since been reproduced in multiple *in vitro* studies, using a variety of antibiotics and pathogens[11]. Further investigations on the effects of electrical factors have demonstrated that electric current alone could also stimulate the detachment of biofilm cells from the substrate[12,13]. As described in Chapter 3, we have revealed that chronic infections associated with biofilm and persister cells of *P. aeruginosa* could be eradicated with 70 μA/cm^2 DC using SS 304 electrodes in the presence of tobramycin (Tob). For instance, co-treatment of *P. aeruginosa* biofilms with DC and 15 μg/mL Tob for 2 h reduced the number of viable persister cells in biofilm by 99.4% compared to the untreated control [14]. These findings motivated us to further evaluate this approach against mucosal biofilms *in vivo* in a model of sinusitis.

The goal of the study outline in this chapter is to assess the effectiveness of electrical current delivered along with Tob in eradicating *P. aeruginosa* in a rabbit model. It also aims to evaluate the safety of such electrochemical treatment. The results can help develop new treatment for patients suffering chronic sinusitis.

9.3. MATERIALS AND METHODS

9.3.1. Experimental setup of the electrochemical treatment

To understand how the impedance of animal tissues affect the delivery of electrochemical currents, different setups of DC treatment were experimented on previously sacrificed mice generously provided by Dr. Jing An at SUNY Upstate Medical University. DC at 1

mA level was delivered using SS 304 electrodes and a series of potentiodynamic curves were recorded. Four main conditions were tested: (1) The working electrode was introduced with the reference electrodes inside the tissue of the mouse, while the counter electrode was attached to the skin outside of the mouse; (2) The counter electrode was inserted inside the tissue with the reference electrodes, while the working electrode was attached to the skin outside; (3) Same as the setup but the skin of the mouse was shaved before the working electrode was placed. (4) Same as the third setup, DC treatment of the mouse snout was performed in the presence of electrolyte to evaluate the effects on the impedance of nasal cavities and tissues. In all the case, a potentiodynamic curve was recorded.

9.3.2. Rabbit model of sinusitis.

Eight New Zealand white male rabbits (3-4 kg each) were used to evaluate the safety and efficacy of electrochemical treatments of *P. aeruginosa* PAO1 involved in sinus infections. To induce the infection, *P. aeruginosa* PAO1 cells were grown overnight in 25 mL Luria-Bertani (LB) medium [15] containing 10 g/L tryptone, 5 g/L yeast extract, and 10 g/L NaCl. The overnight culture was incubated at 37°C with shaking at 200 rpm. On the next day, a subculture of PAO1 was made by adding 25 µL of the overnight culture in 25 mL of fresh LB medium and the cells were grown to the log-phase and collected when the cell density reached an OD_{600} of 0.6. The cells were washed with 0.85% NaCl solution and re-suspended to the same cell density. Then 0.4 mL sample was drawn into 1 mL syringes and stored on ice until needed in surgery.

The rabbits had a hind flank shaved prior to surgery, and a grounding pad was placed on the skin. Each animal was anesthetized with a combination of ketamine (50 mg/kg intramuscularly) and xylazine (5 mg/kg intramuscularly). Once appropriately anesthetized, vital signs were monitored, and the nasal dorsum was shaved and prepped in a sterile fashion. Local anesthetic was administered (1% lidocaine with 1:100,000 epinephrine) subcutaneously over the maxillary sinuses. A vertical incision was made in the midline of the face, and a subperiosteal plane elevated over the maxillary sinuses. The bone overlying the sinuses was drilled to expose the underlying sinus mucosa (Fig. 9.1A). This was incised to gain access to the maxillary sinus. The maxillary ostium was visualized, and a small cotton pledget was cut to fit over the ostium. This functioned as an ostium plug, and was secured with cyanomethacrylate glue, preventing the infection to spread to area other than the sinuses. The previously prepared PAO1 culture was then instilled into the maxillary sinus (Fig. 9.1B). Approximately 200-400 μL of the cell suspension was inoculated to fill each infected sinus. The skin was then closed with suture, and the same procedure repeated on the opposite side. The animals were given buprenorphine (0.05 mg/kg BID) for post-operative analgesia, and kept for 5 days to allow for sufficient biofilm formation within the maxillary sinuses. During this time, the animals were closely monitored and assessed clinically for evidence of complications from the procedure (infection, wound breakdown, hematoma). Minor wound complications were addressed with local wound care if appropriate.

9.3.3. Electrochemical treatment.

To perform the electrochemical treatment, the animals were anesthetized with a combination of ketamine and xylazine, as previously described. After being prepped and draped in a sterile fashion, the previous incisions were reopened to gain access to the maxillary sinuses (Fig. 9.1C). Evidence of successful inoculation was seen as frank purulence within the sinus. After the maxillary sinuses were exposed, purulent material was suctioned to quantify the initial cell count within the sinuses (Fig. 9.1D). Stainless steel (SS) electrodes were connected to a WaveNow potentiostat (PINE Research Instrumentation, Raleigh, NC) to deliver the electrochemical current in a galvanostatic mode. According to the preliminary experiments, the working SS electrode and the Ag/AgCl reference electrode were placed under the skin and skull while the counter electrode was inserted with the treated sinus (Fig. 9.1E). The sinuses were filled with normal saline containing 15 μg/mL Tob during treatment. To minimize the variation among rabbits, each rabbit was used to perform two tests. One sinus was treated with DC and 15 μg/mL Tob only, and the other with 15 μg/mL Tob only as control. A total DC of 1mA was supplied to the DC-treated sinus and the efficacy of the DC treatment was compared to the treatment with 15 μg/mL Tob only. At the completion of each treatment, the electrodes were removed, and the skin overlying each sinus was closed by suture. The animals were given adequate pain control (0.05 mg/kg buprenorphine BID for an additional day), and closely monitored for activity and any development of post-operative complications over the next day (Fig. 9.1F).

9.3.4. Sample collection.

As described above, we first collected purulent materials by suction before the DC treatment was performed (Fig. 9.1D) to evaluate the infection level by quantifying the number of viable PAO1 cells. The day following the electrochemical treatment, the animals were euthanized by an IV bolus of pentobarbital solution (150 mg/kg), followed by thoracotomy to ensure death. After aseptic preparations, the incisions were reopened to gain access to the maxillary sinuses and the purulence secreted was collected and stored on ice until analysis. In addition, the maxillary sinuses were dissected and the side of mucosa that was exposed to the treatments was stripped from the underlying bone for analysis. About 60% of the DC-treated mucosal specimen was collected for the viability test, while 20% was used for SEM analysis and the remaining 20% was used for histological study.

9.3.5. Viability test and Colony Forming Units (CFUs).

To quantify the number of cells in the specimens of purulence and mucosal tissues, the purulence was homogenized for 2 min using the Q125 SONICA sonicator with 500 Watt, 20 KHz and 50% amplitude with 20 sec on and 20 sec off cycles (QSonica, LLC, Newton, CT). Then the samples were placed in LB agar plates to count CFU. Similarly, the sinus mucosa was homogenized to determine the viability of biofilm-associated cells. No significant effects of sonication on the viability of *P. aeruginosa* PAO1 was found (viability was not changed after 2 min of sonication as confirmed by CFU).

9.3.6. Scanning Electron Microscopy (SEM).

The effects of DC treatment on the morphology of PAO1 cells were evaluated in *both in vitro* and *in vivo*. For *in vitro* experiments, stationary phase PAO1 cultures were used to insulate PAO1 biofilm cultures in a 12-well plate insert containing 2 mL LB, and the medium was replenished after 24 h of inoculation. PAO1 biofilms were formed on the inserts, which were cut to fit in an electrochemical cell. The samples were treated with a total DC of 1mA using SS 304 electrodes. Then the DC treated sample and untreated control were fixed with 2.5% gluteraldehyde and dehydrated with increasing concentration of ethanol comprised between 70%-100%. Dehydration in 100% ethanol was repeated three times. To achieve complete drying and preservation of the samples, critical-point drying in CO_2 was performed. Finally, the samples were coated with gold and imaged using a JEOL JSM-5800 LV low vacuum SEM at an accelerating voltage of 10kV. This protocol was also followed to evaluate the morphology of PAO1 in *in vivo* samples.

9.3.7. Histology.

To evaluate the cytotoxicity of the treatments and the inflammatory response within the sinuses, approximately 20% of the collected mucosal specimen was fixed in formalin containing 10% formaldehyde in PBS. The decalcified specimens was sectioned and embedded in paraffin before they were micro-dissected in thin films. Then, the samples were mounted on glass slides and H&E (Hematoxylin and Eosin) staining was performed. Finally, the samples were analyzed using light microscopy to determine if there was any change in histology[16].

9.4. RESULTS

9.4.1. Experimental design of the electrochemical treatment

Preliminary experiments were performed on dead mice to determine appropriate electrochemical setup to deliver low-level DC *in vivo*. Placing the working electrode on mouse skin with the counter and the reference electrodes under the skin resulted in high resistance, and no DC was detected. As shown in Fig. 9.2A, the open circuit potential (4.2V) was recorded instead, showing that in this condition, no electric current was reaching the reference and the counter electrodes. However, insertion of the working electrode and reference electrode under the skin allowed the desired electric current to be established. As shown in Fig. 9.2B, a negative current was crossing the skin of the mouse. The delivery of the electric current was further improved when the counter electrode was placed on a skin previously shaved (Fig. 9.2C). Under that condition, a positive current was delivered, resulting in the decrease of impedance at the working electrode. Because sinusitis was the model of infection in this study, the impedance of the mouse snout was also investigated. As shown in Fig. 9.2D, the impedance of the mouse snout decreased from 2.5 kΩ to 2 kΩ when the pockets of air within the snout were reduced by compressive force. Addition of 0.85% NaCl solution resulted in a major decrease of the impedance. For example, in the presence of 0.85% NaCl saline solution, the impedance was reduced from 2.5 kΩ to 630Ω. These results suggest that filling the sinus with a saline solution could greatly improve the effectiveness of the DC treatment by increasing the conductivity across the tissues.

9.4.2. Efficacy of the electrochemical treatment in rabbits.

To evaluate the efficacy of electrochemical treatment in infection control *in vivo*, rabbit sinusitis was established by instilling *P. aeruginosa* PAO1 in the maxillary sinuses of New Zeeland male rabbits and allowing the infection to develop for 5 days. Then the infections were treated with total DC of 1 mA and/or 15 μg/mL Tob for 1 h. The next day the rabbits were sacrificed to assess the viability of the bacterial cells and evaluate the synergy between DC and 15μg/mL Tob *in vivo*. To verify that DC treatment was successfully delivered, a potentiodynamic curve was recorded to evaluate the change in anodic potential. For a constant total DC of 1mA, the anodic potential decreased from 600 mV to 300 mV during the DC treatment (Fig. 9.3). This indicates that the delivery of DC was successful, reducing the resistance of tissues between the skull and mucosa due to the release of ions from SS electrodes.

The results of the viability test (Fig. 9.4) demonstrated that infection was successfully achieved in all tested rabbits. At 5 days after inoculation that the sinus were infected with $1.58x10^6 \pm 7.6x10^5$ *P. aeruginosa* PAO1 cells/mL. As shown in Fig. 9.2, the total number of PAO1 cells in the untreated sinuses increased by 7 times on the following day compared to the 5^{th} day after inoculation. The number of cells associated with mucosal biofilms was 5 times that of the PAO1 cells collected from the original purulence. The treatment using 15 μg/mL Tob reduced the level of infection significantly; e.g.: the number of PAO1 cells in the pus of Tob-treated sinuses was reduced by 88.3 ± 4.5% compared to the number of cells found in the pus before treatment. While the number of bacteria in the untreated control sample increased by 495.6 ± 1.6%, the growth

of the PAO1 on mucosa treated with 15 μg/mL Tob alone was reduced to 143.6 ± 78.7%, compared to the untreated control, suggesting that Tob alone fails to inhibit biofilm growth on the mucosa. However, treatment combining DC and 15 μg/mL Tob was very effective in killing PAO1. Only 0.18 ± 0.12% of PAO1 cells were found viable after the co-treatment, suggesting a 3-log reduction compared to the number of cells found in the purulence before the treatment. The number of viable biofilm cells attached to the mucosa was reduced to 59.6 ± 53.7%, suggesting that DC and Tob exhibit synergistic lethal effects against PAO1 cells *in vivo*.

9.4.3. Effects of electrochemical treatment on the morphology of PAO1 cells

To directly visualize the PAO1 biofilms on the sinus mucosa and investigate the integrity of cilia of sinus mucosa, SEM imaging was performed to examine control and treated samples. Initially, electron micrographs of *in vitro* cultures of PAO1 biofilms on well-inserts, which were treated with or without 140 $\mu A/cm^2$ DC, were collected to determine if there is any DC-induced morphological change in the PAO1 cells. As shown in Fig. 9.5A, untreated PAO1 biofilms were made up of rod-shape PAO1 cells. However, the DC treatment affected the morphology of the PAO1 cells *in vitro*. The cells, which were originally rod-shape, were found to swell and become round-shape after 1 h electrochemical treatment (Fig 5B).

Representative SEM images of the sinus mucosa are shown in Fig. 9.6 and the images demonstrate that the biofilms were well established on the mucosa of the sinuses. Similarly to the *in vitro* results, both treatments (Tob only vs. DC+Tob) affected the

morphology of PAO1 cells, resulting in round-shaped cells. Many of the PAO1 cells on the specimen treated with DC and Tob were lyzed and misshaped. Treatment of Tob only was not sufficient to eradicate PAO1 cells. In comparison, mucosa tissues free of PAO1 cells were observable after treatment with 1mA DC and 15 μg/mL Tob. These observations are consistent with CFUs data proving that the combination of DC and Tob was more effective in killing the PAO1 cells. Moreover, Fig. 9.6B showed intact cilia on DC+Tob treated samples, suggesting that DC treatment does not damage cilia.

9.4.4. Safety of the electrochemical treatments.

To further evaluate the safety of the DC treatment, specimen were collected from the sinus mucosa and prepared for H&E staining to perform histological analysis. The results of this analysis show that bacterial infection alone could cause damage to the structure of sinus mucosa. As shown in Fig. 9.7A, the infection resulted in the loss of the cilia and the presence of purulence within the tissues. Major ulcerations were found on the mucosa of the PAO1-infected rabbit. These observations were also recorded in the sinus treated with 15 μg/mL Tob only (Fig. 9.7B). The layer of cilia was detached from the rest of the tissue, suggesting that the infections resulted in the loss of the cilia. Tissues underlying the ciliated-epithelial cells were lyzed and presented various vacuoles, which might correlate with the present of purulence materials within the tissues. The specimens collected from the DC-Tob treated sinus were not different from the untreated sample. Fig. 9.7C showed the presence of purulence and no further deformation in the structure of the mucosal tissues.

9.5. DISCUSSION

The medical application of electricity has long been utilized in surgery. For instance, the utilization of the bovie electrocautery is nearly ubiquitous in head and neck surgical procedures. This instrument, which generates high level electrical currents, is able to cut tissues and coagulate blood, while leaving surrounding tissue unharmed. However, the use of electrical current has had little application in the field of infection control. Interestingly, preliminary results show that low-level DC could be effective against bacterial cells in clinical settings.

The *in vivo* study described in this chapter focuses on the ability of low-level DC to eliminate bacterial infection in a rabbit model of sinusitis. Co-current treatment methods of sinusitis using multiple antibiotics are unsatisfactory. In addition to being time consuming and disruptive to the patients daily schedule, the treatments could be irritating to the sensitive nasal mucosa. Chronic use of antibiotics could also contribute to drug-resistance. Henceforth, developing novel approaches that can readily and more effectively eradicate the sinusitis would benefit numerous patients around the world.

Through experimental setups, it was determined that DC was best delivered with the counter electrode (cathode in our case) implanted within the animal tissues, preferably at the site of infection. In order the bypass the impedance of the skin, the working electrode was inserted between the skin and the skull, while the cathode was introduced in the sinus in the presence of a saline solution. As shown by the potentiodynamic curve recorded from the DC treatments of the sinuses, effective level of

DC treatment could be applied to the sinuses and result in significant killing of bacterial cells suspended in the purulence material, as well as those associated with the sinus mucosa. Compared to the treatment with Tob only, more PAO1 cells were eliminated in the combined treatment, suggesting a synergy can be obtained *in vivo* as well. The finding that cell killing was observed around the cathodic electrode is consistent with our previous finding reported in Chapters 3 and 5. The cathodic current/potential was very effective in killing biofilm associated with the counter electrodes[14]. The use of a 2-chamber system connected with a high resistance salt-bridge demonstrated that the high concentration of reactive oxygen species, as well as the cathodic potential, might contribute to the potency of the cathode.

Overall, our data show that the treatment with Tob alone can reduce the number of viable PAO1 cells associated with the pus by 88.3% but it fails to inhibit the growth of the biofilm cells, which represented 143.6%, compared to the original population of cells. A previous study using a rabbit model of PAO1 biofilm infection has shown that Tob at concentrations of 80 μg/mL and 160 μg/mL can kill biofilm-associated *P. aeruginosa* cells by 2 and 2.5 log after a day of antibiotic treatment[17]. However, our results demonstrate that low-level DC delivered for 1 h with 15 μg/mL is more effective in killing *P. aeruginosa* cells. The cidal effects of DC and Tob were of 3 logs for the cells in the purulence and 60.3% for those associated with the mucosal biofilms, suggesting that the use of DC could lead to a decreased reliance on high doses of antibiotics.

In addition to CFU data, SEM imaging of the specimen revealed critical information about the bioactivity of the electrochemical treatments. Treatments of the sinuses with Tob or DC+Tob resulted in morphological changes to the PAO1 cells. The findings that *P. aeruginosa* cells ball up under physicochemical stress is consistent with previous reports. For example, morphological change of *P. aeruginosa* from a rod-shape to a round shape specifically has been reported by Yokochi *et al.*[18] regarding antibiotic treatment with imipenem (a β-lactam) and ceftazidime (a cephalosporin). Under our condition, the cells become round in shape due to the treatment with 15μg/mL Tob and/or 1 mA total DC.

Sanin *et al*. [19] showed that starvation could cause cells of *Pseudomonas sp*. to become round-shape. This report corroborates our finding that many of the round shape cells observed in the electron micrographs were under stress of Tob and DC treatments. On the other hand, the combined treatment resulted in the disruption of the cell membrane and lysis of PAO1 cells. The finding that the electrochemical stresses further disrupted the integrity of the *P. aeruginosa* PAO1 is consistent with our findings reported in Chapter 4.

It was interesting to find that the combined treatment using DC and Tob resulted in the removal of PAO1 cells from the sinus mucosa. Intriguingly, the DC treatment did not exhibit significant detrimental effects on the rabbits. All the animals tested with the DC survived the treatment and did not show any symptom of discomfort following the treatment (Fig. 9.1F). By successfully limiting the infection only to the mucosal tissues,

all animals behaved rather normally throughout the entire trial. These observations demonstrate that the DC treatments used in this study are safe and effective in killing PAO1 *in vivo*. Further tests with more animals will help design clinical studies.

9.6. CONCLUSIONS

In this study, a rabbit model of sinusitis was developed using *P. aeruginosa.* The electrochemical treatment of PAO1 infection using 1mA of total DC and 15 μg/mL Tob demonstrated that DC improved the bioactivity of Tob against *P. aeruginosa in vivo*. The effects of the cathodic potential/current and its related electrochemical products were effective in killing *P. aeruginosa* cells. Overall, these results demonstrated that this technology has a good potential for controlling chronic infections.

9.7. ACKNOWLEDGEMENTS

The authors are grateful to Blue Highway Inc. for supporting the project. We also thank Dr. Thomas K. Wood at Penn State University for sharing the strain of *P. aeruginosa* PAO1. We are grateful to Dr. Jing An (SUNY-Upstate Medical University) for providing the mice used in the preliminary experiments. We are thankful to Jennifer Kiefer (SUNY-Upstate Medical University) and Dr. Robert P. Smith (SUNY-ESF) for helping with rabbit experiment and the SEM imaging, respectively. We would also like to thank Dr. Goyal Parul and Dr. Greg Haveman for performing the rabbit surgeries.

9.8. REFERENCES

1 **Altieri, C., Speranza, B., Del Nobile, M. A. & Sinigaglia, M.** Suitability of bifidobacteria and thymol as biopreservatives in extending the shelf life of fresh packed plaice fillets. *Journal of applied microbiology* **99**, 1294-1302, doi:10.1111/j.1365-2672.2005.02740.x (2005).

2 **Palma, M., DeLuca, D., Worgall, S. & Quadri, L. E.** Transcriptome analysis of the response of *Pseudomonas aeruginosa* to hydrogen peroxide. *Journal of bacteriology* **186**, 248-252 (2004).

3 **Keyer, K. & Imlay, J. A.** Superoxide accelerates DNA damage by elevating free-iron levels. *Proceedings of the National Academy of Sciences* **93**, 13635-13640 (1996).

4 **Lewis, K.** Riddle of biofilm resistance. *Antimicrobial agents and chemotherapy* **45**, 999-1007 (2001).

5 **Li, G. & Young, K. D.** Isolation and identification of new inner membrane-associated proteins that localize to cell poles in *Escherichia coli*. *Molecular microbiology* **84**, 276-295 (2012).

6 **Keyer, K., Gort, A. S. & Imlay, J. A.** Superoxide and the production of oxidative DNA damage. *Journal of bacteriology* **177**, 6782-6790 (1995).

7 **Birbir, Y., Molla, S. & Birbir, M.** Applying electric current to inactivate gram-negative bacteria isolated from salt-packed-cured hides. *Journal of the Society of Leather Technologies and Chemists* **97**, 5-10 (2013).

8 **Shapiro, L. & Losick, R.** Protein localization and cell fate in bacteria. *Science* **276**, 712-718 (1997).

9 **Kasimanickam, R. K., Ranjan, A., Asokan, G. V., Kasimanickam, V. R. & Kastelic, J. P.** Prevention and treatment of biofilms by hybrid- and nanotechnologies. *International journal of nanomedicine* **8**, 2809-2819 (2013).

10 **Francolini, I. & Donelli, G.** Prevention and control of biofilm-based medical-device-related infections. *FEMS immunology and medical microbiology* **59**, 227-238, doi:10.1111/j.1574-695X.2010.00665.x (2010).

11 **Chang, W., Small, D. A., Toghrol, F. & Bentley, W. E.** Microarray analysis of *Pseudomonas aeruginosa* reveals induction of pyocin genes in response to hydrogen peroxide. *BMC genomics* **6**, 115 (2005).

12 **Van Der Borden, A. J., Van Der Mei, H. C. & Busscher, H. J.** Electric block current induced detachment from surgical stainless steel and decreased viability of *Staphylococcus epidermidis*. *Biomaterials* **26**, 6731-6735 (2005).

13 **Van Der Borden, A. J., Van Der Mei, H. C. & Busscher, H. J.** Electric-Current-Induced Detachment of *Staphylococcus Epidermidis* Strains from Surgical Stainless Steel. *Journal of Biomedical Materials Research - Part B Applied Biomaterials* **68**, 160-164 (2004).

14 **Niepa, T. H., Gilbert, J. L. & Ren, D.** Controlling *Pseudomonas aeruginosa* persister cells by weak electrochemical currents and synergistic effects with tobramycin. *Biomaterials* **33**, 7356-7365, doi:10.1016/j.biomaterials.2012.06.092 (2012).

15 **Sambrook, J. & Russell, D. W.** *Molecular cloning: a laboratory manual*. Vol. 3 (Cold spring harbor laboratory press, 2001).

16 **Antunes, M. B., Feldman, M. D., Cohen, N. A. & Chiu, A. G.** Dose-dependent effects of topical tobramycin in an animal model of Pseudomonas sinusitis. *American journal of rhinology* **21**, 423-427 (2007).

17 **Chiu, A. G., Antunes, M. B., Palmer, J. N. & Cohen, N. A.** Evaluation of the in vivo efficacy of topical tobramycin against Pseudomonas sinonasal biofilms. *Journal of antimicrobial chemotherapy* **59**, 1130-1134 (2007).

18 **Yokochi, T., Narita, K., Morikawa, A., Takahashi, K., Kato, Y., Sugiyama, T., Koide, N., Kawai, M., Fukada, M., Yoshida, T.** Morphological Change in *Pseudomonas aeruginosa* following Antibiotic Treatment of Experimental Infection in Mice and Its Relation to Susceptibility to Phagocytosis and to Release of Endotoxin. *Antimicrobial agents and chemotherapy* **44**, 205-206 (2000).

19 **Sanin, S. L., Sanin, F. D. & Bryers, J. D.** Effect of starvation on the adhesive properties of xenobiotic degrading bacteria. *Process Biochemistry* **38**, 909-914 (2003).

FIGURE CAPTIONS

Figure 9.1. Potentiodynamic curves and related impedance from the DC treatment of mice. (A) Anode is placed over the skin and the counter and reference electrodes are under the skin. (B) Counter electrode is over the skin and reference and anodes are placed under the skin. (C) Condition (B) is repeated with the skin of the mouse shaved. (D) DC treatment of mouse snout under the condition presented in (C).

Figure 9.2. Experimental design and electrochemical of rabbit model of sinusitis.

Figure 9.3. Potentiodynamic curve recorded from the electrochemical treatment of the rabbit model of sinusitis.

Figure 9.4. Effects of DC on PAO1 cells in a rabbit model of sinusitis. The number of viable cells was quantified by CFU after the treatment of the infection model with 15μg/mL Tob only or with 1 mA of total DC in the presence of 15μg/mL Tob. The means and standard deviations are shown.

Figure 9.5. Representative SEM images of PAO1 biofilm. *P. aeruginosa* PAO1 cells were culture on a well-insert. The untreated cells (A) maintained their rod-like shape while the cells treated with 140 $\mu A/cm^2$ DC equivalent to 1 mA of total DC for 1 h (B) became round-shape.

Figure 9.6. Effects of DC on PAO1 biofilms associated to the sinus mucosa after treatment with (A) 15μg/mL Tob only or (B) with 1 mA of total DC in the presence of 15μg/mL Tob. Representative SEM image of PAO1 biofilm on the specimen are shown.

Figure 9.7. Effects of DC on the sinus mucosa. The specimen were collected and H &E staining was performed to evaluate the histology of the untreated but infected sinus (A) and compared to the specimen treated with 15μg/mL Tob (B) or with 1 mA of total DC in the presence of with 15μg/mL Tob only.

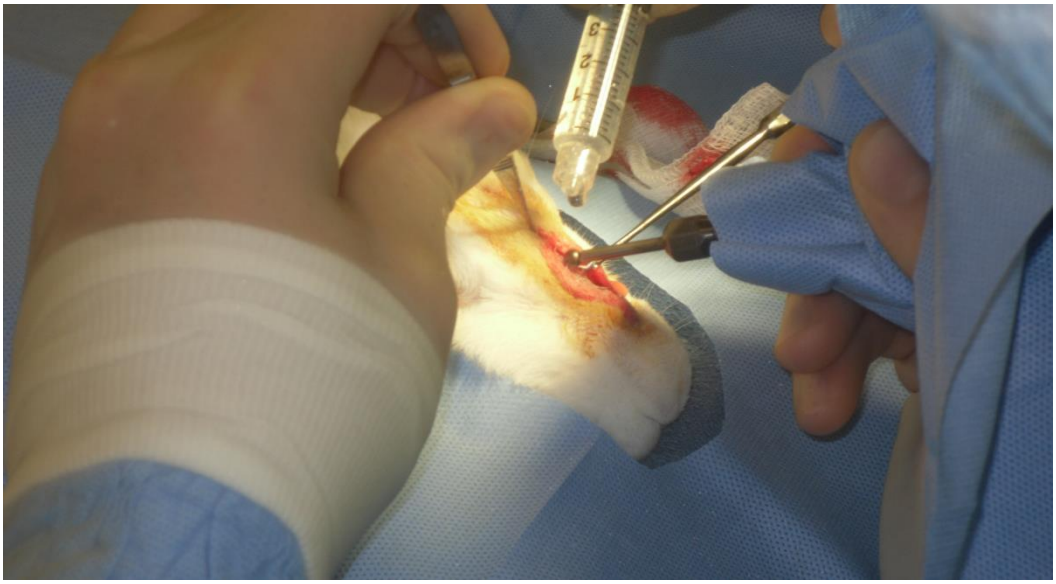

(A)

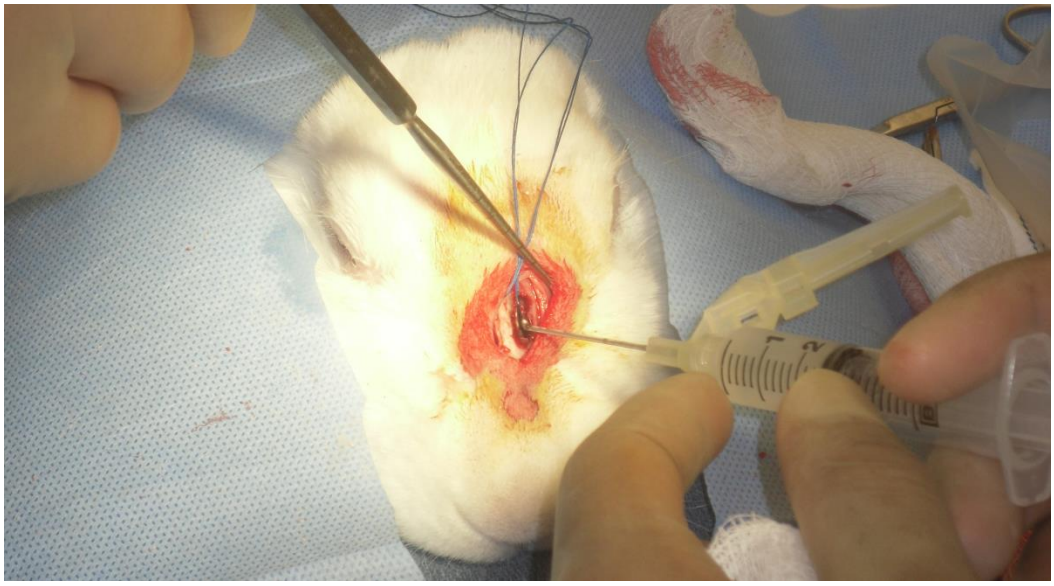

(B)

(C)

(D)

(E)

(F)

Figure 9.1

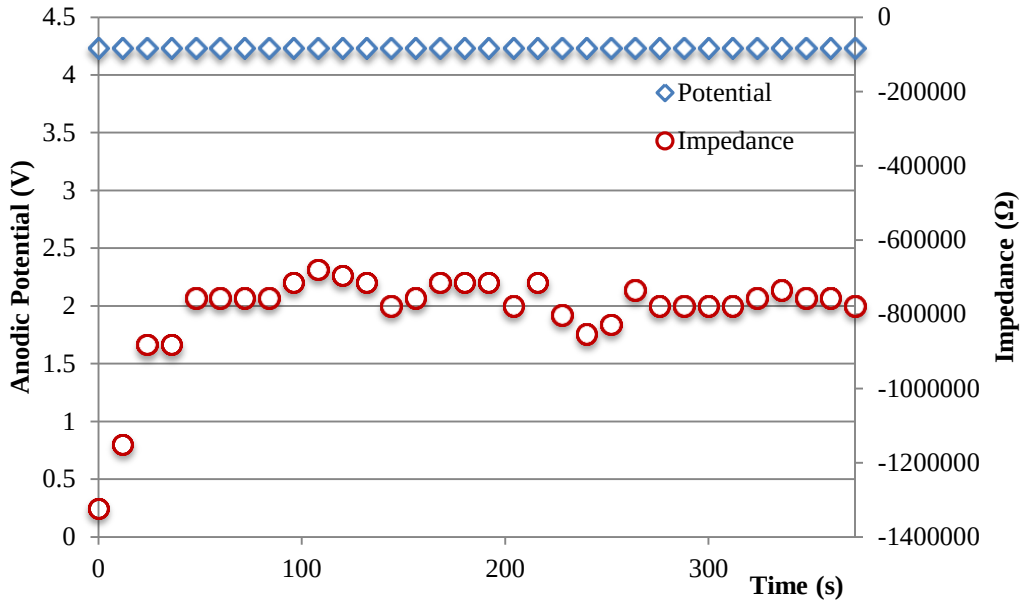
4.5
4
3.5
3
2.5
2
1.5
1
0.5
0
0
-200000
-400000
-600000
-800000
-1000000
-1200000
-1400000
Potential
Impedance
Anodic Potential (V)
Impedance (Ω)
0
100
200
300
Time (s)

(A)

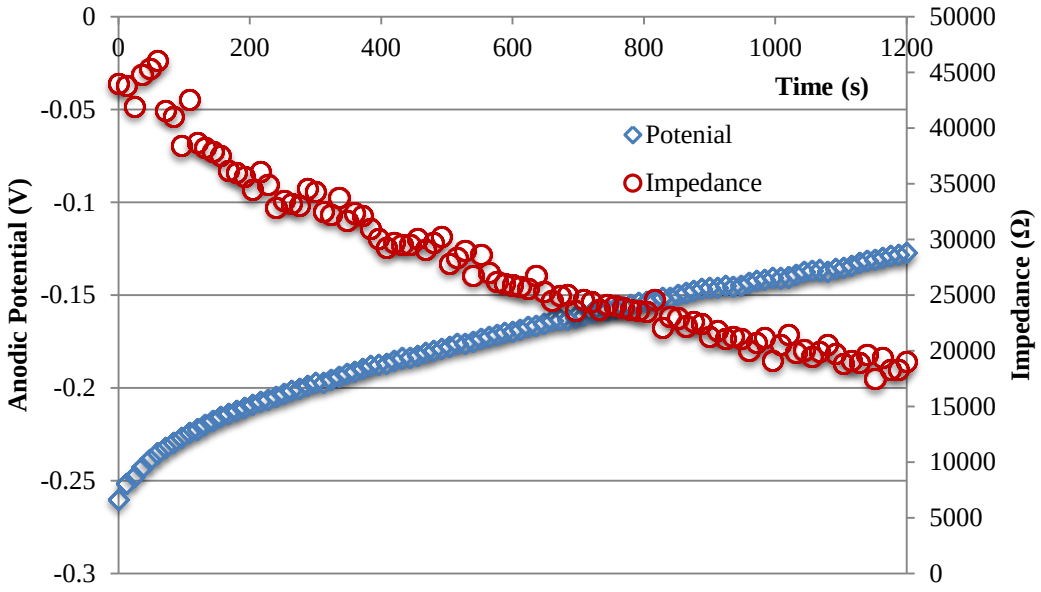
0
-0.05
-0.1
-0.15
-0.2
-0.25
-0.3
0
200
400
600
800
1000
1200
50000
45000
40000
35000
30000
25000
20000
15000
10000
5000
0
Time (s)
Potenial
Impedance
Anodic Potential (V)
Impedance (Ω)

(B)

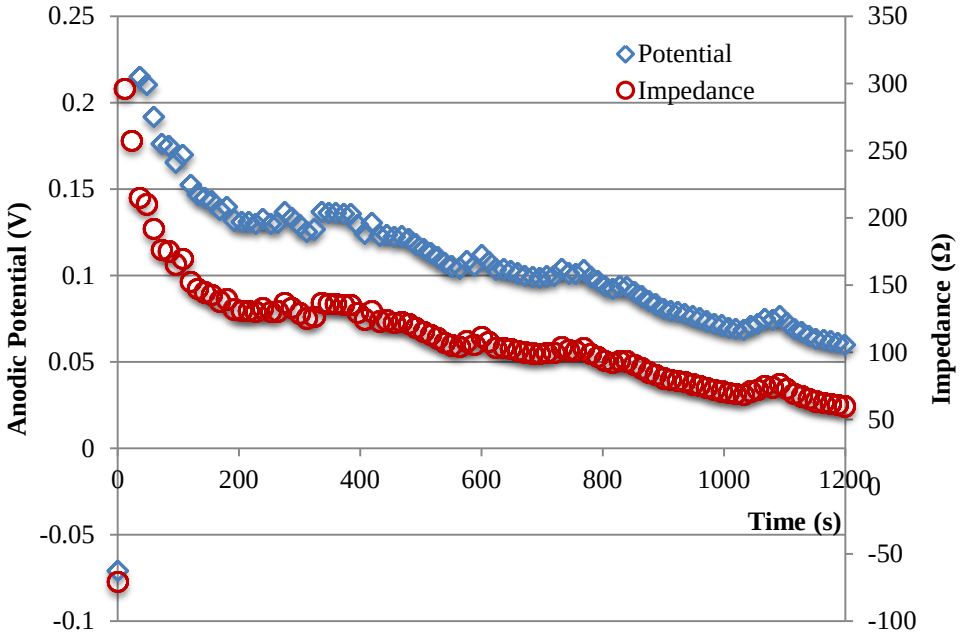
Potential
Impedance
Anodic Potential (V)
Impedance (Ω)
Time (s)
0.25
0.2
0.15
0.1
0.05
0
-0.05
-0.1
350
300
250
200
150
100
50
0
-50
-100
0
200
400
600
800
1000
1200

(C)

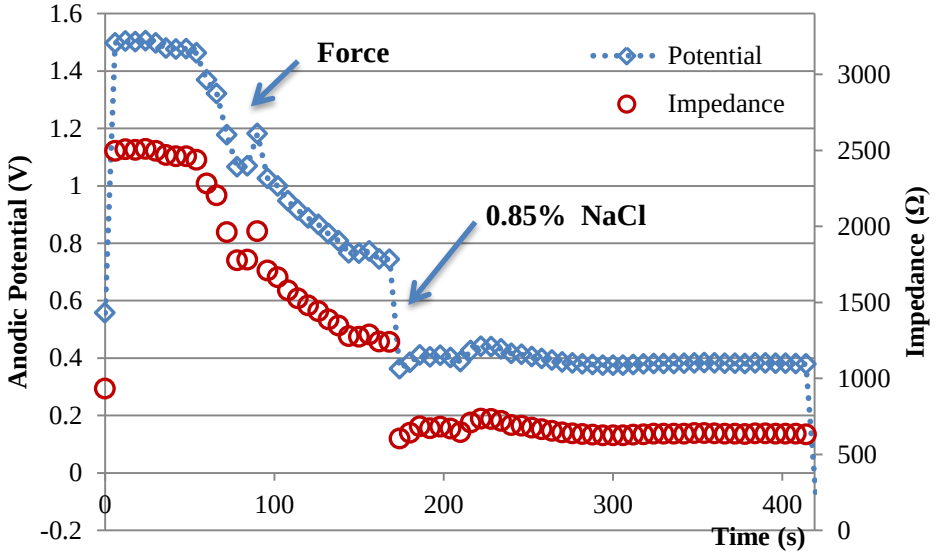
Force
0.85% NaCl
Potential
Impedance
Anodic Potential (V)
Impedance (Ω)
Time (s)
1.6
1.4
1.2
1
0.8
0.6
0.4
0.2
0
-0.2
3000
2500
2000
1500
1000
500
0
0
100
200
300
400

(D)

Figure 9.2

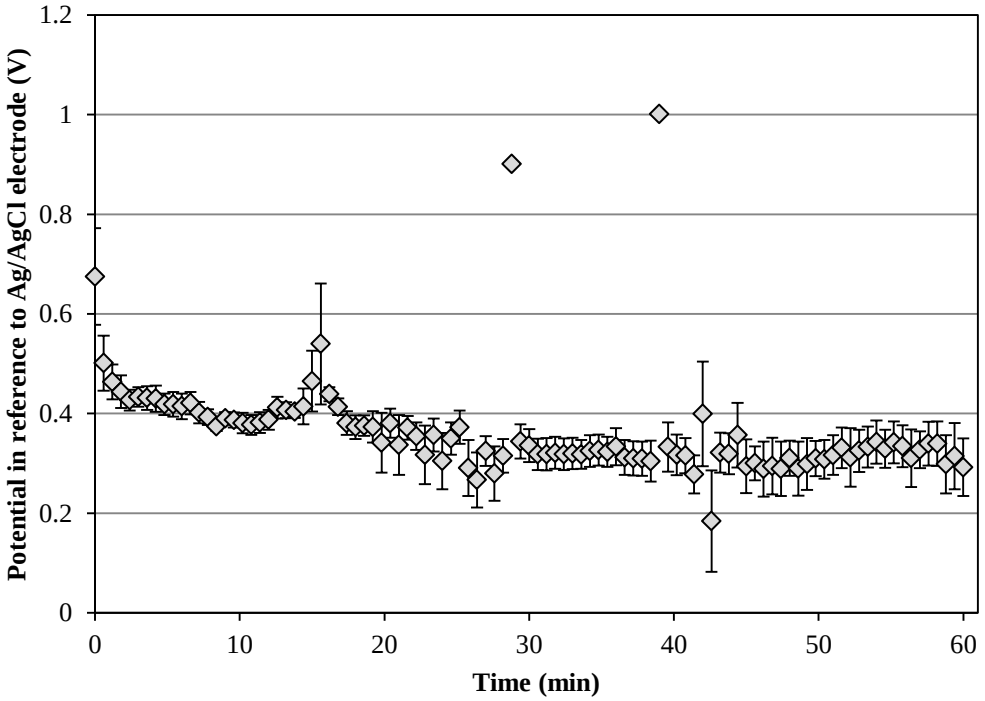
Potential in reference to Ag/AgCl electrode (V)
1.2
1
0.8
0.6
0.4
0.2
0
0
10
20
30
40
50
60
Time (min)

Figure 9.3

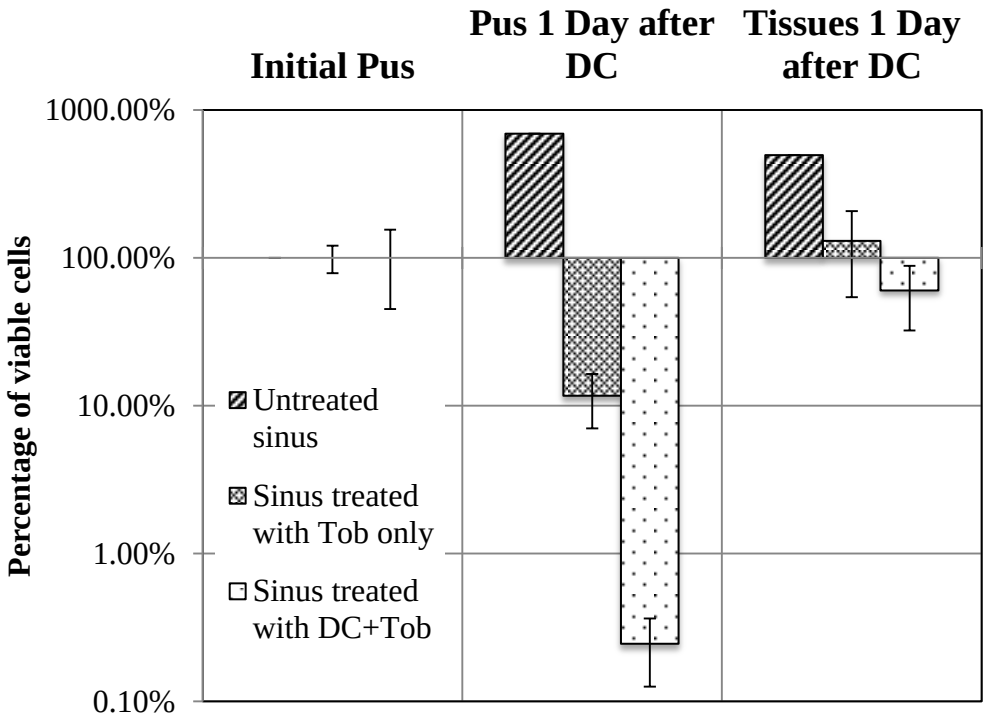
Initial Pus
Pus 1 Day after DC
Tissues 1 Day after DC
1000.00%
100.00%
10.00%
1.00%
0.10%
Percentage of viable cells
Untreated sinus
Sinus treated with Tob only
Sinus treated with DC+Tob

Figure 9.4

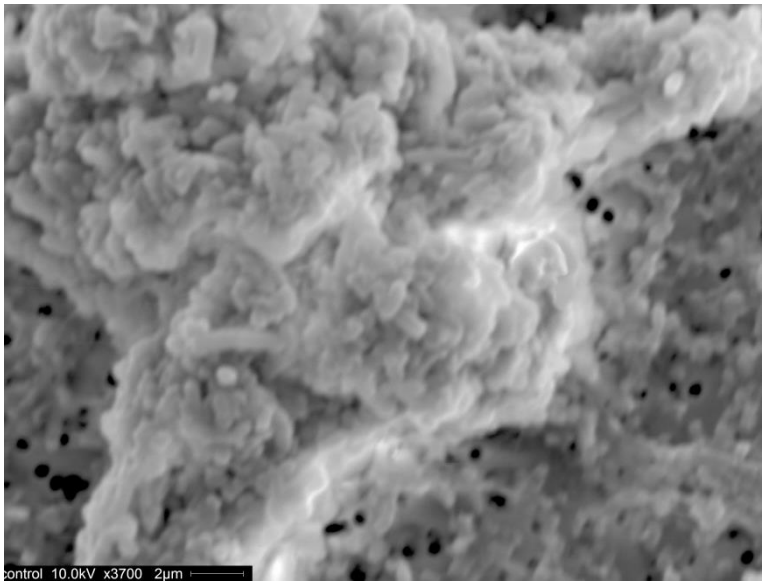

(A)

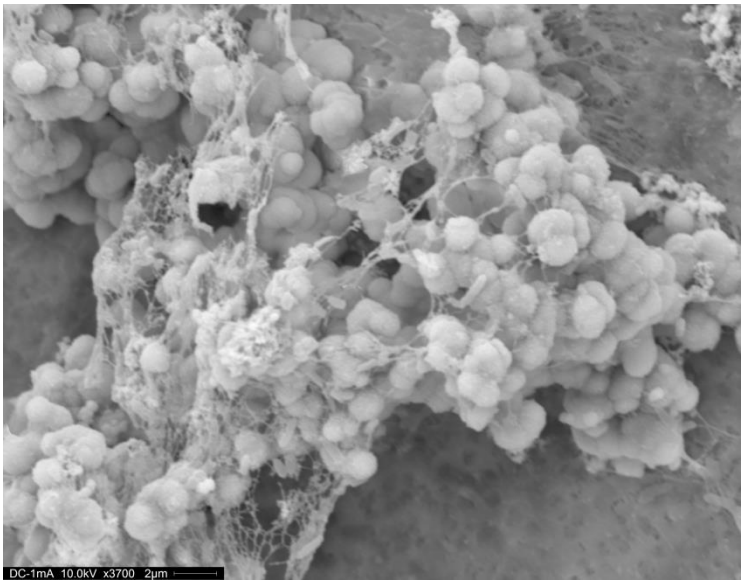

(B)

Figure 9.5

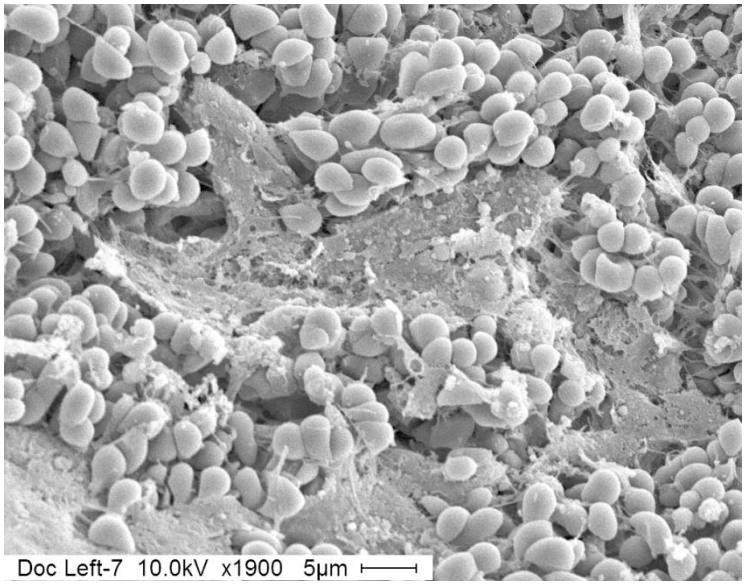
Doc Left-7 10.0kV x1900 5µm

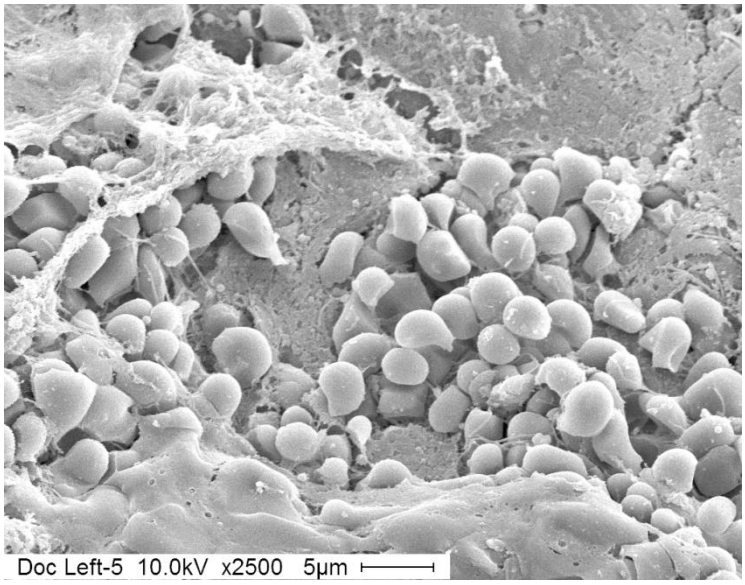
Doc Left-5 10.0kV x2500 5µm

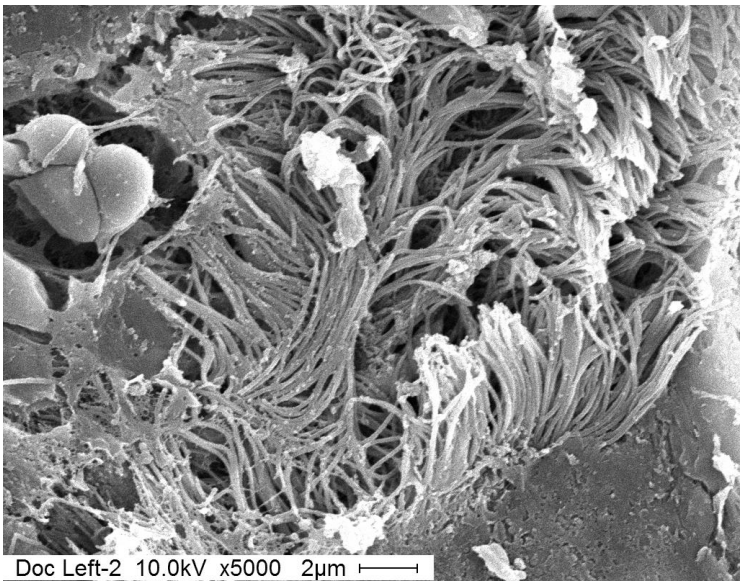

(A)

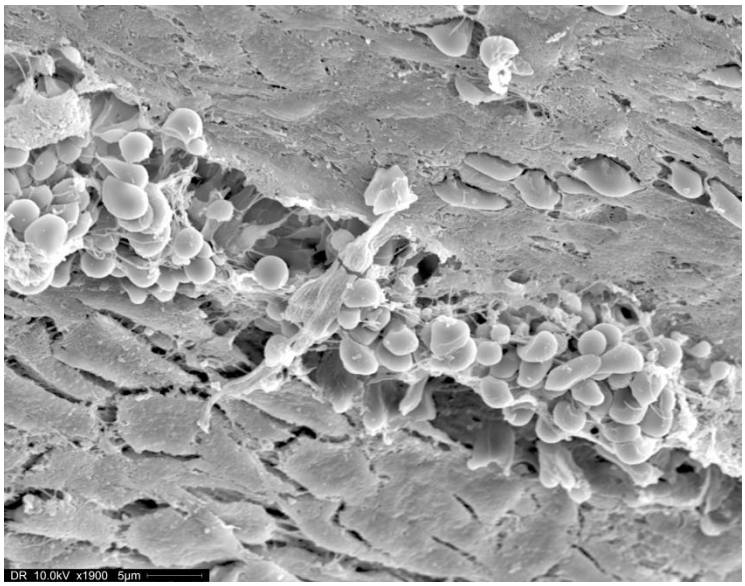

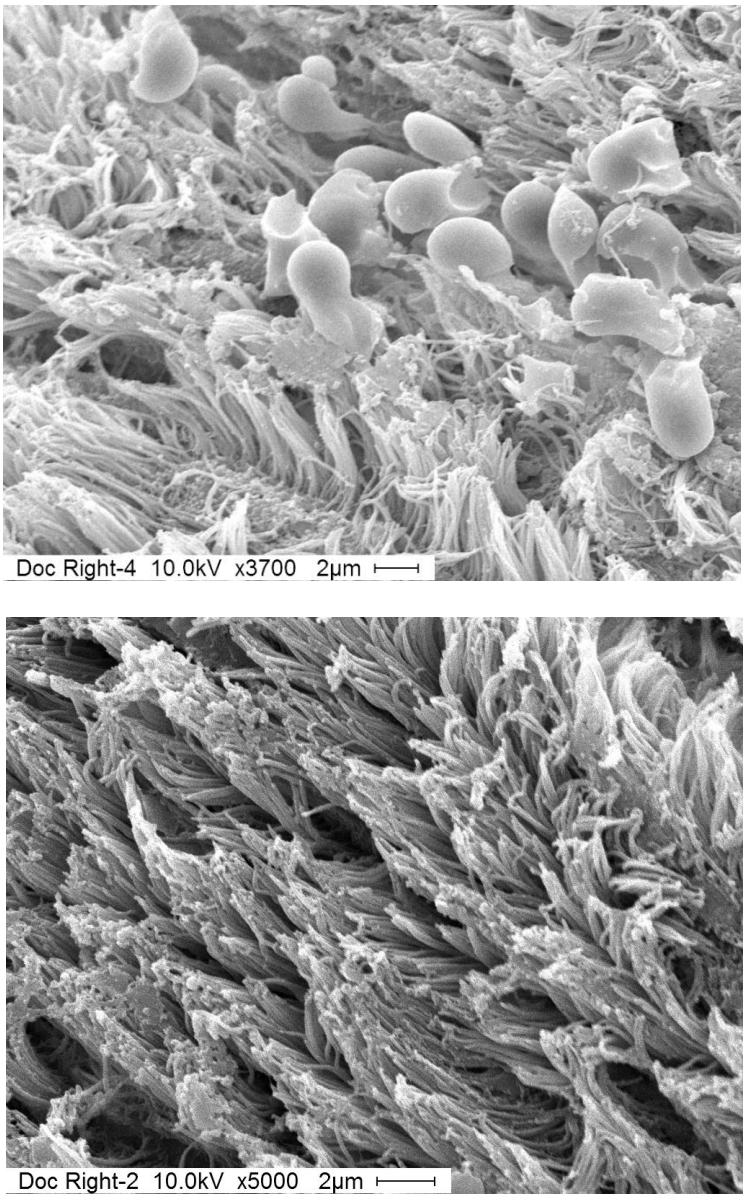

(B)

Figure 9.6

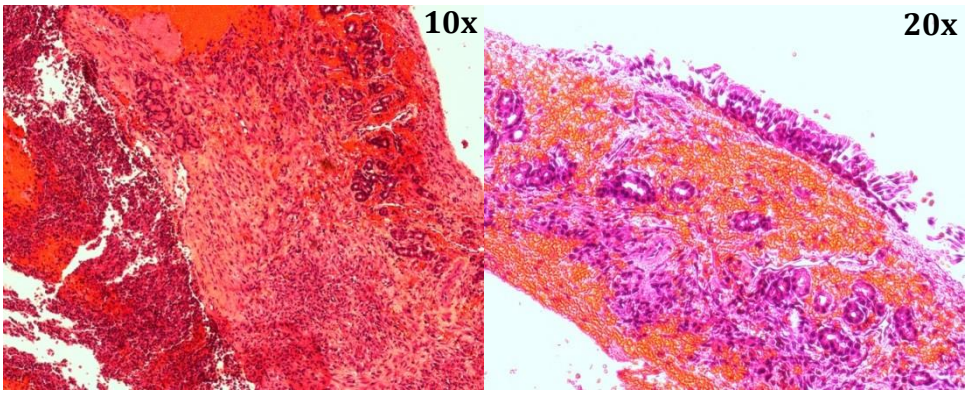

(A)

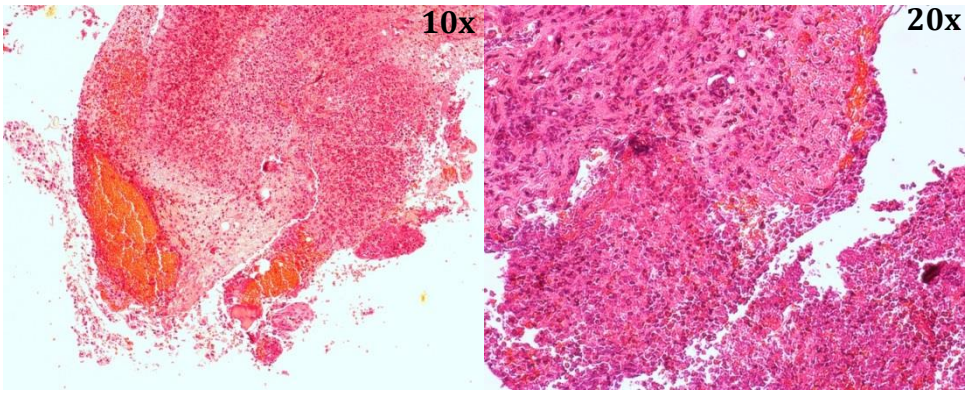

(B)

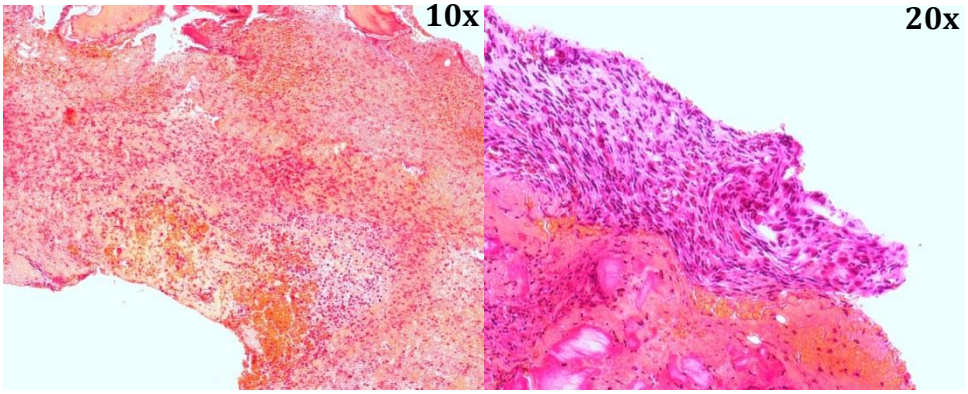

(C)

Figure 9.7

CHAPTER 10

CONCLUSIONS AND RECOMMENDATION FOR FUTURE WORKS

10. 1. CONCLUSIONS

Motivated by the urgent need to control drug resistant infections and previous studies on bioelectric effects, we conducted this thesis research to systematically investigate persister control using low-level electric currents. *P. aeruginosa* was used as a model organism to test the effects of DC in the presence and absence of antibiotics. Our results revealed for the first time that *P. aeruginosa* persister cells can be effectively killed through synergistic effects between DC and antibiotics. For examples treatment using 70 $\mu A/cm^2$ DC using 304 electrodes resulted in 98% killing of the persister cells. However, 5 logs killing were achieved in the presence of 1.5 μg/mL Tob. We named this phenomenon electrochemical control of persister cells (ECCP)

To understand the mechanism of ECCP, we characterized the current level and the generated species in the persister killing. Different effects were observed among the ions studied and the movement of the ions was found to be important. Consistently, the electrode materials used to mediate DC we also found to play an important role . Comparison of carbon-mediated DC with SS-mediated DC revealed that cell death was achieved more quickly with SS-mediated DC. At the same current density synergistic killing effect with Tob was only observed with SS-mediated DC. However, highly potent killing was achieved with sequential treatment using carbon-mediated DC followed by Tob . Further study of ECCP has demonstrated that the treatment could be improved with the choice of the electrode materials. The testing of TGON, a carbon based materials has proven that the persister could be eradicated with 70 $\mu A/cm^2$ DC after 1 h of treatment.

The study of these effects at the cellular level demonstrated that cells lysis occur under DC treatment using SS 304. In comparison, the cells appeared to be intact but with high permeability after DC treatment using carbon electrodes. The measurement of the cells membrane stiffness revealed that carbon treated cells were stiffer compared to SS-treated cells. This finding might explain why the sequential treatment was effective. The treatment using carbon and SS 304 electrodes also cause major differences in the intracellular content of the treated cells. While SS-treated cells released proteins from cell lysis, cells treated with carbon electrodes appeared to have large protein aggregates. Differences in the persister response to DC treatments were also observed at the genetic level; e.g. induction of pyocin genes was observed for cells treated with carbon and SOS response was induced in cells treated with SS 304 electrodes. The following table summarizes the major differences (Table 1).

The fact that the carbon-based electrode did not show any synergistic killing effects led us to investigate the interaction between antibiotic and the DC generated electrochemical species. Specifically, the interaction between metal cations (Cr^{2+}, Cr^{3+}, Cr^{6+}, Fe^{2+}, Fe^{3+}, Mn^{2+}, Ni^{2+}) and antibiotics (Tob and Kan) was investigated. It was found that DC contributes to interaction between Tob and Cr(III) ions, which may play a role in persister control.

Table 10.1: Comparison of persister killing using DC mediated with carbon and SS 304 electrodes

	Electrode materials	
	carbon	***SS 304***
DC condition	70 μA/cm^2 DC, voltage from 0-800mV	70 μA/cm^2 DC, voltage from 0-200mV
Persister killing effects	Synergy in sequential treatment (DC and 1.5 μg/mL Tob) followed by 7-log killing	Synergy in co-treatment with DC and 1.5 μg/mL Tob resulting in 5-log killing
Cellular configuration	No significant accumulation of carbon particles, but compartmentalization of intracellular materials with protein aggregates	Intracellular accumulation of metal cations
Membrane properties	Cells are intact but stiffer and more permeable	Cell lysis observed
	No change in surface charge	Decreased surface charge
Gene expression	Induction of genes related to pyocin and antibiotic resistance	More genes related to transport of small molecules, metabolism, protein secretion /export were affected
	Repression of genes related to SOS response	

Furthermore, the efficacy of the ECCP was studied in co-culture model involving human epithelial cells and P. aeruginosa PAO1. The treatment of such co-cultures demonstrated that *P. aeruginosa* cells could be selectively eliminated through ECCP in the presence of the human cells at appropriate conditions. Finally, these findings were integrated to design an in vivo study in a rabbit model of sinusitis. The results of the animal study demonstrated that, compared to the treatment with Tob only, DC treatment in the presence of 15 μg/mL Tob was more effective in killing PAO1 cells associated to

the sinus mucosa, as well as the cells contained in the purulence materials. Moreover, the treatment was also safe for the animal.

Overall, this study demonstrate that DC treatment has a great potential for developing novel strategies to control bacterial infections associated with biofilms and persister cells. However, more need to be done to optimize the effectiveness of such treatments for real application.

10.2. RECOMMENDATION FOR FUTURE WORK

10.2.1. Genetic basis of persisters' response to electrochemical stress

The study on DC treatment of mutant cells showed that several genes may be important to both persister formation and persister control through ECCP. In Chapter 6, we demonstrated that the mutant of PA1897 has defect in persister formation. Compared to PAO1, which has 1% of persisters in stationary-phase cultures, the number of persister cells in the mutant of PA1897 represented only 0.01% of the total cell population. Also, this mutant exhibited an increased sensitivity to DC treatment mediated with carbon electrodes. It will be important to test the effects on a strain with genetic complementation of this mutation. It will also be helpful to conduct DNA microarrays to understand the genes expression of this mutant to DC treatments.

10.2.2. Interaction between metal cations and Tobramycin

In Chapters 3 and 7, we demonstrated the interactions between Cr^{3+} and Tob could result in both agonistic and antagonistic effects. This led us to speculate that the intracellular

accumulation of such complexes could lead to cell death, through increased interaction with DNA or RNA. This hypothesis could be tested by studying the binding affinity between the Cr^{III}(Tob) complexes and 16 S rRNA. Wang *et al.*[1], studied the interaction 16S rRNA and aminoglycosides including Kan, Tob and their conjugates. Using a similar approach, the interaction between the CrIII(Tob) complexes could be studied to understand if the complex indeed kills persister cells more efficiently.

10.2.3. Design of a prototype for treatment infections in vivo

Our findings reported in Chapter 4 demonstrated that SS 304 is effective in killing persister cells in the 2-chamber system. Because of the resistance of the salt bridge, the results from this 2-chamber system provided existing information that DC treatment may be effective to cross the skin and kill bacteria in vivo, including those attached to implanted devices. Further study can help designing a prototype to treat infection with minimum invasion to ensure safety and efficacy.

10.3. REFERENCE

1 **Wang, H. & Tor, Y.** Electrostatic interactions in RNA aminoglycosides binding. *Journal of the American Chemical Society* **119**, 8734-8735 (1997).

APPENDICES

APPENDIX I

Supplementary Information

For

CHAPTER 3

CONTROLLING *PSEUDOMONAS AERUGINOSA* PERSISTER CELLS BY WEAK ELECTROCHEMICAL CURRENTS AND SYNERGISTIC EFFECTS WITH TOBRAMYCIN

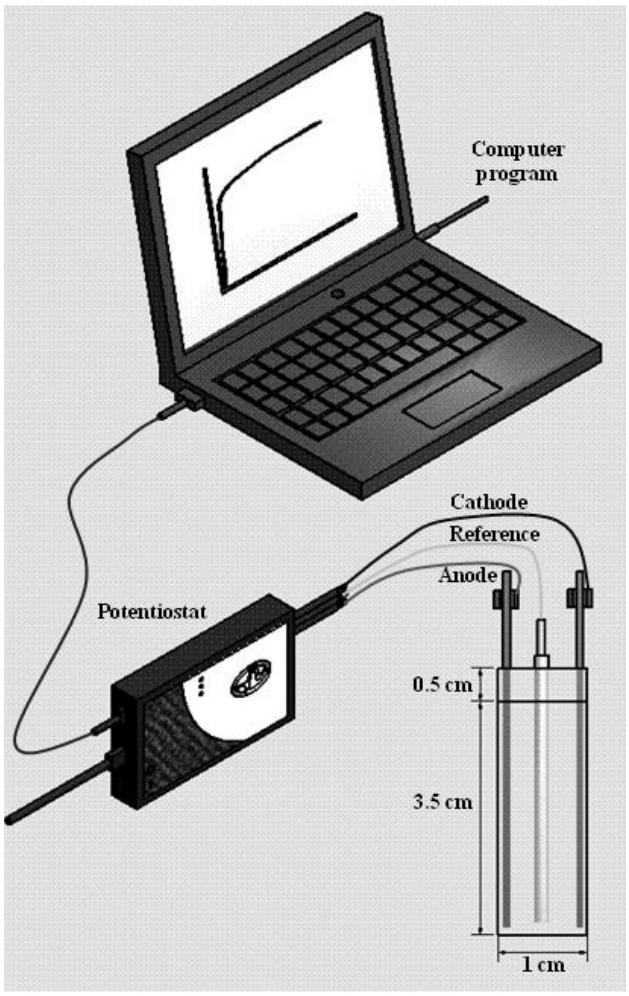

Figure S3.1. Schematic representation of the electrochemical cell system for generating electrochemical current. The electrochemical cell was constructed by inserting two electrodes (4.5 cm x 0.95 cm x 0.05 cm) in a plastic cuvette. The working, counter and reference electrodes were connected to a potentiostat to obtain the desired current.

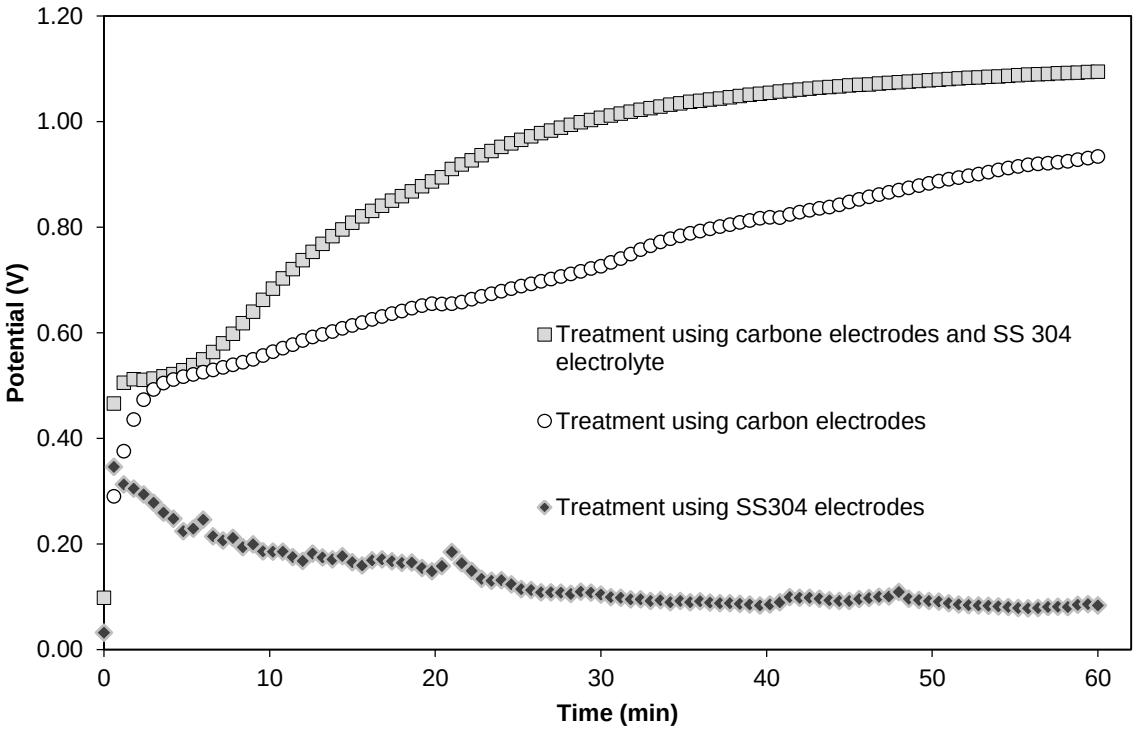

Figure S3.2: Potentiodynamic curves during 70 µA/cm^2 DC treatments of 0.85% NaCl solution.

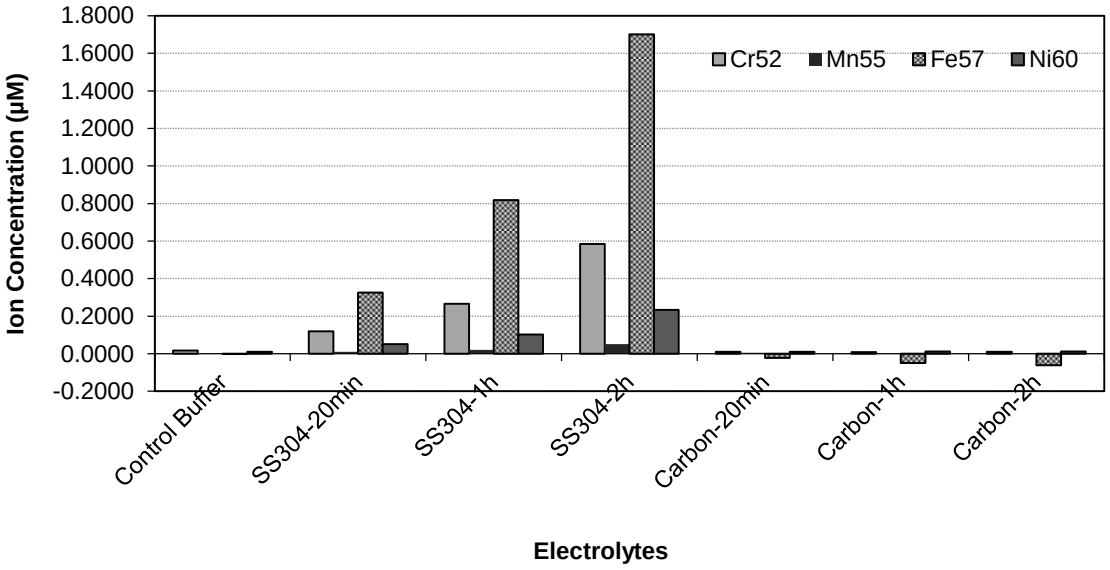

Figure S3.3: ICP-MS analysis of the ions generated during treatments with 70 µA/cm^2 DC using Carbon and SS 304 electrodes.

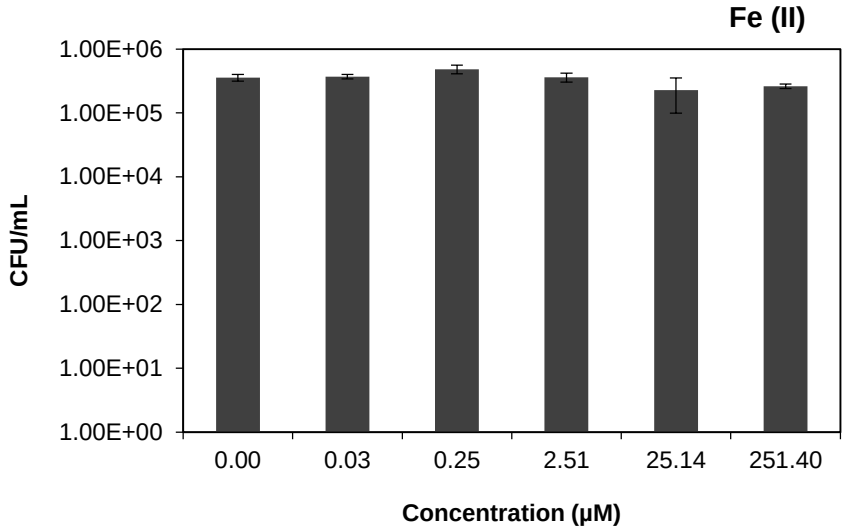
Fe (II)
1.00E+06
1.00E+05
1.00E+04
1.00E+03
1.00E+02
1.00E+01
1.00E+00
CFU/mL
0.00
0.03
0.25
2.51
25.14
251.40
Concentration (µM)

(A)

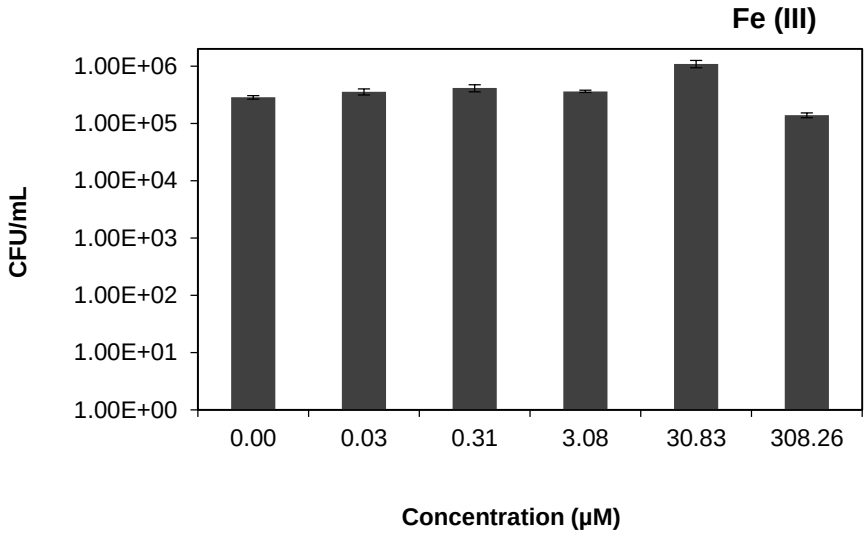
Fe (III)
1.00E+06
1.00E+05
1.00E+04
1.00E+03
1.00E+02
1.00E+01
1.00E+00
CFU/mL
0.00
0.03
0.31
3.08
30.83
308.26
Concentration (µM)

(B)

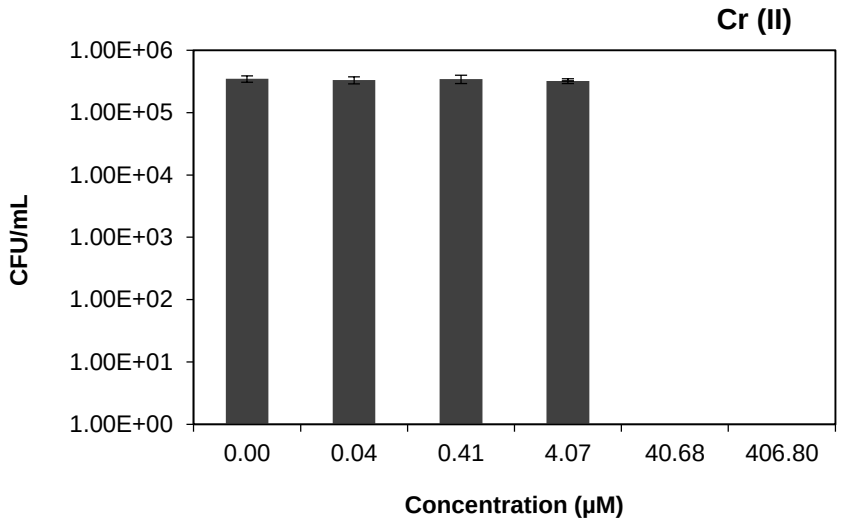
Cr (II)
1.00E+06
1.00E+05
1.00E+04
1.00E+03
1.00E+02
1.00E+01
1.00E+00
CFU/mL
0.00
0.04
0.41
4.07
40.68
406.80
Concentration (µM)

(C)

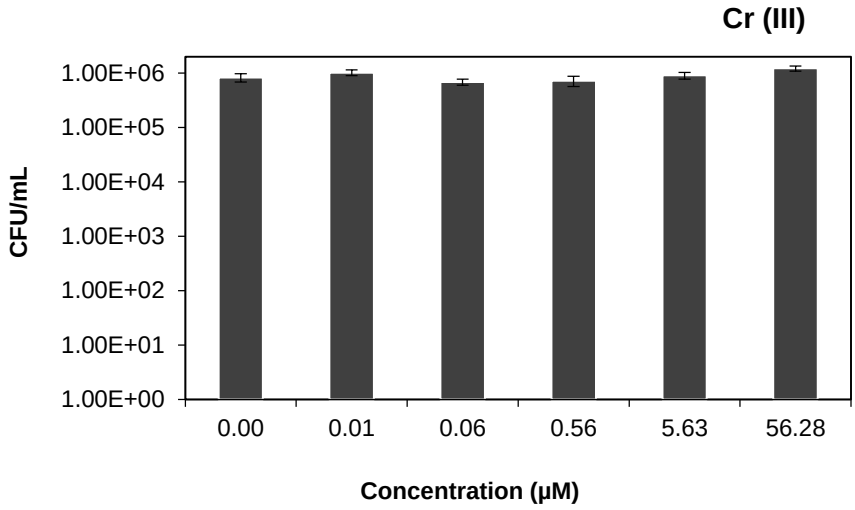
Cr (III)
1.00E+06
1.00E+05
1.00E+04
1.00E+03
1.00E+02
1.00E+01
1.00E+00
CFU/mL
0.00
0.01
0.06
0.56
5.63
56.28
Concentration (µM)

(D)

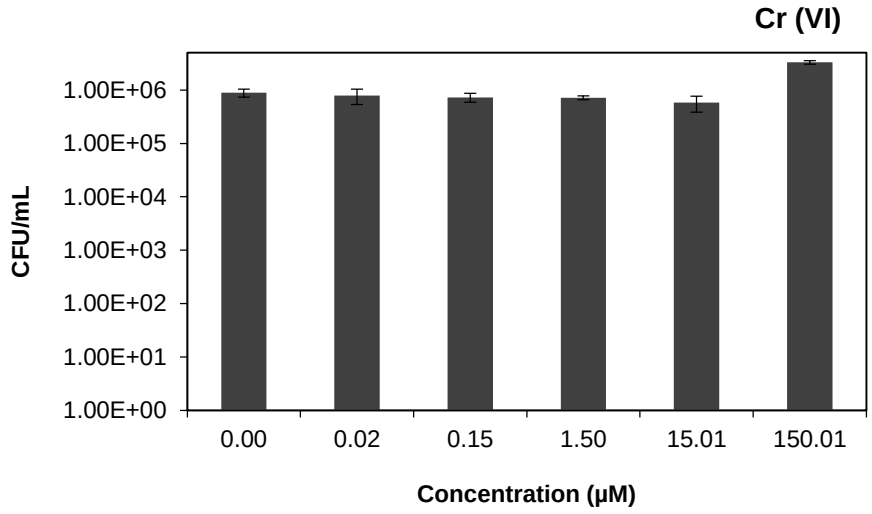
Cr (VI)
1.00E+06
1.00E+05
1.00E+04
1.00E+03
1.00E+02
1.00E+01
1.00E+00
CFU/mL
0.00
0.02
0.15
1.50
15.01
150.01
Concentration (µM)

(E)

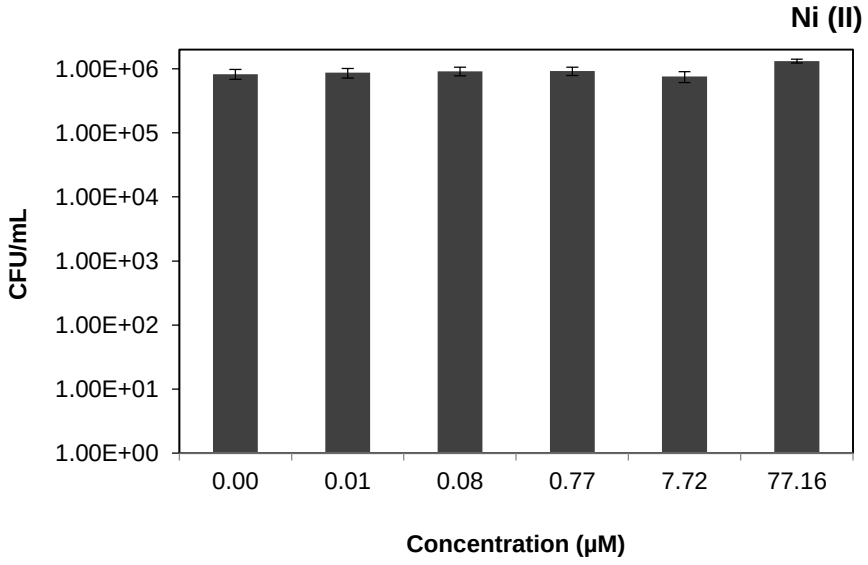
Ni (II)
1.00E+06
1.00E+05
1.00E+04
1.00E+03
1.00E+02
1.00E+01
1.00E+00
CFU/mL
0.00
0.01
0.08
0.77
7.72
77.16
Concentration (µM)

(F)

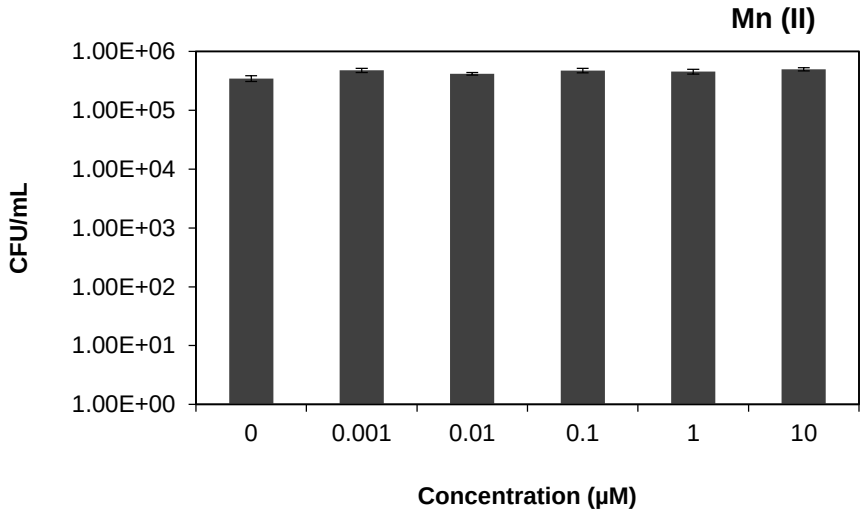

(G)

Figure S3.4: The effects of metal cations with different oxidation states on PAO1 persister cells. The persister cells were exposed for 1 h to Fe^{2+}, Fe^{3+}, Cr^{2+}, Cr^{3+}, Cr^{6+}, Ni^{2+}, Mn^{2+} at various concentrations in the absence of an electrical field.

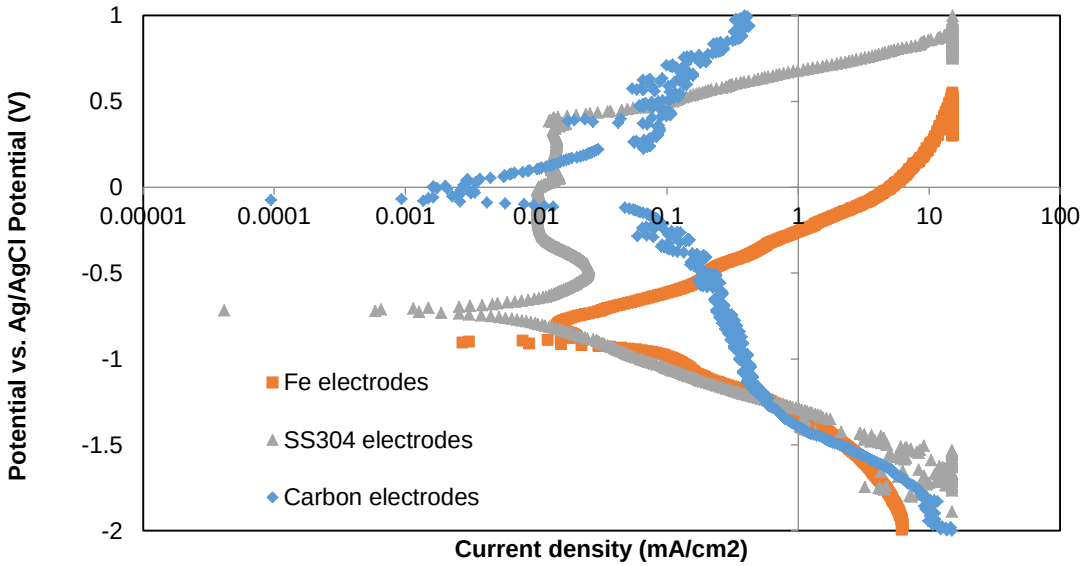

Figure S3.5: Polarization curves of carbon, SS 304 and iron electrodes. Voltages ranging from -2V to 1V (vs. Ag/AgCl potential) were generated across sterile 0.85% NaCl solution using SS 304, carbon or 99.5% c.p. Fe electrodes. Voltammograms were recorded at a polarization scan rate of 1 mV/s.

APPENDIX II

Supplementary Information

For

CHAPTER 5

SENSITIZING *PSEUDOMONAS AERUGINOSA* CELLS TO ANTIBIOTICS BY ELECTROCHEMICAL DISRUPTION OF MEMBRANE FUNCTIONS

1. SEM Imaging of *P. aeruginosa* PAO1 after DC treatment using SS 304

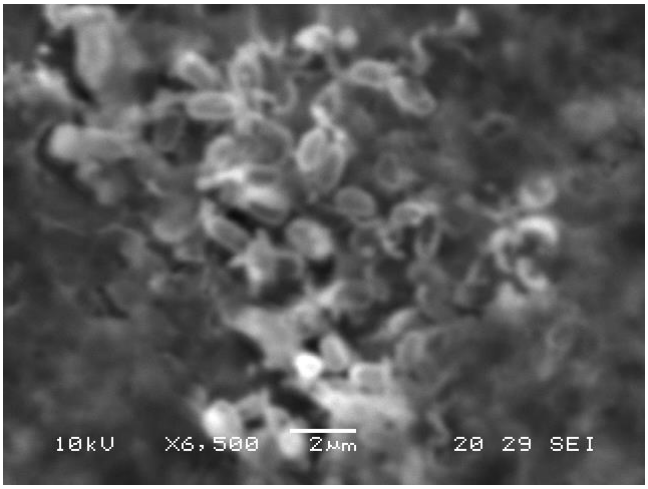

(A)

(B)

Figure S5.1: SEM images of *P. aeruginosa* PAO1 treated with DC using SS 304 electrodes (A) vs. untreated PAO1 cells. The cells were dried on TGON 805, which is a carbon based material, to perform SEM imaging (Joel 5600, Joel, Japan). The

accumulation of metal cations allowed imaging of the cells treated with SS electrodes, which were not previously coated with Au. In contrast, PAO1 control cells did not contain any metal cation and could not be imaged using the Joel 5600 SEM (Joel, Japan).

2. Nano indentation of *P. aeruginosa* after DC treatment.

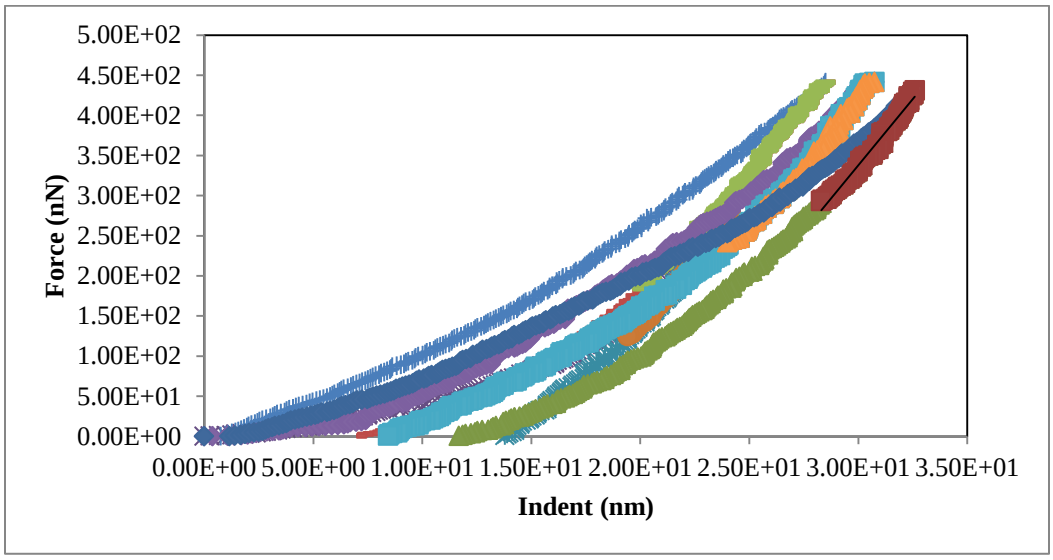

(A)

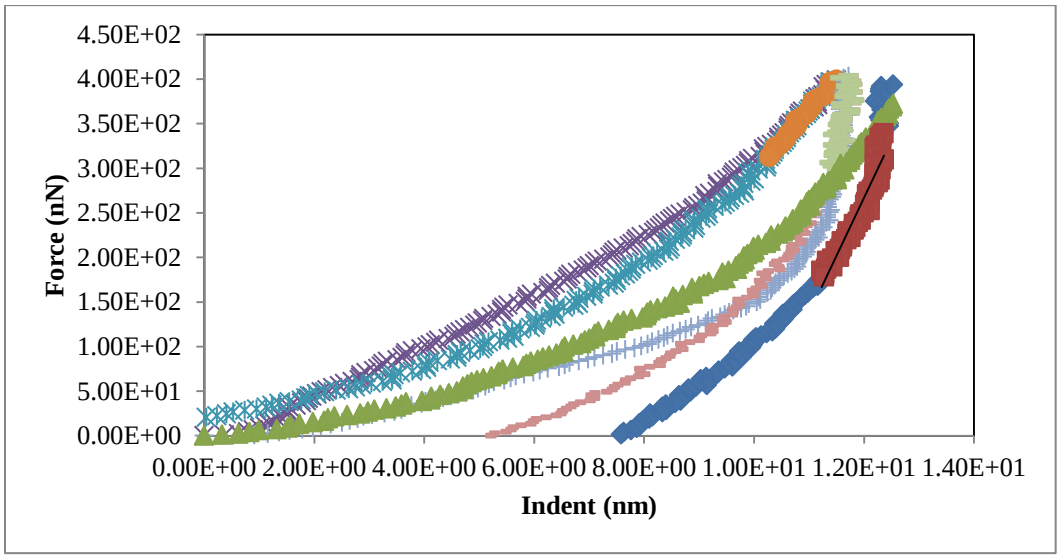

(B)

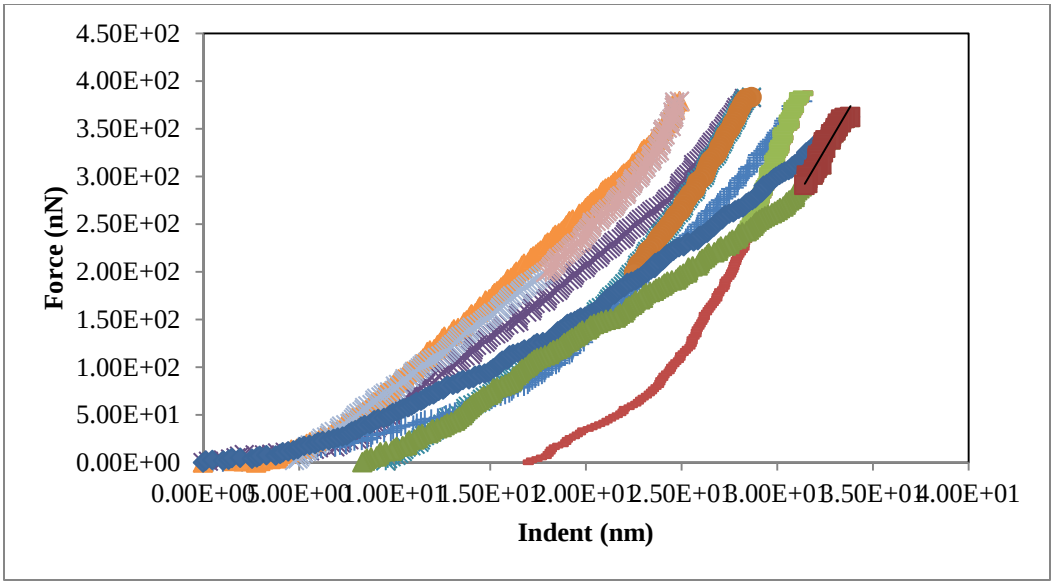

(C)

Figure S5.2: Nonindentation was performed on *P. aeruginosa* cells treated with DC using SS 304 or carbon electrodes. A force curve was derived from the indentation data, which allowed the computation of the elasticity modulus of the cells. (A) Untreated control, (B) PAO1 treated with DC using carbon, and (C) PAO1 treated with DC using SS304.

3. Proteomics of *P. aeruginosa* PAO1 treated with DC using SS304 electrodes for 1h (Contributed by Henry L. Peterson)

The observations of *P. aeruginosa* cells during DC treatments led to the hypothesis that proteins were released from the cells treated using SS 304. To evaluate the significance of the cell response to the DC treatment, the protein expression of DC-treated cells was mapped and compared to the untreated control. Extraction of proteins of *P. aeruginosa* PAO1 was performed according to standard lab protocol described in Appendix VI and VI, and the protein expression between the cells treated with DC using SS304 vs. the

untreated control was analyzed. Extracted protein gel plugs were prepared for LC Mass Spectrometry by the In-Gel Digestion and Extraction Protocol provided by Cornell University's Institute of Biotechnology's Proteomics and Mass Spectrometry Facility.

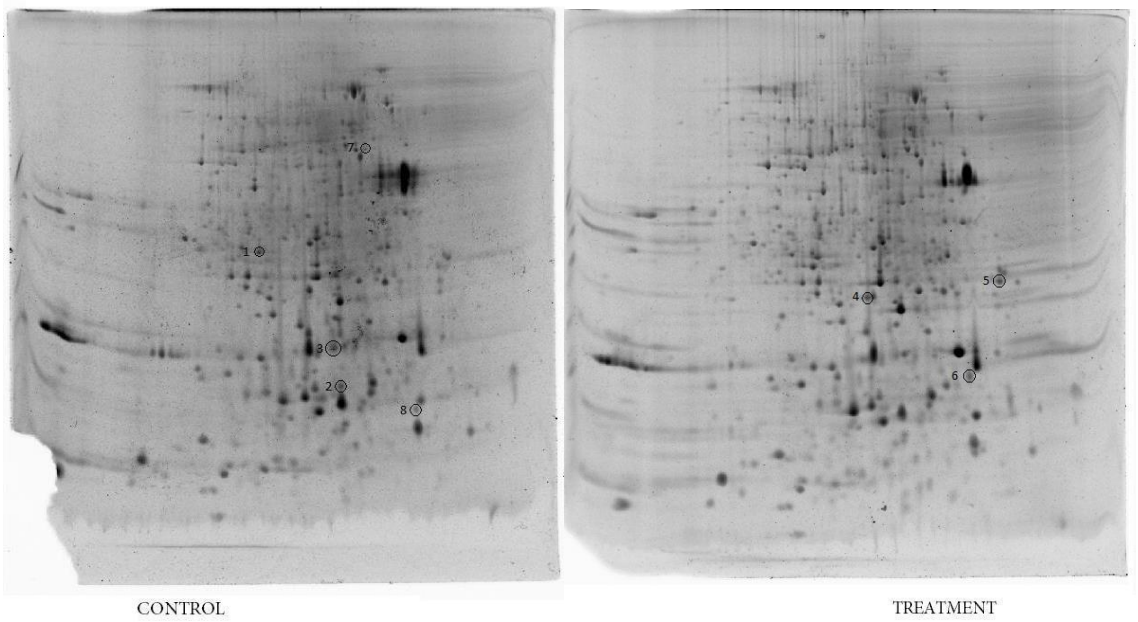

Figure S5.3: 2D protein gels of control and treated samples. Four representative proteins were picked for sequencing. These proteins were found to be: 1) 50s ribosomal protein L25 involved in general stress response. This protein seems to assist in protein formation, and peptidyl hydrolysis 2) a single-stranded DNA binding protein stress protein involved in the inhibition of DNA replication and repair; 3) an outer membrane porin F (OprF) regulating the cross-membrane transport of glucose, nutrients, ions, and water; 4) DsbA (PA5489), a soluble thioldisulfide oxidoreductase periplasmic protein involved in type III secretion system, and detection of eukaryotic cells during bacterial infection.

4. SDS page of protein isolated from *P. aeruginosa* PAO1 treated with DC using carbon electrodes for 1h.

1 Control - Solubilized cell pellet
2 Control - cell pellet
3 Control - intracellular content
4 DC carbon - solubilized cell pellet
5 DC carbon - cell pellet
6 DC carbon – intracellular content

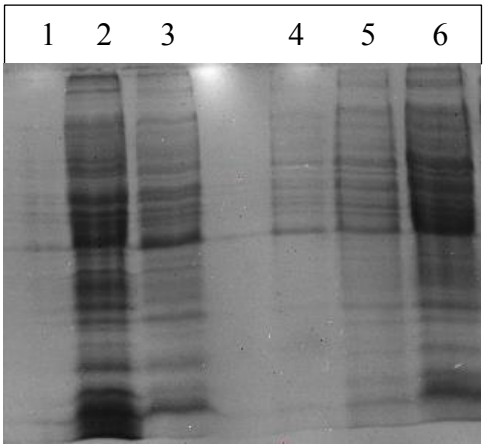

Figure S5.4: SDS gel of membrane and cellular proteins isolated from DC-free control (lane 1-3) and DC-treated *P. aeruginosa* PAO1 cells. Following the protocol for solubilization of expressed proteins from inclusion bodies *(Green, M. R. & Sambrook, J. Molecular cloning: a laboratory manual (Cold Spring Harbor Laboratory Press Cold Spring Harbor, New York:, 2012),* it was found that the level of proteins associated to the cell membrane of *P. aeruginosa* (lane 2) was reduced by the DC treatment (lane 5). In contrast, DC treatment induced the accumulation of intracellular protein as shown on lane 6 (vs lane 3).

APPENDIX III

Supplementary Information

For

CHAPTER 6

EFFECTS OF LOW-LEVEL ELECTRIC CURRENT ON GENE EXPRESSION OF *PEUDOMONAS AERUGINOSA* PERISTER CELLS

Table S6.1: List of genes commonly induced during the DC treatments using carbon electrodes for 20 min and 40 min

Gene	description	fold change at 20 min	fold change at 40 min
	'Biosynthesis of cofactors, prosthetic groups and carriers'		
ribH	riboflavin synthase subunit beta	3.07	2.7
	'Carbon compound catabolism'		
glk	glucokinase	3.2	8.5
	'Hypothetical, unclassified, unknown'		
PA4010	3-methyladenine DNA glycosylase	2.1	4.8
PA0612	hypothetical protein	2.4	2.5
PA1042	hypothetical protein	2.2	2.5
PA1913	hypothetical protein	2.3	5.0
PA1967	hypothetical protein	2.3	2.8
PA2613	hypothetical protein	3.7	2.5
PA3205	hypothetical protein	2.4	2.5
PA3320	hypothetical protein	2.9	2.2
	'Membrane proteins'		
PA1897	hypothetical protein	2.3	4.1
oprG	Outer membrane protein OprG precursor	4.5	2.4
	'Putative enzymes'		
PA1470	probable short-chain dehydrogenase	2.1	2.0
	'Related to phage, transposon, or plasmid'		
PA0627	hypothetical protein	2.5	2.1
PA0628	hypothetical protein	2.1	3.1
PA0629	hypothetical protein	3.0	2.6
PA0633	hypothetical protein	2.4	2.8
PA0636	hypothetical protein	2.1	2.4
PA0617	probable bacteriophage protein	2.7	2.4
	Translation, post-translational modification, degradation'		
fusA2	elongation factor G	4.7	6.1
fusA1	elongation factor G	2.4	3.4
	'Transport of small molecules'		
fruK	1-phosphofructokinase	2.1	2.9
ccmA	heme exporter protein CcmA	2.2	2.7

Table S6.2: List of genes commonly repressed during the DC treatments using carbon electrodes for 20 min and 40 min

Gene	description	fold change at 20 min	fold change at 40 min
	'Energy metabolism'		
PA0510	probable uroporphyrin-III c-methyltransferase	-2.2	-2.1
	'Putative enzymes'		
PA4621	probable oxidoreductase	-2.0	-2.2

Table S6.3: List of genes commonly induced during the DC treatments using SS 304 electrodes for 20 min and 40 min

Gene	description	fold change at 20 min	fold change at 40 min
	'Amino acid biosynthesis and metabolism'		
leuA	2-isopropylmalate synthase	5.1	6.3
	'Biosynthesis of cofactors, prosthetic groups and carriers'		
pqsB	beta-keto-acyl-acyl-carrier protein synthase-like protein	7.0	2.1
	'Carbon compound catabolism'		
PA0810	probable haloacid dehalogenase	5.8	2.6
PA3517	probable lyase	2.2	2.4
	'Cell wall / LPS / capsule'		
wbpB	probable oxidoreductase WpbB	2.2	3.9
comL	competence protein ComL	3.1	2.1
rmlA	glucose-1-phosphate thymidylyltransferase	2.1	2.2
	'DNA replication, recombination, modification and repair'		
gyrA	DNA gyrase subunit A	2.7	2.8
	'Energy metabolism'		
norC	nitric-oxide reductase subunit C	2.1	2.7
norB	nitric-oxide reductase subunit B	2.4	3.0
sdhD	succinate dehydrogenase (D subunit)	17.9	2.7
nuoF	NADH dehydrogenase I chain F	3.2	2.2
nuoJ	NADH dehydrogenase subunit J	2.6	2.1
PA4430	probable cytochrome b	3.1	16.9
	'Fatty acid and phospholipid metabolism'		
fabI	NADH-dependent enoyl-ACP reductase	2.0	2.5
psd	phosphatidylserine decarboxylase	2.6	2.7
	'Hypothetical, unclassified, unknown'		
PA0310	hypothetical protein	3.8	4.8
PA0359	hypothetical protein	3.7	2.2
PA0368	hypothetical protein	3.8	2.0
PA0392	hypothetical protein	2.0	4.2
PA0451	hypothetical protein	3.1	2.0
PA0615	hypothetical protein	2.3	2.1
PA0926	hypothetical protein	2.6	2.8
PA1057	hypothetical protein	6.9	3.2
PA1343	hypothetical protein	5.8	8.0
PA1518	hypothetical protein	3.0	2.1
PA1939	hypothetical protein	10.5	3.5
PA1944	hypothetical protein	3.9	8.5
PA2380	hypothetical protein	3.9	2.4
PA2485	hypothetical protein	2.4	6.6
PA2659	hypothetical protein	4.5	6.2
PA2756	hypothetical protein	2.3	5.9
PA2808	hypothetical protein	2.5	2.3
PA2898	hypothetical protein	4.6	4.4
PA3388	hypothetical protein	2.2	4.6
PA3685	hypothetical protein	2.2	4.0
PA3794	hypothetical protein	2.6	4.1
PA4015	hypothetical protein	2.2	4.0
PA4132	hypothetical protein	2.5	2.1
PA4140	hypothetical protein	3.1	2.9
PA4338	hypothetical protein	3.9	3.2

PA4372	hypothetical protein	2.3	2.1
PA4451	hypothetical protein	2.4	3.9
PA5461	hypothetical protein	9.7	12.5
PA5492	GTP-binding protein	2.4	2.8
PA5502	hypothetical protein	2.1	3.1
	'Protein secretion/export apparatus'		
secE	translocase	6.6	2.0
	'Putative enzymes'		
PA0840	probable oxidoreductase	3.1	2.1
PA1344	probable short-chain dehydrogenase	2.7	2.3
PA2355	probable FMNH2-dependent monooxygenase	3.0	2.0
PA4431	probable iron-sulfur protein	3.5	6.9
	'Related to phage, transposon, or plasmid'		
PA0616	hypothetical protein	2.2	2.0
PA0639	hypothetical protein	2.0	2.1
PA0643	hypothetical protein	3.9	2.7
PA0647	hypothetical protein	3.2	2.3
PA0720	helix destabilizing protein of bacteriophage Pf1	2.4	2.7
	'Secreted Factors (toxins, enzymes, alginate)'		
pvcA	pyoverdine biosynthesis protein PvcA	6.2	2.4
algC	phosphomannomutase AlgC	3.8	2.8
	'Transcription, RNA processing and degradation'		
hepA	ATP-dependent helicase HepA	3.0	2.4
rimM	16S rRNA-processing protein	2.1	2.2
PA1526	probable transcriptional regulator	3.0	6.4
PA3689	probable transcriptional regulator	3.0	2.2
PA4769	probable transcriptional regulator	3.2	2.8
rpsP	30S ribosomal protein S16	3.0	2.4
rplW	50S ribosomal protein L23	2.2	4.4
PA4671	50S ribosomal protein L25	4.1	2.2
	'Transport of small molecules'		
cysW	sulfate transport protein CysW	2.4	2.9
ccmA	heme exporter protein CcmA	1.9	1.9
PA1485	probable amino acid permease	2.8	3.0
PA2135	probable transporter	2.5	5.1
mscL	large-conductance mechanosensitive channel	2.0	2.3
	'Two-component regulatory systems'		
cheY	two-component response regulator CheY	3.6	2.6
PA2479	probable two-component response regulator	3.2	3.0
PA4843	probable two-component response regulator	2.2	2.4

Table S6.4: List of genes commonly repressed during the DC treatments using SS 304 electrodes for 20 min and 40 min

Gene	Description	fold change at 20 min	fold change at 40 min
	'Amino acid biosynthesis and metabolism'		
cysH	phosphoadenosine phosphosulfate reductase	-4.9	-2.4
glyA3	serine hydroxymethyltransferase	-2.5	-2.6
	'Antibiotic resistance and susceptibility'		
PA2018	RND multidrug efflux transporter	-2.5	-2.0
	'DNA replication, recombination, modification and repair'		
PA4282	probable exonuclease	-2.1	-2.0
	'Hypothetical, unclassified, unknown'		
PA0099	hypothetical protein	-2.4	-2.2
PA1972	hypothetical protein	-3.2	-2.1
PA2296	hypothetical protein	-2.6	-2.8
PA2353	hypothetical protein	-2.9	-3.0
PA2768	hypothetical protein	-3.4	-2.8
PA3230	hypothetical protein	-2.1	-2.1
PA4057	hypothetical protein	-2.8	-2.2
PA4347	hypothetical protein	-2.3	-2.3
PA4485	hypothetical protein	-2.0	-2.2
PA4863	hypothetical protein	-2.8	-2.1
	'Membrane proteins'		
PA0345	hypothetical protein	-3.2	-2.0
	'Protein secretion/export apparatus'		
PA2673	probable type II secretion system protein	-2.7	-2.1
pcrG	regulator in type III secretion	-2.2	-2.1
pscF	type III export protein PscF	-3.1	-2.4
pscQ	type III secretion protein	-3.4	-2.1
	'Putative enzymes'		
ispG	4-hydroxy-3-methylbut-2-en-1-yl diphosphate synthase	-2.0	-2.2
PA4724	glutamyl-tRNA synthetase	-2.4	-2.3
PA4008	probable hydrolase	-2.1	-2.2
PA0147	probable oxidoreductase	-2.2	-2.0
PA0364	probable oxidoreductase	-2.4	-2.4
PA1171	probable transglycolase	-2.2	-2.1
	'Transcriptional regulators'		
PA0181	probable transcriptional regulator	-2.0	-2.4
PA1627	probable transcriptional regulator	-2.4	-2.1
PA3630	probable transcriptional regulator	-3.4	-2.0
PA4165	probable transcriptional regulator	-2.6	-2.2
	'Translation, post-translational modification, degradation'		
gatC	aspartyl/glutamyl-tRNA amidotransferase subunit C	-2.5	-2.2
lasB	elastase LasB	-3.2	-2.0
	'Transport of small molecules'		
PA0240	probable porin	-3.1	-2.1
PA0166	probable transporter	-2.4	-2.0
	'Two-component regulatory systems'		
	PmrA: two-component regulator system response regulator		
pmrA	PmrA	-2.1	-2.5
PA0600	probable two-component sensor	-3.1	-2.6

Table S6.5: List of the PAO1 persister genes induced by the treatment with 70µA/cm^2 DC using carbon electrodes for 20 min and 40 min.

Gene	Description	Fold Change 20 min	40 min
	'Adaptation, protection'		
bfrB	bacterioferritin	1.2	3.2
	'Amino acid biosynthesis and metabolism'		
hpd	4-hydroxyphenylpyruvate dioxygenase	1.3	2.5
aroK	shikimate kinase	2.1	1.2
	'Antibiotic resistance and susceptibility'		
PA1032	probable penicillin amidase	1.8	3.5
mexA	Resistance-Nodulation-Cell Division (RND) multidrug efflux membrane fusion protein MexA precursor	-1.4	2.9
	'Biosynthesis of cofactors, prosthetic groups and carriers'		
folD	5,10-methylene-tetrahydrofolate dehydrogenase	1.3	2.2
ribH	riboflavin synthase subunit beta	3.1	2.7
pqsC	beta-keto-acyl-acyl-carrier protein synthase-like protein	2.1	-1.3
thiL	thiamine monophosphate kinase	1.5	2.5
	'Carbon compound catabolism'		
glk	glucokinase	3.2	8.5
mdcC	malonate decarboxylase subunit delta	1.3	3.0
PA0743	probable 3-hydroxyisobutyrate dehydrogenase	1.4	3.0
PA2098	probable esterase/deacetylase	2.4	1.9
cbrA	two-component sensor CbrA	1.2	3.0
	'Cell wall / LPS / capsule'		
mdoH	glucosyltransferase MdoH	3.3	1.7
waaF	heptosyltransferase II	-1.2	2.2
lpxO2	lipopolysaccharide biosynthetic protein LpxO2	1.4	3.0
	'Central intermediary metabolism'		
cpo	chloroperoxidase precursor	-1.1	3.1
PA4880	probable bacterioferritin	1.6	2.2
PA3471	probable malic enzyme	2.8	1.2
	'Chaperones & heat shock proteins'		
grpE	heat shock protein GrpE	-1.0	2.5
	'Chemotaxis'		
aer	aerotaxis receptor Aer	1.5	4.0
pctB	chemotactic transducer PctB	0.9	4.0
	'Energy metabolism'		
atpG	ATP synthase subunit C	4.2	1.0
cioA	cyanide insensitive terminal oxidase	1.0	2.3
nuoA	NADH dehydrogenase alpha subunit	0.8	2.9
nuoB	NADH dehydrogenase beta subunit	-1.1	17.1
PA1554	probable cytochrome oxidase subunit (cbb3-type)	-1.1	2.2
sucD	succinyl-CoA synthetase alpha subunit	-1.0	2.4
	'Fatty acid and phospholipid metabolism'		
fabG	3-oxoacyl-[acyl-carrier-protein] reductase	1.7	3.3
PA1869	probable acyl carrier protein	2.4	-1.1
PA4351	probable acyltransferase	2.6	1.2
	'Hypothetical, unclassified, unknown'		
PA4010	3-methyladenine DNA glycosylase	2.1	4.8
PA1701	conserved hypothetical protein in type III secretion	1.4	2.2
PA0050	hypothetical protein	-1.0	3.3

PA0052	hypothetical protein	1.1	2.9
PA0081	hypothetical protein	2.7	1.9
PA0109	hypothetical protein	1.2	2.4
PA0329	hypothetical protein	1.4	4.2
PA0526	hypothetical protein	1.1	2.1
PA0554	hypothetical protein	1.3	2.4
PA0566	hypothetical protein	1.1	4.4
PA0572	hypothetical protein	1.3	2.1
PA0587	hypothetical protein	1.5	2.6
PA0612	hypothetical protein	2.4	2.5
PA0822	hypothetical protein	2.4	1.3
PA0851	hypothetical protein	2.3	1.7
PA0907	hypothetical protein	-1.1	2.8
PA0959	hypothetical protein	1.4	2.9
PA1042	hypothetical protein	2.2	2.5
PA1134	hypothetical protein	2.8	-1.4
PA1349	hypothetical protein	2.0	-1.2
PA1426	hypothetical protein	1.6	2.4
PA1451	hypothetical protein	1.1	2.9
PA1474	hypothetical protein	-1.3	2.7
PA1679	hypothetical protein	-1.1	3.1
PA1784	hypothetical protein	2.2	1.4
PA1849	hypothetical protein	1.5	2.5
PA1913	hypothetical protein	2.3	5.0
PA1967	hypothetical protein	2.3	2.8
PA1995	hypothetical protein	1.3	3.2
PA2106	hypothetical protein	1.1	2.6
PA2171	hypothetical protein	1.5	2.4
PA2313	hypothetical protein	1.0	4.3
PA2364	hypothetical protein	2.1	1.9
PA2370	hypothetical protein	2.3	-1.0
PA2441	hypothetical protein	1.6	2.5
PA2484	hypothetical protein	2.6	1.3
PA2590	hypothetical protein	1.0	2.2
PA2613	hypothetical protein	3.7	2.5
PA2630	hypothetical protein	1.1	2.8
PA2756	hypothetical protein	-1.6	6.6
PA2774	hypothetical protein	-1.0	3.0
PA2795	hypothetical protein	1.0	6.8
pelE	hypothetical protein	1.2	4.7
PA3127	hypothetical protein	2.1	-1.1
PA3205	hypothetical protein	2.4	2.5
PA3273	hypothetical protein	1.1	2.4
PA3320	hypothetical protein	2.9	2.2
PA3370	hypothetical protein	1.6	2.2
PA3572	hypothetical protein	1.1	2.7
PA3716	hypothetical protein	3.1	1.8
PA3945	hypothetical protein	1.1	2.7
PA3978	hypothetical protein	1.0	2.5
PA4140	hypothetical protein	1.6	2.1
PA4326	hypothetical protein	3.3	1.3
PA4510	hypothetical protein	1.0	2.2
PA4577	hypothetical protein	1.1	2.2
PA4591	hypothetical protein	1.1	2.3
PA4623	hypothetical protein	1.0	3.4

PA4657	hypothetical protein	1.4	5.6
PA4782	hypothetical protein	1.2	2.7
PA4826	hypothetical protein	-1.1	2.2
PA4916	hypothetical protein	-1.3	4.0
PA4918	hypothetical protein	1.4	2.8
PA5061	hypothetical protein	1.4	2.1
PA5306	hypothetical protein	1.1	2.1
PA5444	hypothetical protein	1.3	2.2
PA5506	hypothetical protein	1.1	3.4
	'Membrane proteins'		
PA1897	hypothetical protein	2.3	4.1
oprG	Outer membrane protein OprG precursor	4.5	2.4
	'Motility & Attachment'		
flgL	flagellar hook-associated protein type 3 FlgL	1.7	2.5
fliF	flagellar M-ring protein	-1.0	2.8
	'Putative enzymes'		
PA0421	hypothetical protein	2.8	1.8
PA0836	probable acetate kinase	1.2	2.7
PA0507	probable acyl-CoA dehydrogenase	1.1	2.5
PA2125	probable aldehyde dehydrogenase	3.0	-1.1
PA5508	probable glutamine synthetase	1.7	2.8
PA2865	probable glycosylase	1.1	2.7
PA1470	probable short-chain dehydrogenase	2.1	2.0
PA2554	probable short-chain dehydrogenase	1.7	3.0
PA3128	short chain dehydrogenase	1.5	2.9
PA3277	short chain dehydrogenase	-1.5	3.4
PA4786	short-chain dehydrogenase	1.1	3.5
	'Related to phage, transposon, or plasmid'		
PA0616	hypothetical protein	-1.4	2.5
PA0624	hypothetical protein	2.4	1.4
PA0626	hypothetical protein	1.5	6.1
PA0627	hypothetical protein	2.5	2.1
PA0628	hypothetical protein	2.1	3.1
PA0629	hypothetical protein	3.0	2.6
PA0633	hypothetical protein	2.4	2.8
PA0636	hypothetical protein	2.1	2.4
PA0637	hypothetical protein	1.6	4.6
PA0639	hypothetical protein	1.4	2.2
PA0644	hypothetical protein	-1.1	2.0
PA0717	hypothetical protein of bacteriophage Pf1	-1.2	2.3
PA0617	probable bacteriophage protein	2.7	2.4
PA0619	probable bacteriophage protein	3.7	1.7
PA0622	probable bacteriophage protein	2.3	-1.1
PA0623	probable bacteriophage protein	1.2	4.6
PA0638	probable bacteriophage protein	1.6	2.4
PA0640	probable bacteriophage protein	2.6	1.7
	'Secreted Factors toxins, enzymes, alginate'		
algW	AlgW protein	1.6	2.4
	'Transcription, RNA processing and degradation'		
nusG	transcription antitermination protein NusG	1.6	3.9
nusA	transcription elongation factor NusA	1.1	2.1
PA0207	probable transcriptional regulator	1.0	2.4
PA0225	probable transcriptional regulator	1.1	2.3
PA2897	probable transcriptional regulator	1.5	3.0
PA2930	probable transcriptional regulator	-1.1	2.1

rsaL	regulatory protein RsaL	1.2	2.2
psrA	transcriptional regulator PsrA	-1.3	2.7
	Translation, post-translational modification, degradation'		
rpsL	30S ribosomal protein S12	2.1	1.3
rpsP	30S ribosomal protein S16	1.3	2.8
rpsS	30S ribosomal protein S19	-1.5	2.3
rpsB	30S ribosomal protein S2	-1.3	2.7
rpmE	50S ribosomal protein L31	1.2	2.6
rplL	50S ribosomal protein L7/L12	1.8	2.4
clpB	ClpB protein	-1.1	2.2
fusA2	elongation factor G	4.7	6.1
fusA1	elongation factor G	2.4	3.4
lexA	LexA repressor	1.5	1.9
prc	periplasmic tail-specific protease	1.3	2.8
PA2371	probable ClpA/B-type protease	-1.0	2.5
infA	translation initiation factor IF-1	1.0	2.4
	'Transport of small molecules'		
fruK	1-phosphofructokinase	2.1	2.9
oprD	Basic amino acid, basic peptide and imipenem outer membrane porin OprD precursor	1.6	2.5
braC	branched-chain amino acid transport protein BraC	1.2	2.4
ccmA	heme exporter protein CcmA	2.2	2.7
oprM	Major intrinsic multiple antibiotic resistance efflux outer membrane protein OprM precursor	-1.0	2.5
PA0206	probable ATP-binding component of ABC transporter	1.1	7.3
PA2912	probable ATP-binding component of ABC transporter	-1.0	2.1
PA0273	probable major facilitator superfamily (MFS) transporter	1.5	4.0
PA3647	probable outer membrane protein precursor	1.9	2.0
PA4292	probable phosphate transporter	1.1	3.6
PA4375	probable RND efflux transporter	1.4	2.2
PA2466	probable TonB-dependent receptor	1.4	2.2
	'Two-component regulatory systems'		
PA1243	probable sensor/response regulator hybrid	2.5	1.2
PA1458	probable two-component sensor	1.3	2.3

Table S6.6: List of the PAO1 persister genes repressed after DC treatment with 70 μA/cm^2 DC using carbon electrodes.

Gene	Description	Fold change 20 min	Fold change 40 min
	'Amino acid biosynthesis and metabolism'		
aguB	N-carbamoylputrescine amidohydrolase	-4.7	1.3
PA1818	probable Orn/Arg/Lys decarboxylase	-2.3	-1.1
	'Biosynthesis of cofactors, prosthetic groups and carriers'		
panB	3-methyl-2-oxobutanoate hydroxymethyltransferase	1.0	-2.0
moaA1	molybdopterin biosynthetic protein A1	-1.2	-2.2
serC	phosphoserine aminotransferase	-1.7	-2.1
	'Carbon compound catabolism'		
fbp	fructose-1,6-bisphosphatase	-1.3	-2.1
	'Cell wall / LPS / capsule'		
gmd	GDP-mannose 4,6-dehydratase	-3.9	-1.9
	'Central intermediary metabolism'		
PA5435	oxaloacetate decarboxylase	1.1	-2.0
	'DNA replication, recombination, modification and repair'		
PA2138	DNA ligase	-2.0	1.0
ogt	methylated-DNA--protein-cysteine methyltransferase	-2.0	1.4
recR	recombination protein RecR	-1.7	-2.5
	'Energy metabolism'		
ccmH	cytochrome C-type biogenesis protein CcmH	-1.8	-2.0
cyoD	cytochrome o ubiquinol oxidase subunit IV	-2.9	1.1
nirJ	heme d1 biosynthesis protein NirJ	1.2	-2.2
PA1600	probable cytochrome c	-2.3	1.1
PA2716	probable FMN oxidoreductase	-1.1	-2.5
PA0510	probable uroporphyrin-III c-methyltransferase	-2.2	-2.1
	'Hypothetical, unclassified, unknown'		
PA0238	hypothetical protein	-2.0	-1.1
PA0317	hypothetical protein	1.0	-2.0
PA0486	hypothetical protein	-1.2	-2.1
PA0498	hypothetical protein	-1.1	-2.0
PA0539	hypothetical protein	-1.5	-2.1
PA0549	hypothetical protein	-1.2	-2.0
PA0550	hypothetical protein	1.1	-2.7
PA0709	hypothetical protein	-1.3	-2.0
PA0729	hypothetical protein	-1.2	-2.8
PA0847	hypothetical protein	-2.3	-1.3
PA1866	hypothetical protein	-2.1	1.1
PA1975	hypothetical protein	2.4	-2.3
PA2075	hypothetical protein	-1.7	-2.4
PA2200	hypothetical protein	-2.1	-1.7
PA2404	hypothetical protein	-1.2	-2.0
PA2567	hypothetical protein	-1.4	-3.0
PA2650	hypothetical protein	-3.8	-1.2
PA2765	hypothetical protein	-2.1	1.1
PA2880	hypothetical protein	1.3	-3.0
PA2936	hypothetical protein	-2.1	-1.0
PA3578	hypothetical protein	-1.3	-2.3
PA3892	hypothetical protein	-2.3	-1.4
PA3983	hypothetical protein	-1.3	-2.2
PA4319	hypothetical protein	-2.1	1.7

PA4321	hypothetical protein	-1.6	-2.6
PA4347	hypothetical protein	-1.3	-2.1
PA4872	hypothetical protein	1.1	-2.0
PA4894	hypothetical protein	-1.2	-2.8
PA4929	hypothetical protein	1.2	-2.2
PA5237	hypothetical protein	1.0	-2.2
PA5477	hypothetical protein	1.0	-2.2
	'Protein secretion/export apparatus'		
lepA	GTP-binding protein LepA	-1.2	-2.8
pscF	type III export protein PscF	-2.5	-1.4
	'Putative enzymes'		
PA2324	hypothetical protein	-2.8	-1.5
PA2889	probable acyl-CoA dehydrogenase	-1.4	-2.0
PA2499	probable deaminase	-1.2	-2.5
PA1991	probable iron-containing alcohol dehydrogenase	-2.2	-1.8
PA0237	probable oxidoreductase	-1.3	-2.1
PA4621	probable oxidoreductase	-2.0	-2.2
PA5327	probable oxidoreductase	-1.1	-2.2
PA0975	probable radical activating enzyme	-1.3	-2.1
PA2892	short chain dehydrogenase	1.1	-2.4
	'Secreted Factors (toxins, enzymes, alginate)'		
exoT	exoenzyme T	-2.5	-1.2
	'Transcriptional regulators'		
PA0163	probable transcriptional regulator	1.2	-2.1
PA2047	probable transcriptional regulator	-2.5	-1.6
PA3895	probable transcriptional regulator	-2.2	1.0
PA1911	probable transmembrane sensor	-1.5	-2.3
PA3900	probable transmembrane sensor	-2.5	-1.7
	'Translation, post-translational modification, degradation'		
ileS	isoleucyl-tRNA synthetase	-2.1	-1.0
	'Transport of small molecules'		
hisJ	periplasmic histidine-binding protein HisJ	-2.7	-1.0
trkA	potassium uptake protein TrkA	-1.1	-2.0
PA0458	probable major facilitator superfamily (MFS) transporter	-2.1	-1.7
PA1848	probable major facilitator superfamily (MFS) transporter	-1.2	-2.7
PA4179	probable porin	-1.1	-2.4
PA4898	probable porin	-2.3	-1.2
PA4334	probable transport protein	-2.0	-1.2
PA0322	probable transporter	-2.5	-1.7
msbA	transport protein MsbA	1.2	-2.9
	'Two-component regulatory systems'		
PA2798	probable two-component response regulator	-2.1	-1.6
PA4380	probable two-component sensor	-1.1	-2.3

Table S6.7: List of the PAO1 persister genes induced after DC treatment with 70 μA/cm^2 DC using SS304 electrodes.

Gene	Description	Fold Change 20 min	40 min
	'Adaptation, protection'		
lytB	4-hydroxy-3-methylbut-2-enyl diphosphate reductase	4.2	1.1
dnaJ	DnaJ protein	1.2	2.2
	'Amino acid biosynthesis and metabolism'		
PA0399	cystathionine beta-synthase	3.2	1.9
PA0400	probable cystathionine gamma-lyase	4.7	1.5
trpG	anthranilate synthase component II	1.7	2.6
trpC	indole-3-glycerol-phosphate synthase	1.3	2.3
leuA	2-isopropylmalate synthase	5.1	6.3
	'Biosynthesis of cofactors, prosthetic groups and carriers'		
PA0503	probable biotin synthesis protein BioC	6.3	-1.1
bioD	dithiobiotin synthetase	1.2	2.6
nirF	heme d1 biosynthesis protein NirF	3.1	1.6
nadA	quinolinate synthetase	1.7	2.1
pdxH	pyridoxamine 5'-phosphate oxidase	2.2	1.9
PA1125	probable cobalamin biosynthetic protein	2.6	-1.3
cobO	cob(I)yrinic acid a,c-diamide adenosyltransferase	3.2	1.3
folE1	GTP cyclohydrolase I precursor	1.3	2.5
moaD	molybdopterin converting factor, small subunit	2.2	1.7
ispB	octaprenyl-diphosphate synthase	3.3	-1.2
ipk	4-diphosphocytidyl-2-C-methyl-D-erythritol kinase	2.2	1.8
folP	dihydropteroate synthase	19.3	1.1
nadE	NAD(+) synthetase	4.2	-1.8
pqsB	beta-keto-acyl-acyl-carrier protein synthase-like protein	7.0	2.1
pqsD	3-oxoacyl-[acyl-carrier-protein] synthase III	2.5	1.3
	'Carbon compound catabolism'		
prpC	citrate synthase 2	1.4	2.1
PA0810	probable haloacid dehalogenase	5.8	2.6
xylZ	toluate 1,2-dioxygenase electron transfer component	1.4	2.3
glk	glucokinase	3.7	-1.1
PA3517	probable lyase	2.2	2.4
pgm	phosphoglyceromutase	2.1	-1.3
PA5417	sarcosine oxidase delta subunit	2.2	-1.5
	'Cell wall / LPS / capsule'		
wbpB	probable oxidoreductase WpbB	2.2	3.9
ftsI	penicillin-binding protein 3	2.6	-1.2
comL	competence protein ComL	3.1	2.1
rmlA	glucose-1-phosphate thymidylyltransferase	2.1	2.2
glmU	glucosamine-1-phosphate acetyltransferase/N-acetylglucosamine-1-phosphate uridyltransferase	1.4	2.0
	'Central intermediary metabolism'		
PA2140	probable metallothionein	-1.3	2.2
gloA3	lactoylglutathione lyase	5.2	1.2
	'Chemotaxis'		
chpE	probable chemotaxis protein	4.2	1.0
PA1459	probable methyltransferase	2.6	-1.4
motA	flagellar motor protein	2.8	1.0
	'DNA replication, recombination, modification and repair'		
ruvC	Holliday junction resolvase	2.4	1.1

ruvB	Holliday junction DNA helicase RuvB	3.4	-1.2
uvrB	excinuclease ABC subunit B	2.5	-1.6
ihfB	integration host factor beta subunit	1.8	3.1
gyrA	DNA gyrase subunit A	2.7	2.8
PA5348	probable DNA-binding protein	3.5	-1.2
	'Energy metabolism'		
nirS	nitrite reductase precursor	4.4	1.8
norC	nitric-oxide reductase subunit C	2.1	2.7
norB	nitric-oxide reductase subunit B	2.4	3.0
glpE	thiosulfate sulfurtransferase	2.4	-1.6
napD	NapD protein of periplasmic nitrate reductase	4.6	1.4
ccmG	cytochrome C biogenesis protein CcmG	3.3	1.9
sdhD	succinate dehydrogenase (D subunit)	17.9	2.7
nuoD	NADH dehydrogenase I chain C,D	2.9	1.1
nuoF	NADH dehydrogenase I chain F	3.2	2.2
nuoI	NADH dehydrogenase subunit I	4.9	1.1
nuoJ	NADH dehydrogenase subunit J	2.6	2.1
nosZ	nitrous-oxide reductase precurser	2.0	1.5
PA4430	probable cytochrome b	3.1	16.9
cc4	cytochrome c4 precursor	3.3	1.7
	'Fatty acid and phospholipid metabolism'		
fabI	NADH-dependent enoyl-ACP reductase	2.0	2.5
pgsA	CDP-diacylglycerol--glycerol-3-phosphate 3-phosphatidyltransferase	4.6	1.6
faoA	fatty-acid oxidation complex alpha-subunit	4.7	-1.4
PA3334	probable acyl carrier protein	1.1	4.4
psd	phosphatidylserine decarboxylase	2.6	2.7
	'Hypothetical, unclassified, unknown'		
PA0022	hypothetical protein	2.2	1.1
PA0160	hypothetical protein	3.3	1.5
PA0250	hypothetical protein	2.6	1.8
PA0255	hypothetical protein	2.6	1.3
PA0308	hypothetical protein	2.7	1.8
PA0310	hypothetical protein	3.8	4.8
PA0359	hypothetical protein	3.7	2.2
PA0368	hypothetical protein	3.8	2.0
PA0392	hypothetical protein	2.0	4.2
PA0451	hypothetical protein	3.1	2.0
PA0461	hypothetical protein	2.0	1.1
PA0495	hypothetical protein	4.4	-1.0
PA0565	hypothetical protein	2.1	1.0
PA0614	hypothetical protein	2.9	1.9
PA0615	hypothetical protein	2.3	2.1
PA0713	hypothetical protein	1.7	2.6
PA0777	hypothetical protein	2.7	1.0
PA0808	hypothetical protein	4.7	1.9
PA0862	hypothetical protein	2.3	1.9
PA0907	hypothetical protein	4.8	1.0
PA0915	hypothetical protein	1.4	2.4
PA0926	hypothetical protein	2.6	2.8
PA0943	hypothetical protein	2.4	-1.2
PA0948	hypothetical protein	1.7	2.2
PA0957	hypothetical protein	3.6	1.5
PA1034	hypothetical protein	2.7	1.1
PA1052	hypothetical protein	1.0	2.2
PA1057	hypothetical protein	6.9	3.2

PA1062	hypothetical protein	1.6	2.2
PA1107	hypothetical protein	2.7	1.9
PA1210	hypothetical protein	2.1	1.4
PA1211	hypothetical protein	1.3	2.1
PA1263	hypothetical protein	1.7	2.0
PA1343	hypothetical protein	5.8	8.0
PA1348	hypothetical protein	6.4	-1.2
PA1404	hypothetical protein	2.1	1.8
PA1415	hypothetical protein	14.4	1.7
PA1427	hypothetical protein	2.0	-1.0
PA1503	hypothetical protein	3.1	-1.0
PA1516	hypothetical protein	2.7	-1.3
PA1517	hypothetical protein	2.5	1.5
PA1518	hypothetical protein	3.0	2.1
PA1644	hypothetical protein	2.9	-1.3
exsD	ExsD	4.5	1.6
PA1790	hypothetical protein	2.1	1.3
PA1857	hypothetical protein	4.1	1.8
PA1895	hypothetical protein	1.9	2.5
PA1939	hypothetical protein	10.5	3.5
PA1944	hypothetical protein	3.9	8.5
PA2116	hypothetical protein	4.1	1.1
PA2192	hypothetical protein	2.1	-1.2
PA2287	hypothetical protein	1.7	2.1
PA2313	hypothetical protein	-1.0	2.0
PA2331	hypothetical protein	5.0	1.6
PA2369	hypothetical protein	4.5	1.3
PA2380	hypothetical protein	3.9	2.4
PA2484	hypothetical protein	1.3	2.9
PA2485	hypothetical protein	2.4	6.6
PA2544	hypothetical protein	6.0	1.4
PA2659	hypothetical protein	4.5	6.2
PA2706	hypothetical protein	3.4	1.8
PA2736	hypothetical protein	1.2	2.7
PA2756	hypothetical protein	2.3	5.9
PA2797	hypothetical protein	1.7	2.4
PA2808	hypothetical protein	2.5	2.3
PA2845	hypothetical protein	2.5	1.3
PA2864	hypothetical protein	4.3	1.0
PA2875	hypothetical protein	1.9	3.9
PA2880	hypothetical protein	2.5	-1.4
PA2898	hypothetical protein	4.6	4.4
PA2929	hypothetical protein	2.3	-1.2
PA2946	hypothetical protein	6.8	-1.3
PA2971	hypothetical protein	2.8	1.3
PA3009	hypothetical protein	2.9	1.8
PA3018	hypothetical protein	1.1	2.4
PA3042	hypothetical protein	3.5	1.1
gbt	glycine betaine transmethylase	4.5	1.3
PA3239	hypothetical protein	2.8	-1.3
PA3278	hypothetical protein	2.0	2.4
PA3289	hypothetical protein	2.4	-1.2
PA3323	hypothetical protein	1.2	2.3
PA3388	hypothetical protein	2.2	4.6
PA3435	flavodoxin	2.3	-1.4

PA3496	hypothetical protein	2.9	1.4
PA3539	hypothetical protein	2.6	1.2
PA3552	hypothetical protein	9.7	1.2
PA3634	hypothetical protein	2.0	1.8
PA3685	hypothetical protein	2.2	4.0
PA3726	hypothetical protein	5.2	-1.0
PA3740	hypothetical protein	1.7	3.0
PA3794	hypothetical protein	2.6	4.1
PA3808	hypothetical protein	1.9	3.3
PA3833	hypothetical protein	1.4	2.4
PA3864	hypothetical protein	2.3	1.3
PA3952	hypothetical protein	2.3	1.4
PA3958	hypothetical protein	2.0	1.3
PA3992	hypothetical protein	3.0	-1.2
PA4015	hypothetical protein	2.2	4.0
PA4132	hypothetical protein	2.5	2.1
PA4140	hypothetical protein	3.1	2.9
PA4317	hypothetical protein	2.7	-1.2
PA4324	hypothetical protein	2.9	1.6
PA4338	hypothetical protein	3.9	3.2
PA4372	hypothetical protein	2.3	2.1
PA4379	hypothetical protein	2.9	1.3
PA4395	hypothetical protein	2.1	1.8
PA4451	hypothetical protein	2.4	3.9
PA4460	hypothetical protein	14.6	-1.0
PA4511	hypothetical protein	16.1	1.4
PA4575	hypothetical protein	1.4	2.9
PA4623	hypothetical protein	1.4	2.1
PA4638	hypothetical protein	3.0	-1.3
PA4658	hypothetical protein	-1.2	2.2
PA4736	hypothetical protein	1.7	2.1
PA4792	hypothetical protein	2.5	1.4
PA4842	hypothetical protein	1.7	2.3
PA5002	hypothetical protein	2.8	-2.3
PA5007	hypothetical protein	1.8	2.9
PA5017	hypothetical protein	2.6	1.3
PA5078	hypothetical protein	2.2	1.0
PA5087	hypothetical protein	3.6	1.2
PA5209	hypothetical protein	2.8	1.6
PA5227	hypothetical protein	2.5	1.4
PA5228	hypothetical protein	1.9	2.8
PA5233	flagellar protein	2.4	-1.0
PA5248	hypothetical protein	2.3	-1.2
PA5251	hypothetical protein	2.9	1.5
PA5270	hypothetical protein	3.3	-1.4
PA5271	hypothetical protein	8.1	1.2
PA5329	hypothetical protein	3.1	1.4
PA5359	hypothetical protein	2.8	1.2
PA5423	hypothetical protein	3.3	-1.0
PA5461	hypothetical protein	9.7	12.5
PA5471	hypothetical protein	3.1	-1.6
PA5492	GTP-binding protein	2.4	2.8
PA5502	hypothetical protein	2.1	3.1
	'Membrane proteins'		
PA0452	probable stomatin-like protein	2.1	-1.1

PA1305	hypothetical protein	3.1	1.3
PA4924	hypothetical protein	2.2	1.4
PA5264	hypothetical protein	2.7	1.9
	Motility & Attachment'		
flgJ	peptidoglycan hydrolase	2.2	1.0
cupB6	fimbrial subunit CupB6	2.5	0.9
pilC	still frameshift type 4 fimbrial biogenesis protein PilC	3.5	1.2
pilQ	Type 4 fimbrial biogenesis outer membrane protein PilQ precursor	3.4	2.0
	'Nucleotide biosynthesis and metabolism'		
apaH	diadenosinetetraphosphatase	7.4	1.0
prs	ribose-phosphate pyrophosphokinase	2.0	1.4
	'Protein secretion/export apparatus'		
popD	Translocator outer membrane protein PopD precursor	2.4	-1.0
xcpS	general secretion pathway protein F	1.6	2.8
PA3404	probable outer membrane protein precursor	1.6	2.2
secE	translocase	6.6	2.0
secG	secretion protein SecG	2.3	1.5
	'Putative enzymes'		
PA0562	probable hydrolase	3.0	-1.4
PA0779	probable ATP-dependent protease	1.5	3.3
PA0840	probable oxidoreductase	3.1	2.1
PA1224	probable NAD(P)H dehydrogenase	2.8	1.7
PA1306	probable HIT family protein	1.9	2.0
PA1344	probable short-chain dehydrogenase	2.7	2.3
PA1576	probable 3-hydroxyisobutyrate dehydrogenase	1.9	2.8
PA1628	probable 3-hydroxyacyl-CoA dehydrogenase	1.6	2.7
PA2271	probable acetyltransferase	1.8	2.8
PA2355	probable FMNH2-dependent monooxygenase	3.0	2.0
PA3330	probable short chain dehydrogenase	2.9	1.4
PA3504	probable aldehyde dehydrogenase	1.9	3.1
PA3567	probable oxidoreductase	3.8	1.7
PA3795	probable oxidoreductase	2.9	1.5
PA4431	probable iron-sulfur protein	3.5	6.9
PA4786	short-chain dehydrogenase	2.2	1.0
PA5313	probable pyridoxal-dependent aminotransferase	2.1	1.1
	'Related to phage, transposon, or plasmid'		
PA0616	hypothetical protein	2.2	2.0
PA0631	hypothetical protein	2.3	1.7
PA0639	hypothetical protein	2.0	2.1
PA0643	hypothetical protein	3.9	2.7
PA0644	hypothetical protein	1.8	2.1
PA0645	hypothetical protein	2.4	1.4
PA0647	hypothetical protein	3.2	2.3
PA0648	hypothetical protein	1.2	2.3
PA0718	hypothetical protein of bacteriophage Pf1	13.8	2.0
PA0720	helix destabilizing protein of bacteriophage Pf1	2.4	2.7
PA0725	hypothetical protein of bacteriophage Pf1	2.4	1.3
	'Secreted Factors (toxins, enzymes, alginate)'		
pvcA	pyoverdine biosynthesis protein PvcA	6.2	2.4
algC	phosphomannomutase AlgC	3.8	2.8
	'Transcription, RNA processing and degradation'		
rne	ribonuclease E	2.3	1.3
hepA	ATP-dependent helicase HepA	3.0	2.4
rimM	16S rRNA-processing protein	2.1	2.2

rluD	pseudouridine synthase	1.9	2.5
rnr	exoribonuclease RNase R	2.8	1.3
	'Transcriptional regulators'		
PA0533	probable transcriptional regulator	2.8	-1.1
prtR	transcriptional regulator PrtR	4.3	-1.1
argR	transcriptional regulator ArgR	4.5	-1.3
PA0942	probable transcriptional regulator	1.1	3.2
PA1504	probable transcriptional regulator	-1.7	4.0
PA1526	probable transcriptional regulator	3.0	6.4
cysB	transcriptional regulator CysB	2.0	1.7
PA2432	probable transcriptional regulator	1.1	2.2
PA2885	probable transcriptional regulator	2.1	1.2
PA3689	probable transcriptional regulator	3.0	2.2
PA4184	probable transcriptional regulator	2.0	1.0
PA4203	probable transcriptional regulator	-1.1	2.8
PA4769	probable transcriptional regulator	3.2	2.8
PA4784	probable transcriptional regulator	2.0	-1.9
PA4896	probable sigma-70 factor, ECF subfamily	2.5	0.7
PA5380	probable transcriptional regulator	3.4	1.1
PA5438	probable transcriptional regulator	4.3	1.3
	'Translation, post-translational modification, degradation'		
aspS	aspartyl-tRNA synthetase	2.3	1.1
lexA	LexA repressor	1.8	6.0
map	methionine aminopeptidase	4.0	0.9
rpsP	30S ribosomal protein S16	3.0	2.4
rpsD	30S ribosomal protein S4	3.1	1.7
rplW	50S ribosomal protein L23	2.2	4.4
rpsI	30S ribosomal protein S9	3.0	2.0
PA4671	50S ribosomal protein L25	4.1	2.2
rnpA	ribonuclease P	4.2	1.1
	'Transport of small molecules'		
PA0137	probable permease of ABC transporter	2.5	1.5
PA0206	probable ATP-binding component of ABC transporter	3.0	1.8
PA0215	probable transporter	2.3	1.4
cysW	sulfate transport protein CysW	2.4	2.9
spuG	polyamine transport protein PotH	4.9	1.1
PA0313	probable permease of ABC transporter	-1.2	2.3
PA0314	probable binding protein component of ABC transporter	2.4	1.5
PA0470	probable hydroxamate-type ferrisiderophore receptor	7.8	1.1
exbD2	transport protein ExbD	2.2	1.9
PA0811	probable major facilitator superfamily (MFS) transporter	1.6	2.3
PA0860	probable ATP-binding/permease fusion ABC transporter	2.0	-1.1
aotQ	arginine/ornithine transport protein AotQ	2.7	1.0
tolB	translocation protein TolB precursor	3.3	1.3
PA1108	probable major facilitator superfamily (MFS) transporter	1.1	2.7
PA1194	probable amino acid permease	3.2	1.6
ccmA	heme exporter protein CcmA	1.9	1.9
PA1485	probable amino acid permease	2.8	3.0
PA1808	probable permease of ABC transporter	1.7	2.8
PA1964	probable ATP-binding component of ABC transporter	5.3	1.1
PA2055	probable major facilitator superfamily (MFS) transporter	2.7	1.3
PA2135	probable transporter	2.5	5.1
PA3336	probable major facilitator superfamily (MFS) transporter	-1.2	3.1
PA3441	probable molybdopterin-binding protein	2.4	1.4
potC	polyamine transport protein PotC	2.8	1.2

opmD	probable outer membrane protein precursor	3.3	1.3
PA4374	probable Resistance-Nodulation-Cell Division (RND) efflux membrane fusion protein precursor	2.5	1.4
mscL	large-conductance mechanosensitive channel	2.0	2.3
PA4909	probable ATP-binding component of ABC transporter	1.6	2.5
PA5376	probable ATP-binding component of ABC transporter	2.1	-1.1
	'Two-component regulatory systems'		
cheY	two-component response regulator CheY	3.6	2.6
PA2479	probable two-component response regulator	3.2	3.0
PA4101	probable two-component response regulator	2.3	1.8
PA4843	probable two-component response regulator	2.2	2.4
envZ	two-component sensor EnvZ	2.6	-1.2
ompR	two-component response regulator OmpR	2.2	1.6

Table S6.8: List of the PAO1 persister genes repressed by DC treatment with 70 μA/cm^2 DC using SS304 electrodes.

Gene	Description	Fold Change 20 min	40 min
	'Adaptation, protection'		
ampC	beta-lactamase precursor	-2.5	1.1
betA	choline dehydrogenase	-2.3	-1.0
katN	non-heme catalase KatN	-1.1	-2.1
pmbA	PmbA protein	-1.1	-2.4
PA2314	probable major facilitator superfamily (MFS) transporter	-2.3	-1.4
pvdO	PvdO	-1.4	-2.3
pvdP	PvdP	-1.2	-2.4
	'Amino acid biosynthesis and metabolism'		
ilvI	acetolactate synthase III large subunit	-2.5	1.0
argB	acetylglutamate kinase	-2.9	-1.4
hisF2	imidazole glycerol phosphate synthase subunit HisF	-2.5	1.1
sdaB	L-serine dehydratase	-1.3	-2.3
cysH	phosphoadenosine phosphosulfate reductase	-4.9	-2.4
glyA3	serine hydroxymethyltransferase	-2.5	-2.6
aruE	succinylglutamate desuccinylase	-2.0	-1.3
	'Antibiotic resistance and susceptibility'		
PA1129	probable fosfomycin resistance protein	-2.1	-1.1
PA1237	probable multidrug resistance efflux pump	-2.3	-1.3
PA2018	RND multidrug efflux transporter	-2.5	-2.0
	'Biosynthesis of cofactors, prosthetic groups and carriers'		
panB	3-methyl-2-oxobutanoate hydroxymethyltransferase	-2.0	-1.1
ubiA	4-hydroxybenzoate octaprenyltransferase	-2.3	-1.0
bioA	adenosylmethionine--8-amino-7-oxononanoate transaminase	-2.0	-1.9
ureG	urease accessory protein UreG	-2.0	-1.1
cobA	uroporphyrin-III C-methyltransferase	-3.5	-1.7
	'Carbon compound catabolism'		
PA2040	probable glutamine synthetase	-2.3	-1.1
antA	anthranilate dioxygenase large subunit	-3.4	-1.8
antC	anthranilate dioxygenase reductase	-3.6	-1.7
PA0226	probable CoA transferase, subunit A	-2.2	-1.2
PA0227	probable CoA transferase, subunit B	-2.1	-1.5
PA5411	probable ferredoxin	-3.0	-1.0
PA5410	probable ring hydroxylating dioxygenase, alpha-subunit	-2.5	-1.1
vanB	vanillate O-demethylase oxidoreductase	-1.9	-2.1
	'Cell wall / LPS / capsule'		
rfaD	ADP-L-glycero-D-mannoheptose 6-epimerase	-2.2	-1.4
murI	glutamate racemase	-2.2	1.0
wbpX	glycosyltransferase WbpX	-2.9	-1.1
pbpC	penicillin-binding protein 3A	-3.2	-1.0
sltB1	soluble lytic transglycosylase B	-2.4	-1.2
	'Central intermediary metabolism'		
phaC2	poly(3-hydroxyalkanoic acid) synthase 2	-2.8	1.5
PA2726	probable radical activating enzyme	-2.5	-1.0
ureB	urease beta subunit	1.2	-2.9
	'Chemotaxis'		
motD	flagellar motor protein	-2.4	1.4
PA3349	probable chemotaxis protein	-1.4	-2.1
PA2561	probable chemotaxis transducer	-2.4	-1.5

	'DNA replication, recombination, modification and repair'		
uvrC	excinuclease ABC subunit C	-2.4	-1.5
PA4282	probable exonuclease	-2.1	-2.0
PA1405	probable helicase	-3.5	-1.9
	'Energy metabolism'		
snr1	cytochrome c Snr1	-2.7	-1.2
cycH	cytochrome c-type biogenesis protein	-2.2	1.1
PA2165	glycogen synthase	-2.0	-1.3
nosD	NosD protein	-1.7	-2.8
nirN	probable c-type cytochrome	-2.3	1.0
PA1600	probable cytochrome c	-2.2	-1.6
PA0521	probable cytochrome c oxidase subunit	-2.1	-2.0
PA2714	probable molybdopterin oxidoreductase	-3.1	-1.8
rpe	ribulose-phosphate 3-epimerase	-1.9	-2.4
	'Fatty acid and phospholipid metabolism'		
plsX	fatty acid/phospholipid synthesis protein	-2.0	-1.2
	'Hypothetical, unclassified, unknown'		
engA	GTP-binding protein EngA	-2.2	-1.5
PA0099	hypothetical protein	-2.4	-2.2
PA0161	hypothetical protein	-2.1	1.0
PA0317	hypothetical protein	-1.5	-2.3
PA0328	hypothetical protein	1.1	-2.7
PA0356	hypothetical protein	-2.9	1.1
PA0394	hypothetical protein	-3.0	-1.3
PA0462	hypothetical protein	-3.1	-1.2
PA0497	hypothetical protein	-1.4	-2.0
PA0561	hypothetical protein	2.4	-2.3
PA0574	hypothetical protein	-1.1	-2.5
PA0834	hypothetical protein	-2.0	-1.3
PA0875	hypothetical protein	-2.5	-1.7
PA0878	hypothetical protein	-1.9	-2.2
PA0902	hypothetical protein	-2.7	-1.4
PA0946	hypothetical protein	-3.2	-1.1
PA1059	hypothetical protein	-2.2	-1.3
PA1089	hypothetical protein	-2.7	-1.5
PA1111	hypothetical protein	-2.1	-1.1
PA1192	hypothetical protein	-1.9	-2.2
PA1203	hypothetical protein	-1.7	-2.2
PA1354	hypothetical protein	-2.1	-1.8
PA1371	hypothetical protein	-2.1	1.0
PA1372	hypothetical protein	-2.1	-1.2
PA1378	hypothetical protein	-2.1	-1.6
PA1428	hypothetical protein	-2.1	-1.3
PA1439	hypothetical protein	4.4	-2.0
PA1494	hypothetical protein	-1.9	-2.4
PA1612	hypothetical protein	-2.4	-1.4
PA1640	hypothetical protein	-2.9	-1.5
PA1664	hypothetical protein	-2.1	-1.8
PA1688	hypothetical protein	-2.6	-1.9
PA1755	hypothetical protein	-1.8	-3.9
PA1874	hypothetical protein	-2.2	-1.1
PA1879	hypothetical protein	-2.6	-1.7
PA1906	hypothetical protein	-2.6	1.2
PA1926	hypothetical protein	-1.5	-2.5

PA1956	hypothetical protein	-1.5	-3.0
PA1963	hypothetical protein	-1.1	-2.2
PA1972	hypothetical protein	-3.2	-2.1
PA2033	hypothetical protein	-2.4	-1.7
PA2077	hypothetical protein	-2.5	-1.2
PA2078	hypothetical protein	-2.9	-1.3
PA2110	hypothetical protein	-2.3	-1.4
PA2154	hypothetical protein	-2.1	-1.2
PA2205	hypothetical protein	-2.0	-2.6
PA2268	hypothetical protein	-2.2	-1.2
PA2296	hypothetical protein	-2.6	-2.8
PA2353	hypothetical protein	-2.9	-3.0
PA2428	hypothetical protein	-2.5	-1.0
PA2439	hypothetical protein	-2.9	-1.1
PA2543	hypothetical protein	-3.3	-1.8
PA2610	hypothetical protein	-3.2	-1.0
PA2628	hypothetical protein	-3.6	-1.4
PA2684	hypothetical protein	-1.5	-2.8
PA2720	hypothetical protein	-2.7	-1.5
PA2721	hypothetical protein	-2.3	-1.0
PA2750	hypothetical protein	-1.7	-2.1
PA2768	hypothetical protein	-3.4	-2.8
PA2814	hypothetical protein	-3.0	-1.4
PA2829	hypothetical protein	-2.8	-1.6
PA2839	hypothetical protein	-3.5	-1.5
PA2872	hypothetical protein	-2.2	-1.5
PA3054	hypothetical protein	-2.1	-1.2
PA3057	hypothetical protein	-2.9	-1.0
pelA	hypothetical protein	-2.2	-1.2
PA3130	hypothetical protein	-1.2	-2.4
PA3230	hypothetical protein	-2.1	-2.1
PA3237	hypothetical protein	-2.4	-1.0
PA3282	hypothetical protein	-2.1	-1.5
PA3292	hypothetical protein	-2.3	-1.0
PA3318	hypothetical protein	-2.7	-1.9
PA3419	hypothetical protein	-2.2	-1.4
PA3424	hypothetical protein	-2.6	-1.4
PA3449	hypothetical protein	-2.1	-1.1
PA3670	hypothetical protein	-1.2	-2.2
PA3680	hypothetical protein	-4.0	-1.7
PA3733	hypothetical protein	-3.5	-1.8
PA3772	hypothetical protein	-2.4	-1.1
PA3826	hypothetical protein	-3.4	1.0
PA3851	hypothetical protein	-2.1	-1.1
PA3862	hypothetical protein	-2.7	1.1
PA3868	hypothetical protein	-3.2	1.0
PA3902	hypothetical protein	-2.2	-1.3
PA3904	hypothetical protein	-2.2	-1.7
PA3953	hypothetical protein	-2.1	-1.3
PA4057	hypothetical protein	-2.8	-2.2
PA4095	hypothetical protein	-2.4	1.7
PA4177	hypothetical protein	-2.6	-1.2
PA4181	hypothetical protein	-2.1	-1.5
PA4295	hypothetical protein	-1.5	-2.1
PA4319	hypothetical protein	-2.5	1.1

PA4327	hypothetical protein	-2.6	-1.6
PA4340	hypothetical protein	-1.8	-2.0
PA4347	hypothetical protein	-2.3	-2.3
PA4391	hypothetical protein	-1.9	-2.1
PA4405	hypothetical protein	-2.1	-1.8
PA4438	hypothetical protein	-2.3	-1.5
PA4473	hypothetical protein	1.1	-2.2
PA4485	hypothetical protein	-2.0	-2.2
PA4617	hypothetical protein	-2.3	-1.7
PA4629	hypothetical protein	-2.1	-1.1
PA4639	hypothetical protein	-2.2	-1.2
PA4684	hypothetical protein	-2.5	1.2
PA4734	hypothetical protein	-2.7	-1.1
PA4858	hypothetical protein	-3.0	-1.7
PA4863	hypothetical protein	-2.8	-2.1
PA4866	hypothetical protein	-1.1	-2.4
PA4894	hypothetical protein	-1.8	-2.2
PA5104	hypothetical protein	-2.5	-1.5
PA5109	hypothetical protein	-2.0	-1.5
PA5130	hypothetical protein	-3.1	-1.7
PA5132	hypothetical protein	-2.6	-1.1
PA5135	hypothetical protein	-3.1	1.1
PA5144	hypothetical protein	-2.0	-2.0
PA5180	hypothetical protein	-1.7	-2.5
PA5310	hypothetical protein	-3.1	-1.1
PA5385	hypothetical protein	-2.1	-1.9
PA5396	hypothetical protein	-3.0	-1.3
PA5414	hypothetical protein	-2.4	-1.5
PA3494	NADH-ubiquinone oxidoreductase	-2.3	1.1
PA5568	putative inner membrane protein translocase component YidC	-3.6	-1.1
	'Membrane proteins'		
PA0260	hypothetical protein	-1.0	-2.0
PA0345	hypothetical protein	-3.2	-2.0
	'Motility & Attachment'		
flhF	flagellar biosynthesis protein	-1.5	-2.1
PA5498	probable adhesin	-1.6	-2.4
PA2407	probable adhesion protein	-2.1	-1.6
wspA	probable chemotaxis transducer	-2.2	-1.1
fimT	type 4 fimbrial biogenesis protein FimT	-2.3	-1.8
pilB	type 4 fimbrial biogenesis protein PilB	-2.1	-1.1
	'Nucleotide biosynthesis and metabolism'		
tmk	thymidylate kinase	-2.3	-1.7
	'Protein secretion/export apparatus'		
xcpX	general secretion pathway protein K	-1.2	-2.8
hasE	metalloprotease secretion protein	-2.1	-1.6
PA2673	probable type II secretion system protein	-2.7	-2.1
pcrG	regulator in type III secretion	-2.2	-2.1
pscF	type III export protein PscF	-3.1	-2.4
pscK	type III export protein PscK	-3.0	-1.4
pscQ	type III secretion protein	-3.4	-2.1
pcrV	type III secretion protein PcrV	-2.0	1.0
	'Putative enzymes'		
ispG	4-hydroxy-3-methylbut-2-en-1-yl diphosphate synthase	-2.0	-2.2
PA0494	acetyl-CoA carboxylase	-2.1	-1.3
PA4198	acyl-CoA synthase	-3.4	-1.1

PA0704	amidase	1.4	-2.5
cysQ	CysQ protein	-2.6	-1.1
PA4724	glutamyl-tRNA synthetase	-2.4	-2.3
PA1966	hypothetical protein	-2.0	-1.5
PA2324	hypothetical protein	-3.0	-1.4
PA2263	probable 2-hydroxyacid dehydrogenase	1.1	-2.4
PA4979	probable acyl-CoA dehydrogenase	1.4	-2.4
PA4995	probable acyl-CoA dehydrogenase	-2.6	-1.5
PA3454	probable acyl-CoA thiolase	-2.7	1.1
PA3759	probable aminotransferase	-2.1	-1.3
PA1417	probable decarboxylase	-2.0	-1.7
PA3328	probable FAD-dependent monooxygenase	-2.4	-1.4
PA0842	probable glycosyl transferase	-2.4	-1.8
PA1391	probable glycosyl transferase	-2.2	-1.8
PA4819	probable glycosyl transferase	-2.2	1.0
PA2934	probable hydrolase	-2.5	-1.2
PA4008	probable hydrolase	-2.1	-2.2
PA0147	probable oxidoreductase	-2.2	-2.0
PA0364	probable oxidoreductase	-2.4	-2.4
PA4889	probable oxidoreductase	-3.7	-1.6
PA1832	probable protease	-2.2	-1.1
PA1303	probable signal peptidase	-2.3	-1.2
PA1171	probable transglycolase	-2.2	-2.1
PA0372	probable zinc protease	-1.3	-2.2
PA3957	short chain dehydrogenase	-2.3	-1.5
	'Related to phage, transposon, or plasmid'		
PA0987	hypothetical protein	-2.2	-1.8
	'Secreted Factors (toxins, enzymes, alginate)'		
algI	alginate o-acetyltransferase AlgI	-2.4	-1.1
PA0985	pyocin S5	-2.2	-1.8
algF	alginate o-acetyltransferase AlgF	-2.1	-1.3
	'Transcription, RNA processing and degradation'		
pcnB	poly(A) polymerase	-2.5	-1.5
	'Transcriptional regulators'		
PA0961	probable cold-shock protein	-2.5	-1.3
PA2093	probable sigma-70 factor, ECF subfamily	-2.4	-1.3
PA0181	probable transcriptional regulator	-2.0	-2.4
PA0243	probable transcriptional regulator	-2.8	-1.5
PA0701	probable transcriptional regulator	-2.3	-1.1
PA1138	probable transcriptional regulator	-2.3	-1.4
PA1184	probable transcriptional regulator	-2.3	-1.0
PA1269	probable transcriptional regulator	-2.1	-2.0
PA1309	probable transcriptional regulator	-3.0	-1.6
PA1312	probable transcriptional regulator	-2.3	1.5
PA1520	probable transcriptional regulator	-2.7	-1.6
PA1627	probable transcriptional regulator	-2.4	-2.1
PA1738	probable transcriptional regulator	-3.0	1.5
PA2005	probable transcriptional regulator	-1.0	-2.1
PA2206	probable transcriptional regulator	-2.1	-1.4
PA2758	probable transcriptional regulator	-3.1	-1.5
PA2848	probable transcriptional regulator	-1.3	-2.2
PA3027	probable transcriptional regulator	-3.0	1.2
PA3215	probable transcriptional regulator	-3.5	-2.0
PA3433	probable transcriptional regulator	-2.6	-1.9
PA3630	probable transcriptional regulator	-3.4	-2.0

PA3932	probable transcriptional regulator	-2.9	-1.1
PA4165	probable transcriptional regulator	-2.6	-2.2
PA1364	probable transmembrane sensor	-1.3	-2.0
algU	sigma factor AlgU	-1.3	-2.2
pvdS	sigma factor PvdS	-2.5	-1.1
gpuR	transcriptional activator GpuR	-2.3	1.3
exsA	transcriptional regulator ExsA	-1.0	-3.2
gntR	transcriptional regulator GntR	-3.8	-1.3
pchR	transcriptional regulator PchR	-2.1	-1.0
	'Translation, post-translational modification, degradation'		
gatC	aspartyl/glutamyl-tRNA amidotransferase subunit C	-2.5	-2.2
lasB	elastase LasB	-3.2	-2.0
gatA	glutamyl-tRNA amidotransferase subunit A	-2.0	-1.8
hemA	glutamyl-tRNA reductase	-1.0	-2.5
stk1	serine-threonine kinase Stk1	-1.4	-2.5
	'Transport of small molecules'		
aroP1	aromatic amino acid transport protein AroP1	-1.3	-2.4
phnC	ATP-binding component of ABC phosphonate transporter	-1.1	-2.3
citA	citrate transporter	-2.3	-1.1
gabP	gamma-aminobutyrate permease	-2.1	-1.8
kdpA	potassium-transporting ATPase subunit A	-1.5	-2.1
PA3314	probable ATP-binding component of ABC transporter	-2.2	-1.5
PA3442	probable ATP-binding component of ABC transporter	-1.8	-2.4
PA4910	probable ATP-binding component of ABC transporter	-1.3	-2.2
PA4358	probable ferrous iron transport protein	-2.4	-1.0
PA1908	probable major facilitator superfamily (MFS) transporter	-2.3	1.2
PA2701	probable major facilitator superfamily (MFS) transporter	-2.6	-1.6
PA3595	probable major facilitator superfamily (MFS) transporter	-1.3	-2.5
PA4343	probable major facilitator superfamily (MFS) transporter	-2.2	-1.4
PA5530	probable MFS dicarboxylate transporter	-2.1	-1.8
PA4837	probable outer membrane protein precursor	-2.4	-1.8
PA5377	probable permease of ABC transporter	-2.6	0.5
PA0450	probable phosphate transporter	-2.2	-1.2
PA3760	probable phosphotransferase protein	-2.0	-1.5
PA0162	probable porin	-4.7	-1.6
PA0240	probable porin	-3.1	-2.1
PA4501	probable porin	-2.6	-1.4
PA0156	probable Resistance-Nodulation-Cell Division (RND) efflux membrane fusion protein precursor	-2.5	-1.9
PA2836	probable secretion protein	-2.5	-1.1
PA1365	probable siderophore receptor	-2.3	1.1
PA2533	probable sodium:alanine symporter	-2.6	-1.9
PA2983	probable tolQ-type transport protein	-2.1	-1.4
PA0151	probable TonB-dependent receptor	-2.5	-1.8
PA0166	probable transporter	-2.4	-2.0
PA0322	probable transporter	-1.3	-2.7
PA1507	probable transporter	-3.2	-1.8
gltP	proton-glutamate symporter	-1.6	-2.2
czcB	Resistance-Nodulation-Cell Division (RND) divalent metal cation efflux membrane fusion protein CzcB precursor	-5.3	-1.3
cysP	sulfate-binding protein of ABC transporter	-2.2	-1.1
sbp	sulfate-binding protein precursor	-2.5	-1.3
	'Two-component regulatory systems'		
pmrA	PmrA: two-component regulator system response regulator PmrA	-2.1	-2.5
PA1611	probable sensor/response regulator hybrid	-1.3	-2.1

PA2583	probable sensor/response regulator hybrid	-2.2	-1.9
PA5166	probable two-component response regulator	-2.2	-1.9
PA0600	probable two-component sensor	-3.1	-2.6
PA1798	probable two-component sensor	-2.4	-1.9
PA3191	probable two-component sensor	-2.6	1.1
PA4036	probable two-component sensor	-2.4	-1.8
pfeR	two-component response regulator PfeR	-2.1	-1.1

APPENDIX IV- PROTOCOL:

ELECTROCHEMICAL TREATMENT OF *PSEUDOMONAS AERUGINOSA* PAO1 AND MUTANTS

1. **Overnight Cultures**
    a. Media: LB media (+ 10 μg/mL tetracycline for mutants). 25 mL of LB is poured in a 250 mL flask to and inoculation is performed with a previously sterilized inoculation loop.
    b. Conditions: Incubate overnight at 37 degrees Celsius while shaking at 200 rpm

2. **Preparation of samples for ciprofloxacin testing: Persister isolation**
    a. For each sample to be tested, aliquot 10 mL into to a 50 mL conical tube.
    b. Centrifuge sample(s) at 8000 rpm for 10 minutes at 10 degrees C.
    c. Wash 2X with 30 mL of 0.85% NaCl.
    d. Following second wash, decant and add 10 mL of 0.85% NaCl for restore the sample to the initial concentration.
    e. Add 1 mL of sample to labeled microcentrifuge tubes. Add ciprofloxacin as seen in table below.

Ciprofloxacin Concentration for experiment (Stock 25 mg/mL)	
Desired concentration (μg/mL)	Stock to add (uL/mL)
25	1
50	2
75	3
100	4
200	8

    f. Incubate for 3.5 h at 37 degrees C while shaking at 200 rpm.
    g. Centrifuge and wash 3X with 1 mL of 0.85% NaCl to remove ciprofloxacin and debris. Microcentrifuge settings: 10,000 rpm, 10 °C, 1.5 min.
    h. Following washings add enough 0.85% NaCl to obtain final volume of 1 mL in each vial.
    i. Prepare to perform dilution series and plate.

3. **Plating**
    a. Each sample is performed with five replicates, but the amount of dilution depends on the conditions. For control (no treatment), plate from D3-D8 (dilution 3-8). For the isolated persister cells, plate from D2-D7.
    b. Add 180 uL of 0.85% NaCl to the wells in plate needed per dilution series. Add 20 uL of sample to first row of wells (Dilution 1).
    c. Mixing well, add 20 uL from each dilution row to the next to form a 10x dilution series.
    d. Plate using 10 uL of each sample dilution point.
    e. Let plates dry in biosafety cabinet.
    f. Incubate overnight at 37 degrees C.
    g. Count CFUs the following day
    h. Normalize the cell count based on 1 mL

4. **Preparation of Samples for Electrochemical Experiments**
    a. For each sample to be tested, aliquot 10 mL into to a 50 mL conical tube.
    b. Centrifuge sample(s) at 8000 rpm for 10 minutes at 10 degrees C.
    c. Wash 2X wash with 30 mL of 0.85% NaCl.
    d. Following second wash, decant and add 10 mL of 0.85% NaCl for restore the sample to the initial concentration.
    e. Add 200 μg/mL ciprofloxacin for persister cell isolation (e.g. 80 uL from a 25 mg/mL stock)
    f. Incubate for 3.5 h at 37 degrees C while shaking at 200 rpm.
    g. Centrifuge and wash 2X with 30 mL of 0.85% NaCl, using same centrifuge settings as above.
    h. Following washings add enough 0.85% NaCl to obtain an OD_{600} between ~0.7-0.8. (typically this requires between 30-45 mL of 0.85% NaCl)

5. **Aftermath Software Setup**
    a. Set up the laptop computer that has Aftermath software and connect potentiostat (s).
    b. There is no password to open Aftermath software; enter as a guest.
    c. Under the "Experiments" file menu, select "chronopotentiometric." Enter the following settings: 500 μA and 1 hr. Select the potentiometer serial number you are using and click "perform" to begin the experiment. An mV profile will be able to be observed over the course of the experiment.

6. **Cuvette set up**
    a. Prior the treatment sterilize the electrodes
    b. There are three electrodes in the cuvette: the working electrode (in our case, anode), counter electrode (cathode) and reference electrode.
    c. The carbon and SS304 electrodes were soaked in acetone overnight to remove any potential organic materials (the electrodes are cut by the machine shop). Then Soak in 190 proof ethanol for 1h. Dry the SS304 coupons in the oven, cover the coupons with aluminium foil, insert them in a 50 mL conical tube and autoclave. Keep the carbon electrode in ethanol until use.
    d. The working and counter electrodes (e.g. SS304, carbon, TGON 805) connect to the red and green alligator clips, using copper wire. The reference electrode (Ag/AgCl) connects to the white alligator clip.
    e. The SS304 electrodes need to be discarded following use. The Ag/AgCl can be reused after sterilizing in bleach and ethanol. Carbon was also able to be reused. Soak in acetone and then ethanol. Sand the surface with sandpaper and repeat the same sterilization process. But ideally, carbon electrodes are not reused to avoid variation in experimental results. Indeed, due to the reaction, change of the surface density could occurs and affect the electrochemical properties of the electrodes.

7. **Performing the DC treatment**
    a. Add 3 mL of sample to the experimental cuvette with electrodes and 3 mL of sample to a control cuvette, as needed. For the 2-chamber system, 3 mL of sample is added in each chamber and 0.85% NaCl solution is introduced into the salt bridge. The salt bridge is made out of long Pasteur pipet. The thin end is deformed using a flame.
    b. One the setup is ready, DC treatment is performed
    c. Click “perform” in Aftermath software to start experiment
    d. Plate control (no treatment)
    e. Meanwhile, take 100 uL of sample every 20 minutes for testing (add 20 uL to each of the five wells in D1). Plate D1-D6 for persister experiment.
    f. At 60 minutes, the termination of the experiment, plate D0-D5.

APPENDIX V- PROTOCOL

NANOINDENTATION OF BACTERIAL CELLS USING AN ATOMIC FORCE MICROSCOPE

Data acquisition

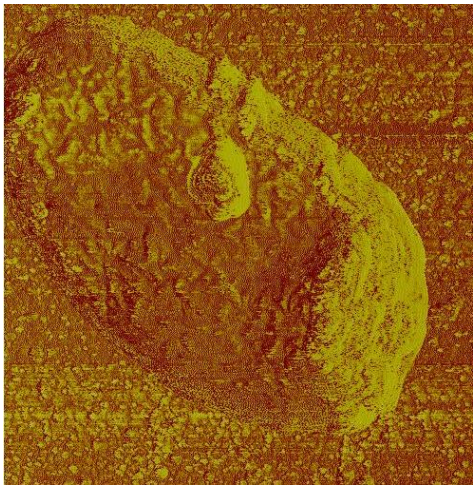

AFM is a useful tool, which could serve to describe the mechanical properties of microstructures such as bacterial cells. In this study, nanoidentation was used to study the change in the mechanical properties of the *P. aeuruginosa* cells following DC treatment using carbon or SS 304 electrodes. The elastic property of the cell membrane was characterized through measurement of the young's modulus and the hardness of the cells using atomic force microscopy (AFM) (Digital Instruments Nanoscope III, Veeco, NY). Here we describe the procedure, which was used:

1) The DC-treated cells and the untreated control cells are fixed with 2.5% glutaraldehyde in PBS for 1 h to conserve the morphology of the cells; 100 µL of the samples were mixed with 400 µL of 2.5% glutaraldehyde (in PBS).
2) The cell suspensions are pipetted onto a gold coated-glass slide. The drops of the samples are allowed to dry on gold-coated glass coupons, which were previously cleaned with 190 proof ethanol. Gold-coated surfaces are used to reduce the charge accumulation on substrate during AFM analysis. The slides are previously cut in a size, which could fit on the AFM sample stage.
3) The samples are washed gently with Milli-Q water to remove the salt from the fixing solution
4) The samples are placed in a petri dish and introduced in a desiccator until dehydration of the cells.
5) Once dried, the samples are ready for imaging.
6) NSC14/AIBS probe (MikroMasch, CA, USA), with a force constant of 5.7 N/m, was used in tapping mode to locate the bacterial cells.
7) For controls use a bare glass coverslip to measure the deflection sensitivity of the AFM tip by performing an Auto tune function and immediately doing a single indent on the hard substrate (without sample). Deflection sensitivity is measured by fitting a line on the descending curve of a force – distance graph using the AFM software. In the recent software, the deflection sensitivity is directly used to compute the deflection of the cantilever.
8) Load the glass slide with the cells on them
9) Image the sample to locate cells on the slide using the tapping mode.

10) Once a cell is located, zoom onto the location where the cell is located to make the total field of view composed of the cell of interest.
11) Offset the sample to that location.
12) Disengage the tip.
13) Switch to contact mode and do a single indent to generate a force curve
14) Save the force distance curve as an ASCI format.
15) Switch to tapping mode, zoom out, and find another cell and repeat the above procedure (8-14) again.

Data processing.

16) Open an Excel spreadsheet
17) Open the ASCI file after selecting the "All files" format
18) Once the "Text Imort Wizard" is opened, select "Tab, semicolon, comma and space" delimiters
19) The column data format should be general
20) The data comprise the *Time (s), Calculated (Z), Deflection (V), Deflection (nm),* and *Deflection (nN)* displayed in 5 separate columns.

The data could also be expressed in Bit: $1V=7.62939x10^{-5}$ Bit. In this case, the *Deflection (V), Deflection (nm),* and *Deflection (nN)* could be derived according to the following formula:

Deflection (V)=Bit * $7.62939x10^{-5}$,

Deflection (nm)= Deflection (V) Deflection sensitivity* (see step 7), and

*Deflection (nN)= Deflection (nm)*Probe Spring constant*

The deflection force is computed based on the spring constant. Therefore, this constant is provided by the manufacturer and should be added as a parameter for the nanoindentation experiment.

21) Since the calculated (Z) described the position of the actuator of the probe (cantilever) in reference to its previous position, the initial position of the probe at the beginning of the "unloading" (labeled as **Retract**) is considered "0". Insert a column to calculate a *"normalized Z"* as a function of the original position before "loading" (labeled as **Extend**). The final value of the "loading" (**Extend**) becomes the initial value of the "unloading" (**Retract**). Any value of the calculated (Z) for the unloading part will be subtracted from the final value of the "loading" in order to generate the "normalized Z".
22) The intramolecular interactions between the probe (tip) and the sample affect the displacement of the cantilever referred to as *Deflection (nm)*. To evaluate the real distance travelled by the probe, the *Deflection (nm)* of the cantilever is subtracted from the *normalized Z (nm)*. Therefore follow the formula *H=normalized Z (nm)-Deflection (nm).*
23) Plot *H* to determine when the indentation begins (characterized by the deformation of the plots).
24) Plot *Deflection (nN)* to determine when the indentation begins and stops. The indentation stop when the deflection force stays at constant value

25) Normalize both H (*normalized H*) and the *Deflection force (nN)* based on the starting point and end point of the indent. The initial values should be "0" and the final value of the "loading curve" should be the initial value of the "unloading curve" for both the *normalized H* and the *normalized deflection force*.
26) Plot the *normalized deflection force* as a function of the *normalized deflection H*.
27) Determine slope of the linear phase of the "unloading curve" by plotting its trendline. This slope corresponds to *k*, the elastic constant of the sample.

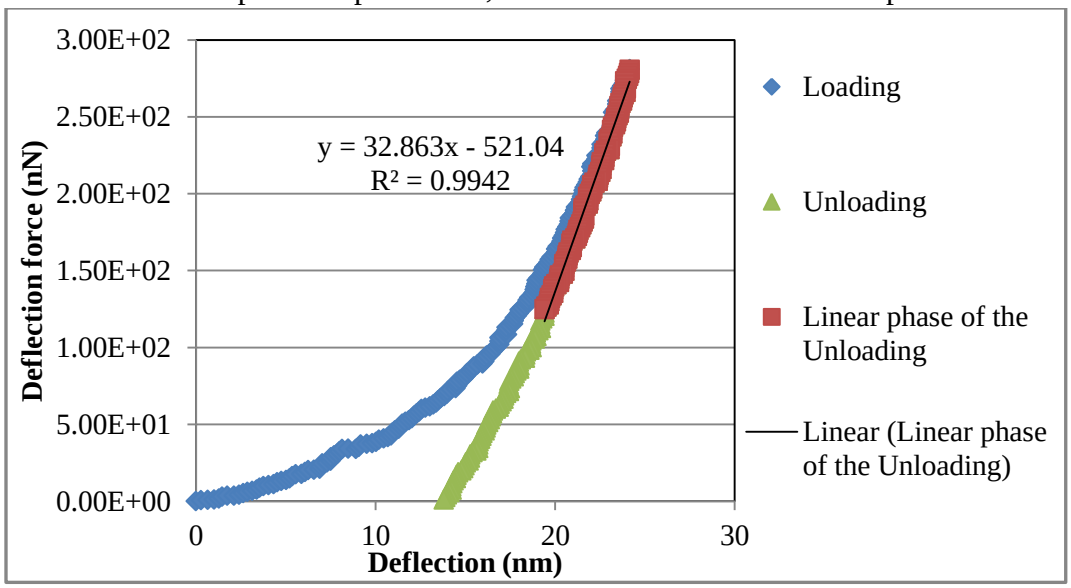

Computation of the mechanical properties

28) The modulus and the Hardness of the cells are calculated according to the following:

$$\text{Modulus: } E = \frac{(1-\nu^2) * \sqrt{\pi} * k}{2\sqrt{A_i}}; \text{ with } \nu = 0.5$$

$$\text{Hardness: } H = \frac{\text{Maximum Load}}{A_i}$$

Ai is the surface area of the tip in contact with the sample during indentation. It is computed based on the characteristics of the tip. The tip of the NSC14/AIBS probe (MikroMasch, CA, USA) is conical, with a radius of curvature of 30º over 10 nm. For an indent "I" using this probe:

$$\text{the Area of indentation: } A_i = [\pi * I * \frac{\tan(30\ degree/2)}{\cos(30\ degree/2)}] + 541.17(nm^2)$$

The value I is derived from the plot in step (26) or from the maximum value of the

normalized deflection H (nm)

The maximum load is maximum value of the *normalized deflection force (nN)*

BIOGRAPHICAL DATA

Tagbo H. R. Niepa
October 23, 1979
7527 Plum Hollow Cir, Liverpool, NY 13090
tniepa@syr.edu/703-344-1525
Citizenship: United States of America

1. EDUCATION

Doctor of Philosophy in Chemical Engineering – (05/2014)
Syracuse University, L.C. Smith College of Engineering and Computer Science, Syracuse, NY
Dissertation Topic: Electrochemical Control of Bacterial Persister Cells
Advisor: Dacheng Ren, PhD.
Committee members: James Dabroviak, PhD.; Jeremy L. Gilbert, PhD.; Jing An, M.D, PhD.; Rebecca Bader, PhD.; Julie Hasenwinkel, PhD.; Dacheng Ren, PhD.

Bachelor of Science in Bioengineering (GPA: 3.59) – (12/2009)
Syracuse University, L.C. Smith College of Engineering and Computer Science, Syracuse, NY

Superior Diploma in Food Engineering (equivalent to **Associate Degree** in the USA**)** – (04/2002)
Food Industry College, Odienné, COTE D'IVOIRE.

2. PEER-REVIEWED PUBLICATIONS

8. **Niepa THR**, Laura M. Shepenger, Marcus B. Jones, and Ren D (2014) Genetic understanding of *Pseudomonas aeruginosa* persister response to electrochemical stress mediated using carbon and stainless steel electrodes (in preparation).
7. **Niepa THR**, and Ren D (2014) Selective Control of *Pseudomonas aeruginosa* by electrochemical treatment of co-cultures involving human epithelial cells (in preparation).
6. **Niepa THR**, James C Dabrowiak, and Ren D (2014) Probing the synergy between Tobramycin and Chromium (III) in the electrochemical treatment of bacterial cells (in preparation).
5. **Niepa THR**, Jeremy L. Gilbert and Ren D (2014) Improving persister cell control through understanding of the effects of electrochemical factors and cell electrophysiology (in preparation).
4. **Niepa THR**, Haveman G, Goyal P, and Ren D (2014) Electrochemical treatment of *Pseudomonas aeruginosa* in a rabbit model of sinusitis (in preparation).
3. **Niepa THR**, Peterson HL, Shiril Sivan, Jeremy L. Gilbert, and Ren D (2014) Sensitizing *Pseudomonas aeruginosa* cells to antibiotics by electrochemical disruption of membrane functions (in preparation).
2. **Niepa THR**, Gilbert JL, & Ren D (2012) Controlling *Pseudomonas aeruginosa* persister cells by weak electrochemical currents and synergistic effects with tobramycin. Biomaterials 33(30):7356-7365.

1. Szkotak R, **Niepa THR**, Jawrani N, Gilbert JL, Jones MB, Ren D. (2011) Differential Gene Expression to Investigate the Effects of Low-level Electrochemical Currents on *Bacillus Subtilis*. AMB Express.

3. CONFERENCE PRESENTATIONS

"Controlling Pseudomonas aeruginosa persister cells by weak electrochemical currents and synergistic effects with tobramycin "- Poster Presentation at the **6th ASM conference on Biofilms**, Miami, FL. Attended the animal models of biofilm infections workshop – (Sept 29-Oct 4, 2012)

"Electrochemical Inhibition of Pseudomonas aeruginosa persister cells"- Oral Presentation at the **Emerging Researcher National (ERN) Conference in STEM**, Atlanta, GA – (February 23-25, 2012)

"Electrochemical Inhibition of bacterial persister cells"- Poster Presentation at the **2011 BMES Annual meeting**, Hartford, CT – (October 12–15, 2011)

"Electrochemical Inhibition of bacterial persister cells"- Oral and Poster Presentation at the **Stevens conference on bacteria-biomaterial interactions**, Stevens Institute of Technology, NJ – (June 9-10, 2011)

"Patterned biofilm formation reveals critical information of bacteria-surface interactions"- Poster Presentation at the **NSF CMMI research and innovation conference**, Atlanta, GA – (January 4-7, 2011)

"Elimination of Pseudomonas aeruginosa persisters with Low Electric Currents"- Oral Presentation at the **AIChE annual meeting**, Salt Lake City, UT – (November 7-12, 2010)

4. PATENT APPLICATIONS

1. Ren, D., M. Zhang, **T. Niepa**, and J. Gilbert. 2010. Systems and Method for Controlling Bacterial Persister Cells with Weak Electric Currents. (Awarded Patent # 8 569 027).
2. Romo, L., N. Garritano, **T. Niepa** (2013). Door Handle Sterilization System, WO Patent 2,013,025,894. (Patent Application)

5. RESEARCH EXPERIENCE

Helios Innovative Technologies Inc., Boston, MA

Title: Founder, Chief Technologies Officer & Director of Research (April 2011-present)

- Developed the alpha and beta prototype of the S1 Automated Door-handle sanitizer
- Performed the testing of the prototype in partnership with the Syracuse Veteran Affairs Medical Center
- Filed the US PTO patent application of the S1 device after validation of the efficacy and efficiency of the device
- Wrote the company's business plan and proposals for venture capital and government funding

Syracuse Biomaterial Institute, Syracuse University, Syracuse, NY
Title: Graduate research assistant, Lab manager & PhD student in Chemical Engineering – (Jan 2010-present)
Thesis Project: Electrochemical Control of Bacterial Persister Cells
Thesis Advisor: Dacheng Ren, PhD., Associate Professor of Biomedical and Chemical Engineering, Syracuse University

- Identified electrophysiological change in bacterial persister cells using DNA-microarray, Inductively Coupled Plasma-Mass Spectrometry (ICP-MS), bacterial zeta-potential, flow cytometry and imaging techniques (fluorescence microscopy, AFM, SEM and TEM)
- Developed methods for electrochemical control of bacterial persister cells (ECCP)
- Performed *in-vitro* study to test the safety and the efficacy in co-cultures involving human cells
- Performed animal testing to evaluate the efficacy of ECCP in a rabbit model of sinusitis
- Helped with lab management including equipment maintenance and organization of weekly lab meetings

Carnegie Mellon University, Pittsburgh, PA
Title: REU (Research Experience for Undergraduate) Summer Researcher – (06/2009–08/2009)
Project: Study of the protein binding to lipids bilayer membranes: case of Lamin-A
Faculty mentor: Mathias Lösche, PhD., Professor of Physics and Biomedical Engineering, Carnegie Mellon University, Pittsburgh, PA

- Studied the protein-lipid binding of what on tethered Bilayer Lipid Membranes
- Used of the Magnetron for the Gold-Chromium coating of a Silicon wafer
- Tested the stability of the tethered Bilayer by Electrochemical Impedance Spectroscopy
- Controlled the binding stability of the Lamin A-protein to the tethered Bilayer Membrane by Surface plasmon Resonance

Syracuse Biomaterial Institute, Syracuse University, Syracuse, NY
Title: LSAMP (Louis-Stokes Alliance for Minority Participation) Biomedical Research Assistant – (06/2008–08/2008)
Project 1: Investigation of the tolerance of Escherichia coli to Butanol and Ethanol
Title: McNair Scholar Biomedical Research Assistant – (08/2008–12/2009)
Project 2: Understanding the multi-drug resistance of Pseudomonas aeruginosa
Faculty Advisor: Dacheng Ren, PhD., Associate Professor of Biomedical and Chemical Engineering, Syracuse University, Syracuse, NY

- Tested butanol and ethanol tolerance of Escherichia coli mutants
- Constructed *Pseudomonas aeruginosa* mutants and tested their antibiotic tolerance
- Identified the mutated genes of selected mutants using PCR
- Helped with lab management including protocol organization and schedule of weekly lab duties

Institut Pasteur de Côte D'Ivoire, Abidjan, Côte D'Ivoire
Title: Lab Technician – (01/2002-08/2003)
Project: Bacteriological analysis of human biological fluids and Control quality of food manufactured in Abidjan-COTE D'IVOIRE.
Title: Lab Manager – (08/2003- 07/2004)
Project: Development of a culture-media and reagents manufacturing unit
Faculty Advisor: Professor Mireille Dosso, Department of Food and Medical Bacteriology-Virology, Institut Pasteur, COTE D'IVOIRE.

- Performed food quality control analysis in the department of food microbiology
- Performed the analysis of biological samples, including blood and urine, in the department of medical bacteriology
- Responsible for the Media & Reagent Manufacturing Unit, overseeing media and reagent production, and maintaining laboratory equipment
- Wrote lab protocols and established good manufacturing procedures for the unit

6. ACADEMIC EXPERIENCE

Relevant Courses

Graduate: Polymer Physics; Biopolymers; Surfaces of Biomaterials; Fundamentals of Heat & Mass Transfer; Chemical Engineering Kinetics; Chemical Reaction Engineering; Fluid Dynamics; Environmental Chemistry & Analysis; Chemical Engineering Methods; Statistics for Engineers; Fluid Mechanics; Biochemical Engineering; Modern NMR Technology II; Modern NMR Technology I; NMR Data Processing Lab; Metals in Medicine; Startup Sandbox.
Undergraduate: Advanced Biomechanics; Advanced Biomechanics Lab; Bioengineering Capstone Design; Senior Thesis; Introduction to Neuroscience; Professional Practice; Engineering Analysis of Living System I and II; Control Systems; Skeleto-Muscular Biomechanics; Biomaterials & Medical Devices; Drug Delivery; Electrical Engineering Laboratory I and II; System & Signal Analysis; Engineering Materials/Properties/Processing; Electrical Engineering Fundamentals I and II; Differential Equation & Matrices Algebra for Engineers; Mechanics of Solids; General Biology II; Genetics & Cell Biology II; Statics; Calculus III.

Professional Development

Participant, Future Faculty Workshop, Georgia Institute of Technology – (July 17-19, 2013)
Session Aide, 2013 AAAS Annual Meeting in Boston, MA – (February 14 -18, 2013)
Participant, NextProf Future Faculty Development Workshop. University of Michigan – (Sept 19-21, 2012)
Participant, NSF sponsored Preparing Future Faculty Summer Institute 2012, Howard University-AGEP and AC-SBES event, Washington DC – (June 6-9, 2012)
Selected participant for the White House Business Council and Business Forward Northeast Business Leaders' Forum, White House, DC – (January 18, 2012)

Teaching Experience and Mentorship Activities

Seminar Speaker at the Department of Chemical and Biological Engineering - University of Pennsylvania. Title: Sensitizing Pseudomonas aeruginosa cells to antibiotics by electrochemical disruption of membrane functions – (August 26, 2013)

Program Coordinator, Emerging Frontiers in Research and Innovation-Research Experience and Mentoring (EFRI-REM), Syracuse University – (summer 2012 - Spring 2014)

- Facilitated, organized and scheduled activities of the EFRI-REM Summer Research Program
- Taught laboratory techniques to the EFRI-REM Summer Students

Mentor, Henry Lars Peterson, Undergraduate Honor's Thesis, Bioengineering – (spring, fall 2012)

Mentor, Simone Gayle, Bioengineering Undergraduate Independent Study – (fall 2012, spring 2013)

Guest-Lecturer, Career and College Workshop in collaboration with High school teacher Suzanne DeTore, Henninger High School-Syracuse, NY – (fall 2012)

Mentor, Jennifer Mary Puthota, Masters' Independent Study in Chemical Engineering – (spring, fall 2011)

Guest-Lecturer, Engineering Computational Tools (ECS 104), Syracuse University – (fall 2011)

7. ACADEMIC AND PROFESSIONAL HONORS & AWARDS

Gordon Research Conference- Carl Storm Underrepresented Minority Fellowship, Gordon Research Conference & Seminar on Microbial Stress Reponses- at Mount Holyoke College, South Hadley, MA (July 26 - August 1, 2014)

University of Pennsylvania-Postdoctoral Fellowship for Academic Diversity, Department of Chemical and Biological Engineering – (2014)

Graduate Research Assistantship, Department of Biomedical and Chemical Engineering, Syracuse University, Syracuse, NY– (2010- 2011, fall 2013, Spring 2014)

Nominated by Syracuse University and MARS, Inc. to attend the 2013 Nobel Laureate meeting in Lindau, Germany from June 30-July 5, 2013 (first and second round of selection) – (2013)

Syracuse University STEM Pre-doctoral Fellow, Syracuse University – (2011-2013)

Travel award, NextProf Future Faculty Development Workshop- University of Michigan – (2012)

Travel award, Emerging Researcher National Conference in STEM, Atlanta, GA – (2012)

Recognition as *GEW TOP 50 Most Promising Startups Globally* with HELIOS – (2011)

Travel award, Stevens Conference on Bacteria-Biomaterial Interactions, Stevens Institute of Technology, NJ – (2011)

1st Place and Grand winner of the NYS Business Plan Competition with HELIOS – (2011)

Travel award, NSF CMMI Research and Innovation Conference, Atlanta, GA – (2011)

8. SOCIETY MEMBERSHIPS

Member since 2009, American Association for the Advancement of Science (AAAS)
Member since 2009, National Society of Black Engineers (NSBE)
Member since 2009, American Society for Microbiology (ASM)
Member since 2010, Biomedical Engineering Society (BMES)
Member since 2012, American Chemical Society (ACS)

9. SKILLS

Entrepreneurship, Scuba diving, Soccer
Language: English, French (native tongue), German (University of Marburg, Germany - Deutsche Sprachprüfung für den Hochschulzugang Zertifikat – 04/2005)